Engin

A REVIEW AND EVALUATION OF BASIC TECHNIQUES FOR PREDICTING THE BEHAVIOR OF SURFACE OIL SLICKS

by

Keith D. Stolzenbach

Ole S. Madsen

E. Eric Adams

Andrew M. Pollack

and

Cortis K. Cooper

RALPH M. PARSONS LABORATORY

FOR WATER RESOURCES AND HYDRODYNAMICS

Report No. 222

February 1977

A REVIEW AND EVALUATION OF BASIC TECHNIQUES
FOR
PREDICTING THE BEHAVIOR OF SURFACE OIL SLICKS

by

Keith D. Stolzenbach
Ole S. Madsen
E. Eric Adams
Andrew M. Pollack
Cortis K. Cooper

Ralph M. Parsons Laboratory
for
Water Resources and Hydrodynamics

Report No. 222

Prepared for the

Marine Assessment Division
Center for Experiment Design and Data Analysis
Environmental Data Service
National Oceanic and Atmospheric Administration
U.S. Department of Commerce

February, 1977

FOREWORD

A preliminary draft version of this report was prepared in May, 1976. A workshop was held at M.I.T. on June 3-4, 1976 for the purpose of reviewing the report and providing further input. The following is a list of the persons who contributed to the workshop:

James M. Austin	Department of Meteorology, M.I.T.
Celso Barrientos	National Weather Service, NOAA
Robert C. Beardsley	Woods Hole Oceanographic Institute
David Behringer	Atlantic Oceanographic and Meteorological Laboratory, NOAA
Joseph Bishop	Deepwater Ports Project Office, NOAA
Dail Brown	Deepwater Ports Project Office, NOAA

TABLE OF CONTENTS

CHAPTER 1

INTRODUCTION

The development of offshore oil production and transportation
facilities has justifiably been accompanied by concern for the possibility
of oil spills and the associated potential for adverse impacts upon
coastlines and coastal waters. Regulatory frameworks have been estab-
lished for the purpose of balancing the risks of such damage against the
benefits of the proposed developments. Decisions within these frameworks
must be based upon predictive analyses of the fate of the oil that are
adequate for risk assessment. In addition, when an oil spill occurs,
protective measures to minimize impacts likewise require a capability to
forecast the short-term and long-term behavior of the spilled oil. The
motivation for the study presented in this report is the need for a de-
tailed review of the basic analytical techniques available for making such
predictive estimates.

1.1 Problem Definition

The major factors that must be considered in an evaluation of
potential or actual oil spills are:

- The location, size, and physical and chemical properties of the
  oil spilled.

- The transport of the oil by wind and currents.

- The physical, biological and chemical transformations that the
  oil undergoes as it is being transported.

The general problem of predicting the behavior of spilled oil

is complicated by the wide variety of conditions that may be present in the receiving waters and the stochastic nature of important environmental factors influencing oil slick transport. In addition, there is a significant lack of data on many of the most important aspects of oil behavior. Accordingly, to accomplish the objectives of the study, it was necessary to define carefully the scope of the problems to be treated. In this regard the following general guidelines were established:

1. Instantaneous rather than continuous or chronic oil spills are emphasized.

2. The review focuses on the transport and transformation of surface oil slicks and does not present an in-depth treatment of techniques relating to the fate of oil beneath the water surface.

Within the general scope defined above, the purpose of the study is to conduct a state-of-the-art review of the basic techniques and knowledge associated with surface oil slick behavior. Of particular importance in this review is the need to delineate the hierarchy of modeling levels that may be achieved on the basis of assumptions of increasing sophistication. In addition to providing a yardstick with which to measure existing modeling efforts, such a review also provides an evaluation of the current needs for additional basic research and data collection.

This report presents the results of this review in the following manner. Because of its significance in determining the fate of oil slicks, the representation and determination of wind fields is discussed first in Chapter 2. Then Chapter 3 presents a treatment of the advection

of oil slicks that is brought about by the combined action of currents and wind-waves. Following this, Chapter 4 deals with the various physical phenomena that _transform_ an oil slick as it is being advected. Finally, a review and evaluation of existing models for oil slick behavior is presented in Chapter 5. A comprehensive bibliography is included at the end of the report, along with an appendix containing a detailed treatment of wind driven currents.

1.2 General Conclusions

Specific conclusions regarding the state-of-the-art in wind field modeling, slick advection, oil transformation, and composite modeling are presented in Chapters 2 through 5. The following are those conclusions considered to be the most important, particularly with respect to the specification of needs for future work:

1. The success of any approach to wind field modeling relies on the availability of measurements with sufficient density in space and time to resolve adequately the significant spatial and temporal scales of wind fluctuations. The complex structure of winds within the nearshore coastal zone presents special problems in this respect because of the combined influence of land and sea masses. Accordingly, the representation of these winds is an area in which future modeling and data collection effort should be directed.

2. Even under idealized conditions, the present capability to quantify the effects of winds and waves on oil slick advection is poor. Whereas waves and wind driven currents by themselves

may be treated, at least in an approximate manner, the lack of reliable data for the combined effects of waves and wind-driven currents results in a predictive capability which is potentially in error by a factor of 2. The solution to the fundamental problem of the advection caused by the combined action of waves and wind-driven currents is urgently needed to improve our ability to predict advection of oil slicks in the offshore environment.

3. In addition to the advection of oil slicks by wind-driven currents and waves, the advection by tidal, density-driven, and general ocean currents may be important,particularly if a spill occurs relatively far offshore. The present capability to predict these currents is poor and reliable estimates must depend heavily on site-specific observations. Continued research into analytical approaches to these problems and systematic data collection efforts should be encouraged.

4. It is clear that present techniques for predicting slick growth yield no better than order of magnitude estimates for slick size and configuration. Given the variability and complexity of the processes affecting slick growth, it is unlikely that significant improvements in these estimations can be made. However, it is important to recognize that in many cases slick size and configuration may be of secondary importance to advection and weathering processes in determining environmental impacts.

5. No adequate technique exists which incorporates the interactions between weathering and spreading. One specific difficulty lies in predicting how changes in oil composition affect the surface tension spreading force. Another is the uncertainty in determining when oil will form a water-in-oil emulsion and how much this emulsification will retard spreading.

6. Weathering of oil involves a variety of physical, chemical and biological reactions, which may take place over time scales ranging from a few hours to a few years. Evaporation is the only one of these processes that can be adequately modeled at present. Evaporation, which takes place during the first days after a spill, is probably the most important short-term mechanism for depleting volume of the slick. Processes which introduce hydrocarbons into the water column, although usually not as important volume-wise as evaporation, are very important ecologically. Dissolution is the only one of these processes that has been modeled at all. It is likely to be less important than vertical dispersion of colloidal-sized and larger oil globules. The dispersion can be aided by surface active substances and by adhesion of oil to sediment, processes that cannot be quantified at present and which are thus important areas for future research.

7. In reviewing existing composite models for oil slick behavior, it is evident that despite numerous attempts, composite models show a remarkable lack of diversity. This conformity in composite modeling is attributable to the state of knowledge of the basic environmental processes affecting slick transport.

It was found in Chapters 2 to 4 that many of these processes have virtually no analytical description. For others, there exists a limited number of analytical techniques of varying complexity, many of which are unproven or too complex for use in a composite model. Hence existing models have tended to use the simpler techniques utilized by previous modelers, despite the fact that these have not necessarily given good results in previous applications.

8. It is concluded that the state-of-the-art in composite modeling is most adequate when applied to relatively protected sites such as harbors and bays. In such areas, predictions of the trajectory of the center of mass can probably be made with adequate accuracy. Other processes for which little is known, such as dispersion, weathering, and wave influence can usually be neglected for the short travel times involved. In more exposed environments, however, these processes can not be neglected. In addition techniques for predicting center of mass movement are much less adequate. Further refinement of the state-of-the-art in composite models for open seas can probably not be achieved until a better fundamental understanding of basic phenomena such as wave-induced drift, weathering processes, etc., is obtained.

9. Individual oil slick modeling efforts must by necessity be focused on a subset of the large number of physical processes involved in oil slick behavior. The choice of which processes

to model must be made on the basis of their relative importance
as determined by site-specific conditions and by the purposes
of the modeling effort. There is a crucial need for
research that will quantify the sensitivity of slick behavior
to the representation of each physical process for a wide range
of generic spill conditions.

CHAPTER 2

MODELING OF WIND FIELDS

2.1 General Considerations

The wind is an important factor in the determination of surface
oil slick behavior. Its primary effect is on the advection of the slick
through the generation of surface waves and near surface currents and through
the creation of shear stress on the slick surface as discussed in Chapter
3. The wind also influences the dispersion and weathering (especially
evaporation) of the slick as discussed in Chapter 4.

Although the wind field is inherently variable in time and space it
is normally the case that measurements are available at a relatively few
locations and for limited periods of observation. Accordingly, in
specifying the wind field for the purpose of predicting oil slick behavior,
it is often necessary to utilize some type of model for the wind field
structure in time and space. The model might calculate winds determinis-
tically from governing equations or it might generate them stochastically
using statistical correlations. Or the model might simply apply spatial
and temporal interpolation and extrapolation schemes to observed data.
The objective of this chapter is to discuss general aspects of coastal wind
fields, to categorize various modeling approaches, and to assess these
approaches in light of the overall objective of predicting the behavior of
surface oil slicks.

2.1.1 Requirements of a Wind Model

The wind field is represented by the three-dimensional vector $\vec{W}(x,y,z,t)$ where x and y are horizontal coordinates, z is elevation and t is time. Because a complete description of $\vec{W}$ is impractical, certain simplifications must be made.

First, and most important, the model should include sufficient detail to describe the regional and local characteristics of the wind at the location being considered. The relationships between the length and time scales which describe a region and the scales of wind variation are discussed below.

Second, the spatial and temporal structure of the wind model should reflect the needs and accuracies of the transport models to be used. For instance the vertical component of wind speed is not usually needed nor is a complete relationship between horizontal wind speed and height because most empirical formulas relating wind to surface shear stress, surface drift, evaporation, etc., require wind speed at only one elevation, z_1 (eg. $z_1 = 10$ meters). Thus the wind may be satisfactorily approximated by the horizontal vector $\vec{W}_H(x,y,z_1,t)$ consisting of either the Cartesian components W_x and W_y or the speed and direction $|\vec{W}|$ and θ. In addition, if advection is being computed in relation to the local wind speed, $\vec{W}_H$ needs to be specified only at the instantaneous position of the slick and not over the entire region.

Finally the model should be consistent with a probabilistic assessment of oil slick behavior. Thus, for example, not only is the probable trajectory of an oil slick important, but so is the distribution of possible trajectories. For risk assessment, the capability of a model to generate

a number of different realizations of the wind field is considered more important than its ability to produce real-time forecasts.

2.1.2   Time and Length Scales of Wind Variation

Figure 2.1.1 shows the approximate relationships among the scales of wind fluctuations, the scales imposed by the nature of the spill and the region under study, and the scales of wind fluctuations which can be resolved with wind measurements. The accompanying discussion is presented as background for assessing different approaches to wind modeling.

Part a) of the figure indicates schematically the most energetic wind scales. Low frequency energy is associated with general circulation and with the passage of synoptic scale weather systems. The nature of these motions depends on the locality and reflects the origin and type of pressure system and possible interaction between systems. These motions have length scales on the order of 10^6-10^7m and contribute energy at periods greater than about 10^4-10^5 seconds.

At the other end of the spectrum are turbulent fluctuations caused by friction and natural convection near the earth's surface. Over the open ocean the contribution of turbulence is limited to periods less than about 10 seconds, while over land, where the surface roughness is greater and conditions of thermal instability more prevalent, periods ranging up to 10^2 to 10^3 seconds may be found. Coastal regions may exhibit a mixture of these characteristics depending on the prevailing wind direction. By assuming a range of prevailing wind speeds the periods associated with the turbulence can be translated into a range of length scales as shown in the figure.

a) Scales of wind variation
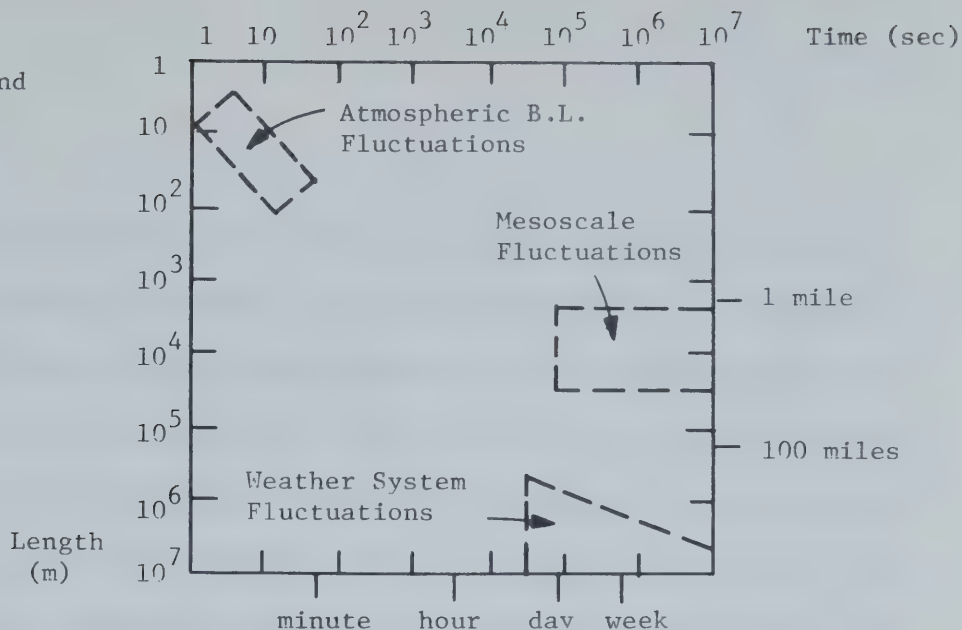
b) Scales related to the spill and the region
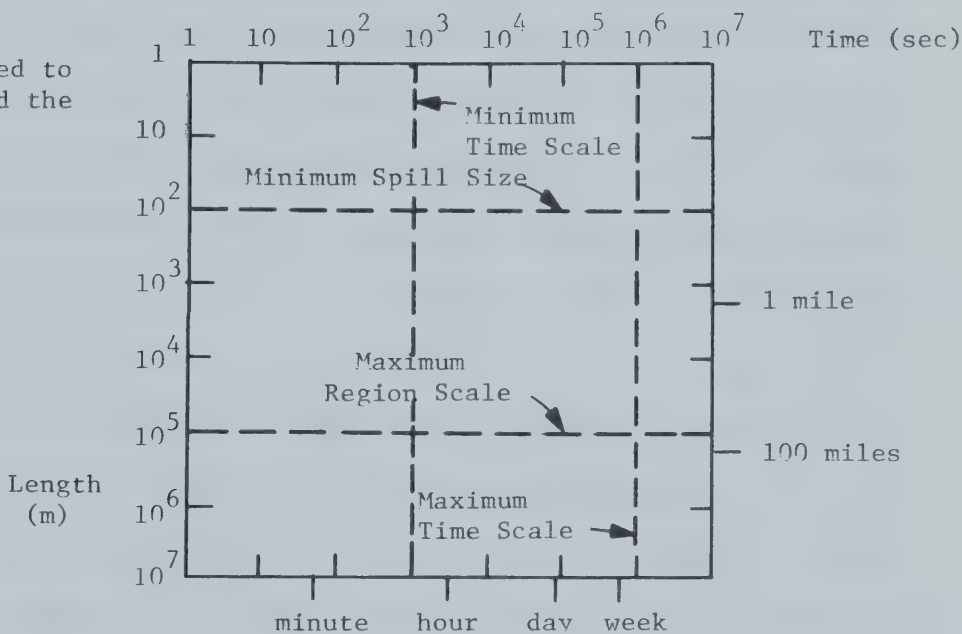
c) Scales resolved with typical measurements
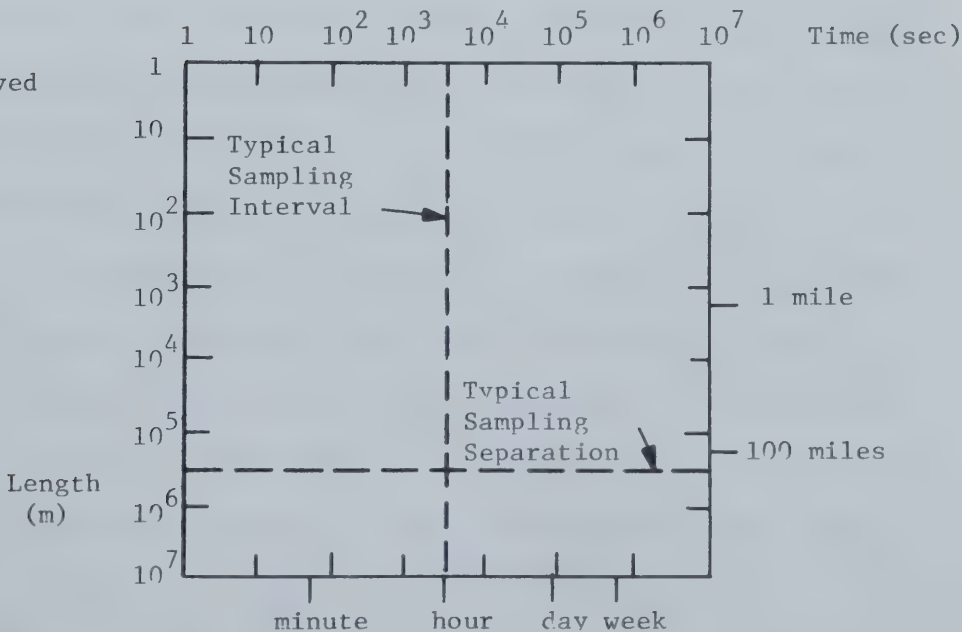
Figure 2.1.1
Length and Time
Scales Charac-
terizing Oil
Transport by Wind

2-4

Coastal regions are often complicated further by mesoscale motions due to thermal and orographic effects. The most common of these are land/ sea breeze systems caused by diurnal variations in atmospheric heating and cooling rates over land and water. A fully developed land/sea breeze system depends on a number of variables including season, latitude and local meteorology (prevailing winds, cloud cover, etc.) and typically extends about 10 km offshore. Near mountainous coastlines land/sea breezes may be amplified by slope or drainage winds and their influences felt at greater offshore distances. Coastal winds may also differ from those inland or further offshore due to the sharp gradient in surface roughness and (non-diurnal) differences in atmospheric heating such as those caused by warm or cold coastal currents.

2.1.3 Time and Length Scales Relating to the Spill and the Region

Part b) of Figure 2.1.1 shows the length and time scales imposed by the size of the spill and the region under study. The maximum length scale of interest is the characteristic length of the region, which for offshore oil facilities, might be about 10^5 meters. Because wind fluctuations with length scales substantially greater than this distance can be treated as uniform, it is not necessary that these fluctuations be resolved. A smaller scale is given by the dimension of the oil slick which is of the order of 10^2m to 10^5m (see Chapter 4). Fluctuations with length scales less than this dimension will contribute to the spreading or "dispersion of the slick about its center of mass," but will not cause significant net advection of the slick. Conversely larger scale fluctuations will act more uniformly on the slick causing

advection or "dispersion of potential slick trajectories about an average trajectory." If we accept the schematic distribution of wind energy in Figure 2.1.1a we conclude that weather scale fluctuations are primarily responsible for advecting oil slicks, while fluctuations associated with the atmospheric boundary layer are primarily responsible for spreading of the slick. Mesoscale effects, such as the land/sea breeze, occur at intermediate scales, and may be responsible for both spreading and advection.

Regional time scales associated with the advection of the slick can be determined by dividing the length scales by a characteristic oil drift rate (order of .1 meter/sec). The corresponding minimum and maximum time scales ($\sim 10^3$ and 10^6 seconds, respectively) are indicated on the figure. As with the length scales, wind fluctuations with periods substantially greater than the larger scale (eg. seasonal variations) can be treated as temporally uniform while fluctuations with periods substantially shorter than the smaller period can be ignored because their contribution towards advection is small in comparison with the size of the slick.

We can also note, that as far as modeling drift due to weather scale fluctuations is concerned, it is more important to model temporal variations than spatial variations. This is because, at the position of the slick, the change in wind speed with respect to time is proportional to the translational speed of the weather system (order of 10 meters/second) while the change in wind speed with respect to the slick position is proportional to the drift speed of the oil (order of .1 meters/second).

2.1.4 Sources and Nature of Wind Data

The ability to detect variations in wind speed depends on the frequency and spacing of meteorological observations (primarily of wind itself, and of pressure). A major source of data is the National Climatic Center in Asheville, N.C. which collects observations from a number of stations operated by the National Weather Service and other federal agencies. The level of service varies but hourly or three-hourly data for many stations is available for periods of at least 10 years. Most stations are inland (eg., at airports) but data from several islands, offshore (Texas) towers, and ocean weatherships is also available. The NCC also collects, archives and summarizes by location meteorological observations reported by ships of opportunity. Coast Guard observing stations represent another major source of data. While these measurements are taken less frequently (typically every 6 hours),they may be more representative of nearshore conditions than measurements from inland stations. Hourly data is also available from a number of environmental data buoys being deployed by NOAA in various areas of the Atlantic Ocean, Gulf of Mexico, and Gulf of Alaska. The data is archived by the National Oceanographic Data Center in Washington, D.C. Several environmental monitoring stations have also been operated privately in specific areas in connection with proposed offshore construction activity. Finally, ocean winds are being measured indirectly from satellite photographs, by for instance, observation of cloud movement or of sunglint patterns (Strong and Ruff, 1970). Although these measurements are not generally available they are distinguished from point measurements in that they cover large areas of the ocean simultaneously.

The length and time scales which can be resolved from typical point source measurements are shown in Figure 2-1c. In comparison with Figure 2.1a it can be seen that a three hour reporting interval is generally satisfactory for describing the time structure associated with wind fluctuations. However, stations are typically separated by distances of several hundred kilometers which means that they are of less use in resolving spatial variability, especially that due to mesoscale motions.

2.2 Dynamically Derived Wind Fields

In principle the three components of $\vec{W}$, along with the atmospheric pressure, density and temperature are governed by six equations: a continuity equation, three equations of motion, an energy equation and an equation of state. In a right-handed coordinate system with x-y plane tangent to the Earth at latitude ϕ and z positive upward these equations may be written

$$\frac{\partial \rho}{\partial t} + \nabla \cdot (\rho\vec{W}) = 0 \tag{2.2.1}$$

$$\rho(\frac{\partial \vec{W}}{\partial t} + (\vec{W}\cdot\nabla)\vec{W}) + \rho\Omega\vec{k}x\vec{W} = -\nabla p - \rho g\vec{k} + F_{fric} \tag{2.2.2}$$

$$\rho c_v(\frac{\partial T}{\partial t} + (\vec{W}\cdot\nabla)\vec{T}) + p(\nabla\cdot\vec{W}) = \Phi_{cond} + \Phi_{dissip} + \Phi_{rad} \tag{2.2.3}$$

$$p = \rho RT \tag{2.2.4}$$

where ρ is density, p is pressure, g is acceleration of gravity, $\vec{k}$ is the unit vector in the z direction, Ω is the Coriolis parameter ($\Omega = \omega_e \sin\phi$), ω_e is the Earth's angular velocity, T is temperature, c_v is the specific heat at constant volume, R is the universal gas constant, F_{fric} is the flux of momentum due to viscous and turbulent stress and Φ_{cond}, Φ_{dissip} and Φ_{rad} are the fluxes of thermal energy due to laminar and turbulent heat conduction, mechanical energy dissipation and absorbed radiation respectively. These equations apply to the turbulent, time averaged components and assume that the atmosphere behaves as an ideal gas.

2.2.1 Synoptic-Scale Motion

Synoptic-scale motion is most easily calculated directly from maps of the pressure field. The approach involves, implicitly or explicitly, three steps: determination of the pressure field, calculation of the wind field above the planetary boundary layer and estimation of surface winds through use of a boundary layer model.

Estimation of Pressure Fields

Synoptic pressure maps are routinely generated by the National Weather Service using numerical models and a network of wind and pressure measurements. Wind fields which are continuous in time can be estimated from sequential weather maps, or for forecasting purposes, the short term forecast maps can be used. Alternatively, representative winds can be computed based on the growth and movement of typical weather systems within a region. The latter approach was used by the Coast Guard (Miller, Bacon and Lissauer, 1975) to study the movement of oil off the New Jersey-Delaware coastline in response to typical wintertime low pressure and summertime high pressure systems.

Winds Above the Boundary Layer

The simplest relationship between wind and the pressure field is geostrophic balance. The resulting flow is calculated by assuming incompressible flow and neglecting vertical velocities, friction and all accelerations in the horizontal equations of motion (Equation 2.2.2), leaving a balance between pressure gradient and Coriolis forces in the form

$$W_{xg} = - \frac{1}{\rho \Omega} \frac{\partial p}{\partial y} \qquad (2.2.5)$$

$$W_{yg} = \frac{1}{\rho \Omega} \frac{\partial p}{\partial x} \qquad (2.2.6)$$

where W_{xg} and W_{yg} are the x and y components of the geostrophic wind

vector. Above the planetary boundary layer, $z \gtrsim 1000m$, the requirements

of geostrophic balance are often satisfied and wind observations generally

show good agreement with Equations (2.2.5-2.2.6). The calculations can

be improved by including corrections to account for centrifugal accelera-

tion due to curvature of the streamlines (gradient wind correction) and

local acceleration due to evolution of the weather system (isallobaric

wind correction). These corrections are discussed in Endlich (1961) and

Haurwitz (1941).

Winds Within the Boundary Layer

Near the Earth's surface, shear stress due to turbulence must enter

the balance. The role of the shear stress can be seen by writing the

horizontal momentum balance in terms of the difference between the actual

wind velocity and the velocity above the planetary boundary layer. For

instance, by assuming geostrophic flow above the boundary layer, and desig-

nating the x and y components of shear stress by τ_x and τ_y, the balance

reads

$$\Omega(W_x - W_{xg}) = \frac{1}{\rho}\frac{\partial \tau_y}{\partial z} \qquad (2.2.7)$$

$$\Omega(W_y - W_{yg}) = -\frac{1}{\rho}\frac{\partial \tau_x}{\partial z} \qquad (2.2.8)$$

Noting that the shear stress opposes the mean motion, these equations

indicate that velocities within the boundary layer are reduced and rotated

(counterclockwise in the Northern Hemisphere) with respect to the overlying

wind.

A solution for the velocity profile (Ekman spiral) can be obtained by postulating a relationship between the shear stress components and the mean velocity components in equations such as (2.2.7-2.2.8) and applying appropriate boundary conditions. The relationship between stress and mean velocity can range from a simple distribution of eddy viscosity for which analytical solutions may be possible (eg. Ellison, 1956) to higher order closure models involving solution of additional equations (eg. Wyngaard, et al., 1974). A discussion of analogous solutions for the ocean Ekman layer is presented in Chapter 3.

Alternatively the form of the profile can be deduced from dimensional considerations along with empirical observations. In a neutrally-stable atmosphere, for instance, the mean velocity distribution near the earth's surface may be defined in terms of the shear velocity u_* and a dynamic roughness height, z_o, so that, when the x axis is oriented in the direction of the surface shear,

$$\frac{W_x}{u_*} = \phi_x (z/z_o) \qquad\qquad (2.2.9)$$

$$\frac{W_y}{u_*} = \phi_y (z/z_o) = 0 \qquad\qquad (2.2.10)$$

At the outer edge of the boundary layer the governing velocity and length scales are u_* and $\frac{u_*}{\Omega}$ respectively, and the appropriate form for the velocity distribution is a velocity defect law,

$$\frac{W_x - W_{xg}}{u_*} = \Phi_x \left(\frac{z\Omega}{u_*}\right) \tag{2.2.11}$$

$$\frac{W_y - W_{yg}}{u_*} = \Phi_y \left(\frac{z\Omega}{u_*}\right) \tag{2.2.12}$$

In the "matched regions", where $z/z_o \gg 1$ and $z\Omega/u_* \ll 1$, both of the above sets of equations hold, and as shown by Blackadar and Tennekes (1968), the velocity distribution must be of the form

$$\kappa \frac{W_{yg}}{u_*} = -A \tag{2.2.13}$$

$$\kappa \frac{W_x}{u_*} = \ln \frac{z}{z_o} + B \tag{2.2.14}$$

$$\kappa \frac{W_x - W_{xg}}{u_*} = \ln \frac{z\Omega}{u_*} + C \tag{2.2.15}$$

$$\kappa \frac{W_{xg}}{u_*} = \ln \frac{u_*}{\Omega z_o} + B - C \tag{2.2.16}$$

where κ is von Karman's constant and the coefficients A, B and C are computed from observed wind profiles. B is often chosen as zero and for $\kappa = 0.4$ the values of A and C are approximately 4.3 and 1.7 (Plate, 1971). For a neutrally stable atmosphere, the relationship between wind speed and direction at elevation z, appropriate for $z/z_o \gg 1$ and $z\Omega/u_* \ll 1$, may now be related to the geostrophic wind velocity by

2-13

$$\frac{W_x}{G} \sim \frac{\ln z/z_o}{[(\ln \frac{u_*}{\Omega z_o} -1.7)^2 + 4.3^2]^{1/2}} \qquad (2.2.17)$$

$$\tan \alpha = \frac{-W_{yg}}{u_*} \sim \frac{4.3}{\ln \frac{u_*}{\Omega z_o} - 1.7} \qquad (2.2.18)$$

where G is the geostrophic wind speed, $G^2 = W_{xg}^2 + W_{xg}^2$, and α is the

angle of the wind at elevation z relative to the geostrophic wind

(positive counterclockwise).

Over the ocean the values of u_* and z_o in the above expressions

are strong functions of the wind speed. Wu (1969) has compiled data from

a number of sources indicating that z_o (computed from the surface rough-

ness parameter, $k_s = 30 \ z_o$) ranges from less than .001 cm for light breezes

(10 meter wind speed, W_{10} < 3m/s) to about .3 cm for strong winds

$(W_{10}$ > 15 m/s) while $c_{10} = \frac{u_*^2}{W_{10}^2}$ ranges from less than 10^{-3} for W_{10} < 5 m/s to

about 2.6×10^{-3} for W_{10} > 15 m/s. For $\Omega = 10^{-4} \ s^{-1}$ (ϕ = 43°N) and values

of u_* and z_o computed from Wu's correlations, Equations (2.2.17-2.2.18) suggest

that the ratio of 10 meter wind speed to geostrophic wind speed varies

from about .80 to about .60 and the corresponding rotation angle α varies

from about 15° to 20° as W_{10} ranges from 3 m/s to 15 m/s.

These numbers are consistent with rule of thumb values of $\frac{W_{10}}{G}$ = 2/3

and α = 10° – 20° which are based on observations of ocean winds under a

variety of conditions. If secondary influences are considered, notably

those arising from vertical and horizontal temperature gradients, the

estimate of near surface winds can be improved. For instance Gordon (1950,

1952) reported that the value of α generally increased and the ratio of $\frac{W_{10}}{G}$ generally decreased with increasing atmospheric stability, and hence decreasing vertical turbulent transport. This dependency can be formalized by including in Equation (2.2.9) a stability dependent term involving the difference between atmospheric and sea surface temperature. If this difference is expressed in terms of the Monin-Obukov length, L, then Equation (2.2.9) may be expressed

$$\frac{W_x}{\bar{u}_*} = \phi_x' \; (z/z_o, \; z/L) \tag{2.2.19}$$

A review of various forms of ϕ_x', appropriate for different stability conditions, is presented by Plate (1971).

The relationship of the geostrophic wind to horizontal temperature gradients, as expressed by the magnitude and orientation of the thermal wind, is also important. On a climatic scale this relationship explains the generally decreasing value of α with increasing latitude found by Sheppard (1954) and Sheppard et al. (1952) (in contradiction of the trend suggested by Equation 2.2.18) while on a mesoscale it accounts for anomalous behavior of wind found near fronts or in coastal regions exhibiting large horizontal temperature gradients. Models of the boundary layer which include thermal wind effects include those of Isozaki and Uji (1974) and Arya and Wyngaard (1975).

Assessment

It is important to note at this point that the accuracy of near surface wind estimates depends on the accuracy of each of the steps outlined above, and in particular, that the accuracy can be no better than the accuracy of the initial estimate of the geostrophic flow. This conclusion is supported by recent studies of winds in the New York Bight by Overland and Gemmill (1976). They found that, while estimates of near surface wind based on synoptic surface pressure fields compared favorably with other estimating techniques such as extrapolations from shore stations, the largest component of error occurred in the calculation of the pressure gradient. This calculation is likely to be best under conditions of strong steady wind and worst near coastlines or under conditions of light winds or rapidly varying winds such as those associated with fronts.

2.2.2 Coastal Wind Models

In coastal regions the relationship between surface winds and synoptic pressure fields is often poor. As illustration, in a recent study of near surface winds 4 km off the New Jersey coast (E.G.&G. Environmental Consultants, 1975) it was found that measured wind speeds generally exceeded the estimated synoptic scale geostrophic wind speed (which was not corrected for friction) while measured wind direction frequently differed from geostrophic wind directions by 90° or more. The poor agreement can be attributed partly to the sudden change in surface roughness between land and water surfaces and to differential heating which produces local changes in surface pressure which cannot be resolved by synoptic weather maps.

In order to study these effects, a number of coastal wind models have been developed. Many, such as the models by Estoque (1961, 1962), Neumann and Mahner (1971) and Walsh (1974) have focused on theoretical aspects of the land/sea breeze. Others have examined the acceleration of offshore winds (eg. Kindle et al., 1976), the effects of coastal topography on wind circulation (Lavoie, 1972) or three-dimensional aspects of land/sea breeze circulation (McPherson, 1970 and Pielko, 1974). Essentially each model solves the governing equations over the depth of the planetary boundary layer within a region extending several hundred kilometers onshore and offshore from the coast.

Often the models are two dimensional. Thus land/sea breeze models commonly neglect alongshore gradients of all variables except pressure and solve for the three components of the wind field as a function of height and distance offshore. If local circulation is due mainly to coastal topography, a formulation involving the two horizontal dimensions and obtained by vertical integration of the governing equations may be appropriate. Other typical assumptions used to simplify the governing equations include hydrostatic pressure, negligible rates of dissipation and radiation and negligible density differences except in gravity terms (Boussinesq approximation). Turbulent transport of heat and momentum is usually parameterized in the form of vertical eddy transport coefficients which, as with single point boundary layer models, can be specified as a function of height and stability. Circulation is driven by specifying the distribution of synoptic scale velocity on lateral and upper boundaries and the distribution of temperature on the surface.

Assessment

Coastal wind models have been able to simulate many of the observed features of coastal winds such as the diurnal variation of wind speed and direction, the location of sea breeze fronts, and differences between inland and offshore wind speed. However, a major obstacle to the use of these models in routine oil spill trajectory simulation is their cost. A practical solution might be obtained by simulating the circulation patterns for a range of representative synoptic scale situations as determined by observations. As an example, Lyons (1972) has shown that properties of the Chicago Lake breeze, and in particular a criterion for its full development, is strongly dependent on the value of the parameter $\psi(\theta) \frac{G^2}{c_p \Delta T}$ where G is geostrophic wind speed, ΔT is the difference between the maximum air temperature at an inland station and a mean water temperature, c_p is the specific heat of air at constant pressure, and ψ is a dimensionless function of the angle θ between the shoreline and the geostrophic wind vector. Thus simulations using various values of $\frac{G^2}{c_p \Delta T}$ and θ could be made and actual winds could be determined by scaling and interpolating in accordance with the values of G and θ.

2.3   Measured or Stochastically Derived Wind Fields

In this section various methods of utilizing wind measurements are suggested starting with simple formulations of the wind field (e.g. constant in space and time) and continuing to more complex formulations involving spatial and temporal variations.

2.3.1   Models with Constant Wind Fields

The simplest assumption regarding the wind field is that it is constant. As indicated in Figure 2.1.1, this approximation is only valid physically if the time and space scales of the problem are short, as would be the case for a spill near shore. However, this assumption can be used to provide crude comparisons between potential spill sites or to yield conservative estimates of risk in situations where the assumption is not really valid.

Values for the constant wind velocity can be obtained from horizontal wind measurements taken near the site of interest and summarized in the form of statistics such as wind roses, tables of wind speed and direction versus frequency, etc. An assumption regarding the vertical profile of velocities (see preceding section) can be used to estimate velocities at one elevation from measured velocities at another elevation. Similarly, any information relating wind speed and direction in the area of interest with that at the measurement station should be used. This is especially true when measurements are taken from inland stations because ocean winds are often substantially greater than corresponding inland winds. The relationship between measured and modeled winds can be obtained either from empirical relationships (e.g. Godshall and Jalickee, 1976) or from the output of a numerical model (e.g. Kindle et al. 1976).

For probability assessments, information regarding the probability of wind events is necessary. Because wind velocity is a vector, enough information should be obtained to approximate the joint probability distribution of the vector components ($|\vec{W}|$ and θ or W_x and W_y), and if there is significant seasonal variation in wind behavior, different distributions should be considered for different seasons of the year. A characteristic wind velocity can then be obtained by finding the mean of the joint distribution, or probabilistic values can be obtained by using repeated samples from the distribution. In the latter regard, analytical probability distribution functions, such as the elliptical bi-variate normal distribution for the two wind components (Crutcher and Baer, 1962), the log-normal distribution for wind speeds (Benjamin and Cornell, 1970) and the type II distribution of largest values for extreme wind speeds (Thom, 1960) have often been used.

2.3.2 Time Dependent Models

The assumption of a constant wind field is usually not warranted and therefore it is not surprising that the majority of oil transport models examined in Chapter 5 specify some sort of time dependence for their wind field. This time dependence is usually ascertained through time series measurements, frequently at a single point, either by using the measured data directly or by generating synthetic time series with similar statistics. Alternatively, the statistics of observed data may be used directly as input to a simple determination of the wind drift.

In determining the time dependence of simulated winds, periodic

components such as seasonal or diurnal variations are often considered separately. By identifying these components first (eg. by harmonic analysis), the remaining (stochastic) components can often be considered stationary which is desirable from the statistical point of view.

The stochastic component is usually represented by a time series of synthetic values generated at discrete time intervals often corresponding to time steps used in the oil transport model. The objective is to match the statistical properties of the synthetic sequence with the statistical properties found in historical sequences. The statistical properties of most interest include the lower order moments of the probability distribution (mean, variance, covariances, etc.) and parameters describing the correlation structure.

The time dependence is often expressed using some sort of autoregression model. The principle behind this type of time series model is that the present value of a process depends in part on previous values of the process, through regression coefficients, and in part on random, uncorrelated perturbations.

Models with no Correlation Between Time Steps

The simplest type of this model assumes that all of the variation between successive time steps is due to random perturbations. For two components, $W_1(t)$ and $W_2(t)$, this may be written

$$W_1(t) = a_1 + e_1(t)$$

$$W_2(t) = a_2 + e_2(t) \tag{2.3.1}$$

in which a_1 and a_2 are the component means and e_1 and e_2 are the random components (zero mean). As in the case of the constant wind field, these parameters can be sampled from the probability distribution of $W(t)$.

Because of its simplicity, this formulation is often used in connection with "random walk" models of advection by assuming that a component of the drift at each time interval is proportional to the (random) wind speed during that interval. The random walk model can then be used in Monte Carlo simulations which allow a number of trajectories to be "tracked" simultaneously (see eg., Tayfun and Wang, 1973). The random walk model is illustrated by a simple formulation in which the drift is proportional to the wind speed through a wind drift factor K_w. After N time steps (elapsed time, $T = N\Delta t$), the mean displacement in each direction and the variance of the displacements about their mean position are

$$\overline{X_{iT}} = K_w \sum_{n=1}^{N} \overline{W_{in}(t)}\Delta t = N K_w a_i \Delta t = K_w a_i T \qquad (2.3.2)$$

$$\overline{X_{iT}^2} = \overline{(K_w \sum_{n=1}^{N} W_{in}(t) \Delta t)^2} - \overline{X_{iT}}^2 = N K_w^2 \Delta t^2 \lambda_i^2 = K_w^2 \lambda_i^2 T\Delta t \qquad (2.3.3)$$

in which λ_i^2 is the variance of each of the random components $e_i(t)$.

A major failing of this simple structure is that the dispersion in the predicted trajectories varies with the size of the time step; to obtain realistic dispersion the time step must be fixed in relation to the integral time scale of observed wind records. This time scale is a measure of the persistence of the wind, as characterized by the auto-correlation function, and is of the order of a day. Unfortunately the time step used in oil transport models is often dictated by other

considerations, such as the rate of change of current speed, and is generally smaller than the integral time scale. It is therefore inappropriate to use models with uncorrelated time steps unless either 1) the random component is small in comparison with the mean (i.e., the time dependence is weak and can be ignored) or 2) values of wind speed are generated at appropriate time steps and are "disaggregated" into shorter time steps which are consistent with model requirements.

First Order Autoregressive Models

A first order or lag-one autoregressive model (Markov model) provides more realistic time structure by allowing the components at time t to be functions of the components at time t-1 in a form such as

$$W_1(t) = a_1 + b_{11}W_1(t-1) + b_{12}W_2(t-1) + e_1(t)$$

$$\text{(2.3.4)}$$

$$W_2(t) = a_2 + b_{21}W_1(t-1) + b_{22}W_2(t-1) + e_2(t)$$

A bi-variate model of this type was used by Shukla and Stark (1974) to enable them to generate synthetic wind components which have similar means, variances and serial and cross correlations as those found in observed wind components. Sometimes the two vector components are considered to be independent in which case the above regression equations can be split into two univariate autoregressive models without the coupling terms b_{12} and b_{21}; the remaining coefficients b_{11} and b_{22} can then be related directly to the autocorrelation function for each component which is of the form $\rho_i(n\Delta t) = b_{ii}^n$.

Simple expressions, analogous to those derived for the random walk process, can be used to estimate the mean and variance due to wind drift from a first order process. Taylor (1921) showed that after N steps of a process having correlation function b_{ii}^{n}

$$\overline{X_{iT}} = K_w \frac{a_i}{1-b_{ii}} T \qquad\qquad (2.3.5)$$

$$\overline{X_{iT}^2} = K_w^2 \frac{\lambda_i^2}{1-b_{ii}^2} \left\{ \frac{1 + b_{ii}}{1 - b_{ii}} \Delta t \, T - \frac{2b_{ii}(1-b_{ii}^{N})}{(1-b_{ii})^2} \Delta t^2 \right\} \qquad (2.3.6)$$

where $\frac{a_i}{1-b_{ii}}$ is the mean and $\frac{\lambda_i^2}{1-b_{ii}^2}$ is the variance of the component $W_i(t)$. Unlike the simple random process, this process has the desirable feature that $\overline{X_{iT}^2}$ approaches a constant as Δt approaches zero.

If the components $W_i(t)$ are thought of as belonging to discrete states, rather than being continuously distributed, then it is not necessary to calculate the parameters of the Markov model directly. Instead a transitional-probability matrix may be generated to assign values to the probability of the process being in a certain discrete state at time t given that it is in another discrete state at time t-1. For instance wind velocities might be discretized into 80 states consisting of 10 intervals of wind speed ranging from zero to infinity and 8 intervals of direction ranging from 0 to 360°. Hourly wind measurements could then be used to construct an 80 x 80 transitional-probability matrix relating the state at time t-1 to the state at time t. The sequence can be initialized by either selecting a known wind state at t=0 or selecting a mean state using the transition matrix. Examples of the use of transition matrices

include two of the models which are reviewed in Chapter 5. The model by Stewart, Devanney and Briggs (1974) used wind data at three-hour intervals to generate transition matrices at a number of sites. The other model, Williams, Hann and James (1975), used the technique to fill in gaps in historical wind data.

Just as models for continuous data require sufficient data to evaluate model parameters, discrete-state models require substantial data for generating transition matrices. In the absence of sufficient data, the size of the intervals may need to be increased or the joint probabilistic structure of the matrix may need to be sacrificed. For instance, in both of the models mentioned above, the authors assumed that the wind direction at time t+1 was correlated with the direction at time t but that the wind speed was a function of only the calculated direction at time t+1.

The adequacy of a simple discrete-state Markov model was examined by Stewart (1973) who compared predicted wind drift using a three-hour lag-one Markov model (nine states for wind direction; a mean wind speed assumed for each direction) with calculations based directly on wind measurements taken on Nantucket Island. He found that for a range of times the observed standard deviations in wind drift (calculated from the data by assuming a constant wind drift factor) were within 10% of the values predicted by the preceding equation for $\overline{X_{iT}^2}$. (Values of b_{ii} used in this calculation were fit to the correlation functions generated by the Markov model.)

Techniques which Preserve Longer Memory

Although the first order Markov process is a considerable improvement over a random walk model, its "memory" is limited by that information which is embodied in the first order autoregression coefficient, and some of the longer time structure, particularly that associated with systematic variations in weather patterns, may be overlooked.

One possibility for incorporating additional "memory" is to utilize a discrete-state Markov model in which the state definition is associated with identifiable features of the weather (high or low pressure system, direction of propagation, etc.). Another possibility is to allow the generated wind components to be functions of lags greater than one. For instance, Tayfun and Wang (1973) treat wind speed and direction as two independent time series using 4th-order univariate autoregressive models. The more realistic behavior of their 4th-order model, compared with their random walk analogy, is clearly shown. In principle any number of lags may be chosen. For instance, an nth order regressive model might be written to preserve statistics relating to serial and cross correlations up to lag-n. For large values of n, however, the process becomes cumbersome, the reliability of the estimates of the coefficients decreases and other techniques are more appropriate.

Several investigators, notably those in hydrology, have endeavored to formulate models which preserve the effects of long-term memory without requiring numerous parameters. These include models of Fractional Gaussian Noise (Mandelbrot, 1971), the autoregressive integrated moving average, ARIMA, model (Box and Jenkins, 1970) and the Broken Line Model

(Hino, 1967; Ditlevsen, 1971; and Mehia et al., 1974). Although none of
these models has been used in the prediction of oil transport, their
ability to handle more complicated time structure, such as extreme events,
runs, and the long-term effect known as the Hurst phenomenon (Hurst, 1951)
may justify their use in the future.

Direct Use of Time Series Statistics

In cases where oil drift is computed as a fraction of wind speed it
is possible to avoid the generation of wind data directly and rely instead
on statistics derived from wind measurements to infer statistics concern-
ing oil slick trajectories. For instance the mean and variance of spill
positions can be estimated from Equations (2.3.5-2.3.6) by calculating the
mean, variance and first order autocorrelation coefficient of the wind
components.

Or the method of Hay-Pasquill (1959) might be considered. Although
this technique has been used mostly in atmospheric diffusion calculations
(Csanady, 1973) it could be applied to oil transport as a surrogate for
Equation (2.3.6). With this technique the displacement in direction i
of an oil slick during time T may be written

$$X_{iT}(T) = K_w T \ W_{iT} \tag{2.3.7}$$

where W_{iT} is the average component velocity during the interval,

$$W_{iT} = \frac{1}{T} \int_{t_o}^{t_o + T} W_i dt \tag{2.3.8}$$

and K_w is the wind drift factor.

For air pollution calculations a major distinction is made between the Lagrangian motion which advects particles and the Eulerian motion which can be measured by a fixed anemometer. W_i is thus the Eulerian velocity and a factor β (typically about 4) multiplies the right hand side of Equation (2.3.8). Because the ratio of oil drift to wind speed is small ($K_w \sim .03$) the oil responds more to Eulerian fluctuations than Lagrangian fluctuations and the factor β is not needed. The variance of the slick position can now be written

$$\overline{X_{iT}^2} = K_w^2 T^2 \overline{W_{iT}^2} - \overline{X_{iT}}^2 \qquad (2.3.9)$$

where the overbar refers to a time average over a period which is much greater than T. The variance at time T thus represents the mean square value of a moving average process formed from the time series W_i by averaging over period T. In order to avoid long averaging times this technique would be most useful for analyzing transport near shore and determining, for instance, the distribution of locations along a shoreline at which a slick might be expected to arrive.

2.3.3 Models with Spatially Dependent Wind Fields

It is more difficult to model spatial dependence than it is to model time dependence. One reason for this is the lack of data. A related problem is that the data which is available is frequently from land based stations so that differences between onshore and offshore winds must be considered. Finally, if data comes from different sources, data management can become tedious. Because of these considerations, most oil transport models do not treat spatial variations or they treat them in a simple way. Nonetheless, given sufficient measurements or statistics based on measurements, a number of interpolation or synthetic data generation techniques exist whereby spatially varying wind fields can be formed.

The simplest, and historically the earliest, technique for interpolation involves fitting polynomials or periodic functions to measured data. The technique can be used by itself or it can be used to remove spatial trends prior to further analysis. In general the interpolation would proceed in two dimensions but because of limited data and the fact that for coastal areas offshore gradients are considerably stronger than alongshore gradients, it is appropriate to treat the wind as a function of only the offshore component of position. As an example of a limiting case involving data at two points, Williams et al. (1975) used piecewise linear interpolation to combine data from an offshore station and an inland station to account for sea breeze effects in their model of oil transport in the Gulf of Mexico.

With more data, a more standard procedure is "optimal linear interpolation". The framework for this approach was presented by Gandin (1965)

and involves estimating the value of a variable at a given location as the weighted sum of measured values at surrounding points. The weights are functions of (previously derived) correlations among the measuring stations and between the measuring stations and the point(s) of interest and are determined by minimizing the expected mean square error between measured and interpolated values. By determining both space and time correlations, data from previous time periods (and future time periods when considering hindcasting) can be utilized to analyze winds in a moving weather system. Similarly, by determining the appropriate cross-correlations the technique can be extended to multivariate applications. Thus other meteorological variables such as pressure can be used to analyze the wind field, or by assuming a horizontally non-divergent wind field, measurements of the independent components W_x and W_y can be combined to derive a distribution for the stream-function, which in turn, can be differentiated to provide fields for W_x and W_y. Several types of interpolation schemes have been compared with measured winds off of the Atlantic Coast in a recent study by Mooers, Fernandez-Partagas and Price (1976).

Measured data can also be used to "update" or "correct" a preliminary estimate of the field of interest. Pressure maps are routinely analyzed this way by obtaining their preliminary estimate from numerical models. However, the estimate could also be obtained by a simple extrapolation from a previous analysis or by simpler dynamic models such as one assuming geostrophic balance.

The correlations required for optimal interpolation of a variable can also be used as the basis for generating synthetic fields of that variable. The correlations are used to construct a spectral density

function which can then be sampled randomly. Each sample represents a

periodic function (e.g., sine wave) of given amplitude, frequency and

phase and their superposition results in the desired field. The procedure

has been used in a number of univariate applications such as the spatial

distribution of rainfall (Mejia and Rodriguez-Iturbe, 1973) or ocean

waves (Borgman, 1969) but it can be used as well in multivariate applica-

tions (see, e.g., Shinozuka and Jan, 1972) such as the distribution of

velocity components. Because these techniques require large quantities

of reliable data, as well as considerable computational effort, however,

it is doubtful that they are presently of much use for oil trajectory

analysis.

2.4   Conclusions

The following conclusions regarding the adequacy of wind field modeling can be drawn from the presentation in this chapter.

1. Wind fields are most easily determined either from wind observations (by using actual measurements or synthetic winds derived from measurements) or from analysis of synoptic pressure fields. Most oil slick transport models use the first approach because it involves wind measurements directly and is thus more appropriate for probabilistic assessments. Disadvantages with this approach include uncertainty regarding the extrapolation of winds from measuring stations (especially inland stations) and the difficulty in modeling spatial variability. Use of pressure fields can provide spatial detail in areas of sparse measurements and has advantages for forecasting purposes since pressure maps are routinely output by numerical weather prediction. However, the approach depends on a correlation between local and synoptic scale motion and may be inaccurate in regions of sea breeze influence or during periods of rapid weather change.

2. Although oil slick models frequently require wind data to be input in space and time, spatially varying wind fields are seldom used or they are used in a simple manner (e.g., by using a weighted average of onshore and offshore observations). The consequences of this representation are most severe in the coastal region extending about 30 kms offshore where dramatically differing winds may be present over a short distance. Farther offshore, time variations are more important than spatial variations and the assumption of spatially uniform winds is probably adequate.

3. Winds in the coastal region are very difficult to model. The
region represents a transition between continental and maritime climates
and exhibits substantial local behavior which is hard to identify with
synoptic scale (wind or pressure) measurements. Dynamic coastal wind
models which include sufficient detail to adequately resolve the flow
field are too expensive to be used for long time series. However, if
they are used in conjunction with observations and empirical forecasting
techniques, they can provide a practical improvement over the direct use
of wind measurements.

4. If wind records are available near a site, their duration is
usually long enough (often 10 years or more) and frequency high enough
(usually hourly or three-hourly) to adequately characterize the time
structure of the wind. This raises the question of whether or not
stochastic time series models, whose parameters can be no better than the
historical data from which they are derived, need to be used for routine
predictions. Synthetic time series are typically generated when there is
insufficient historical data or where extremely long simulations are
needed. Yet the probabilistic studies by CEQ (Steward, Devanney and
Briggs, 1974) and Tayfun and Wang (1973), for instance, perform simula-
tions using fewer runs than could have been generated by using historical
data.

5. If the time structure is modeled stochastically, a first order
model for the autocorrelation is sufficient to characterize the distribu-
tion of slick trajectories due to wind drift (i.e., to determine $\overline{X_{iT}}$,
$\overline{X_{iT}^2}$). This is because measurement errors, and errors associated with

converting wind velocity to oil drift, are generally greater than errors in representing the short term time structure. (Compare, for instance, Stewart's report of a 10% error in predicted oil slick displacement, based on a simple lag-one Markov model, with the variation in wind drift factors presented in Chapter 3.) However, in other applications, such as simulation of extreme wind speeds or the modeling of persistence of a given wind event, models based only on first order statistics may not be adequate and the application of one of the techniques described in Section 2.3.2 is suggested.

CHAPTER 3

ADVECTION OF OIL SLICKS BY WAVES AND CURRENTS

When an oil spill occurs at a large distance offshore the detailed mechanics of the initial spreading of the oil is of minor importance in assessing the possible impact of the oil spill on the shoreline. Assuming therefore that an oil spill results in a thin oil slick covering part of the ocean surface, the problem becomes that of predicting or simulating the movement of this oil slick.

The present part of the report identifies two possible mechanisms for the advection of oil slicks in the coastal environment. These mechanisms are waves and currents and each is discussed separately (Section 3.1 on Waves, Section 3.2 on Currents). The presentation is centered around an examination of our current understanding of and ability to quantify the advection of an oil slick by either waves or currents. The discussion is therefore primarily a critical review of the state of the art of the mathematical modeling of the physical processes contributing to the advection of oil slicks in the coastal environment. These models will form the basis for any simulation technique to be used in assessing the impact of oil spills in a given area and the importance of a thorough evaluation of the strengths and weaknesses of these basic mathematical models can therefore hardly be overemphasized. Finally, Section 3.3 presents a critical review of some of the laboratory and field studies performed leading to a determination of the wind factor, i.e., the ratio of surface velocity to wind velocity, which enjoys much popularity in studies of advection of oil slicks.

3.1 Advection of Oil Slicks By Waves

Linear, first order wave theory for periodic progressive waves in an inviscid fluid of constant depth predicts a sinusoidal surface profile, η, measured from the still water level

$$\eta = a \cos(kx-\omega t) \qquad (3.1.1)$$

in which a is the wave amplitude, $k = 2\pi/L$ is the wave number and $\omega = 2\pi/T$ is the radian frequency of the monochromatic wave motion. The wave number and the radian frequency are related to the water depth, h, through the dispersion relationship

$$\omega^2 = k\ g\ \tanh\ kh \qquad (3.1.2)$$

in which g is the acceleration due to gravity. According to linear wave theory, whose detailed derivation may be found in Eagleson and Dean (1966), individual water particles move in closed orbits, i.e., there is no net movement of water associated with a wave motion to this order of approximation.

Upon carrying out the analysis for periodic progressive waves to second order, Stokes (1847) found that the particle orbits no longer were closed. After one wave period individual water particles do not return to their original location, which indicates that a net drift, a mass transport, is associated with a wave motion when nonlinear effects are considered. For an inviscid fluid Stokes found the mass transport to be given by

$$\bar{U} = \omega k a^2 \frac{\cosh 2k(z+h)}{2 \sinh^2 kh} + C \qquad (3.1.3)$$

in which z is the vertical coordinate (positive upwards and zero in the still
water level) and C is an arbitrary superimposed current of small magnitude.
In general the magnitude of the current C is not readily predicted.
However, for two-dimensional plane waves, as assumed here, in a closed flume
there can be no net transport of water in the direction of propagation.
Thus, by integrating Eq. (3.1.3) over the depth and requiring that $\int_{-h}^{0} \bar{U} \, dz = 0$,
the mass transport velocity profile

$$\bar{U} = \omega k a^2 \left(\frac{\cosh 2k(z+h)}{2 \sinh^2 kh} - \frac{\coth kh}{2kh} \right) \qquad (3.1.4)$$

results.

From Stokes' solution the value of the mass transport velocity at
the free surface, z = 0, is found to be

$$\bar{U}_s = \omega k a^2 \left(\frac{\cosh 2kh}{2\sinh^2 kh} - \frac{\coth kh}{2kh} \right) \qquad (3.1.5)$$

which is always positive, i.e., in the direction of wave propagation. The
value of the gradient of the mass transport velocity at the surface is
found from Eq. (3.1.4) to be

$$\left(\frac{\partial \bar{U}}{\partial z} \right)_s = 2\omega k^2 a^2 \coth kh \qquad (3.1.6)$$

Although not of primary importance in the present context of oil slick advection, Eq. (3.1.4) predicts a mass transport velocity near the bottom, $z = -h$,

$$\overline{U}_b = \omega ka^2 \left(\frac{1}{2 \sinh^2 kh} - \frac{\coth kh}{2 kh} \right) \qquad (3.1.7)$$

which may be shown always to be negative.

Early attempts at experimental verification of Stokes' mass transport velocity profile consistently showed that the near-bottom drift was in the direction of wave propagation, i.e., in the direction opposite that predicted by Stokes. Longuet-Higgins (1953) re-examined the problem of wave induced mass transport accounting for real fluid effects by assuming a viscous fluid and laminar flow. By considering the viscous effects within a thin bottom boundary layer and a thin surface boundary layer, with the condition of zero shear stress imposed on the free surface, Longuet-Higgins found the mass transport velocity in the core to be given by

$$\overline{U} = \frac{\omega ka^2}{2 \sinh^2 kh} \{\cosh 2k(z+h) + \frac{3}{2}$$

$$+ \frac{3}{4} \left(\frac{\sinh 2kh}{2kh} + 3 \right) \left[\left(\frac{z}{h} \right)^2 - 1 \right]$$

$$+ \frac{1}{2} kh \sinh 2kh \left[1 + 4 \frac{z}{h} + 3 \left(\frac{z}{h} \right)^2 \right] \} \qquad (3.1.8)$$

This solution shows that the near-bottom ($z = -h$) mass transport velocity

$$U_b = \frac{5}{4} \frac{\omega k a^2}{\sinh^2 kh} \qquad\qquad (3.1.9)$$

is always positive, i.e., in the direction of wave propagation and

therefore in qualitative agreement with observations. Subsequent experi-

mental investigations by Russell and Osorio (1958) and by Collins (1963)

show excellent agreement with the prediction afforded by Eq. (3.1.9) so

long as the flow in the bottom boundary layer remains laminar.

The experiments by Russell and Osorio (1958) also confirmed the

detailed velocity distribution given by Eq. (3.1.8). However, this con-

firmation of Longuet-Higgins' theory was for a limited range of kh

(0.7 < kh < 1.5). For kh outside this range, i.e., for either relatively

long or relatively short waves, poor agreement between theory and experiments

was obtained. In particular, the predicted drift near the surface was

found experimentally to be much smaller than predicted by Eq. (3.1.8).

From Eq. (3.1.8) the surface drift is found to be

$$\overline{U}_s = \frac{\omega k a^2}{2 \sinh^2 kh} (\cosh 2kh - \frac{3}{4} - \frac{3}{4} \frac{\sinh 2kh}{2kh} + \frac{1}{2} kh \sinh 2kh) \qquad (3.1.10)$$

which is positive for shorter waves but turns negative for longer waves.

A comparison between the mass transport velocity predicted by Stokes

(eq. 3.1.4) and by Longuet-Higgins (Eq.3.1.8) is shown for relatively long

and relatively short waves in Figs. 3.1.1 and 3.1.2 respectively. In

both figures a substantial difference in the mass transport velocity pro-

file is noted. For relatively short waves (Fig. 3.1.2) it is seen that

Longuet-Higgins' solution predicts a substantially larger drift near the

surface. In fact, Eq. (3.1.10) may be seen to have the limit for large kh
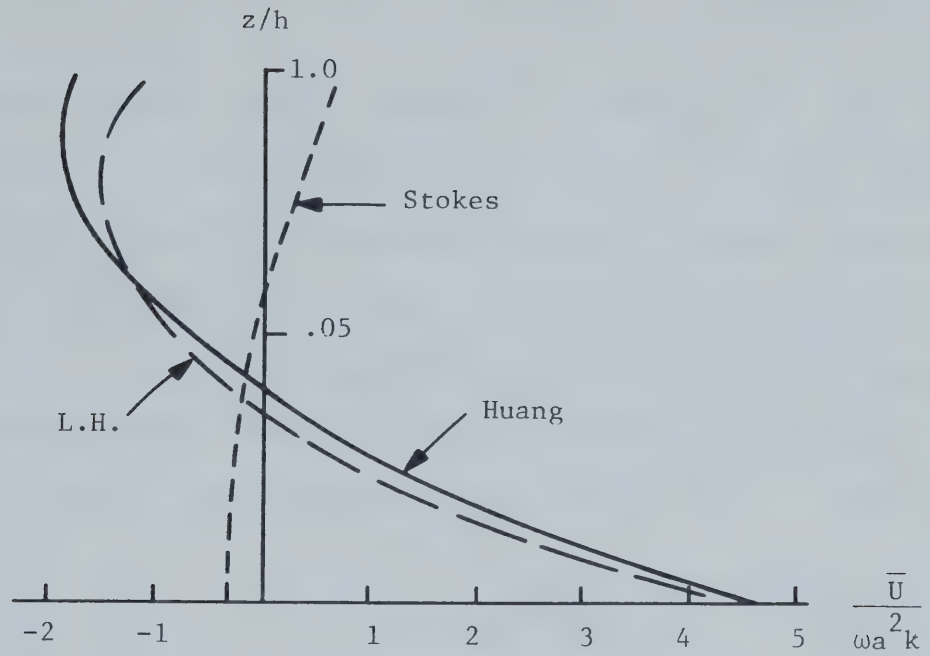
Figure 3.1.1   Mass Transport Velocity Profile for kh = 0.5.
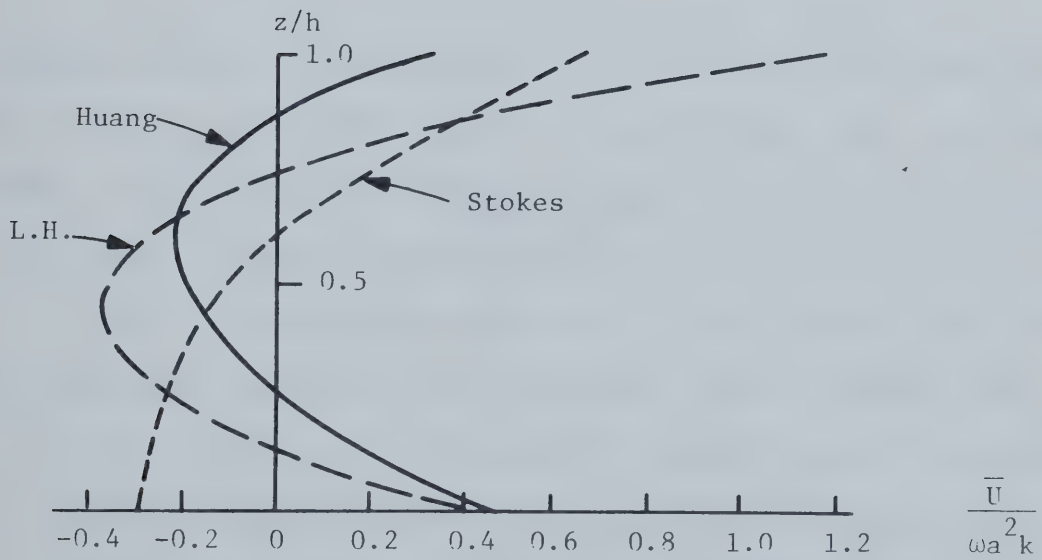
Figure 3.1.2   Mass Transport Velocity Profiles for kh = 1.25

$$\overline{U}_s \rightarrow \omega k a^2 \frac{kh}{2} \quad \text{as} \quad kh \rightarrow \infty \tag{3.1.11}$$

which clearly is unbounded. In contrast, Stokes' solution shows $\overline{U}_s \rightarrow \omega k a^2$ as $kh \rightarrow \infty$, i.e., it remains finite. As seen in Fig. 3.1.3 the experimental results by Russell and Osorio (1958) indicate the surface drift predicted by Stokes' inviscid theory to be superior to the predictions of Longuet-Higgins' viscous solution for $kh \rightarrow \infty$.

From Eq. (3.1.8) the gradient of the mass transport velocity at the outer edge, $z = -\delta_s$, of the surface boundary layer is found to be

$$\left(\frac{\partial \overline{U}}{\partial z}\right)_{z = -\delta_s} = 4\omega k^2 a^2 \coth kh \tag{3.1.12}$$

By comparison with Eq. (3.1.6) it is seen that the "surface" gradient predicted by the viscous solution is twice that predicted by the inviscid solution.

The rather disturbing feature of Longuet-Higgins' viscous solution in the deep water limit was addressed by Huang (1970), whose results raise doubt about the correctness of Longuet-Higgins' solution. Huang's (1970) analysis led to a result similar to that of Longuet-Higgins except that the terms in Eqs. (3.1.8) and (3.1.10) which blow up as $kh \rightarrow \infty$ were absent. Thus, Huang's solution approaches that of Stokes in the deep water limit and that of Longuet-Higgins in the shallow water limit. Unluata and Mei (1970) in re-deriving the results of Longuet-Higgins (1953), however, point out that Huang (1970) adopted an improper free surface boundary condition in his analysis. The correctness of Huang's (1970) analysis is therefore in serious doubt and Longuet-Higgins' solution,
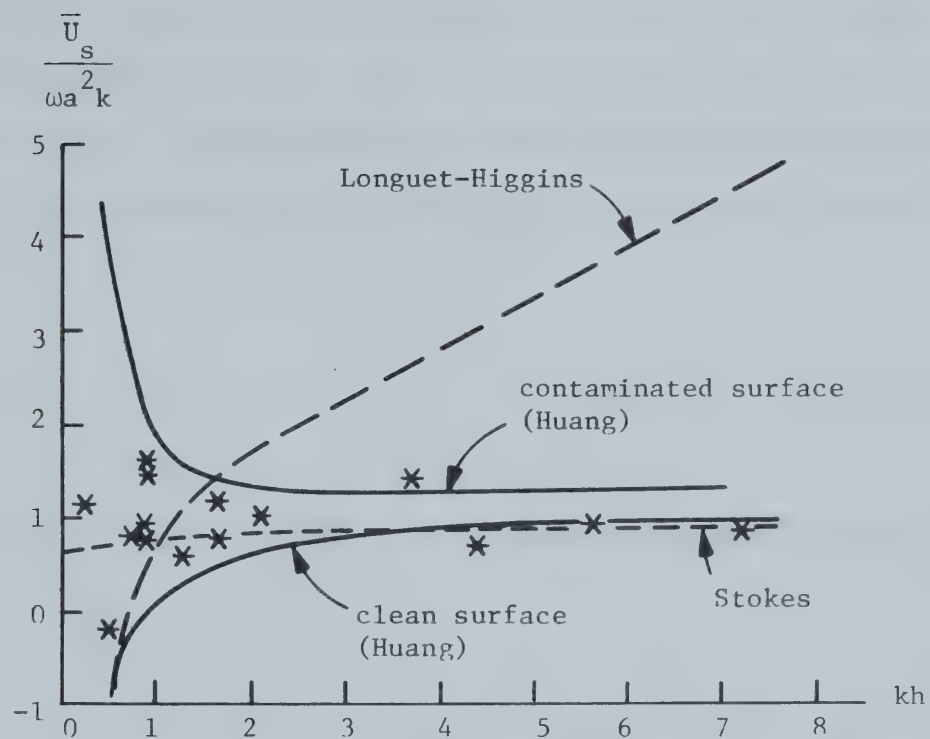
Figure 3.1.3   Surface Drift Velocities * Indicate
            Experimental Observations by Russell
            and Osorio.

although peculiar in the deep water limit, must be considered mathematically correct although physically unrealistic. In spite of this Huang's solution is presented in Figs. 3.1.1, 3.1.2 and 3.1.3 for comparison.

The models for wave induced surface drift discussed up to this point have all been for monochromatic waves with a free surface boundary condition of zero shear stress being imposed on the solution. Chang (1969) extended the solution to include the effect of random waves. For two dimensional, i.e., plane, waves in deep water with an amplitude spectrum, $S(\omega)$, defined by

$$<\eta^2(t)> = 2 \int_0^\infty S(\omega)\,d\omega \qquad (3.1.13)$$

Chang analyzed the wave induced surface drift and found its expected value to be

$$<\overline{U}_s> = 4 \int_0^\infty \frac{\omega^3}{g} S(\omega)\,d\omega \qquad (3.1.14)$$

Chang's analysis was performed for an inviscid as well as for a viscous fluid. In both cases Eq. (3.1.14) was found to hold. Per definition $4\,S(\omega_o)\,d\omega$ is equal to a^2 for a monochromatic wave of frequency ω_o. Thus, Eq. (3.1.14) is seen to reduce to Stokes' solution for deep water regardless of whether the fluid is assumed inviscid or not. The fact that Chang's solution does not reduce to Longuet-Higgins' solution for a monochromatic wave indicates that her solution for a viscous fluid is in error. She did, however, find that the gradient of the mass transport velocity near the surface was given by

$$\left\langle \left(\frac{\partial U}{\partial z} \right)_{z=-\delta_s} \right\rangle = 16 \int_0^\infty \frac{\omega^5}{g^2} S(\omega) d\omega \qquad (3.1.15)$$

for a viscous fluid. This result, which is twice the value obtained for an inviscid fluid, is in agreement with the results obtained for monochromatic waves (Eqs. 3.1.6 and 3.1.12).

Unluata and Mei (1970) generalized Chang's (1969) analysis to include all values of kh. They found, for example, that the expected value of the surface drift was given by

$$\langle \overline{U}_s \rangle = 4 \int_0^\infty \omega k \, H_s(k) \, S(\omega) d\omega \qquad (3.1.16)$$

in which

$$H_s(k) = \frac{\overline{U}_s}{\omega k a^2} \qquad (3.1.17)$$

with $\overline{U}_s$ given by Eq. (3.1.5) for an inviscid fluid and by Eq. (3.1.10) when viscosity is accounted for. To perform the integration indicated by Eq. (3.1.16) the wave number, k, is replaced by a function of the radian frequency, ω, through the use of the dispersion relationship, Eq. (3.1.2). This integration is quite tedious in the general case, but may readily be performed in the deep or shallow water limits, for which the dispersion relationship simplifies considerably.

The preceding discussion has assumed plane, i.e., long crested waves all propagating in the same direction. In ocean waves not all the wave energy propagates in one direction. The distribution of wave energy with direction of propagation may be accounted for by considering

the two-dimensional wave spectrum, the directional spectrum, $S(\omega,\theta)$ defined by

$$\langle \eta^2(t) \rangle = 2 \int_0^\infty d\omega \int_{-\pi}^{\pi} S(\omega,\theta)d\theta \qquad (3,1.18)$$

in which θ is the angle from a fixed direction indicating the direction of propagation. By comparison with Eq. (3.1.13) it is seen that the one-dimensional spectrum is related to the directional spectrum through

$$S(\omega) = \int_{-\pi}^{\pi} S(\omega,\theta)d\theta \qquad (3.1.19)$$

For a wave field specified by its directional spectrum, with being measured from a fixed direction, say from the x-axis, the expected value of the wave induced surface drift becomes a vector quantity, whose components in the x and y directions may be determined from Eq. (3.1.16)

$$\langle \overline{U}_{s,x} \rangle = 4 \int_0^\infty d\omega \{ \omega k H_s(k) \int_{-\pi}^{\pi} \cos\theta \, S(\omega,\theta)d\theta \}$$

$$\qquad (3.1.20)$$

$$\langle \overline{U}_{s,y} \rangle = 4 \int_0^\infty d\omega \{ \omega k H_s(k) \int_{-\pi}^{\pi} \sin\theta \, S(\omega,\theta)d\theta \}$$

The solutions for the mass transport velocity presented so far, with Eq. (3.1.20) being the most general, have been based on an assumption of zero shear stress on the free surface and the possible effects of a thin oil film covering the surface have not been taken into account. For Stokes'

solution the assumption of zero surface shear stress is, of course, consistent with the assumption of an inviscid fluid. The effect of a surface film would appear in Stokes' solution only if this surface film acted as a surface tension effect since a slip velocity between the surface film and the underlying water is allowable for an inviscid solution. An inviscid solution would therefore yield no information about the speed of advection of a thin surface film caused by a wave motion. Only if one argues that there, on the average, can be no slip between an oil film and the underlying fluid can the surface drift velocity predicted by Stokes' solution be taken as an estimate of the speed of advection of an oil slick caused by waves. As discussed in Section 3.1.2 Milgram (1977) has developed a theory which shows the result of the preceding argument to hold in deep water.

For the type of solution for the wave induced mass transport velocity given by Longuet-Higgins, i.e., assuming a viscous fluid, the presence of a thin, highly viscous surface film should be included in the analysis for this to be realistic. Phillips (1966) discusses briefly the first order effects of including the effects of a highly viscous surface film. Phillips (1966) assumes the thin surface film to be "incompressible to tangential shear." It is presently not clear whether or not this assumption is justified for a very thin oil film, but it essentially amounts to regarding the surface film as a thin, highly flexible, plastic sheet. With the above assumption, Phillips (1966) outlines the first order solution for the surface boundary layer with the additional assumption that the surface film is not moving, i.e., zero advection. Since the condition of zero advection of the surface film is imposed on the solution, Phillips'

solution, which was carried out to second order by Huang (1970), is of
limited interest in the present context of determining the speed of advec-
tion caused by waves. As anticipated by Phillips (1966) the solution by
Huang (1970) shows a mass transport velocity outside the surface boundary
layer similar to the induced streaming near a solid bottom, Eq. (3.1.9).
Although of limited interest in the present context the solutions by Phillips
(1966) and Huang (1970) indicate the extreme importance of considering the
surface boundary condition imposed by a viscous surface film when solving
the viscous problem of wave induced mass transport velocity. To emphasize
this Huang's (1970) solution is shown in Fig. 3.1.3. A more realistic
analysis would result if the viscous surface film was assumed to move at
a certain velocity, which would be determined by imposing the condition
that the time average shear stress acting on the film should be zero.
Such a solution, which would correspond to a zero surface shear stress
assumption, has to our knowledge not been attempted. Until a solution for
the advection of oil slicks by waves along this line has been obtained,
it would be nonsensical to adopt the surface drift obtained from a
viscous solution as representing the speed of advection of an oil slick.

3.1.1 Prediction of Advection of Oil Slicks by Waves

As mentioned at the end of the previous section a more realistic
analysis of the advection of an oil slick by waves is called for before it
would make sense to include this effect in a predictive model for oil slick
trajectories. This is certainly true for the results obtained based on an
assumption of a viscous fluid for which the inadequacy of the present state
of the art was evident. The viscous solution for a clean surface has received

only limited experimental confirmation (for intermediate values of kh) and leads to unrealistic results for deep water waves. A viscous model which properly accounts for the influence of a thin surface film must be developed before such a model should even be considered as the basis for predicting oil slick trajectories.

For relatively deep water Stokes' inviscid solution has some experimental support (Fig.3.1.3)and may, based on the heuristic argument of no slip on the average between oil film and the underlying water, be used to examine in quantitative terms the possible advection of oil slicks by waves. It is emphasized that the following discussion is for illustrative purposes and relies on this unsubstantiated "no average slip" condition, i.e., a prediction of the Stokes' surface drift is assumed to be identical to the prediction of the speed of advection of an oil slick by waves.

To predict the Stokes surface drift we must, of course, be able to predict the characteristics of the wind generated waves from knowledge of the wind field at an elevation of, say, 10 meters above the still water level. The simplest wave forecasting relationships are those developed by Sverdrup and Munk and later modified by Bretschneider (SMB-method) which in their latest forms are presented in the Shore Protection Manual (1973), SPM73. An alternative method is that of Pierson, Neuman and James (PNJ-method) also described in SPM73. These forecasting methods do not account for variations in the wind speed during the storm duration, but Wilson (1961) has modified the SMB-method so as to account for a moving storm, i.e., to account for spatial as well as temporal variations of the wind field. These relationships are developed based on deep water wave data and as such are limited to wave forecasting in deep water.

Bretschneider (1966) has, however, developed an approximate method for using the SMB-method to forecast waves in shallow water.

For a fully developed sea the SMB-method gives the significant wave height, H_s, which is the average of the highest one third of the waves, and the average period $<T>$ as a function of the 10 meter wind speed, W,

$$\frac{gH_s}{W^2} = 0.283$$

$$(3.1.21)$$

$$\frac{g<T>}{2\pi W} \simeq 1$$

Thus, for a fully developed sea one might for example choose to represent the waves by the wave of height $H_s = 2a$ and period $<T> = 2\pi/\omega$ propagating in the direction of the wind. For this equivalent wave Stokes' solution, Eq. (3.1.5) yields a surface drift in deep water

$$\bar{U}_s = (\frac{0.283}{2})^2 W = 0.02 W \qquad (3.1.22)$$

i.e., 2 percent of the wind speed. By a similar procedure, i.e., by taking $2a = H_s$ and $\omega = 2\pi/<T>$, the surface drift may be estimated in the general case when H_s and $<T>$ is found from the forecasting relationship. It may be shown by using the SMB-method in this manner that the surface drift essentially is given by Eq. (3.1.22) also for non-fully developed seas.

The preceding choice of H_s and $<T>$ as representing the wave characteristics is rather arbitrary. A better approach would be to represent the waves by their one-dimensional spectrum, defined by Eq. (3.1.13).

Barnett (1968) discusses the various empirical forms of the spectrum of fully developed deep water wind generated waves. Most of these spectra may be expressed as

$$S(\omega) = \alpha \frac{g^2}{\omega^5} e^{-\beta \left(\frac{g}{W\omega}\right)^4} \tag{3.1.23}$$

This is the form suggested by Pierson and Moskowitz (1964) who found $\alpha = 0.00405$ and $\beta = 0.74$. Bretschneider (1966) suggests a spectrum similar to Eq. (3.1.23). For the characteristics of the fully developed sea given by Eq. (3.1.21) the Bretschneider spectrum corresponds to values of $\alpha = 0.0069$ and $\beta = 0.675$ in Eq. (3.1.23).

Introducing Eq. (3.1.23) in Eq. (3.1.14) yields the expected value of the surface drift in deep water

$$\langle \overline{U}_s \rangle = \begin{cases} 1.6 \ 10^{-2} W & \text{(Pierson-Moskowitz)} \\ 2.7 \ 10^{-2} W & \text{(Bretschenider)} \end{cases} \tag{3.1.24}$$

i.e., of the same order of magnitude as the very simplistic approach taken in the development of Eq. (3.1.22). The above result for the Pierson-Moskowitz spectrum agrees with that obtained by Kenyon (1969). For a one-dimensional spectrum the direction of $\langle \overline{U}_s \rangle$ must be assumed to be in the direction of the wind. Kenyon (1969) further considered the effects of the directional spreading of the wave energy by expressing the directional spectrum for a fully developed sea as

$$S(\omega, \theta) = S(\omega) \ S(\theta) \tag{3.1.25}$$

in which θ is measured from the direction of the wind and the spreading factor, $S(\theta)$, according to Eq. (3.1.19) must satisfy

$$\int_{-\pi}^{\pi} S(\theta) d\theta = 1 \qquad (3.1.26)$$

By taking

$$S(\theta) = \begin{cases} C_n \cos^n\theta & |\theta| < \dfrac{\pi}{2} \\ \\ 0 & |\theta| > \dfrac{\pi}{2} \end{cases} \qquad (3.1.27)$$

Kenyon (1969) showed that the effect of angular spreading was to reduce the predicted magnitude of the surface drift by 10 to 15 percent. In view of the variation caused by different choices of the constants α and β in Eq. 3.1.23, the change in $<\overline{U}_s>$ associated with accounting for angular spreading in deep water is minor.

A complete model for wave forecasting has been developed by Cardone et al. (1975). It accounts for wind generation, bottom friction, dissipation through wave breaking, refraction, etc. The details of this model are not clearly described but it is evident that its application is a major undertaking. Other similar models have been developed by Collins (1972). These models lead to a prediction of the directional spectrum of the wind generated waves and may therefore be used in conjunction with Eq. (3.1.20) to predict the Stokes surface drift.

To illustrate the order of magnitude of the Stokes drift in shallow water, let us assume that the relationships, Eq. (3.1.21), for a fully developed sea holds also in shallow water. Taking now the simplistic

approach of representing the waves as an equivalent wave of $2a = H_s$ and $\omega = 2\pi/\langle T \rangle$ and recalling that the shallow water approximation of Eq. (3.1.15) is to be used, we obtain

$$\overline{U}_s = 1.33 \quad 10^{-2} \quad \frac{W}{\sqrt{gh}} \, W \qquad\qquad (3.1.28)$$

By comparison with Eq. (3.1.22) it is seen that the Stokes surface drift under the above, highly conservative, assumptions is of the order of the Stokes drift in deep water only for large values of $W/\sqrt{gh}$, i.e., for either very shallow water or for very high winds.

3.1.2 Conclusions Regarding the Advection of Oil Slicks by Waves

It should be evident from the preceding discussion that no adequate analytical model exists for the prediction of oil slick advection by waves.

In the absense of a highly viscous surface film the solution of Longuet-Higgins, based on a viscous fluid assumption, seems mathematically correct despite its prediction of an infinitely large surface drift in infinitely deep water. The reasons for this seemingly unrealistic result in the deep water limit may be either the neglect of viscous damping of the wave motion or, more likely, the fact that steady state never is reached if the water is truly of infinite depth. The latter reason, which was discussed by Unluata and Mei, is associated with the very slow diffusion of vorticity from the free surface into the fluid. Thus, for shorter times the effects of viscosity may be minor and a solution resembling that of Stokes' may be appropriate. A physically realistic model of wave induced mass transport should therefore include the temporal development

of the viscous solution and also, when used for the purpose of predicting

oil slick advection, the appropriate surface boundary condition including

the effect of the viscous oil slick.

Such a model has recently been developed by Milgram (1977) who finds

that the diffusion of vorticity into the fluid indeed is so slow that

a Stokes' solution, for all practical purposes, may be assumed valid for

infinitely deep water. Milgram (1977) furthermore shows that the speed

of advection of an oil slick on the free surface is practically identical

to the surface drift predicted by Stokes' solution. Thus, Milgram's

result leads to the same speed of advection as does the heuristic model

previously presented. An interesting approach accounting for the presence

of an oil slick on the free surface was recently advanced by Stewart (1976).

This study, however, did not result in a quantitative estimate of the

speed of advection of the oil slick.

Experimental studies of advection of oil slicks by waves are few.

A study by Alofs and Reisbig (1972) reports speeds of advection of plastic

floats exceeding that of Stokes' theory for deep water by 35-100%. In view

of the possible lack of analogy between the behavior of a thin oil film and

a plastic float this result is of limited value, except that it points out

that Stokes' theory tends to underestimate the drift velocity. The demon-

stration by Alofs and Reisbig that small oil slicks and plastic floats of

the same size behaved similarly in waves of a length 4 to 7 times the size

of the slick has little bearing on the problem since the important thing to

show is that they behave in the same manner when their size is large relative

to the wave length. Despite the lack of strong experimental support for

the applicability of Stokes' drift to predicting the speed of advection of oil

slicks by waves, a heuristic model based on Stokes' drift, which is supported

by Milgram's work, shows the possibility of obtaining speeds of advection

comparable to those commonly attributed to wind shear stresses on the free

surface. Thus, it can be concluded that advection by waves may be an

important factor in determining the trajectories of oil slicks.

A series of wave forecasting models of increasing complexity exist

and may be used to predict the wave climate for a given area as a function

of wind speed. However, our fundamental knowledge of the mass transport

velocity induced by waves is, both for a clean and a contaminated surface,

so poor that it would be meaningless to apply a very sophisticated wave

forecasting model to predict the wave climate and then use this result to

infer the advection of an oil slick by waves. A more fundamental knowledge

of the interaction of waves and an oil slick covering the free surface must

be established before the question of the importance of advection by

waves can be answered in a rational manner.

Even if an adequate model for the advection of oil slicks by waves,

based on a viscous fluid assumption, were available, such a model would

in general be of limited value. A complete model should in addition to

accounting for the presence of the oil slick also satisfy a free surface

boundary condition of a non-vanishing shear stress, i.e., the effect of

a wind driven current should be included. This, in turn, necessitates a

description of the wave motion in the presence of a shear current.

Biesel (1950) studied the linear problem of waves superimposed on a linear

shear current. Dalrymple (1974) extended Biesel's model to finite wave

heights using the stream function theory as the basis for numerical compu-

tations and recently (Dalrymple, 1976) extended this analysis to cover

also the case in which the vorticity is assumed to vary linearly with the

value of the stream function. Although the description of waves super-
imposed on a current recently has seen considerable advances, see, e.g.,
Peregrine (1976) for a summary, the prediction of the resulting mass
transport, including the contribution both from waves and from the wind
induced current, still seems far from immediately forthcoming.

Our present lack of ability to describe the oil slick advection by
waves alone, not to mention the combined effect of waves and a wind induced
shear current, leaves us with only one rational approach. This approach
is to deal with the advection of oil slicks as being due to two "separate"
mechanisms: (1) advection by waves, (2) advection by currents. As for
the advection by waves alone the use of Stokes' drift velocity seems to
have limited experimental support and could for that matter be used to
obtain approximate answers. This approach, however, leaves us with
the problem of determining the proportion of the surface wind shear stress
which is supported by the wave induced mass transport. In this respect
it is interesting to note that a formal application of Eq. (3.3.15) for
the inviscid Stokes' solution corresponding to a Pierson-Moskowitz spectrum,
Eq. (3.1.23), leads to a velocity gradient which is infinite at the free
surface. This in turn would indicate that the surface shear stress for a
fluid of finite viscosity would become infinite! This, of course, is an
unrealistic result. However, it does point out the fact that the wave
induced mass transport may support a portion, possibly a large portion, of
the surface wind shear. If this is the case, a separate treatment of the
advection by wave induced mass transport and wind induced currents should
account for this partition of the surface shear stress between a component
supported by the waves and the remaining surface shear stress which will
induce the wind-driven current. At present this is poorly understood

and an improved understanding of this is an absolute necessity if a realistic
and accurate model of oil slick trajectories, accounting for both the effect
of waves and currents, is to be developed.

3.2 Advection of Oil Slicks by Currents

Whereas the inclusion of a thin, highly viscous surface film appears
to be of great importance in the analysis of oil slick advection by waves
it appears to be realistic to analyze the advection of oil slicks due to
currents based on the assumption of a "clean" water surface. For a given
surface shear stress, τ_s, it may be shown that the velocity of a thin oil
slick (of the order 1 mm thick) is practically identical to the velocity at
the oil-water interface due to the high viscosity of the oil. The calming
effect of oil on a water surface subjected to the action of wind is well-
known and appears to dampen the shortest waves and hence reduce the hydro-
dynamic roughness of the sea surface. This in turn would indicate that the
surface shear stress exerted by a given wind speed would be smaller for an
oil film covered water surface than for a clean surface. The results of
Barger et al. (1970) clearly demonstrate this. A simplified argument is,
however, presented in Section 3.2.2 to show that this decrease in surface
roughness of the air-oil interface approximately may be considered balanced
by a corresponding decrease in the surface roughness of the oil-water inter-
face thus leading to a virtually unchanged surface velocity whether or not
the oil slick is included in the analysis. Thus, the following discussion
will be based on the assumption of clean water surface, and it will be
assumed that an accurate prediction of the surface current is identical to
an accurate prediction of the speed of advection of an oil slick.

In the coastal environment a variety of currents may be present.
It would be beyond the scope of even advanced textbooks in oceanography to
attempt a detailed discussion of these currents and our ability to predict
their direction and magnitude. For this reason the present discussion is

limited to tidal and wind-driven currents in a homogeneous ocean. The chapter is, as previously stated, a critical review of our current understanding of and ability to predict these currents.

In the context of prediction of oil slick trajectories the wind-driven current is believed to be of primary importance. The contribution of large scale ocean circulation and density-driven currents may be regarded as very slowly varying and may be estimated, for example, from observations. Tidal currents generally behave more or less as oscillatory flows, i.e., the net advection of an oil slick over one tidal cycle is small relatively to its excursion during the tidal cycle. Thus, the current system may be viewed as a basically steady current consisting of large scale circulations, density-driven currents and residual tidal currents upon which the local rapidly varying wind-induced surface drift is superimposed. The present Chapter is therefore primarily reviewing the mathematical description of wind-driven currents in a homogeneous ocean.

The tidal currents may be considered included in the computational method based on the depth averaged equations, Section 3.2.1, and within the framework of a homogeneous fluid it is still possible to account approximately for density-driven currents as shown in Section 3.2.6.

For a homogeneous ocean the general governing equations for the water movement are derived in several basic texts (e.g., Neumann, 1968). With the assumption of negligible vertical velocity the equations expressing the conservation of horizontal momentum may be written

$$\frac{Du}{Dt} = -\frac{1}{\rho} \frac{\partial p_a}{\partial x} - g \frac{\partial \eta}{\partial x} + \Omega v + F_x \qquad (3.2.1)$$

$$\frac{Dv}{Dt} = -\frac{1}{\rho} \frac{\partial p_a}{\partial y} - g \frac{\partial \eta}{\partial y} - \Omega u + F_y \qquad (3.2.2)$$

in which u and v are the horizontal velocity components in the x and y
directions, respectively. The pressure gradient has been split up into its
two components, one associated with the atmospheric pressure, p_a, and one
associated with the slope of the free surface, η, relative to the still
water level. The effect of earth's rotation is expressed by Coriolis force
with

$$\Omega = 2\omega_e \sin \phi \qquad (3.2.3)$$

where ω_e is the radian frequency of earth's rotation and ϕ is the latitude.
The terms F_x and F_y are the viscous, generally turbulent, frictional forces.
Introducing the concept of a turbulent eddy viscosity, which is analogous
to the kinematic viscosity for laminar flow, the frictional forces may be
written

$$F_x = \frac{\partial}{\partial z} (\epsilon_z \frac{\partial u}{\partial z}) = \frac{1}{\rho} \frac{\partial \tau_{zx}}{\partial z}$$

$$F_y = \frac{\partial}{\partial z} (\epsilon_z \frac{\partial v}{\partial z}) = \frac{1}{\rho} \frac{\partial \tau_{zy}}{\partial z} \qquad (3.2.4)$$

which neglects the shear stresses acting on vertical planes. In Eq. (3.2.4)
the vertical eddy viscosity ϵ_z is in general a function of the vertical
coordinate, z.

In addition to the momentum equations, Eqs. (3.2.1) and (3.2.2), the
conservation of mass requires for an incompressible, homogeneous fluid that

$$\frac{\partial u}{\partial x} + \frac{\partial v}{\partial y} + \frac{\partial w}{\partial z} = 0 \qquad\qquad (3.2.5)$$

where w is the vertical velocity component, which cannot be considered

negligible in the continuity equation for unsteady flow situations.

The problem at hand is therefore the solution of Eqs. (3.2.1), (3.2.2)

and (3.2.5) subject to various boundary conditions such as coastlines and

open boundaries in the xy plane as well as surface shear stress conditions.

Of these boundary conditions the surface shear stress is particularly per-

tinent in the present context and is generally expressed as

$$\vec{\tau}_s = \frac{1}{2} f_a \rho_a \, |\vec{W}|\vec{W} \qquad\qquad (3.2.6)$$

in which $\vec{\tau}_s$ is the surface shear stress vector, f_a is a friction factor,

ρ_a is the air density and $\vec{W}$ is the wind velocity vector at a given elevation,

say 10 meters above the still water level. In the form given by Eq. (3.2.6)

the main problem is that of estimating the value of the friction factor, f_a.

A number of studies have addressed this problem and a relatively recent

and rather complete study is that of Wu (1969). For the sake of simplicity

it will be assumed in the following discussion that the surface shear stress,

$\vec{\tau}_s$, is known if the wind speed, $\vec{W}$, at 10 meters elevation is known. It is,

however, emphasized that the accurate determination of the surface shear

stress, leaving aside the problem of its partition among waves and currents,

for a given wind speed, $|\vec{W}|$, is a problem that by no means can be considered

solved.

Assuming the various boundary conditions to be specified the solution

of Eqs. (3.2.1), (3.2.2) and (3.2.5) rests on an assumed knowledge of the

turbulent eddy viscosity, ε_z, in Eq. (3.2.4). Very little is known about the actual dependency of ε_z on the vertical coordinate. For lack of better information it is often assumed that ε_z is constant, i.e., strictly analogous to its laminar counterpart. It is believed that lack of knowledge and ability to assess the sensitivity of results to the assumption made on the value of ε_z is a serious problem in determining the surface currents in the coastal and offshore environment.

This section will review the various levels of approximate solutions to the governing equations, given here, for the purpose of predicting the speed of advection of oil slicks by currents. Since the wind induced currents have been singled out as the generally most important component the level of a particular solution method is determined by the degree of sophistication involved in accounting for the wind induced surface current.

3.2.1 Depth Averaged Equations

By integrating Eqs. (3.2.1), (3.2.2) and (3.2.5) over the depth of water and applying the appropriate boundary conditions at the free surface $z = \eta$, and at the bottom, $z = -h$, a set of approximate equations governing the depth averaged velocity components (u,v) results

$$\frac{\partial \overline{u}}{\partial t} + \overline{u}\,\frac{\partial \overline{u}}{\partial x} + \overline{v}\,\frac{\partial \overline{u}}{\partial y} = -\frac{1}{\rho}\,\frac{\partial p_a}{\partial x} - g\,\frac{\partial \eta}{\partial x} + \Omega\overline{v} + \frac{\tau_{s,x} - \tau_{b,x}}{\rho(h+\eta)} \qquad (3.2.7)$$

$$\frac{\partial \overline{v}}{\partial t} + \overline{u}\,\frac{\partial \overline{v}}{\partial x} + \overline{v}\,\frac{\partial \overline{v}}{\partial y} = -\frac{1}{\rho}\,\frac{\partial p_a}{\partial y} - g\,\frac{\partial \eta}{\partial y} - \Omega\overline{u} + \frac{\tau_{s,x} - \tau_{b,y}}{\rho(h+\eta)} \qquad (3.2.8)$$

and the continuity equation

$$\frac{\partial}{\partial x} \{\overline{u}(h + \eta)\} + \frac{\partial}{\partial y} \{\overline{v}(h + \eta)\} = - \frac{\partial \eta}{\partial t} \tag{3.2.9}$$

In these equations the surface shear stress is given by Eq. (3.2.6), i.e.,

$$\vec{\tau}_s = (\tau_{s,x}, \tau_{x,y}) = \frac{1}{2} \rho_a f_a |\vec{W}|^2 (\cos\theta, \sin\theta) \tag{3.2.10}$$

where θ is the angle between the x-axis and the 10 meter wind direction, $\vec{W}$. The bottom shear stress $\vec{\tau}_b$ is generally related to the depth averaged velocity through

$$\vec{\tau}_b = (\tau_{b,x}, \tau_{b,y}) = \frac{1}{2} \rho f_b (\overline{u}^2 + \overline{v}^2) \left(\frac{\overline{u}}{\sqrt{\overline{u}^2 + \overline{v}^2}}, \frac{\overline{v}}{\sqrt{\overline{u}^2 + \overline{v}^2}} \right) \tag{3.2.11}$$

in which f_b is a bottom friction factor.

This set of equations have been used extensively in numerical studies of coastal circulation. A large number of numerical schemes are available including finite difference (e.g., Leendertse, 1967) as well as finite element formulations (e.g., Wang, 1975). Recent surveys of some of these numerical techniques are given by Reid (1975) and Hinwood and Wallis (1975). These numerical techniques are quite general and may be used to treat steady as well as unsteady problems. They account for lateral boundary conditions with their main difficulty being in the treatment of the open ocean boundaries. The various models generally need to be calibrated against observations in order to determine the appropriate value of the friction factors, f_a and f_b, in Eqs. (3.2.10) and (3.2.11).

For predominantly wind induced circulation the models are generally quite successful when used for the purpose of predicting the resulting wind set up, i.e., the value of η. As illustrated in Fig. (3.2.1) the vertical velocity profile is poorly represented by its depth averaged value for a wind induced current whereas the depth averaged current may be assumed to give a reasonable representation of pressure gradient or tidal currents.
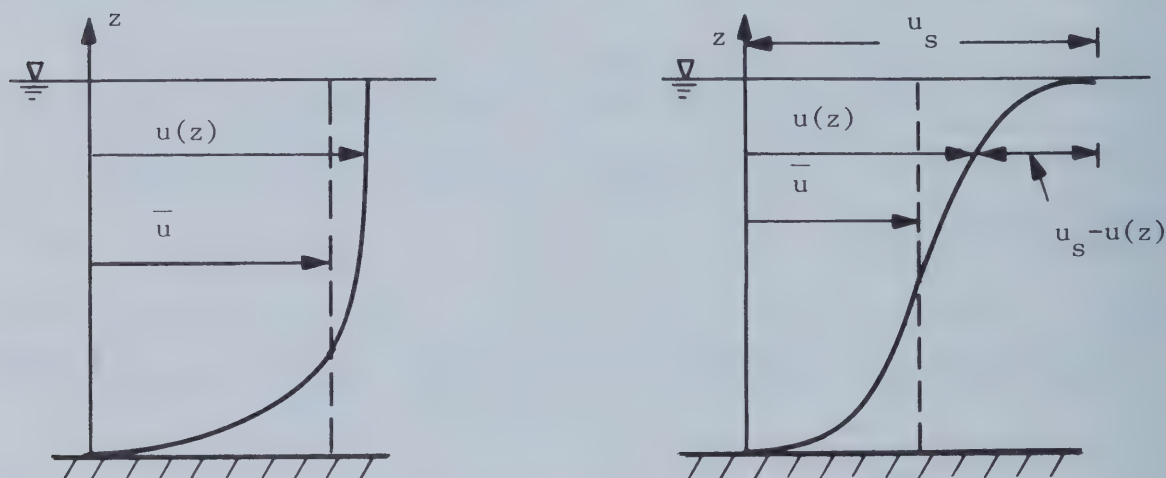
Figure 3.2.1:   Comparison of Actual Vertical Velocity Distribution and the Depth Averaged Velocity.

It is quite evident from Fig. (3.2.1) that the depth averaged velocity because of the pronounced velocity gradient near the surface associated with the surface shear stress is an extremely poor representation of the surface velocity. Thus, although several aspects of the use of numerical models based on the depth averaged equations of motion are quite sophisticated, their use for the purpose of predicting oil slick advection by wind represents a first level of effort which must be supplemented by an estimate of the difference between the depth averaged velocity and the surface current.

3.2.2 Wind Factor Approach

The simplest consideration of the surface current induced by a wind shear stress takes the form of expressing the surface current as a percentage of the wind velocity. The simplest analysis leading to a determination of the wind factor is based on a balance of surface shear stress approaching the surface from the air and from the fluid side. Approaching the free surface from the air the shear stress is given by Eq. (3.2.6)

$$\vec{\tau}_{s,a} = \frac{1}{2} f_a \rho_a \, |\vec{W}| \vec{W} \tag{3.2.12}$$

An assumption of the velocity defect, $\Delta u_s = u_s - u(z)$ where u_s is the surface current, to be logarithmic in the vicinity of the surface (see Fig. 3.2.1) suggests that the surface shear stress approaching the free surface from below may be expressed as

$$\vec{\tau}_{s,w} = \frac{1}{2} f_w \rho_w \, |\Delta \vec{u}_s| \Delta \vec{u}_s \tag{3.2.13}$$

in Eq. (3.2.13) the fluid density is ρ_w and the friction factor is f_w. The velocity defect $\Delta \vec{u}_s$ is rather ill defined, but may be taken to express the velocity which added to the depth averaged velocity yields the surface velocity.

By equating Eqs. (3.2.12) and (3.2.13) one obtains

$$\frac{\Delta \vec{u}_s}{\vec{W}} = \sqrt{\frac{f_a}{f_w}} \, \sqrt{\frac{\rho_a}{\rho_w}} \tag{3.2.14}$$

and following an argument that the friction factors f_a and f_w depend on the hydrodynamic surface roughness which is the same for air and water the much used wind factor

$$\frac{\Delta \vec{u}_s}{\vec{W}} = \sqrt{\frac{\rho_a}{\rho_w}} \simeq 0.03 \qquad (3.2.15)$$

is obtained.

The preceding arguments leading to Eq. (3.2.15) have been advanced in the past without much in the way of actual justification. A recent laboratory study by Shemdin (1972) does, however, lend some credibility to these arguments. It should be pointed out here that, if the preceding argument is advanced for a free surface covered with an oil film, the hydrodynamic roughness of the surface would decrease relative to that of a clean surface. This would tend to produce a smaller value of f_a for an oil covered surface than for a clean surface. However, the decrease in roughness of the oil-air interface would be matched by a corresponding decrease of the roughness of the oil-water interface. Hence, to the extent of the validity of the preceding arguments the equality of f_a and f_w still holds and the wind factor, Eq. (3.2.15), applies to clean as well as contaminated surfaces.

The use of the wind factor approach is clearly extremely simple in that the advection speed of the oil slick is taken as

$$\vec{u}_s = \Delta \vec{u}_s = 0.03 \, \vec{W} \qquad (3.2.16)$$

The direction of the surface current is generally taken as the direction of

the wind. It requires only a knowledge of the wind field at, say 10 meters

elevation, to be used and the effect of other currents may be added if they

are known either from direct measurements (Williams, 1975) or from a num-

erical depth averaged model.

It is felt by the writers that the primary virtue of the wind

factor approach is its extreme simplicity in application. A number of

investigations have attempted to establish the validity of this approach.

A review of some of these investigations is given in Section 3.3 and it is

evident that these investigations generally are not beyond reproach. Based

purely on physical considerations it is evident that the wind factor approach

at best is limited to deep water. In shallow water the bottom roughness

as well as the proximity of lateral boundaries play an important role in

determining the surface velocity resulting from a given surface shear stress.

The experiments by Reichardt (1959) on turbulent Couette flow clearly

demonstrate this. Furthermore, the effects of lateral boundaries are not

readily included except through the use of simple empirical rules of thumb

(Williams, 1975). Because of its simplicity (and popularity) the wind

factor approach is undoubtedly going to be used extensively. It is,

however, felt that at best it can give information of a preliminary

nature. The basic physical principles underlying the wind factor

approach need to be critically examined before its use for other than

preliminary investigations is adopted. A further discussion of the

wind factor is given in Appendix A.

3.2.3 Ekman Approach

A somewhat more sophisticated approach than the wind factor approach is based on an analysis of the details of the vertical structure of the wind induced currents. Analytical solutions to the governing equations are easily obtained under the following simplifying assumptions

(1) Ocean of infinite horizontal extent

(2) Spatially uniform wind field   (3.2.17)

(3) Constant vertical eddy viscosity

These assumptions correspond to those made by Ekman (1905) in his pioneering work on wind induced currents. As an illustration of this approach the problem of the current induced by a uniform surface shear stress, which may vary with time, in an infinitely deep ocean is considered here.

For an infinite ocean there can be no surface slope so the governing equations, Eqs. (3.2.1) and (3.2.2) become

$$\frac{\partial u}{\partial t} = \Omega v + \nu_t \frac{\partial^2 u}{\partial z^2} \qquad\qquad (3.2.18)$$

$$\frac{\partial v}{\partial t} = -\Omega u + \nu_t \frac{\partial^2 v}{\partial z^2} \qquad\qquad (3.2.19)$$

where the convective acceleration terms as well as the terms in the continuity equation, Eq. (3.2.5), are zero by virtue of the spatial uniformity of the motion. The turbulent eddy viscosity ε_z is denoted by ν_t to stress the analogy with laminar flow since ν_t is assumed constant.

Introducing the complex velocity

$$w = u + iv \qquad\qquad (3.2.20)$$

in which $i = \sqrt{-1}$, equations (3.2.18) and (3.2.19) may conveniently be written

$$\frac{\partial w}{\partial t} + i\Omega w = \nu_t \frac{\partial^2 w}{\partial z^2} \tag{3.2.21}$$

This equation is to be solved subject to the following boundary conditions

$$w \to 0 \quad \text{as } z \to -\infty \tag{3.2.22}$$

$$\nu_t \frac{\partial w}{\partial z} = \frac{\tau_{s,x} + i\tau_{s,y}}{\rho} \qquad \text{at } z = 0 \tag{3.2.23}$$

with the initial condition of fluid at rest, i.e.,

$$w = 0 \quad \text{at} \quad t \leq 0 \tag{3.2.24}$$

Introducing Laplace transforms defined by

$$F(s) = \hat{f}(t) = \int_0^\infty e^{-st} f(t) \, dt \tag{3.2.25}$$

we have that

$$\int_0^\infty e^{-st} \frac{\partial w}{\partial t} \, dt = [e^{-st} w]_0^\infty + s \int_0^\infty e^{-st} w \, dt = s\tilde{w} \tag{3.2.26}$$

since the bracketed term vanishes at $t = \infty$ for $s > 0$ and at $t = 0$ by virtue of the initial condition, Eq. (3.2.24).

Equation (21) may therefore be written in terms of its Laplace transform

$$(s + i\Omega)\tilde{w} = \nu_t \frac{\partial^2 \tilde{w}}{\partial z^2} \tag{3.2.27}$$

which has the solution

$$\tilde{w} = A\ e^{\alpha z} + B\ e^{-\alpha z} \tag{3.2.28}$$

in which

$$\alpha = \sqrt{\frac{s + i\Omega}{\nu_t}} \tag{3.2.29}$$

Choosing the solution of Eq. (3.2.29) with a positive real part it is

seen that B = 0 in Eq. (3.2.28) in order for Eq. (3.2.22) to be satisfied.

The remaining boundary condition therefore becomes

$$\nu_t \frac{\partial \tilde{w}}{\partial z} = \nu_t\ A\ \alpha\ e^{\alpha z} = \nu_t\ \alpha\ A = \frac{\overset{\sim}{\tau}_s}{\rho} \tag{3.2.30}$$

where $\overset{\sim}{\tau}_s$ is the Laplace transform of the time varying surface shear

stress expressed by Eq. (3.2.23). From Eq. (3.2.30) the value of the

constant A is found and the solution of Eq. (3.2.27) is

$$\tilde{w} = \frac{1}{\rho \nu_t} \overset{\sim}{\tau}_s\ \frac{e^{\sqrt{\frac{s + i\Omega}{\nu_t}}\ z}}{\sqrt{\frac{s + i\Omega}{\nu_t}}} \tag{3.2.31}$$

From tables of Laplace transform it may be found that

$$\frac{e^{\sqrt{\frac{s + i\Omega}{\nu_t}}\ z}}{\sqrt{\frac{s + i\Omega}{\nu_t}}} = \mathcal{L}\{\nu_t\ e^{-i\Omega t}\ \frac{1}{\sqrt{\nu_t \pi t}}\ \exp\ (-\frac{z^2}{4\nu_t t}) \} \tag{3.2.32}$$

in which $\mathcal{L}\{\ \}$ designates the Laplace transform of the term in the brackets.

The Laplace transform of the solution for the complex velocity may therefore be written as the product of two Laplace transforms which is a convolution integral. Hence, the solution is found as

$$w = \frac{1}{\rho \sqrt{\nu_t \pi}} \int_0^t (\tau_{s,x}(t-\beta) + i\tau_{s,y}(t-\beta))e^{-i\Omega\beta}\, \frac{1}{\sqrt{\beta}}\, e^{-\frac{z^2}{4\nu_t \beta}}\, d\beta \tag{3.2.33}$$

Equating the real part of (3.2.33) with u and the imaginary part with v this result is readily seen to be identical to the result obtained by Warner et al. (1972), who used this procedure with some success to track the Arrow oil spill off the coast of Nova Scotia. In their application they limited the integration of Eq. (3.2.33) to the 96 hour period preceding the time of interest. The best results were obtained for a value of $\nu_t = 0.16$ ft^2/sec.

For the particular choice of temporal variation of the surface shear stress

$$\vec{\tau}_s = \begin{cases} 0 & t \le 0 \\ \tau_{s,x} + i\tau_{x,y} & t > 0 \end{cases} \tag{3.2.34}$$

the solution becomes the classical solutions of Ekman. In particular, the steady solution is obtained from Eq. (3.2.33) when $\tau_{s,x} = 0$ and $\tau \to \infty$

$$w = \frac{\tau_{s,y}}{\rho \sqrt{\nu_t \Omega}} \exp\left\{ \sqrt{\frac{\Omega}{2\nu_t}}\, (1+i)z + i\, \frac{\pi}{4} \right\} \tag{3.2.35}$$

which shows that the surface velocity on the Northern Hemisphere is at an angle of 45° (clockwise) from the wind direction.

A similar but somewhat more complicated solution may be obtained for the case of a finite depth. This solution along with the inclusion of a possible surface slope in the analysis will be outlined in the following section since it, in the present context, is related to the approach taken by Forristall (1974).

By integrating Eq. (3.2.35) over the depth the transport associated with an Ekman current is found to be

$$\int_{-\infty}^{0} w \, dz = q_x + iq_y = \frac{\tau_{s,y}}{\rho\Omega} \tag{3.2.36}$$

which shows that there is a net transport in the direction perpendicular to the direction of the surface shear stress (90° in the clockwise direction on the northern hemisphere). For the simple case of a lateral boundary parallel to the y-axis, the boundary condition of zero mass flux in the x-direction will cause the water to pile up along the coast, thus creating a slope of the water surface perpendicular to the shore. This slope will in turn produce a flow in the x-direction which balances the Ekman transport. Murray (1975) discusses this simple case for finite depth and steady conditions.

The use of the Ekman approach to predict surface drift currents is as seen from the preceding discussion limited to large distances from shorelines or to cases where the shore may be regarded as long and straight. Although analytical solutions may be obtained their application generally requires the use of computers to evaluate relatively complicated integrals

such as Eq. (3.2.33). Also, this particular approach is limited to cases

where the wind field may be assumed uniform over the area of interest.

The use of the Ekman approach has in addition to the limitations

mentioned above a severe limitation in that it is based on an assumed

constant vertical eddy viscosity, whose value is at best ill defined.

If data are available one might calibrate the model, as did Warner et al.

(1972) to find the best fit value of ν_t. This, of course, is a generally

acceptable approach, but unless generally valid expressions for ν_t are

available such calibration becomes a necessity for a particular area of

interest. An alternative approach is to tie the Ekman solution to the wind

factor approach by requiring that the steady surface velocity be a certain

percentage of the wind speed. Taking, for example, the surface current

given by Eqs. (3.2.15) and (3.2.35) one obtains

$$\sqrt{\frac{\rho_a}{\rho}}\, W = \frac{\tau_{s,y}}{\rho\sqrt{\nu_t \Omega}} = \frac{\frac{1}{2} f_a \rho_a W^2}{\rho\sqrt{\nu_t \Omega}}$$

which with values of $f_a = 3.2 \; 10^{-3}$ and $\rho_a/\rho = 1/800$ yields a formula for
ν_t

$$\nu_t = 2.3 \; 10^{-5} \frac{W^2}{\sin\phi} \; ; \quad [\,cm^2/sec \;\; if \; W \; in \; cm/sec] \qquad (3.2.37)$$

The ill defined value of ν_t (see Section 3.3 for the variations of

observed wind factors) presents in the writers' opinion a serious limitation

of this approach. The constant eddy viscosity leads in deep water to a

deflection angle of 45° between wind and surface current. It is believed

that this deflection angle is unrealistically high. In shallow water the value of ν_t must somehow reflect not only the turbulence generated at the surface but also that associated with the flow over a rough bottom. In relatively shallow water a constant eddy viscosity leads to a triangular velocity profile which only vaguely resembles the turbulent Couette flow velocity profile found by Reichardt (1959). The lack of more fundamentally sound understanding of the proper parameterization of the eddy viscosity is one of the major shortcomings of the Ekman approach.

3.2.4 Forristall Approach

The limitations of the Ekman approach to cases of spatially uniform wind fields and simple boundary geometry were elegantly overcome by Forristall (1974). Foristall suggested a combined use of the numerical solution of the depth averaged equations and the Ekman approach. As mentioned in Section 3.2.1 the numerical solution of the depth averaged equations may be performed for spatially and temporally varying surface shear stress and for very complex boundary geometries. The solution for the surface elevation, η, can generally be considered quite reliable whereas the vertical structure of the velocity field is poorly represented by the depth averaged results.

From the numerical solution the values of the surface slope, $\partial\eta/\partial x$ and $\partial\eta/\partial y$, may be obtained as a function of time for any point in the computational region. With the continuity equation satisfied by the numerical solution the vertical structure of the velocity field may be approximately resolved by employing the horizontal momentum equations, Eqs. (3.2.1) and (3.2.2). Writing Eqs. (3.2.1) and (3.2.2) in a form

analogous to Eq. (3.2.21) and linearizing the acceleration terms, the governing equation becomes

$$\frac{\partial w}{\partial t} + i\Omega w = -P + \nu_t \frac{\partial^2 w}{\partial z^2} \qquad (3.2.38)$$

in which w is the complex horizontal velocity defined by Eq. (3.2.20) and

$$P = (\frac{1}{\rho} \frac{\partial p_a}{\partial x} + g \frac{\partial \eta}{\partial x}) + i(\frac{1}{\rho} \frac{\partial p_a}{\partial y} + g \frac{\partial \eta}{\partial y}) \qquad (3.2.39)$$

may be regarded as known from the numerical solution of the depth averaged equations. It should be pointed out that Forristall's definition of the term P (denoted by q in his paper) appears to be missing a minus sign.

Forristall (1974) presents an outline of the solution of Eq. (3.2.39). In addition to the misleading typographical error already noted, Forristall's paper contains another very unfortunate misprint which may go unnoticed unless the reader repeats the entire derivation. An alternative reference to the equations given by Forristall is the paper by Welander (1957). Welander's paper appears, however, to be typographically as unreliable as the paper by Forristall. The original solution to Eq. (3.2.39) appears to be due to Fjeldstad (1930) and Hidaka (1933). These references are, however, not readily available to most researchers and with the misprints in later publications, noted above, it is found justified to repeat the derivation of the solution of Eq. (3.2.39) here.

Since Eq. (3.2.38) is linear the solution for w may be assumed to consist of the sum of two solutions

$$w = w_t + w_p \tag{3.2.40}$$

of which w_t is the current due to the surface shear stress and w_p is the current associated with the pressure gradient. Thus, the problem may be considered as finding the solutions to the following equations and boundary conditions

$$\frac{\partial w_t}{\partial t} + i\Omega w_t = \nu_t \frac{\partial^2 w_t}{\partial z^2}$$

$$w_t = 0 \text{ at the bottom, } z = -h \tag{3.2.41}$$

$$\nu_t \frac{\partial w_t}{\partial z} = \frac{\tau_{s,x} + i\tau_{s,y}}{\rho} \text{ at the surface, } z = 0$$

and

$$\frac{\partial w_p}{\partial z} + i\Omega w_p = -P + \nu_t \frac{\partial^2 w_p}{\partial z^2}$$

$$w_p = 0 \text{ at the bottom, } z = -h \tag{3.2.42}$$

$$\nu_t \frac{\partial w_p}{\partial z} = 0 \text{ at the surface, } z = 0.$$

with the initial condition being a motion starting from rest, i.e.,

$$w_t = w_p = 0 \quad \text{for } t \leq 0. \tag{3.2.43}$$

The solution of Eq. (3.2.41) proceeds as outlined in the previous section by taking the Laplace transform denoted by $\sim$

$$(s + i\Omega) \; \tilde{w}_t = \nu_t \; \frac{\partial^2 \tilde{w}_t}{\partial z^2} \tag{3.2.44}$$

which has the solution

$$\tilde{w}_t = A \; \sinh\alpha(z+h) + B \; \cosh\alpha(z + h) \tag{3.2.45}$$

in which α is given by Eq. (3.2.29). The arbitrary constant B is zero by virtue of the bottom boundary condition.

For the particular choice of the time varying surface shear stress

$$\vec{\tau}_s = \begin{matrix} 0 & t \leq 0 \\ \tau_{s,x} = \text{constant} & t > 0 \end{matrix} \tag{3.2.46}$$

whose Laplace transform is

$$\tilde{\tau}_{s,x} = \int_0^\infty e^{-st} \; \tau_{s,x} \; dt = \frac{\tau_{s,x}}{s} \tag{3.2.47}$$

the constant A is determined from the surface boundary condition

$$\nu_t \quad \cosh\alpha h \; A = \frac{1}{s} \; \frac{\tau_{s,x}}{\rho} \tag{3.2.48}$$

The solution of Eq. (3.2.44) is therefore

$$\tilde{w}_t = \frac{\tau_{s,x}}{\rho \nu_t s\alpha} \; \frac{\sinh\alpha(z + h)}{\cosh\alpha h} \tag{3.2.49}$$

which is identical to the solution of Forristall (1974, Eq. 11).

To invert the Laplace transform the inversion integral (the Brom-wich integral, Hildebrand, 1965, p. 601-603) is used

$$w_t = \frac{1}{2\pi i} \int_{c-i\infty}^{c+i\infty} e^{ts}\, \tilde{w}_t \; ds = \frac{1}{2\pi i} \int_{c-i\infty}^{c+i\infty} F(s) \; ds \qquad (3.2.50)$$

in which the real constant c is chosen to the "positive side" of all singularities of $F(s)$.

The solution of the contour integral, Eq. (3.2.51), may be expressed as the sum of the residues, i.e.,

$$w_t = \sum_{s_R} \mathrm{Res}\,\{F(s);\; s_R\} \qquad (3.2.51)$$

where s_R are the values of s for which $F(s)$ is singular.

Examining Eqs. (3.2.49) and (3.2.50) it is seen that $F(s)$ is singular for

$$s = 0;\; \alpha = 0;\; \cosh\alpha h = 0 \qquad (3.2.52)$$

Of these singularities the one corresponding to $\alpha = 0$ is removeable since $\sinh\alpha(z + h) = \alpha(z + h)$ as $\alpha \to 0$. Using $\cosh ix = \cos x$ we obtain

$$\cosh\alpha h = \cosh i(n + \tfrac{1}{2})\pi = \cos(n + \tfrac{1}{2})\pi = 0 \quad n = 0,1\ldots \qquad (3.2.53)$$

which shows that the singularities correspond to

$$\alpha h = i(n + \tfrac{1}{2})\pi \;;\; n = 0,1,2\ldots \qquad (3.2.54)$$

3-43

or, by introducing α from Eq. (3.2.29), the singularities of $F(s)$ correspond to values of

$$s_R = 0; \quad s_R = s_n = -(i\Omega + \frac{\nu_t (n + \frac{1}{2})^2 \pi^2}{h^2})$$

(3.2.55)

With the singularities given by Eq. (3.2.55) and $F(s)$ defined by Equations (3.2.49) and (3.2.50) we obtain

$$\text{Res } \{F(s); \ s_R = 0\} = \frac{\tau_{s,x}}{\rho \sqrt{i\Omega \nu_t}} \frac{\sinh \sqrt{\frac{i\Omega}{\nu_t}}(h + z)}{\cosh \sqrt{\frac{i\Omega}{\nu_t}} h}$$

(3.2.56)

which for $h \to \infty$ is readily seen to correspond to the steady state solution for infinitely deep water, Eq. (3.2.35). Thus, Eq. (3.2.56) corresponds to the steady state solution.

The remaining residues are obtained from

$$\text{Res}\{F(s) = e^{ts} \tilde{w}_t; \ s_R = s_n\} = \frac{\tau_{s,x}}{\rho \nu_t \ \alpha s_n \ \frac{\partial (\alpha h)}{\partial x}} e^{ts} \frac{\sinh \alpha h(1 + \frac{z}{h})}{\sinh \alpha h} =$$

$$- \frac{2\tau_{s,x}}{\rho\Omega(i + \mu_n^2)h} e^{-(i + \mu_n^2)\Omega t} \cos (n + \frac{1}{2})\pi\frac{z}{h}$$

(3.2.57)

in which

$$\mu_n = (n + \frac{1}{2}) \ \pi \ \frac{1}{h}\sqrt{\frac{\nu_t}{\Omega}}$$

(3.2.58)

The solution therefore becomes

3-44

$$w_t = \frac{\tau_{s,x}}{\rho\sqrt{i\Omega\nu_t}} \; \frac{\sinh \sqrt{\frac{i\Omega}{\nu_t}}\,(z+h)}{\cosh \sqrt{\frac{i\Omega}{\nu_t}}\,h}$$

$$-\frac{2\tau_{s,x}}{\rho\Omega\,h} \sum_{n=0}^{\infty} \frac{1}{i + \mu_n^2} \; e^{-(i+\mu_n^2)\Omega t} \cos\left(n+\tfrac{1}{2}\right)\pi \frac{z}{h} \tag{3.2.59}$$

which may be shown to be identical to the solutions given by Welander (1957) and Forristall (1974) when it is realized that Welander's (1974, Eq. 31) definition of μ_n contains a misprint and that the same is true for Forristall's (1974) definition of his quantity A_n.

Eq. (3.2.59) corresponds to a sudden application of a finite shear stress. To obtain the soltuion for a continuously time varying surface shear stress

$$\tau_s(t) = \tau_{s,x}(t) + i\,\tau_{s,y}(t) \tag{3.2.60}$$

this variation is treated as a series of infinitesimal steps given by

$$\Delta\tau_s = \frac{\partial\tau_s}{\partial t}\,\Delta\beta \tag{3.2.61}$$

assumed to occur at time $t - \beta$. At time $t = t$ the contribution of all infinitesimal steps may be expressed as an integral

$$w_t(t) = \int_0^t \frac{\partial\tau_s(t-\beta)}{\partial t} \; w_{t,1}(\beta)\,d\beta \tag{3.2.62}$$

in which $w_{t,1}(\beta)$ is given by Eq. (3.2.59) with $\tau_{s,x} = 1$ and t replaced by

the dummy variable β.

Integrating Eq. (3.2.62) by parts we obtain

$$w_t(t) = \int_0^t \tau_s(t-\beta) \frac{\partial w_{t,1}}{\partial \beta} \, d\beta \ =$$

$$\frac{2}{\rho h} \sum_{n=0}^{\infty} \cos(n + \frac{1}{2})\pi \, \frac{z}{h} \int_0^t \tau_s(t-\beta) e^{-(i + \mu_n^2)\Omega\beta} \, d\beta \qquad (3.2.63)$$

which is identical to the solution given by Forristall (1974). By integrating Eq. (3.2.63) over the depth, i.e., from z = -h to z = 0, we obtain the volume flux

$$\int_{-h}^0 w_t(t) \, dz = q_x + iq_y = \frac{2}{\rho} \sum_{n=0}^{\infty} \frac{(-1)^n}{(n + \frac{1}{2})\pi} \int_0^t \tau_s(t-\beta) e^{-(i+\mu_n^2)\Omega\beta} \, d\beta$$

$$(3.2.64)$$

For the solution corresponding to the contribution of the pressure gradient (the "slope current") given by Eq. (3.2.42) the procedure is identical to that followed for the solution of the shear current, i.e., the Laplace transform of Eq. (3.2.42) is taken

$$(s + i\Omega) \, \tilde{w}_p = -\frac{1}{s} P + \nu_t \frac{\partial^2 \tilde{w}}{\partial z^2} \qquad (3.2.65)$$

The solution of Eq. (3.2.65) satisfying the surface and bottom boundary conditions for a suddenly applied pressure gradient, i.e., corresponding to

$$P = \begin{cases} 0 & t \leq 0 \\ P & t > 0 \end{cases} \tag{3.2.66}$$

is given by

$$\tilde{w}_p = \frac{P}{\nu_t s \alpha^2} \left(\frac{\cosh \alpha z}{\cosh \alpha h} - 1 \right) \tag{3.2.67}$$

in which   is given by Eq. (3.2.29) as before.

To invert Eq. (3.2.67) it is again recognized that the singularity corresponding to $\alpha = 0$ is removeable. The singularity at $s = 0$ corresponds to the steady state solution. Thus we obtain

$$w_p(t) = \Sigma \text{ Res } \{e^{ts} \tilde{w}_p(s); s_R\} \tag{3.2.68}$$

where s_R is given by Eq. (3.2.55). The result is

$$w_p(t) = \frac{P}{i\Omega} \left(\frac{\cosh \sqrt{\frac{i\Omega}{\nu_t}} z}{\cosh \sqrt{\frac{i\Omega}{\nu_t}} h} - 1 \right)$$

$$+ \frac{2P}{\Omega} \sum_{n=0}^{\infty} \frac{(-1)^n}{(n + \frac{1}{2})\pi} \frac{1}{i + \mu_n^2} \cos(n + \frac{1}{2})\pi \frac{z}{h} e^{-(i + \mu_n^2)\Omega t} \tag{3.2.69}$$

This result may be shown to be identical to the result given by Forristall (1974) when the misprint in Forristall's definition of the quantity A_n is kept in mind. The solution resembles the solution given by Welander (1957) but complete agreement is not obtained. Thus, the term $1/\{(n + \frac{1}{2})\pi\}$ seems absent in Welander's (1957, Eq. 30b) solution.

Looking for a solution corresponding to a continuously varying pressure gradient, i.e., taking

$$\Delta P = \frac{\partial P}{\partial t} \Delta \beta \qquad (3.2.70)$$

as the infinitesimal step in P occurring at $t = t-\beta$, the summation of contributions at $t = t$ may be expressed as the integral

$$w_p(t) = \int_0^t \frac{\partial P(t-\beta)}{\partial t} \; w_{p,1}(\beta) d\beta \qquad (3.2.71)$$

where $w_{p,1}(\beta)$ is given by Eq. (3.2.69) with $P = 1$ and t replaced by the dummy variable β.

Integrating Eq. (3.2.71) by parts we obtain

$$w_p(t) = \int_0^t P(t-\beta) \; \frac{w_{p,1}(\beta)}{\partial \beta} \; d\beta \quad =$$

$$-2 \sum_{n=0}^{\infty} \frac{(-1)^n \cos(n + \frac{1}{2})\pi\frac{z}{h}}{(n + \frac{1}{2})\pi} \int_0^t P(t-\beta) e^{-(i + \mu_n^2)\Omega\beta} \; d\beta \qquad (3.2.72)$$

which is readily shown to be identical to Forristall's (1974, Eq. 19) expression when the sign difference between his q and the present equivalent P is recognized.

To obtain the volume flux Eq. (3.2.72) is integrated over the depth and we obtain

$$\int_{-h}^{0} w_p(t)\,dz = q_x + iq_y =$$

$$-2h \sum_{n=0}^{\infty} \frac{1}{[(n + \frac{1}{2})\pi]^2} \int_{0}^{t} P(t'-\beta) e^{-(i + \mu_n^2)\Omega\beta} \, d\beta \qquad (3.2.73)$$

which again is similar to the result given by Forristal (1974, Eq. 20) when accounting for the difference in definition of the sign of the pressure gradient and allowing for an omission of the depth, h, in Foristall's equation.

For a given $\tau_s(t)$, Eq. (3.2.60), and a known value of P(t), Eq. (3.2.39), the latter obtained from a numerical solution of the depth averaged equations the complete solution is obtained from Eq. (3.2.40) by evaluating Eqs. (3.2.63) and (3.2.72). A check of the solution is obtained by comparing the volume fluxes given by the sum of Eqs. (3.2.64) and (3.2.73) and the volume flux obtained from the numerical solution of the depth averaged equations.

Forristall (1974) presents sample calculations using this approach. The approach, which produces three-dimensional results, is clearly more involved computationally than the Ekman approach. It does seem to offer an excellent alternative to the ultimate numerical model: a three-dimensional numerical model. It is, however, severely limited by the necessity of having to assume a constant eddy viscosity, ν_t. The "accuracy" gained by using a sophisticated model, such as Forristall's, may therefore not be commensurate with the considerable computational effort.

3.2.5 Three-Dimensional Numerical Models

The ultimate numerical simulation of coastal circulation is a three-dimensional model solving the basic governing equations, Eqs. (3.2.1), (3.2.2) and (3.2.5). Leendertse and Liu (1975) outline such an approach based on an assumed multilayered model where the fluid density as well as the vertical eddy viscosity may be assumed different from layer to layer, but constant within each layer. A model of this type is clearly very involved, computationally. It is doubtful that sufficient accuracy is gained by this approach so long as our basic knowledge of the vertical eddy viscosity is as limited as it is.

An alternative approach to a complete numerical solution of the three-dimensional governing equations was outlined by Welander (1957). The approach is readily illustrated based on the results given in the previous section where the value of the pressure gradient, P, was assumed known at any point in the xy-plane. From Eqs. (3.2.64) and (3.2.73) we obtain the volume flux

$$q_x + iq_y = \frac{2}{\rho} \sum_{n=0}^{\infty} \frac{(-1)^n}{(n + \frac{1}{2})\pi} \int_0^t \tau_s(t-\beta)\, e^{-(i + \mu_n^2)\Omega\beta}\, d\beta$$

$$-2h \sum_{n=0}^{\infty} \frac{1}{[(n + \frac{1}{2})\pi]^2} \int_0^t P(t-\beta)\, e^{-(i + \mu_n^2)\Omega\beta}\, d\beta \tag{3.2.74}$$

Now, in the discussion presented in the previous section it was assumed that P(t), given by Eq. (3.2.39), was known. This quantity is seen to depend on the value of the slope of the free surface, $(\partial\eta/\partial x, \partial\eta/\partial y)$.

Whether this surface slope is known or not does not change the analysis

presented in the previous section. Thus, regarding η, the free surface

elevation to be unknown, Eq. (3.2.74) may be regarded as a relationship

between the volume flux and the surface slope. Introducing now the depth

integrated continuity equation, Eq. (3.2.9), in its linearized form we

have

$$-\frac{\partial \eta}{\partial t} = \frac{\partial (hu)}{\partial x} + \frac{\partial (hv)}{\partial y} = \frac{\partial q_x}{\partial x} + \frac{\partial q_y}{\partial y} \qquad (3.2.75)$$

in which q_x and q_y are found as the real and imaginary part of Eq. (3.2.74),

respectively. The resulting equation, (3.2.75), involves the temporal

derivative of the surface elevation as well as the integral of the surface

slope. Although complicated, Eq. (3.2.75) may be taken as the governing

integro-differential equation for the surface elevation, η. Welander (1957)

suggests this solution method. It is not known whether a solution to an

unsteady flow problem has ever been carried out based on Eq. (3.2.75).

For steady flow problems the solution by Murray (1975) is a simple appli-

cation of the above concepts. More elaborate models, in terms of the

boundary geometry, have been advanced by Thomas (1975) and by Witten and

Thomas (1976). It is noted that these applications have been for assumed

steady state conditions, i.e., $\partial \eta / \partial t = 0$ in Eq. (3.2.75). They have,

however, incorporated more or less realistic models of a spatially varying

eddy viscosity. Thus, Murray (1975) assumes an eddy viscosity which varies

with distance from the bottom according to the empirical relationship

obtained by Fjeldstad (1929). Thomas (1975) assumes an eddy viscosity which

varies linearly with distance from the bottom and thus closely resembles the

variation found by Fjeldstad (1929). For mathematical convenience, Witten and Thomas (1976) assume an exponentially decaying eddy viscosity from the surface down. These investigations represent the first attempts at incorporating more realistic models of the vertical eddy viscosity, than have previously been proposed, into the analysis of wind driven circulation in coastal waters.

These recent models of the vertical eddy viscosity seem more realistic than the mathematically convenient assumption of a constant ν_t. Not only would one expect the eddy viscosity to exhibit a spatial dependency, but one would also expect its value to be a function of the flow parameters, i.e., it cannot be specified a priori but is itself a function of the solution. The latter of these expectations is borne out by Thomas' (1975) assumed eddy viscosity.

Thomas' linearly varying eddy viscosity with distance from the bottom boundary furthermore reproduces the classical logarithmic velocity profile in the vicinity of the bottom. It does not, however, reproduce the logarithmic behavior of the velocity deficit near the surface which was found experimentally by Reichardt (1959), Wu (1968) and Shemdin (1972). This experimentally observed behavior of the velocity distribution near the surface is only obtained if the eddy viscosity vanishes at the free surface as is the case for Reichardt's (1959) results. The physical realism of the assumption of a finite eddy viscosity near the surface made by Thomas (1975) and by Witten and Thomas (1976) is therefore in doubt and the considerable computational effort associated with the adoption of these sophisticated models can hardly be considered justified.

3.2.6 Approximate Evaluation of Density Driven Currents

As mentioned in the introduction to this section on advection of oil slicks by currents, it was for simplicity assumed that the fluid was homogeneous. The effect of a varying fluid density enters the dynamics of the problem through the vertical momentum equation

$$\frac{\partial p}{\partial z} = -\rho g \tag{3.2.76}$$

If the assumption made in the previous sections of a constant fluid density is relaxed by taking

$$\rho = \rho(x,y,z,t) \tag{3.2.77}$$

we may integrate Eq. (76) formally to obtain

$$\int_z^\eta \frac{\partial p}{\partial z} \, dz = p(\eta) - p(z) = p_a - p(z) = -g \int_z^\eta \rho \, dz \tag{3.2.78}$$

in which p_a is the atmospheric pressure acting on the free surface.

The pressure distribution in the vertical is therefore given by

$$p(z) = p_a + g \int_z^\eta \rho \, dz \tag{3.2.79}$$

and the pressure gradients in the x and y directions may be found by employing Leibnitz's rule(Hildebrand, 1965, p. 360)

$$\frac{\partial p}{\partial x} = \frac{\partial p_a}{\partial x} + \rho_s g \frac{\partial \eta}{\partial x} + g \int_z^\eta \frac{\partial \rho}{\partial x} \, dz$$

$$\frac{\partial p}{\partial y} = \frac{\partial p_a}{\partial y} + \rho_s g \frac{\partial \eta}{\partial y} + g \int_z^\eta \frac{\partial \rho}{\partial y} \, dz \tag{3.2.80}$$

in which ρ_s is the fluid density at the free surface. The first two terms on the right-hand side of Eq. (3.2.80) are seen to be the terms included in the governing equations, Eqs. (3.2.1) and (3.2.2), for the homogeneous case, and the effect of a varying fluid density consequently enters through the integrals of the density gradients. If it is assumed that $\rho(x,y,z,t)$ is known from measurements the integrals in Eq. (3.2.80) may be evaluated and the resulting expressions for the pressure gradients may be introduced in the analysis, for example, through Eq. (3.2.39).

If it is assumed that the fluid density may be expressed as

$$\rho = \rho_s(x,y,t) + \rho'(x,y,z,t) \tag{3.2.81}$$

Eq. (3.2.80) becomes

$$\frac{\partial p}{\partial x} = \frac{\partial p_a}{\partial x} + \rho_s g \frac{\partial \eta}{\partial x} + g(\eta-z) \frac{\partial \rho_s}{\partial x} + g \int_z^\eta \frac{\partial \rho'}{\partial x} \, dz$$

$$\tag{3.2.82}$$

$$\frac{\partial p}{\partial y} = \frac{\partial p_a}{\partial y} + \rho_s g \frac{\partial \eta}{\partial y} + g(\eta-z) \frac{\partial \rho_s}{\partial y} + g \int_z^\eta \frac{\partial \rho'}{\partial y} \, dz$$

It is difficult to advance a convincing argument for the smallness of the integral terms in Eq. (3.2.82). However, an order of magnitude assessment of the influence of density driven currents in a particular region may be obtained by neglecting these terms. This was done by Bishop and Overland (1977) and resulted in the expression analogous to Eq. (3.2.39)

$$\frac{\partial p}{\partial x} + i \frac{\partial p}{\partial y} = P = \left(\frac{\partial p_a}{\partial x} + \rho_s g \frac{\partial \eta}{\partial x} - gz \frac{\partial \rho_s}{\partial x}\right) + i\left(\frac{\partial p_a}{\partial y} + \rho_s g \frac{\partial \eta}{\partial y} - gz \frac{\partial \rho_s}{\partial y}\right)$$

$$\tag{3.2.83}$$

With this expression for P the analysis presented in Section 3.2.4 still holds, i.e., Eq. (3.2.72) with P given by Eq. (3.2.83). The assumption of the negligible effect of ρ' suggests that a more realistic density variable would be the depth averaged fluid density, $\bar{\rho}$, rather than ρ_s. This was, in fact, the density variable used by Bishop and Overland (1977).

The preceeding simplified analysis of the effect of density driven currents within the framework of the analysis presented for a homogeneous fluid is clearly an oversimplification. It is, however, felt that density driven currents often may play a secondary role in the advection of oil slicks so that an approximate analysis of their contribution should suffice. A more elaborate analysis of density driven currents rapidly becomes very involved as seen from the idealized analysis presented by Stommel and Leetmaa (1972). The preceeding simplified analysis is therefore suggested as reasonable for situations where the density varies slowly with depth. The effect of a stably stratified fluid on the vertical momentum exchange should, however, be kept in mind. For a strong stratification, e.g., associated with the build-up of a thermocline during summer months, a two-layer model may be considered.

The average circulation in a given region, on which the wind driven currents are superimposed, may be estimated from direct measurements, use of a diagnostic model (e.g., Galt, 1975) or predicted from mean circulation models (e.g., Csanady, 1976).

3.2.7 Discussion of Important Parameters

The preceding sections have reviewed some of the available models for predicting the wind-induced surface drift. The important parameters, which must be quantified, in order to carry out the analysis are: (1) the surface shear stress (2) the bottom shear stress (3) the vertical eddy viscosity. A discussion of these parameters, the uncertainty involved in their determination and the resulting uncertainty in the determination of the surface drift current is presented in the following sections.

3.2.7.1 The Surface Wind Shear Stress

Methods for the determination and simulation of the wind field at an elevation of, say, 10 meters above the still water level were discussed in Chapter 2 of this report. In all models, except the Wind Factor Approach (Section 3.2.1), for the prediction of the wind induced current the knowledge of the surface shear stress associated with a given wind field is necessary to implement the model.

The wind shear stress is generally related to the square of the 10 meter wind velocity, W, as given by Eq. (3.2.6). Several investigators have found the wind velocity profile in the lower atmosphere to be approximately logarithmic, i.e.,

$$\frac{u_a}{u_{a*}} = \frac{1}{\kappa} \ln \frac{z}{z_o} \qquad\qquad (3.2.84)$$

in which u_a is the wind velocity at elevation z above the still water level, κ is von Karman's constant ($\kappa \approx 0.4$) and u_{a*} is the shear velocity defined by

$$u_{a*} = \sqrt{\tau_s / \rho_a} = \sqrt{\frac{f_a}{2}} \ W \qquad (3.2.85)$$

where Eq. (3.2.6) has been introduced. The quantity z_0 in Eq. (3.2.84) is the characteristic roughness length of the boundary and is clearly the level at which $u_a = 0$. From an analogy with turbulent shear flow over a fully rough boundary (Schlichting, 1960) one may take

$$z_0 = k_s / 30 \qquad (3.2.86)$$

in which k_s is the equivalent Nikuradse sand roughness of the boundary.

By measuring wind velocity profiles above the sea surface and fitting the observations to Eq. (3.2.84) a value of z_0 or k_s may be obtained. By introducing Eq. (3.2.85) in Eq. (3.2.84) evaluated at $z = 10$ m $= 1000$ cm, the friction factor f_a is found as a function of the surface roughness

$$\sqrt{\frac{2}{f_a}} = 2.5 \ \ell n \ \frac{1000}{z_0} = 2.5 \ \ell n \ \frac{30000}{k_s} \qquad (3.2.87)$$

in which z_0 and k_s are in centimeters.

The above procedure is essentially that followed by Wu (1969) and by Ruggles (1970). A rough examination of Ruggles' data, which are for a range of wind speeds 3 m/s $< W <$ 10 m/s, shows that most of his determinations of the friction factor fall within $\pm$ 40% of the mean value which is $f_a = 3.2 \ 10^{-3}$. From Eq. (3.2.87) it is found that $f_a = 3.2 \ 10^{-3}$ corresponds to a value of $k_s = 1.4$ cm. For the range of wind speeds investigated by Ruggles the friction factor is found by Wu to decrease with wind speed from $f_a = 3.2 \ 10^{-3}$ for $W = 10$ m/s to $f_a = 2.0$ for $W = 3$ m/s. Wu's

results indicated a standard deviation of the various results obtained for f_a, expressed in percent of f_a, to be of the order 22%.

From the preceding examination of a subset of the available data on wind friction factors it may be concluded that the order of accuracy obtained by adopting Wu's results as the basis for evaluating the surface shear stress is approximately $\pm$ 25%. This uncertainty is reflected in the determination of the surface drift current. Thus, it follows from Eq. (3.2.35) that the surface drift current is proportional to the surface shear stress if a value of the constant eddy viscosity, ν_t, is taken to be a function of wind speed only (as suggested by Eq. 3.2.37). If, however, ν_t is determined by the method employed in deriving Eq. (3.2.37), the surface current is independent of the assumed value of the surface roughness since the approach then is nothing more than a disguised wind factor approach.

3.2.7.2 The Bottom Shear Stress

In the procedure employing the depth averaged equations, Section 3.2.1, it is seen from Eq. (3.2.11) that a knowledge of the value of the bottom friction factor is necessary in order to evaluate the bottom shear stress. In the models based on a constant eddy viscosity assumption the knowledge of the bottom shear stress is not necessary since it may be evaluated from the assumed value of ν_t and the solution based on satisfying a no slip condition at the bottom.

In reality the flow over the bottom will be turbulent and a logarithmic velocity profile similar to that given by Eq. (3.2.84) is expected. For the turbulent case an analysis similar to that presented in

the previous section, referencing the shear stress to the velocity at, say, 1 m = 100 cm above the bed would result in expressions for f_b defined by

$$\tau_b = \frac{1}{2} f_b \, \rho \, u_{100}^2 \qquad\qquad (3.2.88)$$

similar to Eq. (3.2.87). Thus, the problem associated with the determination of the bottom shear stress is that of determining the value of the equivalent Nikuradse sand roughness of the bottom k_b.

For a moveable bed, which may exhibit bed forms (ripples), it is by no means easy to estimate the value of k_b. A further difficulty is associated with the presence of waves of sufficient length to feel the bottom. The presence of an oscillatory boundary layer associated with the waves will effectively increase the bottom roughness experienced by the current, i.e., the equivalent bottom roughness is a function of the physical bottom roughness and the wave climate. Research aimed at clarifying this aspect of the interaction of waves and currents is presently being pursued at MIT.

3.2.7.3 The Vertical Eddy Viscosity

The proper parameterization of the vertical eddy viscosity has repeatedly been emphasized as one of the major problems in predicting wind driven currents (Reid, 1975). Various proposed models have been briefly discussed in the preceeding sections. The best way to illustrate the sensitivity of computed results for the surface drift current to the assumption made regarding the vertical eddy viscosity seems to be through example calculations.

As a simple example we consider the two dimensional problem of the wind induced steady current in a flume. Neglecting the influence of a varying atmospheric pressure and Coriolis force the governing equation reads

$$0 = -g \frac{\partial \eta}{\partial x} + \frac{\partial}{\partial z} \left(\varepsilon_z \frac{\partial u}{\partial z} \right)$$
(3.2.89)

with a surface boundary condition of

$$\tau_{s,x} = \frac{1}{2} f_a \rho_a W^2 = \left(\frac{1}{2} f_a \frac{\rho_a}{\rho} \right) \rho W^2 = c_f \rho W^2$$
(3.2.90)

The following characteristics are assumed

Water Depth = h = 10 m

Wind Velocity = W = 20 m/sec

Bottom Roughness = k_b = 2 cm
(3.2.91)

Surface Roughness = k_s = 8 cm (Wu, 1969)

and calculations are carried out for the two cases of an infinite channel, for which $\partial \eta / \partial x = 0$, and for a finite closed channel, for which $\int_0^h u \, dz = 0$.

To determine the surface shear stress Wu's (1969) result is used which gives a value of c_f in Eq. (3.2.90) of $3.1 \ 10^{-6}$. The assumptions made regarding the vertical eddy viscosity as well as the expressions for the resulting velocity profiles are shown in Tables 3.2.1 and 3.2.2 and in graphical form in Figs. 3.2.2 and 3.2.3. Figs. 3.2.2 and 3.2.3 speak for themselves and clearly point out just how crucial the assumption regarding the vertical eddy viscosity is.

Figure 3.2.1 shows the obvious result that the inability of the depth averaged equations to reproduce the strong velocity gradient near

TABLE 3.2.1: VELOCITY PROFILES - INFINITE CHANNEL

Case	Description	Form of Vert. Eddy Viscosity	Velocity Profile	Surf.Veloc. (m/sec)	Mass Flux (m^3/sec-m)
1	depth averaged	N. A.	$\sqrt{\dfrac{2}{f_b c_f}}\, W$	0.69	6.4
2	3% fixed wind factor	N. A.	N.A.	.60	N. A.
3	const. vertical eddy viscosity; no slip bottom boundary condition	$\left[\dfrac{c_f W}{.03\sqrt{\Omega}}\right]^2$	$\dfrac{c_f W^2}{\nu_t}\, z$	.29	2.9
4	const. vertical eddy viscosity slip at bottom	"	$\sqrt{\dfrac{2c_f}{f_b}}\, W + \dfrac{c_f W^2}{\nu_t}\, z$	.93	7.85
5	linear eddy viscosity	$.4\sqrt{c_f}\, Wz$	$\sqrt{\dfrac{c_f W}{.4}}\, \ell n\, \dfrac{30z}{k_b}$	.85	7.5
6	parabolic eddy viscosity	$.4\sqrt{c_f}\, Wz(1-\dfrac{z}{h})$	$\sqrt{\dfrac{c_f W}{.4}}\, \{\ell n\dfrac{30z}{k_b} - \ell n(1-\dfrac{z}{h})\}$	1.55	8.5

TABLE 3.2.3: VELOCITY PROFILES – FINITE CLOSED CHANNEL

Case	Description	Form of Vert. Eddy Viscosity	Velocity Profile	Surf.Veloc. (m/sec)	Surf.Slope $(\partial\eta/\partial x \ 10^5)$
1	depth averaged	N. A.	0	0	1.27
2	3% fixed wind factor	N. A.	N. A.	.60	N. A.
3	const. vertical eddy viscosity, no slip bottom boundary condition	$\left[\dfrac{c_f W}{.03\sqrt{\Omega}}\right]$	$\dfrac{g}{\nu_t}\dfrac{\partial\eta}{\partial x}(\dfrac{1}{2}z^2 - hz) + \dfrac{c_f W^2}{\nu_t}z$	.072	1.90
4	const. vertical eddy viscosity slip at bottom	"	$\dfrac{g}{\nu_t}\dfrac{\partial\eta}{\partial x}(\dfrac{1}{2}z^2 - hz) + \dfrac{c_f W^2}{\nu_t}z + u_b$	.097	1.27
5	linear eddy viscosity	$.4 u_{*b} z$	$\dfrac{g}{.4\|u_{*b}\|}\dfrac{\partial\eta}{\partial x}[z - h\ln\dfrac{30z}{k_b}] + \dfrac{c_f W^2}{0.4\|u_{*b}\|}\ln\dfrac{30z}{k_b}$	.166	1.34
6	parabolic eddy viscosity	$.4\sqrt{c_f}\,Wz(1-\dfrac{z}{h})$	$\dfrac{-gh}{[.4\sqrt{c_f}W}\dfrac{\partial\eta}{\partial x} + \dfrac{\sqrt{c_f}W}{.4}]\ln\dfrac{30z}{k_b} - \dfrac{\sqrt{c_f}W}{.4}\ln(\dfrac{h-z}{h})$	.75	1.41
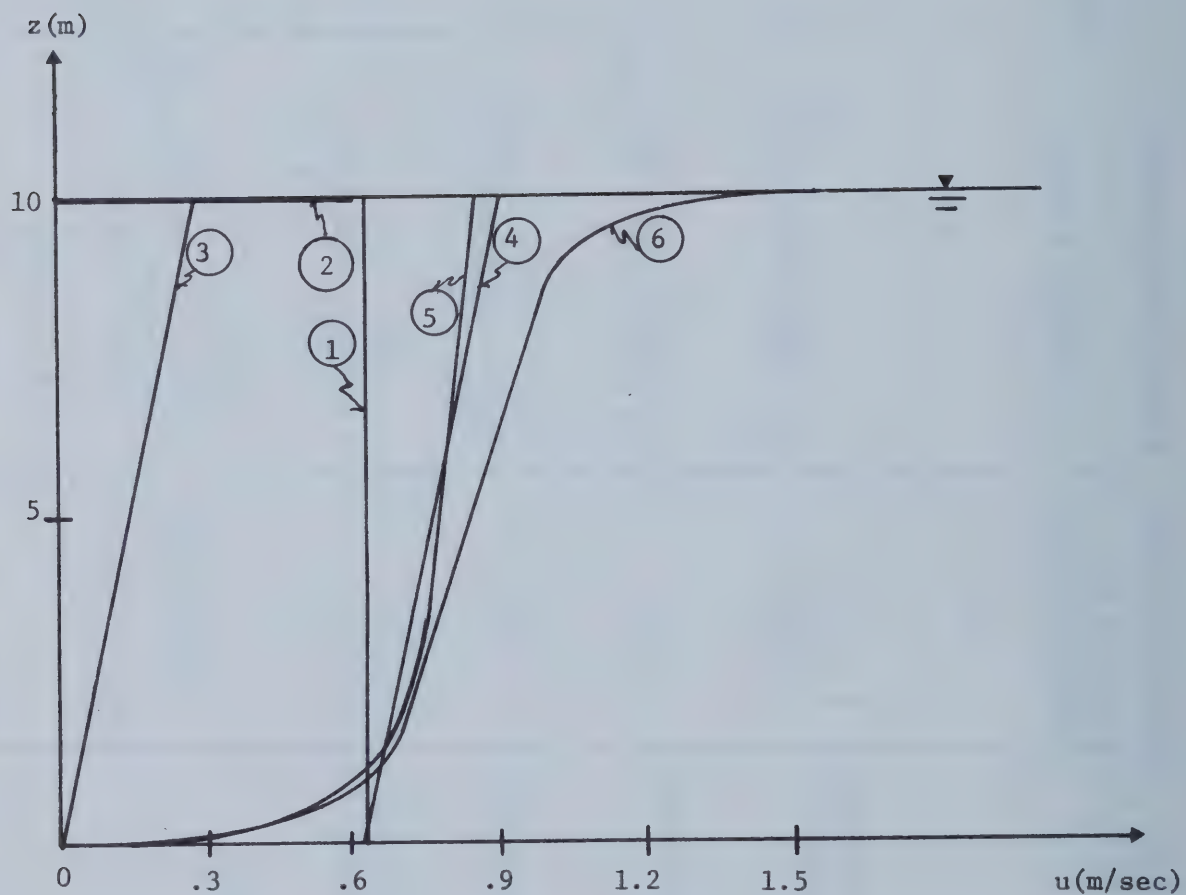
Figure 3.2.2: Velocity Profiles in Infinite Channel as a Function of the Assumed Vertical Eddy Viscosity. (Numbers refer to case number given in Table 3.2.1)
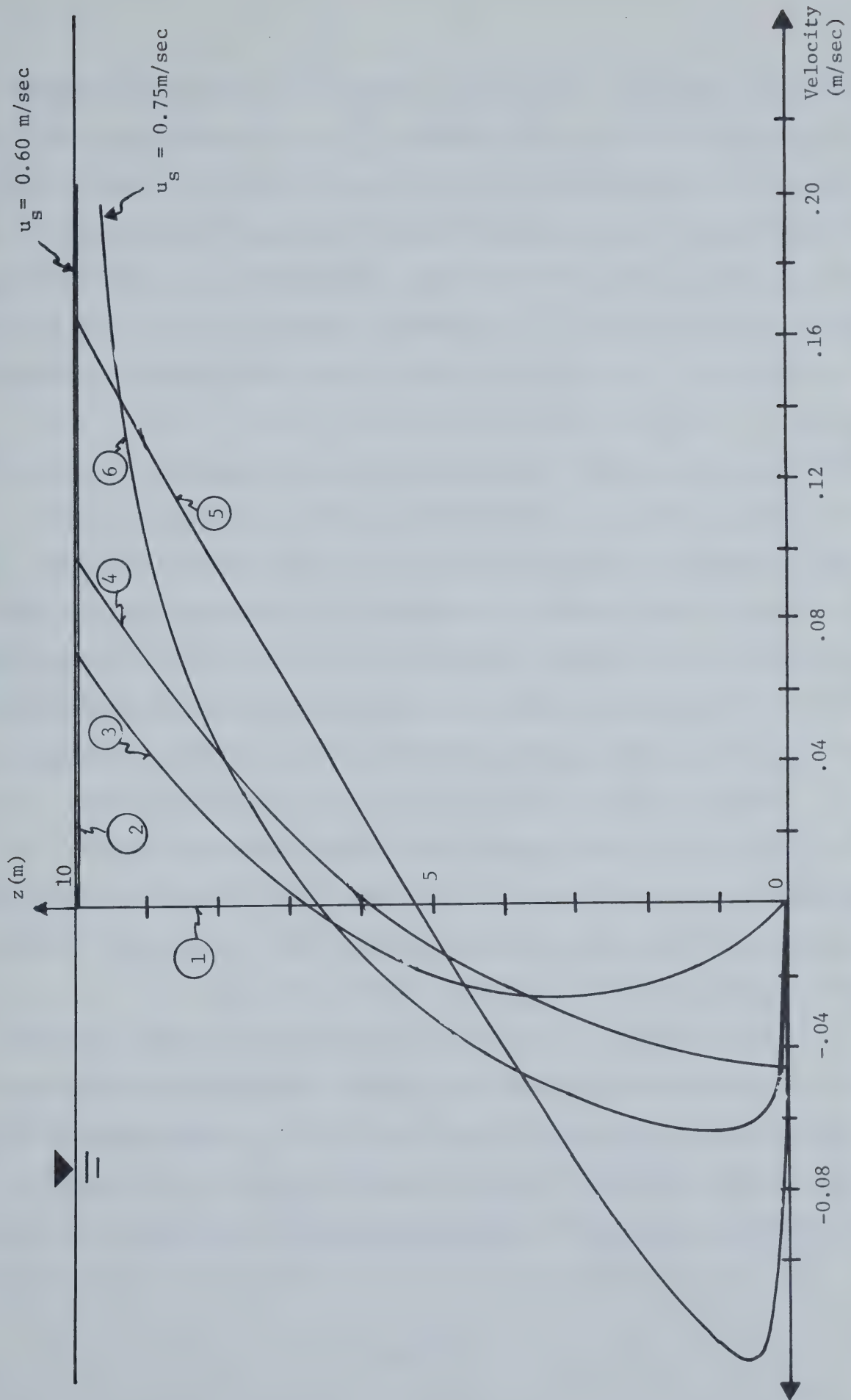
Figure 3.2.3: Velocity Profiles in Closed Channel as a Function of the Assumed Vertical Eddy Viscosity. (Numbers indicate case number given in Table 3.2.2)

3-64

the surface leads to a low estimate of the surface current when compared

with the turbulent Couette flow solution, ⑥ . The constant eddy vis-

cosity with no slip at the bottom is known (Murray, 1975) to lead to much

lower estimates of u_s than observed and a more realistic estimate is ob-

tained by allowing for a slip velocity at the bottom ④ . The linearly

varying eddy viscosity, ⑤ , suggested by Thomas (1975) is seen to lead

to an expression (Table 3.2.1) for the velocity profile which is identical

to that of a turbulent pressure gradient flow, since $\sqrt{c_f}\ W = u_{*_b} = u_{*_s}$,

which seems to be a rather unrealistic result. The parabolic variation of

eddy viscosity, which for turbulent Couette flow is supported by experi-

ments by Reichardt (1959) gives the most physically realistic profile.

The absence of a wave motion in Reichardt's experiments may call for some

adjustments in ε_z. However, the logarithmic velocity defect law near the

free surface, which is a result of the vanishing ε_z at $z = h$, is supported

by experimental evidence given by Shemdin (1972) when waves are present.

Remarks similar to those made above for the infinite channel

(Fig. 3.2.2), can be made for the finite channel case (Fig. 3.2.3). For

the finite channel case it is, however, noticed that the models, which do

not account for the near surface velocity gradient lead to predicted sur-

face velocities an order of magnitude smaller than ⑥ .

In conclusion it is felt that the most realistic models must incor-

porate the features of a logarithmic velocity defect near the surface and

a logarithmic velocity profile near the bottom, i.e., using models of the

vertical eddy viscosity of the type suggested by ⑥ . It is, however,

interesting to note that if, for example, case ⑥ is adopted as the more

realistic one then the surface velocity may with good approximation be
obtained from the sum of the depth averaged and the wind factor approach
for both cases. The depth averaged approach may be regarded as accounting
for the strong velocity gradient near the bottom whereas the wind factor
approach accounts in an approximate manner for the contribution from the
near surface velocity gradients. A further discussion of a model for
the vertical eddy viscosity may be found in Appendix A.

3.2.8 Conclusions Regarding the Advection of Oil Slicks by Currents

The preceding sections have reviewed a hierarchy of models which
may be employed for the purpose of predicting the wind-driven surface
current and hence the speed of advection of oil slicks in the coastal
environment. The applicability of these models was discussed primarily
based on their apparent ability to provide accurate estimates of the sur-
face current with little attention being paid to their practical use in
studies simulating impacts of oil spills.

Re-examining these models in the light of their intended use, the
depth averaged numerical model falls short both because of its poor ability
to predict the surface current and because of its high level of computational
effort.

For simulation of oil spills the wind factor approach has definite
virtues, mainly because of its simplicity. All the models discussed
would require a simulation of the wind field to be applied. For the wind
factor approach a simulation of the wind field is identical to simulating
the oil slick advection, which clearly minimizes the computational effort.
Currents other than wind induced may be computed once and for all using,

for example, the depth averaged equations and prevailing conditions or may be obtained from field measurements. In this respect it should be noted that tidal currents being periodic generally will give rise to only small net advections over several tidal cycles, so the detailed knowledge of tidal currents does not seem crucial to the problem of simulating oil spills occurring far off shore. The value of the wind factor has been found to vary considerably and a more fundamentally sound knowledge of its actual value and its dependency on local conditions, such as water depth, is necessary to render the wind factor approach predictive.

The wind factor approach tacitly assumes the surface current to respond immediately to changes in the surface shear stress. The Ekman approach may to some extent account for the response of the surface current to changing wind stress and the results by Warner et al. (1972) indicate that improved results may be obtained using the Ekman rather than the wind factor approach. This conclusion, however, may not be strictly valid since Warner et al. used a best fit value of ν_t in their use of the Ekman approach whereas no "best fit" value of the wind factor was established. The use of the Ekman approach, based on a physically more realistic model of the vertical eddy viscosity, is discussed by Madsen (1977) and this paper is reproduced in Appendix A. The results of this analysis indicate the response time of the surface drift to be relatively short, of the order 6 hours, thus lending credibility to models which assume instantaneous response.

The Forristall approach, although elegant, does not seem to present a viable tool for the simulation of oil slick advection. A large computational effort is involved and with the surface current being eventually

obtained from an analysis assuming a constant eddy viscosity, i.e., similar to the Ekman approach, it is doubtful whether the increased effort is worthwhile.

As demonstrated in Section 3.2.7, Figs. 3.2.2 and 3.2.3, the lack of a physically realistic model of the vertical eddy viscosity seems to be the main problem in our ability to model wind driven currents. A model, such as the parabolic eddy viscosity variation, which assumes the vertical eddy viscosity to vanish near the free surface and near the bottom seems to be the physically most realistic. An initial attempt at establishing such a model is presented in Appendix A, but further research into this important aspect seems warranted.

3.3   Experimental Basis for Fixed Drift Factors*

The basis for the fixed drift factors commonly used in state-of-the art oil spill drift models originates from two sources: observation of actual spills and controlled experiments, the latter being performed both in the field and in the laboratory.

The approach taken in this section is to examine in a relatively thorough manner representative examples from each of the two major sources. An effort is made to point out not only the specific deficiencies of the representative example but also the weaknesses of the general approach of which the example was taken to be representative.

3.3.1 Observation of Actual Spills

Typical of the first group is Smith's (1968) analysis of the trajectories of various spills from the Torrey Canyon tanker. Basically Smith measured distances and directions traveled by a particular slick, derived from aerial observations and then used wind data from the nearest meteorological station (land-based) to compute the appropriate wind factor and deflection angle. For a particular slick, Smith found the average wind factor to be 3.4% with a deflection angle of 3.3° to the right, but the data upon which these values are based showed a standard deviation of .7% for the wind factor and 11° for the deflection angle.

---

*The term "fixed drift factors" refers to the assumption of a constant wind factor and deflection angle.

This high variability should not be surprising. In his analysis, Smith neglected contributions to overall drift from currents (e.g., tides) and waves. He did not consider the effect of water depth which varied from 0 feet to 350 feet. In addition his calculations were based on the assumption that the slick had moved in a straight line in the time interval between aerial observations. This interval ranged from 24 hrs. to 120 hrs. In addition, wind data were taken from land-based stations which are routinely influenced by such effects as diurnal land/sea breezes.

Smith did apply the 3% rule (0° angle) to a slick observed off the coast of Brittany with fairly good results. However, certain important details such as depth, wave climate, wind magnitude, subsurface current structure, etc., are omitted.

Other investigators have attempted to apply fixed drift factors in hindcasting oil slick movement. Warner et al. (1972) made use of data collected from the 1970 Arrow tanker oil spill which occurred off the coast of Nova Scotia in waters of 300 feet. Knowing the final location and the approximate time of impact of the slick the authors showed that a simple model based upon a 3% wind factor and 0° deflection angle was clearly in error. Part of this discrepancy was due to the omission of subsurface currents which current meter data showed to be important.

Another example of hindcasting was included in a paper by Tomczak (1964). He used slick position and wind data gathered from the 1955 Gerd Maersk tanker spill which occurred in water depths of less than 100 feet, to show that a 4.3% wind factor and 0° deflection angle pre-

dicted the slick position after 11 days. It should be noted that this factor deviates by more than 25% from the 3.4% factor suggested by Smith.

Hence one can conclude that arguments for use of a constant wind factor (and deflection angle) based upon observations of actual spills at sea are weak at best and in fact these observations can be taken to indicate that the drift factors are heavily dependent on local geography, meteorology, and sea state.

3.3.2 Controlled Field Experiments

Controlled field experiments from which fixed drift factors have often been justified, can be broken up into two subsets: experiments utilizing oil and experiments utilizing other drifting bodies such as drift cards or polyethylene plastic sheets.

An often quoted example of a field experiment utilizing drift cards is the research performed by Tomczak (1964). Tomczak placed 2000 drift cards in the North Sea off the coast of Germany in water of up to 1000 feet. The resulting analysis was based upon 960 cards which were returned. Wind velocities at 10 meters were calculated every 6 hrs. from the geostrophic winds (which in turn were derived from the isobars from weather maps). A deflection angle of 0° was assumed.

To determine the value for the wind factor the movement of an imaginary card whose initial location and time of release corresponded to that of a real card, was traced using a given wind factor which was varied from 1.5 to 5.5% in increments of .5%. The trajectory of the imaginary card was traced until either the card reached land or the time at which its real world analog was retrieved. If this final position of

the card was within a certain allowable radius, the imaginary card was
considered a "hit." If the imaginary card did not fall within the
allowable radius, the wind factor was incremented by .5% and the process
was continued. A plot of frequency of hits vs. wind factor was then made
for a given radius of error and a mean value for the wind factor derived.
Tomczak found that for a radius of 50 km, the mean value for the
wind factor was 4.2%.

Tomczak's experiment has many shortcomings, some of which are
common to all classical "drift card" type experiments. These include:

a) the fact that a majority of the drift cards are never re-
    covered (52% - Tomczak, Highs (1956) - 70%). Only those cards
    that drift towards the coast will ever have a chance of being
    recovered.

b) the unknown influence of currents induced by waves, tides, and
    large scale circulation. It has been shown for instance
    (see Section 3.1.1) that wave induced transport can approach
    a 3% drift factor and thus contribute significantly to
    total transport. Thus the so called wind factor derived from
    classical drift card experiments normally includes components
    which are not directly traceable to immediate surface winds.

c) the question of exactly what time the cards were retrieved.
    Because drift card experiments depend mainly upon the general
    public to return the cards, a considerable time lag can exist
    between the time that the card lands and the time it is dis-
    covered.

Other weak points of Tomczak's paper originate from his method of analysis. For example:

i) Recall from the above discussion that the simulated card is followed until either the card reaches land or the time at which its real world analog was retrieved, whichever occurs first. If the meteorology of the area is such that a predominate wind blows primarily inland and perpendicular to the coast (as is the case for the portion of the North Sea, where the author performed his experiments), then it can be seen that the author's method of analysis will tend to predict higher wind factors than may actually exist.

ii) predicted mean value for the wind factor is highly sensitive to variations in the allowable radius of the area of hit. For example if one takes a radius of 40, 50 and 60 km then the predicted mean value is 3.8, 4.2, 4.7% respectively.

iii) the assumption of a 0° deflection angle.

In conclusion, the use of Tomczak's research to justify use of fixed drift factors appears flawed. The experimental weaknesses are due in part to the methods of analysis that the author used and in part to the general, inherent deficiencies of classical drift card experiments. In fact, because of a, b, c above it can probably be concluded that only a very rough, order of magnitude approximation of the wind factor can be gained from Tomczak's work and similar experiments such as Hughs (1956), Neumann (1966) and Tolbert et al. (1964).

Another popular method used to measure drift factors which has been employed in the past by several experimentors (e.g., Smith et al. (1974) and Teeson et al. (1970)), has been to release a drifting body at sea and constantly monitor its movement for a period of time, generally of the order 1 hour or less. In such experiments, subsurface currents are usually monitored using drogues (both Teeson and Smith measured these at a 1 m depth). Wind direction and magnitude are also recorded. Knowing this information and assuming that the drift path is simply a vector sum of the subsurface current plus a component due to the wind,one can find the average deflection angle and average wind factor. Using this method and utilizing plastic polyethelene drifting bodies, Teeson found a mean wind factor of 2.8%[*] and mean deflection angle of 13° right with standard deviations of 1.07% and 7°, respectively, in water depths of 50 to 90 feet. Smith, who used small oil slicks as the drift body found the average wind factor to be .8% with a standard deviation of .67% in water depths of 40 feet.

Though this method is very attractive in theory, it has many shortcomings when applied, as is suggested from the very high standard deviations above. For instance there is the problem that a portion of the subsurface drift is induced directly by the immediate surface wind. Thus the wind effect on surface drift is accounted for twice; once in the wind factored component and once in the subsurface current component.

---

[*]If one of the data points (5.3% associated with a very low wind speed of 2.4 knts) is discarded then the mean becomes 2.41% with a standard deviation of .33%.

Refinement of the procedure would dictate that the wind-induced portion of the subsurface component should somehow be subtracted. To do this one can make use of research performed by Shemdin (1972) who through a series of careful laboratory experiments derived a relationship for the vertical profile of a wind induced current. Using this formula on the work done by Teeson et al. one can arrive at a rough estimate that the wind induced portion of the subsurface current amounted to approximately 10% of the total subsurface current. Thus in the case of Teeson's experiment the effect was relatively small. However, this is due in part to the fact that the wind speeds included in the author's work were small (i.e., less than 7 knots) and therefore the subsurface currents at 1 meter were outside the zone of major influence. This zone increases proportionately to the wind velocity. An additional factor contributing to this relatively low contribution is the fact that the experiment was performed in a relatively shallow, narrow bight area where tidal currents are relatively high.

Another closely related deficiency of this method arises from the fact that the water velocity profile is generally not measured. Instead the subsurface current is usually taken to be the value measured at a single particular depth which may or may not give a representative value. If velocity gradients do exist, as they certainly do in shallower waters, they will affect slick movement. Neither Teeson or Smith took vertical velocity profiles.

In summary, the results of Smith et al. and Teeson et al. offer very little proof as to the fixity of the drift factors. Smith's results

are extremely variable and can be almost immediately disregarded. On the other hand Teeson's results are quite consistent (with the exception of the one data point) but it must be remembered that these experiments were conducted in one location and with a relatively low wind level and thus it is speculative to conclude that the factors calculated are appropriate for all wind speeds and local geometries.

3.3.3 Laboratory Experiments

Justification of the 3% rule has often been based on laboratory experiments including work done by Swartzberg (1971), Keulegan (1951) and Wu (1968). These experiments have typically been conducted in laboratory flumes of narrow width relative to length and with flow in essentially one direction. In these experiments which correspond closely to the conditions assumed for the computational example presented in Section 3.2.7.3, it is fairly easy to reproduce the conditions corresponding to a closed channel whereas the conditions corresponding to an infinite channel are extremely difficult to achieve.

Take for example a closed channel in which a wind shear stress is applied at the free surface by having the top part of the flume enclosed and acting as a wind duct. To drive the air flow above the water there must exist a pressure gradient in the air along the flume direction. This pressure gradient is necessary to overcome the frictional forces resisting the air flow, and is balanced in the water by a water surface slope. In a closed channel, i.e., in the case of no net flow, this surface slope balances the pressure gradient and produces no flow in the water. An additional surface slope is required to balance the surface

shear stress and this slope contributes a return current so that the net flow is zero. Thus, it is, in principle, possible to test in the laboratory the wind induced surface current under conditions corresponding to zero net flow.

To reproduce the conditions corresponding to an infinite open channel, which is unable to sustain a surface slope, is however, not easy, if possible at all. To avoid the establishment of a surface slope balancing the surface shear stress and giving rise to a return current Swartzberg (1971) introduced return channels to allow the return flow to take place in these rather than in the main channel. Swartzberg's equipment consisted of a laboratory flume 19 feet long and 5 feet wide which was partitioned into 3 channels, the one in the middle being 3 feet wide and covered by a wind duct. The two side channels were open on either end of the flume which allowed relatively unrestricted flow of water to and from the middle channel. Thus return currents would hopefully be established in the two side channels, leaving the middle channel to be affected primarily by the wind. Unfortunately Swartzberg did not take vertical velocity profiles in the middle channel and thus it is unclear how successful his attempt to minimize return currents was. It is, however, conceivable that while return channels may reduce return currents in the main channel they may also induce an important extraneous pressure driven current, making this approach unattractive.

For a single channel laboratory flume and for the prototype the pressure gradient will induce a water surface slope but will not result in return currents since the surface slope is supported by the pressure

gradient. However, for a laboratory flume utilizing return channels the existence of this pressure gradient has important consequences. This can best be seen by first noting that the water surface at the end of the flume will be 'flipped-up' relative to the beginning of the flume to balance the pressure gradient. This surface slope will induce a current in the return channels since, unlike the main channel, the surface slope here is not balanced by a pressure gradient. This pressure induced flow in the return channels will be in a direction opposite to the wind in the main channel and will, due to continuity, induce a main channel current. Thus an extraneous current, with no prototype analog, has been induced in the laboratory by the use of return channels.

It is revealing to examine the magnitude of this pressure induced current. The atmospheric pressure at the beginning of the wind tunnel is simply the head loss due to boundary frictional losses times the specific weight of air. The rise in water level at the end of the flume is the pressure drop in the tunnel divided by the specific weight of water. So for Swartzberg's experiment with a 22 inch wind duct height, 30 ft/sec mean wind velocity and 10 inch water depth, the water level rise at the end of the flume will be about .02 inches. The velocity in the main channel can be approximated by equating this elevation head to the boundary frictional losses in the return and main channel. Using the values in the paragraph above one finds the pressure induced current in the main channel to be of the order .3 ft/sec. The wind induced surface current is of the order .9 ft/sec, and thus we see that the pressure induced velocity is of the same order of magnitude as the wind-

induced velocity, thereby raising serious doubts as to the applicability
of return channels in the study of wind induced currents.

The preceeding discussion has demonstrated that it is practically
impossible to model a pure Couette flow in a laboratory wind wave
facility. Since the depth of water in a laboratory flume necessarily
is finite the surface velocity in a pure Couette flow would, as illus-
trated in Section 3.2.7.3 (Fig. 2), be a function of the bottom rough-
ness as well as of the surface shear stress which further would compli-
cate the interpretation of laboratory results. Thus, it is at best
possible to model the case of zero net flow in a laboratory environment.
The flow conditions in the laboratory being significantly different from
prototype conditions even for this special case raises doubt about the
validity of inferring prototype behavior from laboratory model tests.
In the model a limited fetch length limits the surface wave development
and a complete similarity can hardly be achieved. The air flow in the
laboratory is likely to correspond to smooth turbulent flow. This in
turn means that the equivalent boundary roughness and resulting shear
stress in the model are functions of ν_a, the kinematic viscosity of air,
whereas prototype beahvior corresponds to fully rough turbulent flow for
wind speeds exceeding 10 m/sec. To establish the 3% rule from laboratory
experiments can therefore hardly be considered a convincing argument for
the accuracy of this simple rule.

3.3.4 Conclusions Regarding Experimental Basis for Fixed Drift Factors

Many experiments have been performed on the topic of wind induced
surface drift. These works can be broken up into various categories

and it was attempted here to explore, in moderate detail, representative examples from each category which are often quoted as justification for models using fixed wind factors. Various inherent weaknesses of each category were pointed out as well as specific weaknesses peculiar to the particular experiment which was examined. It is important when reviewing research in this field that these weaknesses be kept in mind.

Table 1 is a summary of the results from most of the papers which were mentioned as well as a few additional ones. This table serves to point out two important facts. First, that there exists a high degree of variability in the results of each individual experimentor as indicated by the standard deviations. And second, there exist large discrepancies between the mean drift factors found by individual investigators. More specifically, the wind factor has been found by some investigators to be as low as 0.8% and by others to be as high as 5.8%. The deflection angle suffers from an equally high degree of variability. Thus in the writers' opinion this table coupled with the discussion in the preceeding section lends firm credibility to one of the important conclusions reached in Section 3.2, namely that the fixed drift factor approach represents a considerable oversimplification of a very complex process.

TABLE I

SUMMARY OF VARIOUS EXPERIMENTS INVESTIGATING THE EFFECT OF WIND ON SURFACE DRIFT

Name of Investigator	Nature of Experiment	mean wind factor (%)	standard deviation (%)	deflection angle (degrees)	standard deviation (degrees)
Smith (1968)	hindcasting of observed oil slick	3.4	0.7	3.3 right	11.0
Tomczak (1964)	hindcasting of observed oil slick	4.3	N.A.	0.0	N.A.
"	field experiment with drift cards	4.2	"	"	"
Hughs (1956)	field experiment with drift cards	2.1	0.4	3.5 right	10.7
"	" " "	2.2	0.4	0.3 left	8.6
Neumann (1966)	" " "	4.2	N.A.	0.0	N.A.
Teeson et al (1970)	field experiment with plastic sheets	2.8	1.1	13 right	7.0
Smith et al (1974)	field experiment with drifting oil	0.8	0.7	none	none
Swartzberg (1971)	lab experiments with oil as drift medium	3.7	0.2	N.A.	N.A.
Keulegan (1951)	lab experiments (at high Reynolds #'s)	3.3	none	N.A.	N.A.
Van Dorn (1953)	field experiments in a small basin	3.3	none	N.A.	N.A.
Doebler (1966)	field experiments made off fixed platform	1.6	none	5.2 right	none
"	using a drifting current pole	1.2	none	13.2 right	none
"	"	4.3	none	1.9 right	none
"	"	5.8	none	4.8 right	none
Wu (1968)*	lab experiment	4.1	0.9	N.A.	N.A.

* Wu actually found the wind factor to be a function of wind speed. The mean wind factor is derived by simply taking the mean of all Wu's data points.

3.4   General Conclusions Regarding the Advection of Oil Slicks

The preceding critical examination of two of the possible mechanisms for advection of oil slicks in the coastal environment has revealed our rather poor basic understanding of and ability to quantify these mechanisms.

For the advection of oil slicks by wave induced mass transport it seems evident from the limited information available that a realistic analysis should account for the presence of a highly viscous surface film. Yet, no such analysis has been performed.* In fact, even when the surface is considered clean the results for the wave induced surface drift in a viscous fluid yield physically unrealistic results (the surface drift increases proportionally to the depth). Thus, in order to tentatively assess the importance of waves in the advection of oil slicks one is left with Stokes inviscid solution, whose validity in the present context at best can be considered doubtful. For a fully developed sea in deep water the application of Stokes theory shows that the surface drift can be expressed as a percentage of the wind velocity. This result coincides with the wind factor approach often used in oil slick advection studies and may therefore, at first sight, seem pleasing. The wind factor approach is, however, based on considerations of the surface shear stress associated with the wind, i.e., entirely ignoring the waves, and one is therefore left with the unpleasant dilemma: are the advective processes of waves and wind shear additive or not? This question could readily be ignored if it were not for the fact that the two contributions are of the same order of magnitude (waves of the order 2% of the wind speed, wind shear considerations of the order 3%).

_____

*Except for Milgram (1977)

A heuristic argument is presented here, which suggests that the wave induced mass transport velocity is capable of supporting part of the surface shear stress exerted by the wind. This conjecture, which presently is unsubstantiated, means that the advective processes of waves and wind shear are not additive in a simple manner. It is emphasized that this partition of surface shear stress among waves and a wind-driven current is of major importance to the prediction of oil spill trajectories.

It remains to be shown decisively whether or not wave induced mass transport contributes significantly to the advection of oil slicks in the coastal environment. Until this question is resolved modeling oil slick advection based solely on considerations of currents is potentially in error by a factor of the order 2. What is needed is a thorough theoretical analysis of mass transport in water waves which in a physically realistic manner accounts for the presence of a thin, highly viscous and moveable surface film. This analysis should be performed for the case of a pure wave motion, i.e., with a free surface condition of zero shear stress and for the case of the combined action of waves and a surface shear stress. In view of the limited success of past efforts by prominent hydrodynamicists attempting to clarify the complicated problem of mass transport in water waves it should be recognized that such a study is no easy undertaking and that long term funding of basic research would be called for.

In comparison with the advection of oil slicks by waves the problem of advection by currents, primarily wind induced, is on a somewhat firmer foundation. At least there are a number of relevant models which may be used to quantify this mechanism. The main shortcoming of the more elaborate

of these models is that they rest on an assumed constant eddy viscosity.
This constant eddy viscosity assumption severely limits the physical
realism of these models and an improved ability to parameterize the vertical
eddy viscosity in particular to determine its spatial variation, is
tantamount to the viability of these models.

As a result of the present review a physically more realistic model
of the vertical eddy viscosity is suggested to be one which reproduces
the logarithmic velocity profile near the solid bottom and a logarithmic
velocity deficit near the free surface. The features are reproduced if
the vertical eddy viscosity is assumed to vary linearly with distance
from a sheared boundary. An initial paper employing such a vertical eddy
viscosity model, Madsen (1977), has been accepted for publication and is
reproduced in Appendix A.

Even if the more elaborate models, Ekman and Forristall approaches,
were based on a more fundamentally sound parameterization of the vertical
eddy viscosity as for example that suggested by Madsen (1977) the consid-
erable computational effort involved in their application would conceivably
make them impractical for use in simulation studies of oil slick advection.
The main reason for seeking to establish an elaborate model, based on
fundamentally sound physical principles, would be that such a model could
be used to clarify the dependency of the wind factor on water depth, wind
field and location in a given area. Basically an elaborate and truly
predictive model could be used to replace the need for field measurements
for the purpose of obtaining empirical wind factors. For the purpose
of simulating oil slick trajectories the wind factor approach seems to

offer the best solution. As clearly demonstrated by the compilation of available information on experimentally determined wind factors our ability to "predict" its appropriate value leaves a lot to be desired. Depending on method of analysis and location, wind factors obtained empirically vary from less than 1% to more than 4%. This range of possible values clearly indicates that a fixed wind factor approach potentially may be in error by a factor of 2.

The main conclusion of this examination of our ability to predict the advection of oil slicks in the coastal environment is rather discouraging: we can't do it with any degree of confidence in the results. What is needed is an improved understanding of the fundamental mechanisms governing advection of oil slicks by waves and currents.

CHAPTER 4

OIL SLICK TRANSFORMATIONS

In addition to being able to predict the transport of the oil spill, it is often of value to know the areal extent, volume, and physical and chemical characteristics of the slick as a function of time after the spill. Such information may be vital in adapting oil containment and clean-up measures to the physical characteristics of the slick. Also, the ecological consequences of a spill are largely determined by the relative concentrations of toxic components in the slick or in the water column.

Accordingly, the purpose of this chapter is to treat the physical, chemical and biological processes that bring about changes in the shape, size, and composition of the slick. As with the previous chapters, the emphasis in this treatment will be on the state-of-the-art level of understanding of the basic transformation processes and on the various conceptual models that have been formulated on the basis of this knowledge. First, section 4.1 will present information on the relevant physical and chemical properties of oil. Next, in section 4.2 an attempt is made to discuss the various transformation processes in terms of a single analytical framework that will be of use in the later treatments of individual processes. Section 4.3 then analyzes the physical processes of spreading and dispersion that tend to change the distribution of oil about the center of mass of the slick. Section 4.4 discusses the various physical, chemical, and biological weathering processes that change the total mass and composition of the slick. Finally, section 4.5 presents general conclusions regarding the state of the art in modeling oil slick transformations with an emphasis on a discussion of the possible interaction between the various processes as determined by the time scale within which the slick transformations are considered important.

4.1 Oil Properties

Oil is a mixture of hundred or thousands of hydrocarbons whose individual chemical and physical properties vary widely. The properties of the oil as a whole depend in some manner on the properties of the individual constituents. Since these constituents weather at different rates, the slick's properties change with time. Knowledge of the physical and chemical properties of hydrocarbons is also necessary in order to predict the rate and direction these weathering reactions will take and what the environmental harm might be. The composition of the oil is at least as important as climatic and environmental conditions during a spill in determining the fate of oil on natural waters.

Compounds in oil can be categorized either by chemical structure or by boiling point. Structurally, the main types of hydrocarbons in oil are the alkanes (or paraffins), the cycloparaffins (naphthenes) and the aromatics. Paraffins can be either normal (straight carbon chains) or iso-paraffins (branched chains). Petroleum also contains some organic compounds containing other elements such as nitrogen, sulfur, oxygen and metals, which are commonly referred to as NSO's or asphaltenes. It is not necessary for purposes of this report to further discuss the details of the various chemical structures.

The boiling point classification is often used in the refining industry because the various refined petroleum products are separated from one another by distillation. The boiling point of a hydrocarbon is closely related to the number of carbon atoms in its molecule. Substances with more carbons boil at higher temperatures. Hydrocarbons with the same number of carbons boil at nearly the same temperature, with iso-

paraffins boiling at slightly lower temperatures than paraffins and
aromatics at slightly higher levels. The boiling point classification,
then, is essentially equivalent to a classification by carbon number.

The gas fraction boils at temperatures below 40°C and contains
paraffins C_2 to C_5 which exist as gases at room temperature. The gaso-
line fraction boils between 40°C and 180°C and contains paraffins C_6 -
C_{10} and lighter aromatics such as benzenes. Kerosene boils from 180° -
230°C and encompasses carbon numbers 10-12. Light gas oil (C_{13} - C_{17})
boils between 230°C and 305°C. Heavy gas oil and light lubricating dis-
tillate (C_{18} - C_{25}) boil between 305°C and 405°C. The lubricant fraction
(C_{26} - C_{38}) boils between 405°C and 515°C. Still heavier hydrocarbons
are classified as the residuum. Often, information on the boiling point
distribution of oil is presented not in terms of discrete fractions but
as a continuous distillation curve showing the cumulative percentage
of the oil which will boil by a certain temperature.

Crude oils contain all of the above fractions. Fuel oils and
diesel oils are blends of several of the fractions and boil between
170°C and 370°C. Bunker C fuel oil, a variety commonly involved in
spills, contains mostly compounds with 30 or more carbons, representing
the heaviest fractions of the crude oil. Crudes and refined products
vary widely in composition with respect to distribution of both carbon
numbers and hydrocarbon types, although the refined products in general
contain larger proportions of aromatics than do crude oils. In general,
also, whatever paraffins are present tend to be concentrated at the lower
end of the molecular weight scale. The upper end is comprised mainly of
cycloparaffins, NSO's, and naphtheno-aromatics, compounds with both

cycloparaffin and aromatic rings (Moore et al., 1973).

The physical and chemical properties of hydrocarbons vary with both carbon number and chemical structure, although for a given property one classification scheme may be far more useful than the other. Toxicity and solubility are correlated more strongly with chemical structure, whereas density, vapor pressure (and boiling point itself) depend on carbon number. Brief summaries of the useful physical and chemical properties of hydrocarbons follow.

Slick Characteristics

The three physical properties of most interest, particularly for calculations of oil spreading, are density, viscosity and surface tension.

Crude and fuel oils have densities slightly lower than that of water. Specific gravities range from 0.8 to 0.95. The specific gravity of a slick is equal to the average of the specific gravities of each component, weighted by the fraction of the oil represented by that component. The density of a crude oil is often reported in terms of API gravity, given by

$$\text{API gravity} = \frac{141.5}{\text{specific gravity}} - 131.5 \qquad (4.1.1)$$

Denser oils have lower API gravities and the API gravity of a mixture is not a simple weighted average of individual API gravities. Hence it is better to work with specific gravities or densities whenever possible. The density of a slick increases with weathering because the lighter fractions are the most volatile.

Viscosities of crude and fuel oils vary widely, with most falling in the range between 5 and 50 centipoises. By comparison, water's viscosity at 20°C is 1 cp. Viscosities of the various oil fractions vary from less than 1 cp for gasoline to about 10,000 cp for the heaviest residuals. Viscosity is not an additive property, so the viscosity of a mixture cannot be figured from an average of component values. There are several techniques, however, for estimating the viscosity of a mixture (see e.g., Nelson, 1958). The heavier hydrocarbons are more viscous, so viscosity increases with weathering, often by several orders of magnitude (Hellmann, 1971).

Three slick surface tension coefficients are defined:

σ_{aw} = surface tension of water with respect to air

σ_{oa} = surface tension of oil with respect to air

σ_{ow} = oil-water interfacial tension.

Since σ_{aw} (72.75 dynes/cm at 20°C) does not change, it is the two other terms that are of most interest. σ_{oa} is typically around 24 dyne/cm for many crudes (Berridge, Dean et al., 1968). σ_{ow} varies from 15 to 25 dyne/cm. Thus a typical value for f_n, the surface tension spreading force (as described in Equation 4.3.4), is 30 dyne/cm. Surface tension coefficients for individual components vary over a wider range and those of heavier hydrocarbons have negative values (Phillips and Groseva, 1975). The surface tension coefficient of a mixture is not easily determined from the surface tension of the components. It appears that certain compounds with high positive coefficients spread out first, clearing the way for other components to follow (Berridge, Dean et al., 1968; Phillips and Groseva, 1975).

One other physical property of an oil that deserves a brief mention is the pour point. This is the temperature at which an oil will congeal, behaving as a semi-solid mass instead of a liquid. The pour point of Bunker C oil is about 20°C (National Academy of Sciences, 1975). Pour points of crude oils have been reported as high as 7°C (Berridge, Dean et al., 1968) but most crudes have pour points well below 0°C. Hence for most oils other than Bunker C, and under most conditions other than winter at high latitudes, the slick can be treated as a liquid.

Vapor Pressure

The rate of evaporation of a substance depends on the vapor pressure of the substance, as will be discussed further in Section 4.4.1. There are several means of calculating or finding the vapor pressure of a hydrocarbon as a function of temperature. It is obvious that the vapor pressures for all compounds in a given boiling fraction will be similar.

The exact relationship between vapor pressure and temperature is a result of the first two laws of thermodynamics (Kirk and Othmer, 1955):

$$\frac{dP}{dT} = L(V_G - V_L)T \qquad\qquad (4.1.2)$$

where P is the vapor pressure, L is the molar heat of vaporization, T the absolute temperature, V_G the molar volume of the vapor and V_L the volume of an equal mass of liquid. If we assume V_L is negligible compared to V_G and if we treat the vapor as an ideal gas for which

$V_G = \dfrac{RT}{P}$, we arrive at the commonly used Clausius-Clapeyron equation:

$$\frac{dP}{dT} = LP/RT^2 \tag{4.1.3}$$

If we assume constant L and integrate we get:

$$\ln P = -\frac{L}{RT} + B \tag{4.1.4}$$

where B is a constant of integration.

Another common relationship is the Antoine equation:

$$\log_{10}P = B - A/(C+T) \tag{4.1.5}$$

when T is the temperature in °C. A, B and C are characteristic of a given hydrocarbon. It can be seen that if C = 273.15, the Antoine equation reduces to the integrated form of the Clausius-Clapeyron equation (4.1.4). Since it has been found that C does not equal 273, the Antoine equation is generally the more accurate of the two.

Values of vapor pressure of many hydrocarbons have been catalogued. The most complete compilation is that of Zwolinski and Wilhoit (1971), who give values for the Antoine coefficients. Stull (1947) also presents a good collection. There are several other methods for estimating vapor pressure from boiling point or from molar latent heat of evaporation. Kirk and Othmer (1955) present a survey of such methods.

Solubility

The solubility of a hydrocarbon is useful in predicting both weathering pathways and possible biological harm. Solubility figures, however, are difficult to utilize correctly for predictive purposes. For one, dissolution is not the only means by which oil can enter the water column. Also, figures quoted for the solubility of various hydrocarbons are inconsistent owing to difficulties both in measuring small concentrations and in distinguishing between true dissolution and other processes. The use of solubility figures in modeling will be discussed more fully in Section 4.4.2.

Suffice it to say for now that while oil and water are generally considered immiscible, the solubilities of certain hydrocarbons are not negligible. As Table 4.1.1 shows, the lower aromatics are far more soluble than the paraffins, with benzene (1780 ppm) and toluene (515 ppm) the most soluble of all.

Hydrocarbon dissolution can be conceptualized as a reorienting of water molecules around a hydrocarbon molecule (Shaw, 1976). Hydrocarbons whose molecules require larger cavities in the water have lower solubilities. More exactly, several researchers (Hermann, 1972; Harris et al., 1973) have found that the logarithm of solubility varies linearly with the surface area of the cavity just large enough to accommodate a solute molecule. The presence of salt, in effect, makes cavity formation energetically more difficult. As can be seen in Table 4.1.1, solubilities in salt water are lower (by about 30 per cent for many hydrocarbons) than those in distilled water.

Toxicity

Inasmuch as oil spill trajectory and weathering models might be used in the assessment of potential ecological harm, it is necessary to know something of the toxicities of the various petroleum hydrocarbons. The effects of hydrocarbon exposure depend on the species, the life stage of the organism and the duration of exposure.

The most harmful hydrocarbons are the lower and middle aromatics. Paraffins with 10 or fewer carbons can cause narcosis, but only in concentrations greater than are likely to be found beneath a slick (Moore et al., 1973). Polycyclic aromatics, while not as immediately harmful as the lower aromatics, can cause cancer and may pose a hazard to humans if they are passed up the food web. Among the single and double ring aromatics, toxicity increases with increasing substitution in the molecular structure. Hence ethyl benzene is more toxic than toluene, which in turn is more toxic than benzene; the dimethylnaphthalenes are more toxic than methylnaphthalenes, which in turn are more toxic than naphthalene (Rice, 1976). This is the reverse of the order of increasing solubility. The tradeoff between the toxicity of the hydrocarbons and the amount of them which may dissolve makes it difficult to pinpoint one specific compound as the most dangerous.

Reviewing the literature in existence as of 1973, Moore et al. (1973) found that adult organisms can suffer sublethal effects when exposed to aromatic concentrations on the order of 1 ppm and lethal effects from 10-100 ppm. Most aquatic plant life is not harmed by 100 ppm aromatic levels. Larvae are susceptible to concentrations of .1 ppm.

Objectionable tastes in fish can result from water concentrations
of 1-10 ppb over a few days. Studies and reviews done since Moore's
have discovered sublethal effects, such as impairment of growth, in
juveniles and larvae, from exposure to naphthalene concentrations less
than .1 ppm (See, e.g. Rice, 1976; Anderson, 1976).

The fact that aromatics are the most toxic compounds has several
implications. One is that spills of refined oil products are potentially
more harmful than spills of crude oil, because the refined products con-
tain greater amounts of aromatics in the proper ranges (Lasday and
Mertens, 1976). Another is that weathering will make the slick less
toxic, since aromatics are both very volatile and fairly soluble.
The biological harm resulting from a spill will be determined to a
large extent by the competition for aromatics between the atmosphere
and the water column. It is unfortunate from a biological point of view
that the aromatics are both the most soluble of petroleum hydrocarbons
and the most toxic.

Table 4.1.1 Solubilities of Hydrocarbons in Water

Room Temperature Solubility (PPM) in

Hydrocarbon	Salt Water	Distilled Water	Source
N-Paraffins			
n-hexane	11(b)	9.5(a), 15(b)	a = McAuliffe (1966)
n-octane	1.0(b)	0.66(a), 1.4(b)	b = Freegarde, et al. (1971)
n-C_{12}	.0029	.0037	Sutton and Calder (1974)
n-C_{15}	.0008	.0021	Sutton and Calder (1974)
n-C_{26}	.0001	.0017	Sutton and Calder (1974)
Cycloparaffins			
Cyclohexane		55	McAuliffe (1966)
Cyclooctane		7.9	McAuliffe (1966)
Aromatics			
Benzene	1250(b)	1780(a)	a = McAuliffe (1966)
Toluene		515(a)	b = Lassiter (1974)
O-Xylene		175	McAuliffe (1966)
Ethylbenzene		152	McAuliffe (1966)
Isopropyl benzene		50	McAuliffe (1966)
Naphthalene	22	31	Eganhouse and Calder (1976)
1-Methylnaphthalene		25	Eganhouse and Calder (1976)
Biphenyl	4.8	7.5	Eganhouse and Calder (1976)
1,5 Dimethylnaph- thalene		2.7	Eganhouse and Calder (1976)
Phenanthrene	0.7	1.1	Eganhouse and Calder (1976)

4.2 Analytical framework for Describing Oil Slick Transformations

Oil slick transformation is influenced by a number of physical processes that are complex in their own right and in their interactions. The basic investigations and attempts to model these processes, which will be reviewed in this chapter, involve many different analytical and descriptive approaches that are often difficult to compare and contrast. Accordingly, it is useful to specify a single analytical framework for describing oil slick transformations that will provide a consistent notation with which to summarize the collective achievements of previous individual efforts.

Consistent with the scope of this review outlined in Chapter 1, the following framework will be used to describe transformations of surface oil slicks:
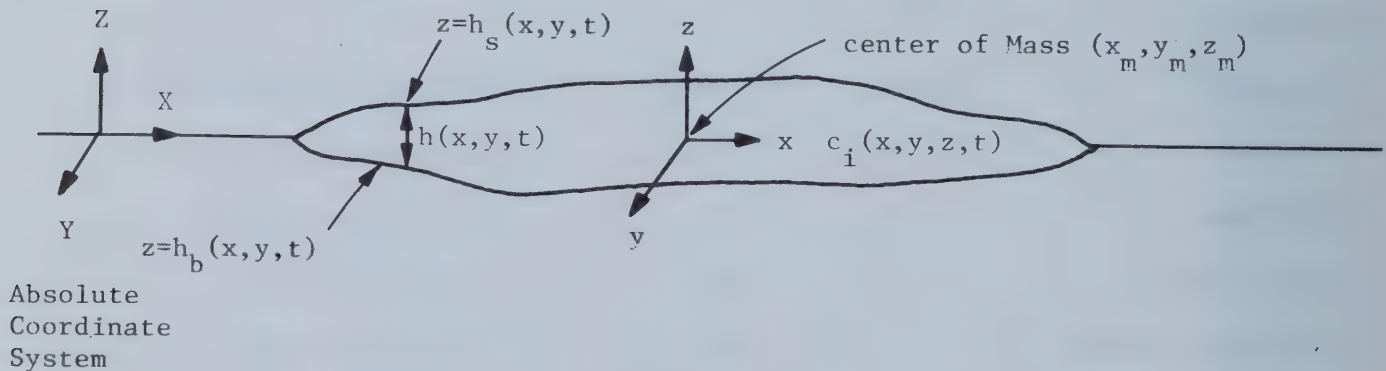
where:

   c_i = mass per unit volume of oil of the ith oil fraction

   h_s = vertical position of the slick surface

   h_b = vertical position of the slick bottom

The average slick density ρ, at any point is given by:

$$\rho = \sum_i c_i \qquad\qquad (4.2.1)$$

The coordinates of the center of mass are then given by:

$$X_m = \frac{\int_{-\infty}^{\infty} \int_{-\infty}^{\infty} \int_{h_s}^{h_b} \rho X \, dX \, dY \, dZ}{\int_{-\infty}^{\infty} \int_{-\infty}^{\infty} \int_{h_s}^{h_b} \rho \, dX \, dY \, dZ}$$

$$Y_m = \frac{\int_{-\infty}^{\infty} \int_{-\infty}^{\infty} \int_{h_s}^{h_b} \rho Y \, dX \, dY \, dZ}{\int_{-\infty}^{\infty} \int_{-\infty}^{\infty} \int_{h_s}^{h_b} \rho dX \, dY \, dZ} \qquad (4.2.2)$$

$$Z_m = \frac{\int_{-\infty}^{\infty} \int_{-\infty}^{\infty} \int_{h_s}^{h_b} \rho Z \, dX \, dY \, dZ}{\int_{-\infty}^{\infty} \int_{-\infty}^{\infty} \int_{h_s}^{h_b} \rho \, dX \, dY \, dZ}$$

If each oil fraction has a density ρ_i, then the following volumetric re-lationship also holds:

$$\int_{h_b}^{h_s} (\Sigma \frac{c_i}{\rho_i}) \, dz = h_s - h_b = h = \text{local slick thickness} \qquad (4.2.3)$$

In terms of the notation defined above, the oil slick transformations to be discussed in this chapter are represented by variations in the oil concentration distribution function $c_i(x,y,z,t)$ and the slick thickness function, $h(x,y,t)$. These functions are governed by the following differential conservation law for the mass of the ith oil fraction

$$\frac{\partial c_i}{\partial t} + \frac{\partial uc_i}{\partial x} + \frac{\partial vc_i}{\partial y} + \frac{\partial wc_i}{\partial z} = k_i \left(\frac{\partial^2 c_i}{\partial x^2} + \frac{\partial^2 c_i}{\partial y^2} + \frac{\partial^2 c_i}{\partial z^2}\right) - R_i$$

$$-k_i \left.\frac{\partial c_i}{\partial z}\right|_{z = h_s} = \phi_{si}$$

(4.2.4)

$$k_i \left.\frac{\partial c_i}{\partial z}\right|_{z = h_b} = \phi_{bi}$$

where k_i = molecular diffusion rate for the ith oil fraction within the slick

R_i = rate of removal of the ith oil fraction per unit volume

ϕ_{si} = flux of the ith oil fraction outward through the surface of the slick

ϕ_{bi} = flux of the ith oil fraction outward through the bottom of the slick

u,v,w = components of the oil motion relative to the center of mass of the slick.

The above equation expresses the changes in $c_i(x,y,z,t)$ that are brought about by advection relative to the center of mass diffusion through the slick boundary, and internal decay. These physical processes are treated in detail separately in the following sections of this chapter.

4.3 Spreading and Dispersion of Oil Slicks

This section will analyze the changes in $c_i(x,y,z,t)$ and $h(x,y,t)$ that result from the oil motion (u,v,w) relative to its center of mass. Accordingly, it is first necessary to write the basic differential momentum equations governing the oil movement. The use of simplified forms of the total governing equation set (mass and momentum) to analyze oil behavior will then be discussed.

4.3.1 Basic Momentum Laws for Surface Oil Slicks

The momentum equations for the oil slick are developed assuming (1) the acceleration of the center of mass is small; (2) Coriolis effects are negligible; (3) the pressure is hydrostatically distributed; (4) the oil density variations are important only in determining the pressure gradients (Boussinesq assumption) (5) the oil is non-turbulent:

$$\frac{\partial u}{\partial t} + u\frac{\partial u}{\partial x} + v\frac{\partial u}{\partial y} + w\frac{\partial u}{\partial z} = -\frac{g}{\rho}\int_z^{-\infty}\frac{(\rho-\rho_w)}{\partial x}\,dz + \nu\left[\frac{\partial^2 u}{\partial x^2} + \frac{\partial^2 u}{\partial y^2} + \frac{\partial^2 u}{\partial z^2}\right]$$

$$\frac{\partial v}{\partial t} + u\frac{\partial v}{\partial x} + v\frac{\partial v}{\partial y} + w\frac{\partial v}{\partial y} = -\frac{g}{\rho}\int_z^{-\infty}\frac{(\rho-\rho_w)}{\partial y}\,dz + \nu\left[\frac{\partial^2 v}{\partial x^2} + \frac{\partial^2 v}{\partial y^2} + \frac{\partial^2 v}{\partial z^2}\right]$$

$$(4.3.1)$$

where ρ_w = the density of the water underlying the oil slick (assumed constant) and ν = kinematic viscosity of oil. The significant surface and bottom boundary conditions related to the above equations are:

$$\nu \left. \left(\frac{\partial u}{\partial z} + \frac{\partial w}{\partial x} \right) \right|_{z = h_s} = \frac{\tau_{sx}}{\rho} \qquad \nu \left. \left(\frac{\partial v}{\partial z} + \frac{\partial w}{\partial y} \right) \right|_{z = h_s} = \frac{\tau_{sy}}{\rho}$$

$$(4.3.2)$$

$$\nu \left. \left(\frac{\partial u}{\partial z} + \frac{\partial w}{\partial x} \right) \right|_{z = h_b} = \frac{\tau_{bx}}{\rho} \qquad \nu \left. \left(\frac{\partial v}{\partial z} + \frac{\partial w}{\partial y} \right) \right|_{z = h_b} = \frac{\tau_{by}}{\rho}$$

where τ_{sx}, τ_{sy} = shear stresses on the oil slick surface

τ_{bx}, τ_{by} = shear stresses on the oil slick bottom.

In addition, at the lateral boundary of the slick, the following force
balance exists between the oil and water surface tensions
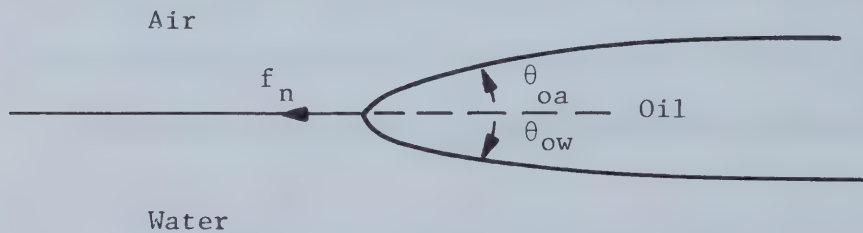
f_n = net surface tension force per unit length of slick boundary =

$$\sigma_{aw} - \sigma_{oa} \cos\theta_{oa} - \sigma_{ow} \cos\theta_{ow} \qquad\qquad (4.3.3)$$

where σ_{aw} = surface tension of air-water surface

σ_{oa} = surface tension of air-oil surface

σ_{ow} = surface tension of oil-water interface.

In most cases it is reasonable to assume that θ_{oa} and θ_{ow} are small so that f_n is given by

$$f_n = \sigma_{aw} - \sigma_{oa} - \sigma_{ow} \qquad\qquad (4.3.4)$$

4.3.2 Vertically Averaged Equations

The full set of governing differential equations developed in the previous section is clearly not tractable by either analytical or numerical methods, primarily because of the three-dimensional framework. For this reason, all analyses of oil motion utilize a simpler form of the governing equations obtained by considering vertically averaged values of c_i, u, and v (w drops out). This approximation is justified by the typically small thicknesses of oil slicks and by the large ratio of oil viscosity to water viscosity, both of which tend to produce relatively uniform profiles of u and v within the slick and negligibly small vertical velocities. It should be noted, however, that the averaging is justified on this basis only for the analysis of the oil motion and may not in some cases be a good approximation for studying the diffusion of oil through the slick boundaries.

Depth average values of c_i, u, v, and R are defined by:

$$\overline{c}_i = \frac{1}{h} \int_{h_b}^{h_s} c_i \, dz$$

$$\overline{u} = \frac{1}{h} \int_{h_b}^{h_s} u \, dz \qquad\qquad (4.3.5)$$

$$\overline{v} = \frac{1}{h} \int_{h_b}^{h_s} v \, dz$$

$$\overline{R}_i = \frac{1}{h} \int_{h_b}^{h_s} R \, dz$$

The governing equations for these averaged quantities are obtained by averaging the basic equations in the same manner, yielding the following:

$$\frac{\partial \overline{c}_i h}{\partial t} + \frac{\partial \overline{u} h \overline{c}_i}{\partial x} + \frac{\partial \overline{v} h \overline{c}_i}{\partial y} = k_i \left[\frac{\partial}{\partial x} \left(h \frac{\partial \overline{c}}{\partial x} \right) + \frac{\partial}{\partial y} \left(h \frac{\partial \overline{c}}{\partial y} \right) \right] - \phi_{si} - \phi_{bi} - \overline{R}_i h$$

$$\frac{\partial \overline{u}}{\partial t} + \overline{u} \frac{\partial \overline{u}}{\partial x} + \overline{v} \frac{\partial \overline{u}}{\partial y} = -g \left(\frac{\rho_w - \overline{\rho}}{\overline{\rho}} \right) \frac{\partial h}{\partial x} - \frac{\tau_{bx}}{\rho h} + \frac{\tau_{sx}}{\rho h} \qquad\qquad (4.3.6)$$

$$\frac{\partial \overline{v}}{\partial t} + \overline{u} \frac{\partial \overline{v}}{\partial x} + \overline{v} \frac{\partial \overline{u}}{\partial y} = -g \left(\frac{\rho_w - \overline{\rho}}{\overline{\rho}} \right) \frac{\partial h}{\partial y} - \frac{\tau_{by}}{\rho h} + \frac{\tau_{sy}}{\rho h}$$

The surface tension relationship on the slick boundary (Equation 4.3.4) is unchanged.

The above equation set clearly indicates that the movement of an oil

slick about its center of mass is determined by gravitational, viscous and

surface tension forces and by the processes that tend to change the mass

of oil in the slick. As will be seen in the next subsections, all attempts

to analyze this problem have by necessity addressed only a subset of these

influences, assuming the remainder to be negligible. Accordingly, a

categorization of these efforts is best done in terms of which processes

are treated. In this regard there are two main categories of approaches,

designated spreading and dispersion, depending upon whether the motion is

induced primarily by the oil properties (density difference and surface

tension) or by the external shear forces on the bottom and surface of the

slick. These two general approaches are discussed separately in the next

two subsections.

4.3.3 Spreading Models

The basic assumptions of spreading models of oil slick movement are

the following:

1. There is no shear on the surface of the slick ($\tau_{sx} = \tau_{sy} = 0$) and

the bottom shear is generated solely by the relative motion of the oil over

a water body assumed to be at rest with respect to the center of mass of

the oil slick. This assumption is consistent with the basic premise of

this chapter that net motions of the water with respect to the oil slick

tend to advect the center of mass and are therefore not to be considered

in the treatment of slick transformation.

2. The oil is assumed to be composed of a single component of concen-

tration $\bar{c} = \rho$ which is constant in space.

3.   The horizontal configuration of the slick is assumed to be an idealized shape described by a single length scale. Many laboratory and theoretical studies have addressed the one-dimensional case in which the slick spreads only in one horizontal direction. However, this case is hardly ever applicable to real oil slicks and the discussion here will be confined to radially symmetric slicks that are described by specifying the total slick diameter, D, and the variation of the slick thickness, h, with r, the distance from the geometric slick center (which is also the center of mass).

4.   The rate of oil removal per unit volume, $\overline{R}$, is zero.

With these assumptions, the governing equations in radial coordinates are:

$$\frac{\partial h}{\partial t} + \frac{1}{r}\frac{\partial}{\partial r}(rUh) = \frac{-1}{\rho}(\phi_s + \phi_b)$$

$$\frac{\partial U}{\partial t} + U\frac{\partial U}{\partial r} = -g(\frac{\rho_w - \rho}{\rho})\frac{\partial h}{\partial r} - \frac{\tau_{br}}{\rho h} \tag{4.3.7}$$

$$f_n = f_r = \sigma_{aw} - \sigma_{ow} - \sigma_{oa}$$

where U is the radial spreading velocity.

The solution to these equations depends upon which of several remaining simplifying assumptions are made, as will now be discussed.

The Blokker Approach

Blokker (1964) formulated a spreading model that retained the effects of gravity and of mass loss at the cost of neglecting surface tension and viscous forces. He correctly integrated the mass conservation equation over the slick area, producing the following equation for the change in total slick volume, V:

$$\frac{dV}{dt} = -\frac{1}{\rho} (\phi_s + \phi_b) \frac{\pi D^2}{4}$$

(4.3.8)

However, his second basic equation was not based upon the correct momentum equation, but upon a purely empirical assumption:

$$\frac{dD}{dt} \sim (\rho_w - \rho)h \sim (\rho_w - \rho) \frac{V}{D^2}$$

(4.3.9)

which was intended to represent gravitational spreading. As will be discussed later, Blokker's equations have not compared well with field data, largely because of the theoretical inadequacy of the basic spreading assumption and because of the neglect of surface tension and viscous forces. However, Blokker's work is significant in its combined treatment of spreading and mass transfer, a feature that is not present in the constant volume spreading models discussed below.

Constant Volume Spreading Models

In an attempt to formulate more rigorously derived spreading expressions that could account for the effects of surface tension and viscous drag as well as gravity, a number of investigators have neglected the loss of mass from the slick and obtain the following governing equations:

$$\frac{\partial h}{\partial t} + \frac{1}{r} \frac{\partial}{\partial r}(rUh) = 0$$

$$\frac{\partial U}{\partial t} + U \frac{\partial U}{\partial r} = -g \left(\frac{\rho_w - \rho}{\rho}\right) \frac{\partial h}{\partial r} - \frac{\tau_{br}}{\partial h} \tag{4.3.10}$$

$$f_r = \sigma_{aw} - \sigma_{ow} - \sigma_{oa}$$

As first demonstrated by Fay (1969, 1971), the solution to the above equation for a given initial slick volume, V, is best obtained by considering the solution in regions characterized by which terms in Equation 4.3.10 are dominant.

1. Acceleration phase: If it is assumed that the oil is initially motionless with $h \simeq D$ (i.e. a "blob"), then the initial motion consists of an accelerating collapse of the blob caused by the density difference between the oil and water. The corresponding momentum equation is:

$$\frac{\partial U}{\partial t} + U \frac{\partial U}{\partial r} = -g \left(\frac{\rho_w - \rho}{\rho}\right) \frac{\partial h}{\partial r} \tag{4.3.11}$$

4-22

This initial collapse is similar to a classical dam break problem, in which the edge of the accelerating mass moves with velocity

$$\frac{dD}{dt} \sim \sqrt{g(\frac{\rho_w-\rho}{\rho})h_o} \qquad\qquad (4.3.12)$$

where h_o is the initial slick height.

Thus the initial increase in the slick diameter is linear with time. However, this mode of spreading lasts only for a time $\sqrt{\frac{h_o}{g(\frac{\rho_w-\rho}{\rho})}}$

until the height of the slick at its center begins to decrease because of the necessity to conserve mass. If an average slick thickness $h \sim V/D^2$ is used in equation 4.3.12, the change in slick diameter is then given by:

$$\frac{dD}{dt} \sim \frac{1}{D} \sqrt{g(\frac{\rho_w-\rho}{\rho})V}$$

$$\qquad\qquad (4.3.13)$$

$$\text{or} \qquad D \sim \sqrt[4]{g(\frac{\rho_w-\rho}{\rho})Vt^2}$$

From this result it is seen that the rate of spreading of the edge of the slick actually decreases with time. However, the outward net acceleration of the slick remains positive.

2. <u>Non-accelerating density current phase</u>: In the analysis of oil slick spreading, it has been a common error to confuse the acceleration phase described above with a second mode of spreading in which the gravitational buoyant force is balanced by a dynamic pressure at the front edge of the slick caused by the relative motion of the slick and the water. This type of non-accelerated gravitational spreading, discussed in detail by Benjamin (1968), is not adequately represented in the basic governing

equations (4.3.1) because the presence of a dynamic pressure force conflicts with the assumption of hydrostatic conditions. This discrepancy has not been of great consequence because the rate of spreading in this region is also given by equation 4.3.13 and is thus difficult to distinguish this stage from the later accelerating collapse stage.

   3. Viscous-Gravitational spreading: A third phase of spreading occurs for slicks that are sufficiently large and have been spreading for a sufficiently long time that the viscous shear on the bottom of the slick becomes the primary force balancing the buoyant gravitational force as expressed by the following governing equation:

$$0 = -g \; (\frac{\rho_w - \rho}{\rho}) \; \frac{\partial h}{\partial r} - \frac{\tau_{br}}{h} \qquad (4.3.14)$$

Analyses by Fay (1969), Fannelop and Waldman (1972), and Buckminster (1973), assume that the bottom stress, τ_{br}, is associated with a laminar boundary layer that develops in the water below the slick. These analyses, which vary in their degree of complexity, such as whether radial changes in h are treated, all result in the following spreading rate:

$$\frac{dD}{dt} \sim (\frac{\rho_w - \rho}{\rho}) \; g \; \frac{h^2}{D} \sqrt{\frac{t}{\nu_w}} \qquad (4.3.15)$$

where ν_w is the viscosity of water and t is the time since spreading began. Again, using $h \sim V/D^2$ the above equation yields

$$D \sim [(\frac{\rho_w - \rho}{\rho}) \; \frac{gV^2}{\sqrt{\nu_w}}]^{1/6} \; t^{1/4} \qquad (4.3.16)$$

4. Surface tension - viscous regime: The final spreading stage occurs when the slick has thinned sufficiently so that surface tension is the dominant spreading mechanism. The balance of surface tension and viscous forces leads to the following spreading rate:

$$\frac{dD}{dt} \sim \frac{f_r}{\rho_w}\sqrt{\frac{t}{\nu_w}}\frac{1}{D}$$

or   (4.3.17)

$$D \sim [\frac{f_r}{\rho_w\sqrt{\nu_w}}]^{1/2} t^{3/4}$$

Table 4.3.1 presents a summary of the spreading formulae for radial oil slicks based on the constant volume approach.

Table 4.3.1. Summary of Radial Spreading Laws for Successive Regimes

Spreading Force	Retarding Force	Spreading Formula
Gravitational	Inertial	$D = 2k_1[(\frac{\rho_w-\rho}{\rho_w})gVt^2]^{1/4}$
Gravitational	Viscous	$D = 2k_2[(\frac{\rho_w-\rho}{\rho})gV^2 t^{3/2}/\nu_w^{1/2}]^{1/6}$
Surface Tension	Viscous	$D = 2k_3[f_r^2 t^3/\rho_w^2\nu_w]^{1/4}$

Constants

k_1 = 1.14 (Fay) k_2 = 0.98 (Fannelop and Waldman) k_3 = 1.6 (Fannelop
                                    1.12 (Hoult)   Waldman)
                                    1.45 (Fay)

4-25

In addition to the above empirical results, Fay has proposed that changes
in slick properties caused by weathering may result in eventual cessation
of spreading. Assuming that molecular diffusion is the dominant mode of
mass transfer from the slick, Fay reasons that the depth of oil so affected
increases as $\sqrt{t}$ and thus the slick would be affected over its full depth
at a time $t \sim h^2 \sim \dfrac{V^2}{D^4}$. Substituting this relationship in the surface
tension growth law (equation 4.3.17) results in the following dependence
of the final slick area A_f on initial slick volume:

$$A_f \sim V^{3/4} \qquad\qquad (4.3.18)$$

On the basis of a number of empirical observations, Fay proposes the
following correlation:

$$A_f (m^2) = 10^5 \, V^{3/4} \, (m^3) \qquad\qquad (4.3.19)$$

4.3.4 Dispersion Models

The basic concept behind the dispersion approach to oil slick move-
ment is that the physical spreading processes related to the oil properties
(density differences and surface tension) are subordinate to the effects of
the shear on the slick boundary produced by random motions in the water.
In general the direct effect of wind in this regard is not considered to be
significant. Accordingly, the following assumptions are made in formulating
dispersion models:

1. The momentum equations are replaced by an assumption that the effect of the shears on the slicks is to make the velocities $\bar{u}$ and $\bar{v}$ random functions of time and space with zero means.

2. The product $(\widetilde{c_i h})$ is itself assumed to be a random quantity with a mean value $\overline{\widetilde{c_i h}}$ and a fluctuating component $(\overline{c_i h})'$.

3. Horizontal diffusive transfer by molecular processes is negligible with respect to the mean transfers induced by the random motions. With the above assumptions the mass conservation equation may itself be averaged (in the ensemble sense) to produce the following equation for the mean value $\overline{\widetilde{c_i h}}$:

$$\frac{\partial \overline{\widetilde{c_i h}}}{\partial t} + \frac{\partial \overline{\widetilde{uc_i h}}}{\partial x} + \frac{\partial \overline{\widetilde{vc_i h}}}{\partial y} = - [\widetilde{\phi_{si}} + \widetilde{\phi_{hi}} + \widetilde{R_i h}] \tag{4.3.20}$$

A final assumption is made regarding the averaged correlations of $\bar{u}$ and $\bar{v}$ with $\overline{\widetilde{c_i h}}$:

$$\overline{\widetilde{u\,\overline{c_i}h}} = -K_x \frac{\partial \overline{\widetilde{c_i h}}}{\partial x}$$

$$\overline{\widetilde{v\,\overline{c_i}h}} = -K_y \frac{\partial \overline{\widetilde{c_i h}}}{\partial y} \tag{4.3.21}$$

where K_x and K_y are dispersion coefficients that are assumed to be constant in space. This formulation is purely empirical and should be regarded as a means of parameterizing the basic assumption of random motion. Substituting the above into equation 4.3.11 yields:

$$\frac{\partial \overline{\widetilde{c_i h}}}{\partial t} = K_x \frac{\partial^2 \overline{\widetilde{c_i h}}}{\partial x^2} + K_y \frac{\partial^2 \overline{\widetilde{c_i h}}}{\partial y^2} - [\widetilde{\phi_{si}} + \widetilde{\phi_{bi}} + \widetilde{R_i h}] \tag{4.3.22}$$

At this point another equation may be generated by dividing equation 4.3.13 by ρ_i, summing over all i, and using equation 4.2.3 which yields:

$$\frac{\partial \widetilde{h}}{\partial t} = K_x \frac{\partial^2 \widetilde{h}}{\partial x^2} + K_y \frac{\partial^2 \widetilde{h}}{\partial y^2} - \sum_i \frac{\widetilde{\phi}_{si} + \widetilde{\phi}_{bi} + \widetilde{R_i h}}{\rho_i} \qquad (4.3.23)$$

in which it is assumed that the K_x and K_y apply to all the oil fractions.

The solution to the above equations depends upon the time dependence assumed for K_x and K_y, the nature of the mass flux terms and the number of oil fractions considered. For a single component system, if K_x and K_y are assumed to be constant in time as well as space and if the mass flux terms are given by a first order relationship

$$\widetilde{\phi}_s + \widetilde{\phi}_b + \widetilde{Rh} = k \, \widetilde{h} \, \rho \qquad (4.3.24)$$

then equations 4.3.22 and 4.3.23 are identical and have the following solution:

$$\widetilde{h} = \frac{M_o \, e^{-kt}}{4\pi\rho\sqrt{K_x K_y} \, t} \, \exp \left\{ - \frac{x^2}{4K_x t} - \frac{y^2}{4K_y t} \right\} \qquad (4.3.25)$$

in which M_o = the initial mass of the slick which is assumed to be spilled instantaneously at x = y = 0 at time t = 0.

The above solution turns out to be a special case of a slightly more general solution to the governing equations for a single component spill which is obtained by considering zeroth and the second moments of $\widetilde{h}$ about the origin of the spill:

zeroth moment: $m = \rho \int_{-\infty}^{\infty} \int_{-\infty}^{\infty} \tilde{h} \, dxdy = $ total slick mass

$$\sigma_x^2 = \rho \int_{-\infty}^{\infty} \tilde{h} \, x^2 \, dxdy/m \qquad (4.3.26)$$

second moments:

$$\sigma_y^2 = \rho \int_{-\infty}^{\infty} \tilde{h} \, x^2 \, dxdy/m$$

Performing the same integrations on the governing equation for $\breve{h}$ yields the following result:

$$\frac{\partial m}{\partial t} = - \int_{-\infty}^{\infty} \int_{-\infty}^{\infty} (\breve{\phi}_s + \tilde{\phi}_b + \breve{Rh}) \, dxdy$$

$$\frac{\partial \sigma_x^2}{\partial t} = 2K_x \qquad (4.3.27)$$

$$\frac{\partial \sigma_y^2}{\partial t} = 2K_y$$

The final solution for h is obtained by solving equations 4.3.27 for m, σ_x and σ_y, and assuming a Gaussian form for the spatial variation:

$$\tilde{h} = \frac{m}{2\pi\rho\sigma_x \sigma_y} \exp \left\{ - \frac{x^2}{2\sigma_x^2} - \frac{y^2}{2\sigma_y^2} \right\} \qquad (4.3.28)$$

Other, non-Gaussian, distributions may be utilized as long as the formulation preserves the total slick mass and second moments.

The above formulation does not restrict the specification of the
form of the mass losses or the time variability of K_x and K_y. This is
particularly important because previous investigations of dispersion in open
coastal environments have shown that K_x and K_y are likely to be strong
functions of σ_x and σ_y and thus of time. A commonly used form for the
time dependence of K_x and K_y is (Csanady, 1974)

$$K \sim t^n \qquad\qquad (4.3.29)$$

which in combination with equations 4.3.27 yields the following dependence
of K on σ:

$$K \sim \sigma^{(2n/n+1)} \qquad\qquad (4.3.30)$$

A typical pattern of growth of σ vs time for surface dye plumes is shown in
Figure 4.3.1. Although it is not clear that the relationship between
K and σ will be the same for an oil slick or for a dye plume, it is expected
that the dispersion coefficient for oil will show the same general tendency
to increase with increasing slick size.

4.3.5 Comparison of Actual Slick Observations with Spreading and Dispersion
       Theories

Real open sea slicks rarely fit the assumptions made in formulating
the previously discussed spreading and dispersion models. This is largely
because (1) oil is a complex mixture of hydrocarbons with properties that
change as the constituents of the mixture change and (2) actual slick con-
figurations rarely match the idealized geometry assumed by the analytical
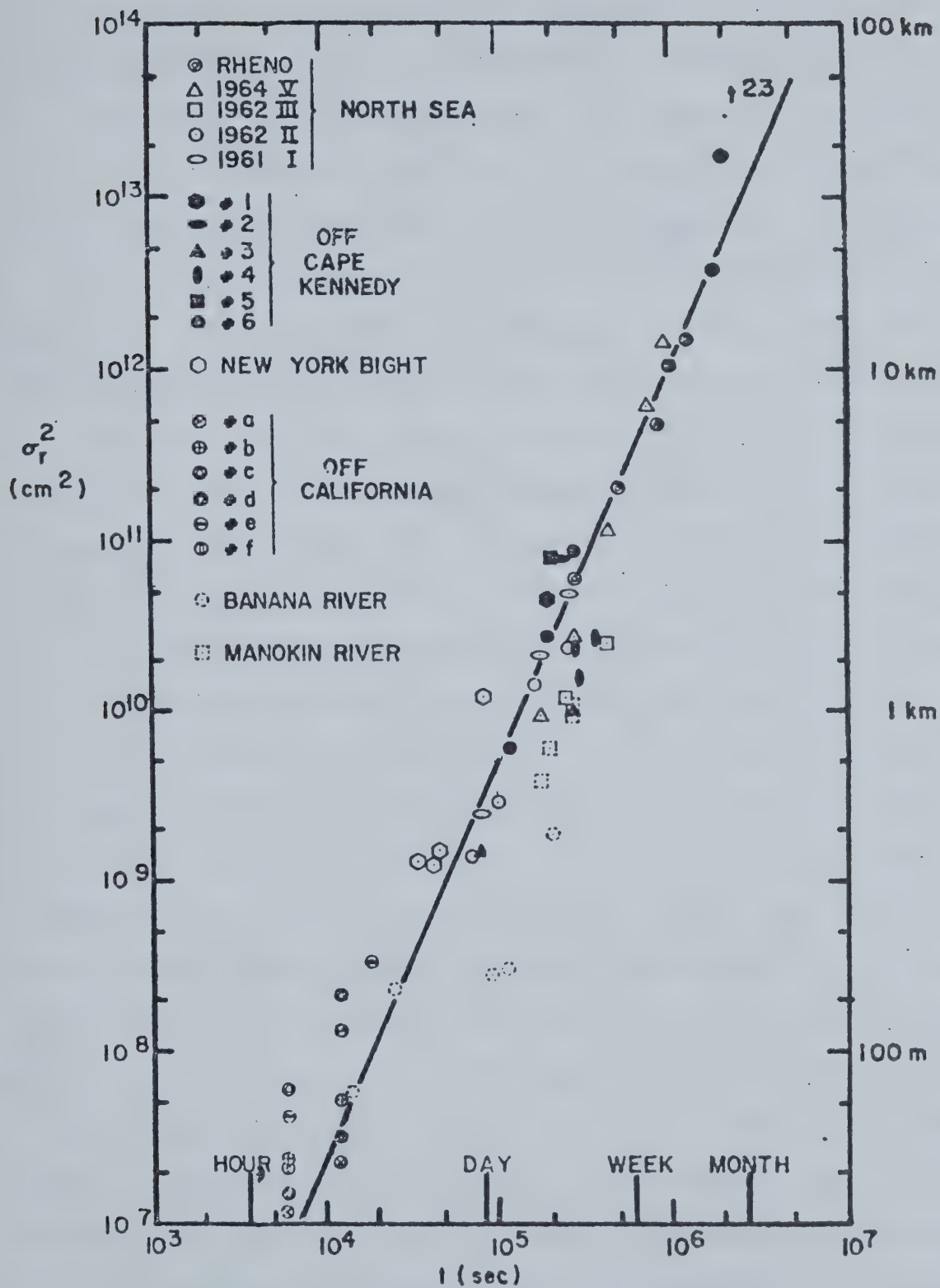
Figure 4.3.1 Surface Dye Patch Size, σ, as a Function of Time
(Okubo, 1962)

4-31

approaches.

The different oil components, for instance, may not spread at the same rate, as shown by the work of Phillips and Groseva (1975). Hence the assumption that the oil can be treated as a single component with properties and concentrations that do not vary horizontally is not generally valid. Berridge, Dean et al. (1968) also ovserved that certain surface active components would spread much faster than the rest of the oil. The result of this is that oil tends to fractionate into thick clumps of more viscous hydrocarbons and wider thinner patches of faster spreading components (Jeffery, 1973; Kennedy and Wermund, 1972) (see Figure 4.3.2). Eventually the oil breaks up into discrete blobs which can be advected independently. Observations of a spill in San Francisco Bay (Conomos, 1975) show that the area actually covered with oil may be only about 10 percent of the area spanned by the oil around its center of mass.

Open sea slicks are rarely round but are distorted by wind and currents into irregular shapes. This also makes it extremely difficult to compare the predictions of radial spreading models with field data. When this comparison is made, the results are mixed. Glaeser and Vance (1971) found that spreading in an Arctic pool fit Fay's gravity-viscous regime well, but noted no gravity-inertial phase. Jeffery (1973) noticed no abrupt changes in spreading mechanism. Field data from Conomos (1975) show that Fay's theory greatly underestimates slick growth using an equivalent radius equal to $(A/\pi)^{1/2}$ for the field data. Murray (1972) also found that Fay's theory underestimates the growth of a slick, probably because it neglects dispersion due to random water motions. This neglect becomes more serious as the slick grows larger. Similarly, experimental oil
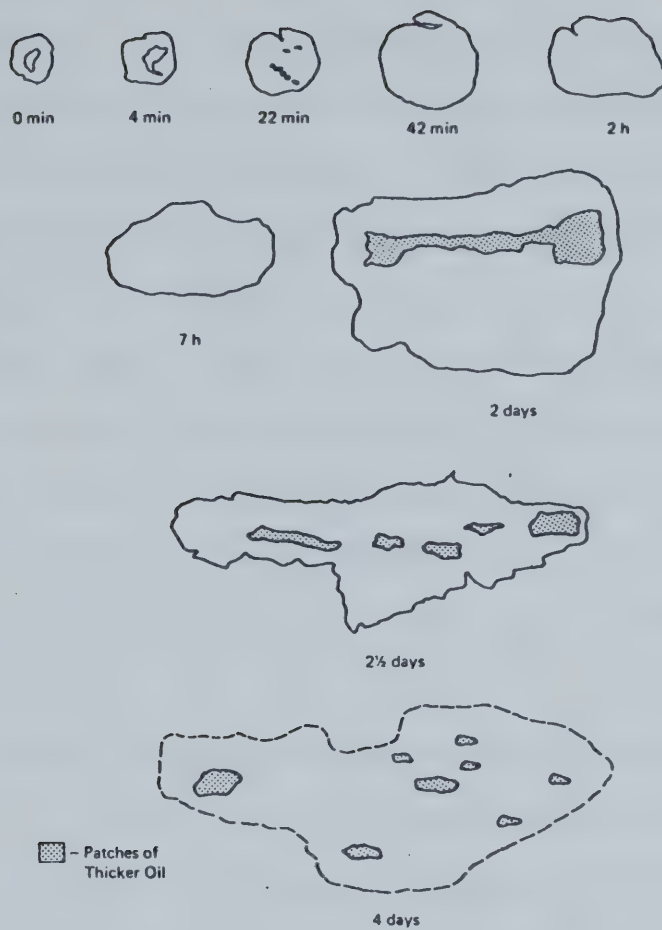
Figure 4.3.2 A series of diagrams showing the
outline development and subsequent breakup of
the oil slick (P.G. Jeffery, 1973).

slick areas varied as about t^3 in the St. Lawrence estuary (Drapeau et al., 1974) while all of Fay's regimes predict slick area growing as t^a where $a \leq 1.5$. Blokker's model has been fit to several sets of spreading observations (Jeffery, 1973; Sivadier and Mikolaj, 1973; Berridge, Dean et al., 1968) but the constants used differ widely for the different cases.

Fewer observations have been made which can be used to test dispersion models. Most of what has been done (e.g., Murray, 1972) has been hind-casting, rather than forecasting, to obtain values for diffusivity. Kennedy and Wermund (1972) noted that a real oil spill slick had the same shape as could be predicted by Murray's theory, but did not discuss the magnitude of the dispersive spread. Figure 4.3.3 shows a plot of slick size data compared with both spreading and dispersion relationships.

On the basis of the observations discussed above, it may be concluded that:

1. Both spreading and dispersion processes may be important in determining the total growth of the slick.

2. Existing techniques for estimating the growth of surface oil slicks provide at best only an order of magnitude estimate of what the actual slick size will be.

3. Because of the complex and usually random nature of the processes controlling slick growth, it is unlikely that a significant improvement in deterministic capability will be possible. However, estimates of the variance in slick sizes should become more accurate as additional observations are obtained.

4. The applicability of available spreading and dispersion models should be judged on a case by case basis in terms of the site specific conditions. The factors involved in this judgment will be discussed more fully in Section 4.5. of this chapter and in Chapter 5.
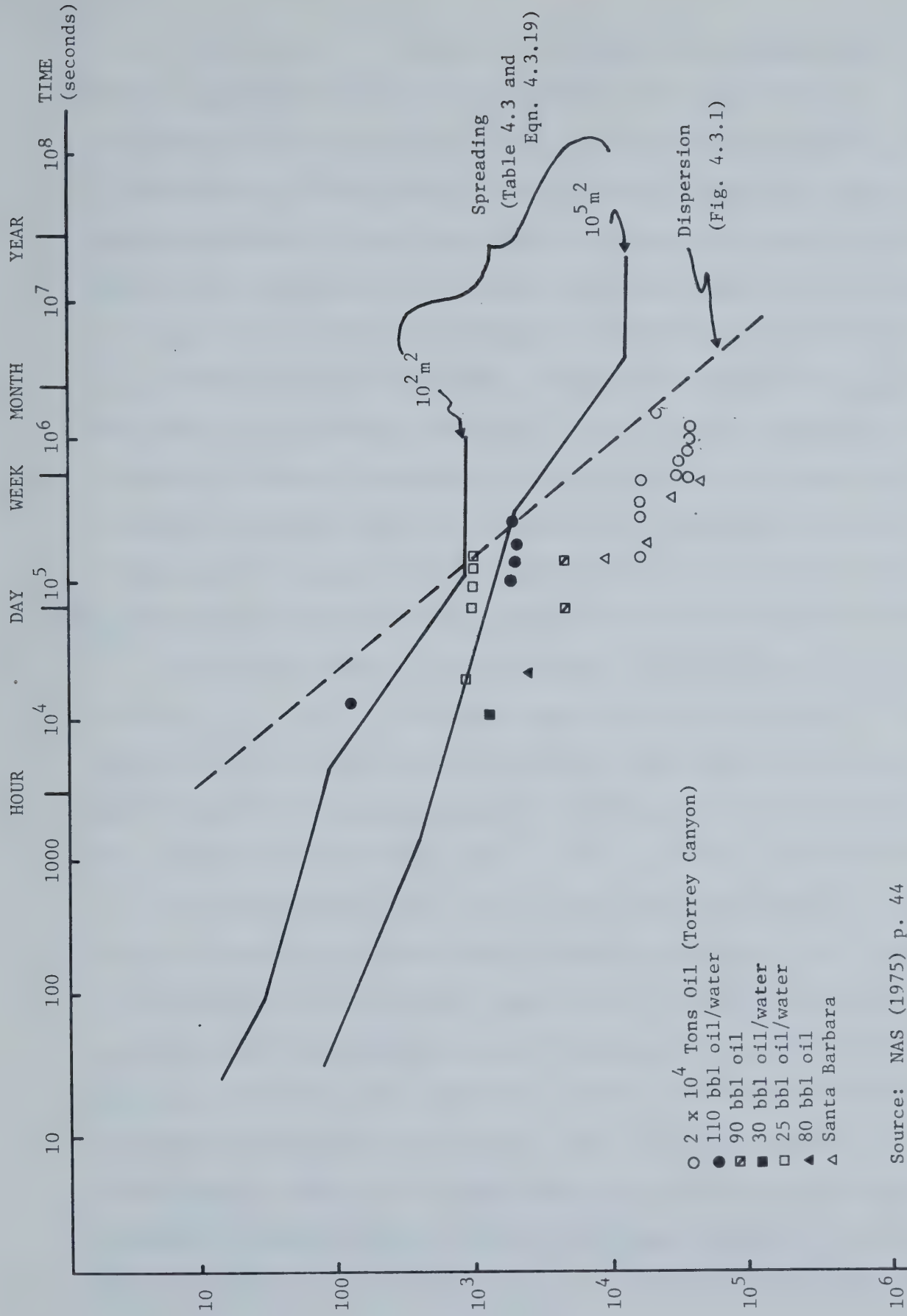
Figure 4.3.3 Comparison of Theoretical and Observed Slick Sizes (NAS(1975))

4.4 Mass Transfer (Weathering) in Oil Slicks

The purpose of this section is to treat the processes of boundary and internal mass transfer (ϕ_s, ϕ_b and R) that affect the distribution functions for $c_i(x,y,z,t)$ and $h(x,y,t)$. This subject is particularly complex because of the number of potentially significant mass transfer processes and because the basic nature of the transfers are poorly understood in comparison with our capability to write (if not solve) the basic fluid mechanics equations governing advection, spreading and dispersion of the oil slick. The state of knowledge concerning the various mechanisms and our ability to predict the rates and magnitudes of the various processes vary widely. For evaporation, for instance, fairly reliable models are already in use. For other processes such as photo-oxidation and biodegradation, the basic mechanisms are still not completely understood. For these processes the most that can be specified is a characteristic time frame.

The following sections give separate treatments of evaporation, subsurface transport processes, emulsification and chemical and biological degradation. Models of some of these processes are discussed. For those processes for which no models exist, the underlying physical, chemical or biological mechanism is described and the factors affecting the rate of the process are discussed qualitatively. An extremely important matter is the relative rates and importance of the various, often competitive, mass transfer processes. When this matter is examined it is found that there are many situations where inability to model a particular process is not important because the process itself is not important relative to some other one which can be modelled. Further discussion of this aspect of oil slick modeling is presented in section 4.5.

4.4.1 Evaporation

Evaporation, the major component* of the surface flux, ϕ_s, is the primary means by which oil is removed from the slick during the first few days of its existence. Many laboratory and field studies have been performed and several predictive models developed. These models are based largely on techniques developed previously for water evaporation or petroleum distillation. It is fair to say that the state-of-the-art is more advanced and more quantitative for evaporation modeling than it is for modeling any of the other weathering processes. Since evaporation is also the single most important mass transport process from the point of view of slick dissipation, the discussion of evaporation will be more quantitative and lengthy than the treatment of the other processes.

At present, it is possible to predict fairly accurately how much and which parts of an oil slick will eventually evaporate. Only the lower boiling fractions evaporate to any appreciable degree, so the extent of evaporation depends on the amount of these volatiles in the oil.

It is more difficult to say how fast this evaporation will proceed since this depends on several environmental factors. Wind speed (Smith and MacIntyre, 1971) and temperature are the most important, although other variables such as solar radiation also have some influence.

---

* The other component of ϕ_s is the transport of oil into the atmosphere from bubble bursting and on ocean spray. Little is known about the magnitude of this process but it is no doubt of minor significance when compared to evaporation (NAS, 1975). Also, oil particles ejected this way tend to fall back onto the water anyway. This mechanism, therefore, will not be discussed further.

For a constant volume of oil, the rate of evaporation increases with increasing surface area. Evaporation per unit area, however, may actually decrease slightly with increasing surface area (Mackay and Matsugu, 1973) because edge effects (the enhanced evaporation thought to occur at the upwind edge of a slick) become relatively less important for larger slicks. Kreider (1971) found that evaporation is faster for thinner slicks; thus oil spreading tends to accelerate evaporation, both by increasing surface area and reducing slick thickness. Kreider did not suggest an explanation for his observation, but it has been suggested elsewhere (Mackay and Matsugu, 1973; Harrison et al. 1975) that evaporation from thick slicks can be limited by the rate at which volatiles diffuse from within the slick to the oil-air interface. This will be especially true if evaporation of volatiles from the top of the slick allows the remaining, viscous component to form a skin at the oil-air interface and impede further evaporation, an effect noted by Blokker (1964) and Ramseier (1971).

Finally, the state of agitation is a crucial determinant of evaporation rates. Both Smith and MacIntyre (1971) and Harrison et al. (1975) found that the rate of evaporation took a sharp, discontinuous jump with the onset of whitecapping. Similarly, Sivadier and Mikolaj (1973) found that rough sea conditions could triple the early rate of evaporation, keeping the wind speed constant. The enhancement of evaporation by sea turbulence can be explained by some combination of greater air turbulence (Wu, 1971), faster spreading, greater surface area exposed to the atmosphere and greater ejection of oil as sprays and aerosols.

There are two degrees of freedom which determine the complexity of an evaporation model. The first is the degree to which oil is broken up into its various components, all of which evaporate at different rates. At the simplest extreme, oil can be treated as a single pure substance and a curve could be fit to experimentally observed evaporation data. Such a curve, however, would be valid only for that particular brand of oil. The most general model, on the other hand, would be one that weathers each hydrocarbon in the oil separately. Such a model would work for any oil (providing its composition is known) and has other advantages as well. It can be focused on one particular compound of interest (say, a particularly toxic compound) and at each time step can compute the composition (and thereby some of the physical properties) as well as the volume of the remaining slick. However, such a complete breakdown is impossible for crude oils, which contain upwards of a thousand different compounds. Compromises can be made between these two extremes, such as grouping hydrocarbons together on the basis of chemical structure or boiling point. As always there is a tradeoff between greater applicability and greater output on the one hand and higher costs and larger data requirement on the other.

The other variable in model development is the degree to which the environmental factors mentioned above are incorporated. Those models that do not account for many of the independent environmental variables tend to utilize empirical constants which are valid only for a limited range of conditions.

It should be noted that the two degrees of complexity can vary independently. A model might be very detailed in treating separate components yet very simple in modeling the kinetics, or vice-versa. It seems that some of the benefits of increasing a model's sophistication in one of these directions would be lost if treatment of the other aspect is too simple.

Approaches to modeling the effect of the processes described above on the evaporation of oil from a surface slick will now be discussed in terms of the form of the basic mass conservation law (equation 4.2.4).

Diffusion Models

The use of the evaporative mass flux as a true boundary condition requires the consideration of vertical gradients of c_i within the oil slick and thus requires the use of the mass conservation equation (4.2.4) without vertically averaging.

Lassiter et al. (1974) use such a model to study the dissipation of benzene and naphthalene from a slick by both dissolution and evaporation. The equation used is a simplified form of equation (4.2.4) in which advection, horizontal mass transport, and internal decay are neglected:

$$\frac{\partial c_i}{\partial t} = k_i \frac{\partial^2 c_i}{\partial z^2}$$

$$-k_i \left. \frac{\partial c_i}{\partial z} \right|_{z=h_s} = \phi_s = \text{evaporative flux} \qquad (4.4\text{-}1)$$

$$k_i \left. \frac{\partial c_i}{\partial z} \right|_{z=h_b} = \phi_b = \text{dissolutive flux}$$

They use a five layered model - the slick surrounded by the laminar water and air layers surrounded in turn by turbulent air and water layers. The model results were fairly sensitive to the thicknesses assumed for each layer. Since the model was really designed to compute water column concentration, it will be discussed further in the section on dissolution. Of interest here, however, is that in only one situation - diffusion of benzene from a thick (1 cm) slick - was a concentration gradient set up within the slick, indicating that diffusion within the slick was slower than evaporation from the surface. For thinner slicks there was no noticeable concentration gradient, nor was there any gradient for less volatile naphthalene, even for thick slicks. The value used for diffusivity within the slick was 1.0×10^{-5} cm^2/sec. It is not discussed how this figure was determined.

The results of Lassiter's work indicate that vertical diffusion of oil within the slick usually will not be the rate-limiting process.

Accordingly, the remaining discussion of evaporation will be based on the assumption that the rate is determined by vertically averaged oil concentrations and the corresponding vertically averaged mass conservation law (equation 4.3.6) in which the evaporation surface flux, ϕ_e, appears as a term in the equation rather than as a boundary condition. Thus the discussion of evaporation centers around the factors affecting ϕ_e and the functional forms assumed in various levels of approach.

Models Accounting for Environmental Factors

The most sophisticated formulations for the evaporative flux term, ϕ_e, have utilized an empirical expression that has been highly successful in water and heat budget studies:

$$\phi_{ei} = k_i (P_i - P_{ai}) \qquad (4.4-2)$$

in which

ϕ_{ei} = the evaporative flux of a substance i

P_i = the vapor pressure of the liquid substance

P_{ai} = the vapor pressure of the substance in the atmosphere above the slick

k_i = a mass transfer coefficient that accounts for environmental factors.

This formulation is an expression of the fact that the driving force of evaporation is the difference in vapor pressure between the liquid phase and the air. In the cases of hydrocarbons, it is safe to

assume that $P_{ai} = 0$, making the evaporation directly proportional to the vapor pressure P_i for given environmental conditions as reflected in the constant k_i.

The above equation holds for the evaporation of a single liquid substance. It has already been discussed in Section 4.1 how to find the vapor pressure, P, of a particular hydrocarbon. However, oil is a mixture of liquids, and in such a mixture the effective vapor pressure of a single component is reduced below the value it would have were it alone. The following relationship holds approximately for mixtures of liquids:

$$P_i = X_i P_i \qquad\qquad (4.4-3)$$

in which P_i is the effective vapor pressure of substance i in the mixture, P_i the vapor pressure of pure substance i, and X_i the mole fraction of the substance in the mixture. In other words, the escape tendency of a substance is reduced in a mixture by a factor which reflects the fact that the substance covers only a fraction (X_i) of the available surface area. The relationship, known as Raoult's law, is valid for an ideal mixture, i.e., one in which intermolecular forces between different species can be neglected and each component can be viewed as behaving independently.

Evaporation Constant

The functional form of the coefficient k_i in equation (4.4-2) may be based upon theoretical considerations but is generally con- sidered as an empirical parameter to be fit to data. Most expressions derived for water or heat loss from natural water bodies make k_i a function primarily of wind speed but also of temperature and surface area. A review of these forms may be found in Ryan and Harleman (1973).

Blokker (1964) used the following form for k (after Sutton, 1947):

$$k = CU^{2-n/2+n}D^{-n/2+n} \qquad (4.4-4)$$

in which U = wind velocity, D = slick diameter, and in which n is a turbulence parameter and C a constant.

Other models have been developed using the same basic equations (4.4-2 to 4.4-4). Mackay and Matsugu (1973) performed a heat balance across the upper surface of the slick in an attempt to better cal- culate the constant C in equation (4.4-4). The heat balance equation could be solved to yield the slick temperature over time. The authors used experimental values of slick temperature and fit a constant C to generate the observed evaporation profile for Cumene. This value of C holds only for Cumene, but it is claimed that for two different systems the constants are related by

$$C_2 = C_1(S_{c_1}/S_{c_2})^{0.67} \qquad (4.4-5)$$

in which S_c is the Schmidt number of the system.

Their results for Cumene yielded C = .0150, which applies when the mass transfer coefficient, wind speed and diameter are measured in m/hr, m/hr and m respectively. Since the Schmidt number for Cumene evaporation at 30°C is 2.70, the value of C for the evaporation of other hydrocarbons can be found by:

$$C_i = .0292 \ S_{c_i}^{-0.67} \tag{4.4.6}$$

This formulation avoids the assumption implicitly made in Blokker's formulation (see next page) that oil slick temperature is the same as air temperature. Mackay and Matsugu's data show that slick temperature may be as much as 20°C higher than air temperature owing to the greater absorption of sunlight by the dark slick. On the other hand, use of the heat budget requires far more input data such as the albedo and emissivity of the oil. In addition, both Blokker's and Mackay and Matsugu's approaches neglect the influence of the sea surface water temperature on the heat balance and thus the temperature of the slick.

Fallah and Stark (1976) manipulated equations (4.4.2) to (4.4.4) to permit the use of random wind speeds and temperatures.

Multicomponent Evaporation Computations

Discussion so far has dealt with modeling the evaporation of either a single pure substance or a single substance within a mixture. A straightforward extension of this approach to the problem of modeling a mixture of hydrocarbons would be to compute the evaporation of each component separately for a certain time step. At the end of each time step, the volume and composition of the remaining slick can be calculated, new mole fractions computed for each component and

evaporation then taken another step. Since most oils have too many
components for each one to be handled individually, several components
must be grouped together. It makes much sense to group compounds
together on the basis of boiling point rather than chemical structure,
since evaporation and boiling point are so closely interrelated. The
higher boiling fractions can be considered not to evaporate at all,
reducing the amount of computation required during and after each
time step.

Blokker (1964) used a similar, though slightly different
approach. He treats the oil as a single substance. Substituting
equations (4.4-2) and (4.4-4) into the averaged mass transfer equation
for a circular slick and integrating over slick area yields

$$\frac{dV}{dt} = -\frac{\pi}{4} KU^{2-n/2+n} D^{2-n/2+n} PM \qquad (4.4-7)$$

In this equation P is the total vapor pressure of the oil,
equal to the sum of the effective vapor pressure of the components,
$p_i = P_i X_i$. M is the average molecular weight of the oil.

To account for the fact that oil is a mixture, the value of PM
changes during the course of evaporation. Given a distillation curve
for the oil or a breakdown by boiling point classifications, the value
of PM as a function of the percentage of oil evaporated can be found
fairly easily. From the average boiling point of a fraction, an
average vapor pressure can be computed using, for example, the integrated
form of the Clausius-Clapeyron equation (4.1-4):

$$\log P_b/P = \frac{qM}{4.57} \left(\frac{1}{T} - \frac{1}{T_b}\right) \qquad (4.4\text{-}8)$$

in which

T = absolute temperature

T_b = boiling point (°K)

q = heat of evaporation

M = molecular weight

P_b = vapor pressure at the boiling point (= 760 mm Hg).

Since $qM/4.57\,T_b$ is nearly a constant (5.0 ± 0.2) for hydrocarbons, Blokker simplifies the expression to

$$\log P_b/P = 5.0 \left(\frac{T_b - T}{T}\right) \qquad (4.4\text{-}9)$$

An average molecular weight for each fraction can easily be estimated from the number of carbons in the molecules of the fraction. Using Raoult's law, PM can be calculated as a function of percentage evaporated.

The evaporation equation can then be applied stepwise to compute the time needed for a certain percentage to evaporate:

$$t = \frac{\Delta h D^{2-n/2+n}}{KU^{2n/2+n}} \; \Sigma \; \frac{1}{PM} \qquad (4.4\text{-}10)$$

where, assuming a constant area and a uniform slick thickness, Δh is the decrease in slick thickness, $\dfrac{\Delta V}{\frac{\pi}{4} D^2}$.

Blokker compared his model's predictions to experimental laboratory data for the evaporation of crude oil and gasoline. He found his model overestimated the early evaporation rate for crude oil and underestimated subsequent evaporation. For gasoline the situation was reversed. The predicted time for evaporation of the first 20% of the gasoline was 3 times shorter than the observed time.

Blokker's model is oriented toward overall volume calculations and cannot follow individual components. However, information on the physical properties of the remaining slick can be inferred from the distillation curves just as values of PM were determined as a function of percentage evaporated.

First Order Models

Most (but not all) lab and field studies have found that evaporation starts off relatively rapidly and gradually slows down. This pattern, which holds both for oil as a whole and for individual hydrocarbons in the slick, is susceptible to modeling as a first order process, in which the loss of mass (or drop in concentration) is proportional to the mass (or concentration) in the slick.

$$\phi_{ei} = k_{ei} M_i \qquad\qquad (4.4\text{-}11)$$

Williams et al. (1975) developed such a first order model based on the work of Moore et al. (1973). The oil is divided into eight groups based on chemical structure and carbon number. The breakdown and first order coefficients are shown in Table 4.4-1.

4-48

Table 4.4.1 First Order Mass Transfer Coefficients
for Eight Oil Fractions

Fraction	Description	Evaporation[b] (K_e)	Dissolution (K_d)	Ratio (Diss/Evap)
1	Paraffin C_6-C_{12}	$0.8e^{0.2W}$	0.1	1/60
2	Paraffin $C_{13}-C_{22}$	0.002	0	0
3	Cycloparaffin C_6-C_{12}	$0.8e^{0.2W}$	0.5	1/12
4	Cycloparaffin $C_{13}-C_{23}$	0.002	0^c	0
5	Aromatic (Mono- and di-cyclic) C_6-C_{11}	$0.8e^{0.2W}$	1.0	1/6
6	Aromatic (Poly-cyclic) $C_{12}-C_{18}$	0.02	0.001	1/20
7	Naphtheno-Aromatic C_9-C_{25}	0.02	0.001^d	1/20
8	Residual	0	0	0

a   These values are approximate and are probably all dependent upon temperature and oil film thickness.

b   W is the wind speed in knots.

c   Estimated from fraction 2.

d   Estimated from fraction 6.

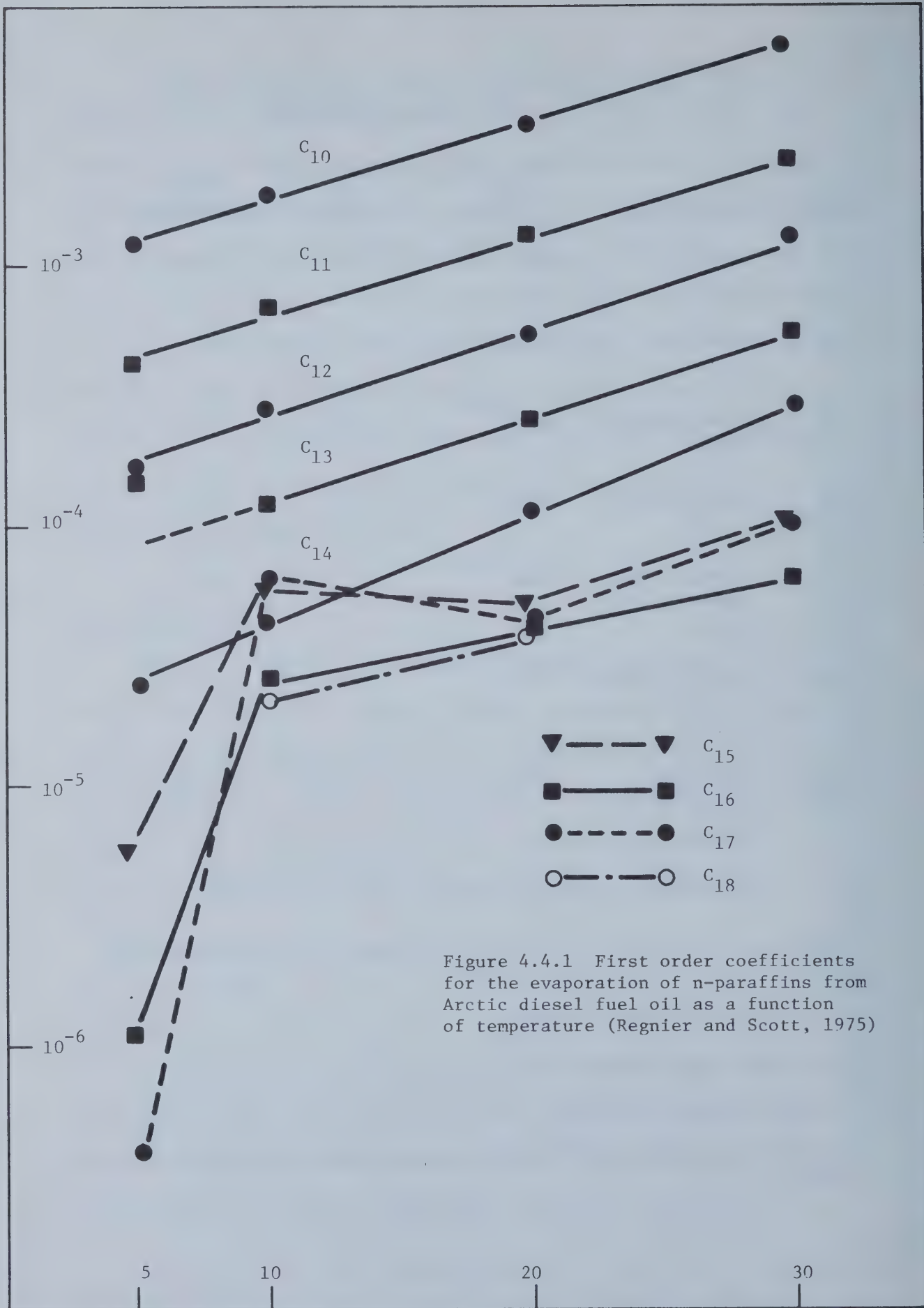(from Williams et al. (1975) based on data supplied by Moore et al. (1973))

Figure 4.4.1 First order coefficients for the evaporation of n-paraffins from Arctic diesel fuel oil as a function of temperature (Regnier and Scott, 1975)

Temperature (°C)

Each group is weathered separately and the remaining fractions combined at the end of each time step to yield a picture of the remaining slick. The model handles both evaporation and dissolution, though evaporation accounts for most of the mass transport.

The values for the first order empirical constants are derived from a limited set of observations. The evaporative constant for groups 1, 3 and 5 is based on weathering curves for C_{11} hydrocarbons from Kinney et al. (1969) and Smith and MacIntyre (1971). Both studies were at temperatures near 5°C, which will lead to underestimates of evaporation at higher temperatures, and there was no apparent control for the effects of spreading and thinning in either of the works. The constants for the other groups have even less of an empirical foundation. However, since evaporation of these groups is extremely slow, the model is not as sensitive to these values.

The relationship between K_e and wind speed indicated in Table 4.4.1 is also only approximate and might be overestimated since Moore et al. included Smith and MacIntyre data for the 18 knot wind in their analysis. At this speed whitecapping began, leading to a discontinuity in the evaporation rate. The faster evaporation at 18 knots is a function of sea roughness not wind speed.

Regnier and Scott (1975) calculated first order evaporative coefficients for the n-alkanes C_{10} through C_{18} at various temperatures based on laboratory tests under simulated field conditions. Their results are shown in Figure 4.4-1. The coefficient varies regularly with temperature, approximately doubling for each 10°C rise. This is probably due to the regular variation of vapor pressure with

temperature. The authors found that the following relationship holds approximately for each hydrocarbon tested:

$$\frac{K_{eT}}{K_{e30°}} = \frac{P_T}{P_{30°}} \tag{4.4-12}$$

where K_{eT}, P_T, $K_{e30°}$ and $P_{30°}$ are the first order coefficients and vapor pressure at temperatures T and 30°C. This allows us to calculate K_e for any temperature knowing K_e at 30°C. Also, for all the hydrocarbons tested, a regression analysis yielded:

$$logP = 1.25 \ log \ K_e + 0.160 \tag{4.4-13}$$

Presumably this relationship holds only for wind speeds of 21 km/hr, the speed under which the data were taken.

Since volatility is so strongly linked to carbon number, the coefficients for n-alkanes can be used for all hydrocarbons with the same number of carbons with little error. Mackay and Matsugu (1973) suggest that the n-alkane coefficients can be used by carrying out evaporation on a hypothetical slick made up of only n-alkanes in such proportions that their distillation curve resembles that of the actual oil.

The coefficients proposed by Regnier and Scott and by Moore et al. are directly comparable in only one instance - evaporation of $n-C_{11}$ at 5°C and a wind speed of 21 km/hr. For this situation, Moore's coefficient is 5.35×10^{-3} min^{-1} whereas Regnier and Scott's is 4.15×10^{-4} min^{-1}.

There are several possible explanations for this discrepancy. One is that Moore overestimates the effects of wind speed, as has been mentioned. Another is that Moore's data comes from field experiments and Regnier and Scott's from laboratory work. Smith and MacIntyre (1971) found that evaporation on the open sea was 7 times greater than in their lab setup, even though in the laboratory air was bubbled through the oil, temperatures were kept higher and oil was exposed for 7 times longer than in the field. In any case, the discrepancy shows that the current state of knowledge is advanced enough to yield evaporation data correct only to one order of magnitude.

While first order models are useful approximations and computationally easy, it should be kept in mind that there is nothing inherently first order about the process of evaporation, whether of the slick as a whole or of individual components from the slick. Interestingly, the mechanism accounting for the characteristic pattern of evaporation with time is not the same for the slick as a whole as it is for individual components. For the slick as a whole, evaporation rates decline with time simply because the fastest-evaporating substances vaporize first. After they are gone, evaporation slows down. This pattern would be observed whether or not the evaporation of individual components were a first order process.

For individual components, changes in the rate of evaporation are related to changes in the mole fraction of the substance, not to any loss of mass per se, so that equations like (4.4-11) are not strictly valid. In fact, the evaporation rate of a component might even increase with time if its mole fraction increases.

4-53

This possibility may be illustrated by use of the vertically averaged mass conservation equation (4.3.6), neglecting horizontal advective and diffusive transport:

$$\frac{\partial \overline{c}_i h}{\partial t} = -\phi_{si} - \phi_{bi} - \overline{R}_i h \tag{4.4-14}$$

Dividing by ρ_i, summing over all i, and using equation (4.2.3), one obtains

$$\frac{\partial h}{\partial t} = -\sum_i \frac{\phi_{si} + \phi_{bi} + \overline{R}_i h}{\rho_i} \tag{4.4-15}$$

Combining these two equations yields: an expression for the changes in c_i with time:

$$\frac{\partial c_i}{\partial t} = \overline{c}_i \sum_i \frac{\phi_{si} + \phi_{bi} + \overline{R}_i h}{\rho_i} - \frac{1}{h}(\phi_{si} + \phi_{bi} + \overline{R}_i h) \tag{4.4-16}$$

The first term on the right hand side of the above equation accounts for increases in c_i brought by decreases in the total slick volume that tend to increase c_i; the second term accounts for actual loss of the ith fraction. It is clear that c_i may either increase or decrease depending upon the relative rates at which other fractions are being lost from the slick. Finally, because the mole fraction of the ith oil fraction is given by

$$X_i = \frac{c_i/M_i}{\sum_i c_i/M_i} \qquad\qquad (4.4\text{-}17)$$

where M_i is the molecular weight of each fraction, the same conclusions hold regarding the possibility for X_i to either increase or decrease with time.

The non-first-order nature of oil evaporation is further illustrated by the data from Kreider (1971) in Figure 4.4-2. The arrows on each curve show the approximate position of the change from an accelerating to a decelerating evaporation rate. It appears that each component experiences an increasing evaporation rate at first, as its concentration in the slick increases owing to the more rapid evaporation of even more volatile components. Only after the more volatile components are gone does evaporation cause a decrease in concentration and a declining evaporation rate. A similar pattern can be seen in the field data reported by Harrison et al. (1975). In short, there is nothing inherently first-order about the evaporation of individual components from an oil slick. The first-order-like pattern is caused by relative concentration changes of the various components. The buildup of partial pressure above the slick, which heretofore has been neglected, also contributes to a deceleration of evaporation with time by decreasing the $P_i - P_{ai}$ term in equation (4.4-2). The implications of this are (1) that the simple first order models are only approximate and more importantly, (2) the empirically determined first order constants depend on the oil as a whole since the evaporation rate reflects shifting relative concentration. Hence, Regnier and Scott's constants, for instance, determined for Arctic Diesel

Figure 4.4.2 Evaporative losses from a crude oil as a function of time. Less volatile hydrocarbons experience an increasing evaporation rate at first. (Kreider, 1971).
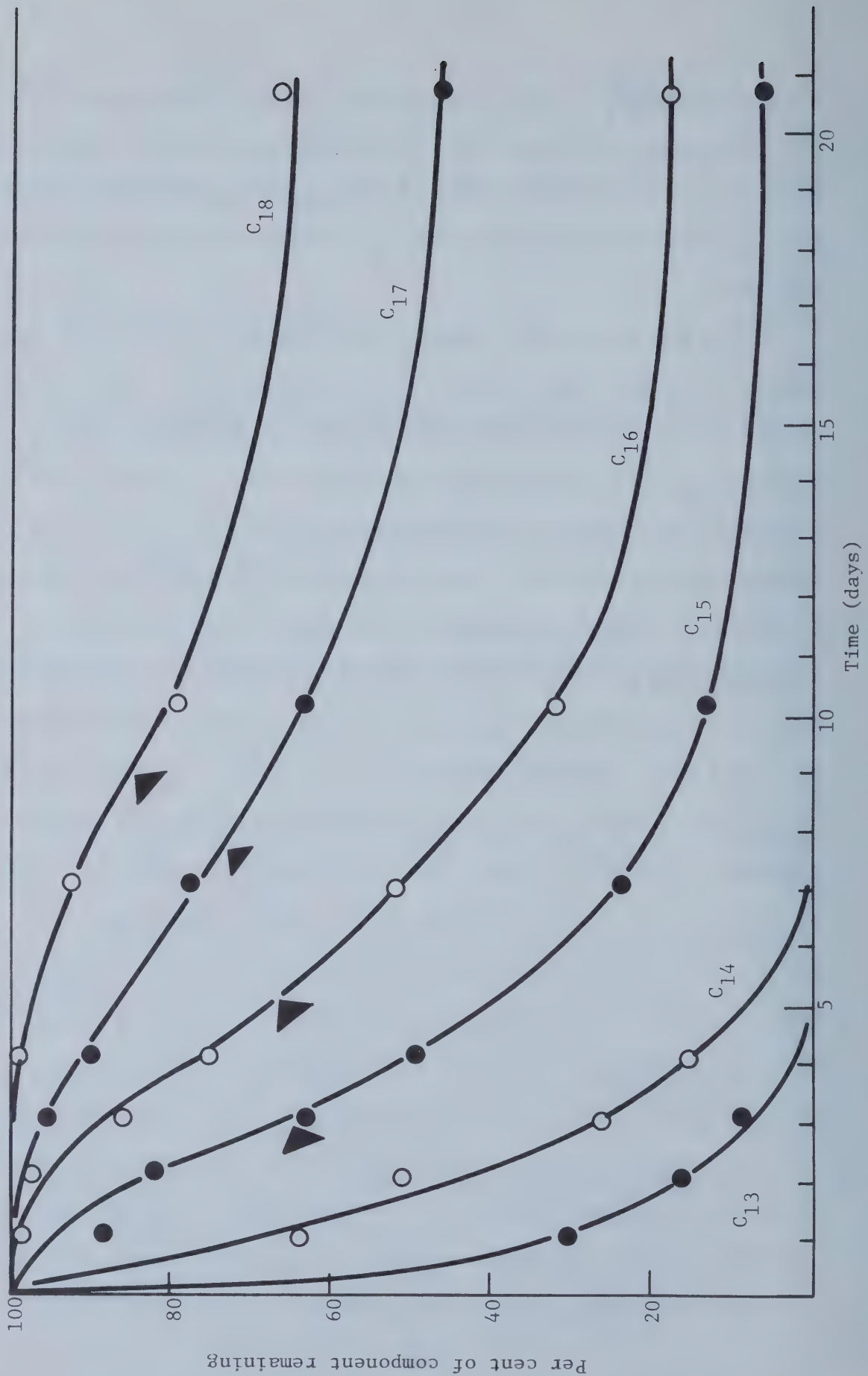
fuel oil, might be valid only for that oil, although the error in applying them to the other oils may not be very serious.

Single-Step Evaporation

In many situations interest in the slick may begin after a time period long enough for virtually all of the evaporation to have occurred. For instance, we might be interested in the volume and density of a slick that impacts the beach after a week or more at sea. In such cases, evaporation can be modeled as a step function in which the oil that is eventually to evaporate is removed all at once.

There is no abrupt cutoff between fractions that do and fractions that do not evaporate. However, Smith and MacIntyre (1971) found that very little of the fraction boiling above 270°C (518°F) evaporates. Frankenfeld (1973a) found that nearly all components boiling below 500°F and most boiling below 600°F are lost in a week. In general, any value between 500°F and 600°F will adequately serve as a cutoff point for the accuracy desired with this model. A value to the high end of the range can be chosen for conditions favorable to evaporation (high wind speed, high temperature) and a value to the lower end for unfavorable conditions. As Figure 4.4-3 shows, calculated evaporations differs by at most 10 per cent of oil volume for the two extremes of this temperature range.

All that is needed to use this method is information on the boiling point distribution of the oil in question. Such distillation

data are published for many crudes (see e.g., Ferrero and Nichols, 1972). Some typical distillation curves are shown in Figure 4.4-3*. It can be seen, for instance, that if 500°F is used as a cutoff, 40 percent of the typical crude with API gravity 35 would be expected to evaporate. Sometimes distillation curves are accompanied by information on the density of the fraction remaining at each boiling point. This permits an easy estimate of whether, for instance, the oil remaining after evaporation will be prone to sink.

If a breakdown of the oil by number of carbons is available insteady of distillation data, a cutoff number of carbons per molecule can be used, taking either C_{15} (boiling point of $n-C_{15} = 270°C$), C_{16} or C_{17} (boiling point of $n-C_{17} = 302°C$). Compounds with the same or fewer carbons are assumed to evaporate fully, others not at all.

It cannot be said with certainty how much time must elapse for this model to be valid since this depends on several environmental variables. A period of a week or more is certainly adequate for the potential evaporation to have taken place. The model will also be valid or only slightly off for periods of 2-3 days, sometimes for even shorter periods.

_____

* Figure 4.4-3 shows true boiling point distillation curves, i.e., curves drawn for a distillation in which all of each component, and only that component, boils off at its boiling point. For purposes of single step evaporation it is probably better to use standard ASTM distillation curves. In this process no attempt is made to fractionate the oil into components. Many different components boil at each temperature and each component boils off at least partly at temperatures above and below its true boiling point. This is more like the situation in oil evaporation, in which all components are evaporating simultaneously, albeit at different rates. In practice, the two types of curves do not differ very much. (Nelson, 1958).
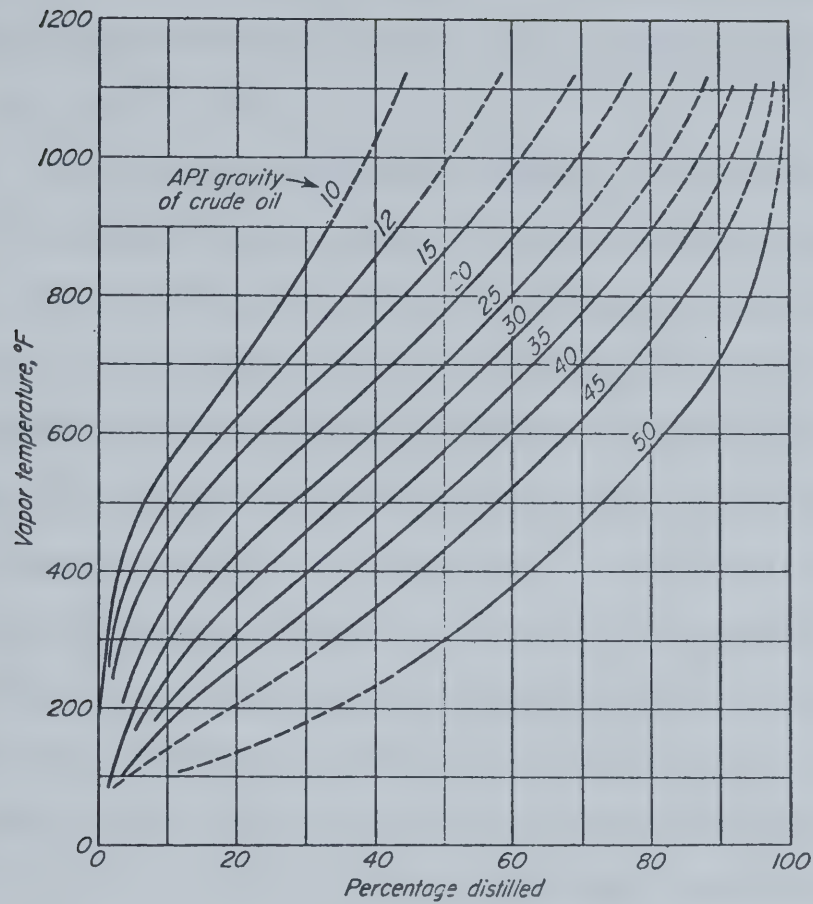
Figure 4.4-3: Typical distillation curves for crude
oils based on data for more than 350 different crudes
(Nelson, 1958, p. 90)

Summary of Evaporation Models

The models discussed represent the state-of-the-art of oil spill evaporation modeling. It is instructive to review and discuss their many common assumptions in order to assess how far the field still must go.

The first group of assumptions idealizes the oil slick. The slick is modeled as one of uniform thickness which remains perfectly mixed both horizontally and vertically. In actuality, different components spread at different rates and the slick tends to fractionate, as has been mentioned. Assuming perfect vertical mixing is equivalent to assuming that diffusion within the slick can keep up with evaporation from the slick surface. This generally is a good assumption for thin, less viscous slicks. However, at the beginning of the slick's life, the slick is at its thickest and evaporation at its fastest, presenting the proper conditions for diffusion within the slick to be the rate-limiting process. This can be corrected for by modeling diffusion within the slick.

The ideal slick assumptions are the same as those used in the spreading models and improving them would require building a more sophisticated model of spreading. Without better knowledge of these non-ideal phenomena, it is impossible to say exactly how predicted evaporation will differ from the real thing. It is conceivable that a non-ideal, fractionated slick would evaporate faster than a model slick because the components that spread slowly and remain in the thick blobs are also the least volatile components. Better to have them segregated in a few small areas than to have them interfere with

evaporation of the more volatile components elsewhere in the slick.

A second group of approximations is that oil is a perfect mixture, that the behavior and properties of one hydrocarbon are not affected by the presence of others. This assumption is inherent in the use of Raoult's Law.

In reality, of course, most mixtures are not ideal. There is a heat of solution caused by the mixing of different liquids that must be overcome in addition to the heat of vaporization, for evaporation to occur. Evaporation of non-ideal mixtures is thus more difficult than predicted by Raoult's Law. This can theoretically be corrected for by adding an activity coefficient to Raoult's expression. Hence

$$p_i = P_i X_i \gamma_i \qquad\qquad (4.4\text{-}18)$$

where γ_i is slightly less than 1.

It has been found that ideal conditions are approached most closely when the elements of the mixture are of nearly the same molecular size. Benzene-toluene is an oft-cited example. For most oils with their large range of components the ideal assumption is not valid. Regnier and Scott (1975) found that the evaporation energies for the n-alkanes in diesel fuel oil were significantly higher than the energy of the pure compounds. Similar evidence of inter-molecular interaction was noted by Wall et al. (1970). The ideal-mixture models tend to overestimate the rate of evaporation, although it is hard to separate out this effect from that of limited diffusion within the slick.

Another major group of assumptions and approximations are those used in deriving equation (4.4-4) for the evaporative constant. These are primarily reflected in the values of the exponents on wind speed and slick diameter, respectively. While these equations are not the only possible choices they are quite similar to others that have been successfully used in computing heat loss from water surfaces (Ryan and Harleman, 1973).

Finally, the models cannot properly account for the roughness of the sea, since there is a discontinuity noted when whitecapping begins. Models fitted for lower wind speeds and calm oceans cannot properly be used under rough conditions. As a start in surmounting this problem, the mechanisms behind the increased evaporation under rough conditions must be understood. It has been suggested that the effect is due mainly to a greater surface area being exposed in rough conditions. Wu (1971), however, has suggested that increased roughness alters the wind structure over the slick. If the first hypothesis is correct, it would suggest merely multiplying the area term in the evaporation constant by some corrective factor. If the second suggestion proves correct it would require altering the exponent on the wind speed or possibly developing a whole new functional form for the dependence of evaporation on wind speed.

4.4.2 Subsurface Fluxes

There are several mechanisms by which oil can enter the water
column. Dissolution is usually the most important one for aromatics and
other hydrocarbons with fewer than 11 carbon atoms. Larger, less
soluble molecules may undergo photochemical oxidation reactions trans-
forming them into soluble compounds. These larger molecules may also
form colloidal-sized particles which can be "accommodated" in water, a
process that is not true dissolution but which has often been confused
with it in the literature. The presence of surface active organic matter
in the water promotes this accommodation (Boehm and Quinn, 1973). Oil
globules may also simply be dispersed mechanically in the water column,
be carried downward   by adsorption to sediment, sink from their own
weight or be ingested and then excreted by marine organisms. Oil that
enters the water column may remain suspended for long periods of time, may
settle into the bottom sediments, or may be drawn back up to the surface
or atmosphere. Oil that remains in the water column or bottom sediments
will be subject to biodegradation (see Section 4.4.4).

Each of the mechanisms which contribute to ϕ_b, the subsurface flux,
will now be discussed in turn.

Dissolution

The solubility of oil has already been discussed in Section 4.1.
The values presented there say little in themselves about how much oil
will actually dissolve. For while solubilities are low, the volume of
water potentially available is huge. Rather, the determinant of how
much of a hydrocarbon will dissolve is the rate of dissolution and how

that rate compares to the rates of competitive processes. Dissolution tends to occur in the first hours of a slick's life, meaning that it must compete with evaporation. Numerous investigators have found that oil losses from solution will be two or more orders of magnitude smaller than from evaporation (Smith and MacIntyre, 1971; Moore et al., 1973; Harrison et al., 1975; McAuliffe, 1976b). A study of the fate of oil from the Chevron Main Pass Block 41 spill (McAuliffe et al., 1975) found that less than 1 per cent of the oil dissolved compared to 25-30 per cent which evaporated, although the study could not account at all for more than half the oil. Evaporation will deplete the slick of most volatiles before they get a chance to dissolve. Those that do dissolve will eventually be drawn back up into the atmosphere (Frankenfeld, 1973; Lassiter et al., 1974). Hence the equilibrium solubility values for water in the absence of air are rarely likely to be reached after real spills.

Field studies in which concentrations of dissolved oil from a spill have been measured are few and probably flawed in that it is difficult to distinguish solution from dispersion and accommodation. McAuliffe (1976b) found concentrations no higher than 60 ppb of total dissolved C_2 to C_{10} hydrocarbons beneath four experimental spills. Measurable concentrations were found at depths of 5 feet, but not at 10 feet, and at 15 minutes after the spill but not at 30 minutes, indicating rapid evaporation of any dissolved volatiles. And McAuliffe suspected that even these low concentrations were measures not of solution, but of dispersed oil that had dissolved between the time the sample was collected and the time it was filtered.

Nevertheless, in certain circumstances concentrations of dissolved oil may reach biologically significant levels. Such a case is when a thick slick completely covers a shallow lake or near-shore sheltered area, or when the oil is rapidly churned into the water column before much of it has a chance to evaporate. In both these cases, solution may be particularly important when the spill involves a highly aromatic refined oil. In these cases it may be necessary for biological reasons to model dissolution of the oil or of selected components.* The state-of-the-art of modeling dissolution is somewhat behind that of evaporation, owing largely to the scarcity of good field data. The different approaches to modeling dissolution have parallels for evaporation and, in fact, dissolution cannot be modeled adequately unless evaporation is modeled simultaneously.

As for evaporation, a vertical diffusion model permits treatment of flux into the water column as a boundary condition. Lassiter's (1974) model, discussed in Section 4.4.1, was used to predict water column concentrations of benzene and naphthalene. Three stages of mass transfer were found for benzene. First, a period of evaporation and dissolution. Then, a period in which evaporative losses halted the transport of hydrocarbons into the water. Finally, a period in which evaporation drew the dissolved benzene back into the air. For benzene in a slick

---

* Which single compound to concentrate on for, say, a worst case analysis, is difficult to say. In so far as equilibrium solubility values apply to these cases, benzene and toluene can be expected to be the most abundant dissolved hydrocarbons immediately following the spill. However, these compounds are very volatile and will be quickly drawn up into the atmosphere. The less soluble but also-less-volatile higher aromatics will persist for longer times in the water column, albeit in lower concentrations. Yet, as has been mentioned in Section 4.1, the most soluble of these are also the least toxic, so no clear cut choice stands out. A lot of recent attention however has focused on naphthalene as being highly toxic and fairly soluble, if also fairly volatile (Lassiter et al., 1974; Anderson, 1976).

1 mm thick, the first and second stages were found to take three hours apiece. After five days the concentration was practically constant for the first 5 meters below the slick. Then the hydrocarbon was sucked back into the atmosphere.

There is very little data with which to compare the results of the model, but the general pattern of dissolution followed by evaporation has been found experimentally for benzene and other volatile hydrocarbons. The approach, then, seems promising, although this particular model cannot account for the effect of temperature, wind, slick movement and spreading.

In Lassiter's model, transport into the water column is proportional to the concentration gradient across the oil-water interface subject to the condition:

$$C_{iw} = K_s C_{io} \qquad\qquad (4.4.19)$$

where C_{iw} and C_{io} are the concentrations of substance i in the water and in the oil respectively and K_s represents the relative solubility of the substance in the two media. If it can be assumed that the water immediately below the slick is saturated with respect to oil, we can use the solubility figures reported in Table 4.1. to compute the gradient across the interface.

The vapor pressure models for evaporation also have their parallel for dissolution. However, the driving force for dissolution is the concentration gradient across the oil-water interface, rather than the vapor pressure gradient.

Assuming (Leinonen and Mackay, 1973) as was done for the diffusion

model, that the water immediately below the slick is saturated with hydrocarbons, Harrison et al. (1975) propose the following relationship for the dissolutive flux:

$$\phi_d = K_D \, S_i \, X_i \gamma_i \qquad\qquad (4.4.20)$$

where K_D is a constant, S_i is the solubility of substance i, X_i its mole fraction and γ_i an activity coefficient. This is clearly analogous to the evaporation expression for one component of a mixture obtained by substituting equation (4.4.18) into (4.4.2). Leinonen and Mackay (1973) found that the activity coefficients are likely to be greater than unity. They found that the solubilities of both hydrocarbons in a binary mixture were 6 to 35 per cent greater than would be predicted by an ideal linear dependence on mole fraction.

Williams et al. (1975) and Moore et al. (1973) used a simple first-order model. Such models are less sophisticated than the ones discussed above and accurate data does not exist for the first order coefficients. Most of the problems associated with using simple first order schemes for evaporation apply to dissolution as well.

Dispersion and Accommodation

In addition to dissolving, oil may enter the water column as colloidal or suspended particles in amounts greater than can be expected from dissolution. These particles may range in size from less than a micron to larger than a millimeter in diameter. Peake and Hodgson (1967) found that 75 per cent of the accommodated $C_{20} - C_{33}$ hydrocarbons in their experiment were removed by a 5μ filter and almost 100 percent by a

.05μ filter. After the Arrow oil spill in Nova Scotia, particles ranging from 5 microns to a millimeter were found as far as 250 km from their source (Forrester, 1971).

Some of these suspended particles may be formed by simple mechanical dispersion. Water turbulence may tear off globules of oil and entrain them, forming an oil-in-water emulsion. These emulsions, by themselves, are not stable and the oil will coalesce (Berridge, Thew et al., 1968) unless the particles are dispersed very quickly.

These emulsions can also be stabilized by surface active agents which can coat the oil-water interface and prevent oil from coalescing. The formation of semi-stable colloids has been called accommodation or "solubilization" to distinguish it from true solubility. It is hard to make a clear distinction between accommodation and mechanical dispersion, accommodation really being nothing more than chemically assisted dispersion. However, while simple mechanical dispersion would be expected to affect all slick hydrocarbons equally, accommodation is more selective (Peake and Hodgson, 1966, 1967).

In natural waters, dissolved organics may serve as the surface active agents to solubilize oil. Sources of this organic matter include sediments and sewage outfall. Boehm and Quinn (1973) found that the amounts of $n-C_{16}$ and $n-C_{20}$ accommodated in Narragansett Bay water varied with the level of dissolved organic carbon. The solubilization of $n-C_{16}$ fell 75 per cent after a 35 per cent reduction in DOC. Significantly, the solubility of phenanthrene, an aromatic, was not affected by the presence of dissolved organics, indicating that this mechanism is not important for aromatics.

Surface active agents within the oil itself conceivably can also bring about solubilization, since accommodation has been observed in distilled water (Peake and Hodgson, 1966, 1967; Franks, 1966).

It has been proposed that accommodated hydrocarbons exist in colloidal forms called micelles (Boehm and Quinn, 1973). A micelle is a cluster of surface active compounds, whose molecules have hydrocarbon chains at one end and a polar group at the other (Elworthy et al., 1968). The hydrophobic hydrocarbon parts of these molecules huddle together in the center of the micelle as remote from the water as possible, thereby reducing the high free energy associated with the hydrocarbon-water interface. The polar groups stay on the outside of the micelle in contact with the water. Other hydrocarbons can dissolve in the hydrocarbon interior of the micelle. In this way, normally insoluble hydrocarbons are "solubilized." This is the means by which the detergents and chemical dispersants used in oil spill cleanups act to disperse the oil.

It is impossible to give an accurate figure for the amount of hydrocarbons which may be accommodated. It depends to a large extent on the quantities of organics present in the surface water as well as on the waters pH and salinity. Also, since accommodated particles are not in equilibrium, the levels of accommodation are determined to a large extent by the degree of agitation and length of settling time before a measurement is taken. Finally, accommodation of each hydrocarbon is dependent upon the quantities of other hydrocarbons present.

Peake and Hodgson (1967) found that individual hydrocarbons in the C_{12} to C_{17} range could be accommodated in levels of 10 to 100 ppm. But these high values did not persist very long and were reached only after

vigorous agitation. After 15 days, the accommodated levels had dropped
to .3 ppm. Most laboratory values reported for accommodation are on the
order of .01 to .1 ppm for individual alkanes (Peake and Hodgson, 1967;
Sutton and Calder, 1974) and on the order of .1 to 1 ppm for total
accommodation of all hydrocarbons (Boehm and Quinn, 1973; Peake and
Hodgson, 1966). Solubilities of the n-alkanes in distilled water range
from .0037 ppm for n-C_{12} to .0017 for n-C_{26} (Sutton and Calder, 1974),
so accommodation of these n-alkanes is about 2 orders of magnitude
greater than dissolution.

As is the case for solution of oil, laboratory studies do not
necessarily give an accurate idea of how much of the oil from a real
spill may be accommodated or dispersed. There have been a few field
studies in which subsurface concentrations of oil have been measured.
Freegarde et al. (1970) found levels of dissolved and dispersed hydro-
carbons beneath a slick on the order of .1 ppm at a depth of 1 meter
and .01 ppm at 5 meters in the first few hours after a spill. As a
guide to these figures, a concentration of 1 ppm in a meter of water
below a slick accounts for only 1 per cent of a .1 mm thick slick.
Hence, dispersion in this case accounted for a few per cent of the oil at
most. Forrester (1971) found concentrations of suspended particles from
the Arrow Oil Spill in concentrations as high as .02 ppm at depths of 5 to
10 meters. He estimated that suspended particles left the slick at the
rate of 6 m^3/day during the first two weeks and at about 1 m^3/day for
the following twenty days. It is clear that the suspended oil represents
only a small fraction of the total spill, whose volume was several thousand
cubic meters.

Photochemical Oxidation

In the presence of sunlight, compounds in oil can undergo oxidation to form a variety of products including hydroxy-compounds, aldehydes, ketones and carboxylic acids (Freegarde et al., 1971). Since these products are often more soluble than the original hydrocarbons, photo-oxidation tends to reduce the volume of the slick through solution.

In the first few days after a spill photo-oxidation is negligible compared to evaporation and dissolution of the slick's original hydrocarbons. After a week or more, however, the effects of photo-oxidation - on both the quantity of dissolved organics and the spreading properties of the slick - become noticeable.

Lysyj and Russell (1974) found that the combined concentration of dissolved and accommodated hydrocarbons from fuel oils and gasoline increased in two distinct stages. Within one day, concentrations reached levels ranging from 36 ppm to 220 ppm and stayed that way for a period of two days to several weeks, depending on the type of oil. Concentrations then began to rise again so that after 42 days the levels of dissolved organics were hundreds of ppm higher than after the first plateau was reached. The authors attributed the initial rise to dissolution of indigenous oil compounds and the second rise to chemical modifications of initially insoluble hydrocarbons. The amount of hydrocarbons solubilized by these oxidation reactions was greater than the initial dissolution, often twice as great.

Burwood and Speers (1974) also noticed a five-fold increase of dissolved C_{15} - C_{23} polar compounds after a month. They identified these as thiacyclane-I-oxides, products of the oxidation of indigenous crude oil

thiacyclanes. Exposure to greater illumination accelerated the formation of these compounds. Hellmann (1971), noted that the viscosity of an open ocean slick increased in two steps. The first order-of-magnitude rise in viscosity occurred in the first few days and was attributed to loss of volatiles by evaporation. The second increment, of two to three orders of magnitude, occurred over a period of weeks and months and was attributed to chemical oxidation effects.

Probably the best estimate of the rate of photo-oxidation is provided by Freegarde et al. (1971). Extrapolating the results of laboratory experiments to open ocean slicks, they predicted that photo-oxidation could result in the destruction of 2.5 µm of slick thickness per 100 hours of sunlight for a slick 1 mm thick, or about 0.25 per cent of the slick in 10 days, assuming 10 hours of sunlight per day. For slicks .01 and .001 mm thick, the absolute destruction rate is only 1/2 and 1/10 respectively of the above value since thinner slicks absorb less sunlight. However the percentage of the thinner slicks decomposed in a given time is greater than for the thicker slick.

Much research is required to better determine the rates, mechanisms and products of photo-oxidation as they vary with the different oil compositions and different degrees of illumination. The scanty data cited above, however, indicate that photo-oxidation can be as important a weathering process, if not moreso, than dissolution of indigenous slick hydrocarbons. However, photo-oxidation acts over a much longer time span, on the order of weeks and months rather than days.

Modeling photo-oxidation should be possible once the kinetics are known. Majewski et al. (1974) showed that an auto-catalytic model produced

the best statistical fit to kinetic data. According to this envisioned

mechanism, a molecule of reactant would react with oxygen to form a

free radical which would form an oxidation product. The oxidation product

would be capable of forming free radicals itself which would join in the

reaction, and so on. They propose modeling such a reaction by the

following equation:

$$\ln (P/R) = (R_o + P_o)kt - \ln(R_o/P_o) \qquad (4.4.21)$$

in which R_o, P_o = initial concentrations of reactant and product

R, P = concentrations of reactant and product at time t.

The value of the rate constant would depend on factors such as the speci-

fic reactant and product and the wavelength and intensity of the solar

radiation. Absorption of light by oil is greatest for wavelengths in

the 200-300 nm range, shorter than the wavelengths found in sunlight.

Absorption drops off with increasing wavelength, although crude oil can

absorb all wavelengths in sunlight well except reds (Freegarde et al.,

 1971).

Spreading and photo-oxidation are also intertwined. Oxidation

reactions increase with increasing surface area but decrease with

thinning because less light is absorbed by thinner slicks. Going in the

opposite direction, Klein and Pilpel (1974) found that irradiation of oil

by artificial sunlight increased the spreading coefficient from 22 to 28

dyne/cm in an hour. This is largely from a reduction of oil-water inter-

facial tension caused by absorption at the interface of the products of

the oxidations, some of which are probably surface active.

Sinking and Sedimentation

There are several other mechanisms by which oil, either in the slick or dispersed in the water column, may be carried downward, eventually to the bottom sediments.

The first is gravity-induced sinking, which will occur if the oil density exceeds that of the water. This will happen only for some oils and then only after weathering. It has been suggested that such sinking was responsible for the otherwise inexplicable disappearance of the slick from the Anne Mildred Brovig spill (Berridge, Dean et al., 1968). An evaporation model and some knowledge of the chemical composition of the oil are usually enough to enable prediction of a slick's tendency to sink.

More interesting is the interaction of oil with sediments. Oil globules can adhere to suspended particles and be carried downward. Or, oil already dispersed in the water column can come into contact with bottom sediments and be held there.

This mechanism can result in significant buildup of hydrocarbons in both bottom and suspended sediments, especially after spills occurring in estuaries with high suspended solids loads. Conomos (1975) noted that much of the oil from a San Francisco Bay spill reached and was transported along the bottom. In another study of San Francisco Bay, DiSalvo and Guard (1975) measured hydrocarbon concentrations averaging 1200 ppm in suspended sediments and 1588 ppm in bottom sediments. They estimated that 13.2 metric tons of hydrocarbons were suspended in the bay, an amount that would accommodate the daily input into the bay of hydrocarbons from industrial effluent.

McAuliffe et al. (1975) observed hydrocarbon concentrations averaging

31 mg/l in the sediments in the vicinity of the Chevron spill in the Gulf of Mexico, compared to background concentrations of 1 mg/l. Nevertheless, they estimated that oil in the sediments accounted for less than 1 per cent of the total spill volume. Oil-sediment interactions were also reported important in the West Falmouth and Santa Barbara incidents. In short, it can be concluded from these limited field studies that oil-sediment interactions can increase the bottom and water column concentrations of hydrocarbons substantially above ambient levels. Oil which reaches the bottom can coat and kill shellfish and other benthic organisms. It is still not known whether sediment-sorbed hydrocarbons are available for uptake by aquatic organisms (Anderson and Moore, 1976).

There is virtually no field data on the rates at which oil can be removed from the slick by this mechanism. Most of the studies of this process have concerned artificial addition of massive doses of particles to sink oil as a slick removal technique. These tests show that the actual physical process of adhesion and removal is a rapid one. But for untreated spills the rate-determining factors will be the nature and quantity of naturally suspended sediments and the rate at which these particles are brought into contact with the oil. Artificial sinking tests obviously cannot shed much light on this.

These tests do, however, point out what factors are likely to be important. The size of the particles seems to be of foremost importance in determining the ability of a substance to sink oil (Poirier and Thiel, 1941; Tobias, 1971). Smaller particles are more efficient in sinking oil, probably because of their relatively larger surface area per unit volume. Another factor is the nature of the sediment, particularly the

wetting factor. To be an effective sinking agent the material should be preferentially wet by oil and resistant to wetting by water (Houston, 1971). Sand, for instance, is easily water wet and is never used as a sinking agent without first being chemically treated. Ho and Karim (1976) found that high levels of iron or aluminum hydrous oxides increased a sediment's ability to adsorb oil. Finally, the degree of turbulence is a crucial parameter. Greater turbulence disperses oil globules into the water column, deflocculates sediments to decrease particle size and promotes mixing of oil and sediments. On the other hand, greater water turbulence will also impede the descent of the oil-sediment conglomerate.

After oil has been adsorbed by suspended or bottom sediments it may yet free itself and resurface. After the sinking of 100 tons of Kuwait oil with treated sand in the North Sea, about 10 per cent of the oil resurfaced over a period of a month, initially at the rate of about 1 ton per day (Tobias, 1971). Disturbance of bottom sediments, as by subsurface currents, promotes this release of oil (Roshore, 1972).

A final method of oil deposition involves the uptake of oil droplets by marine organisms. Filter-feeding zooplankton such as copepods ingest oil particles and excrete them in fecal pellets which sink. Freegarde et al. (1971) estimate that under the most favorable conditions copepods could remove .3 g of oil per m^3 of seawater per day. The authors point out that for a spill covering 1 km^3 and a copepod population at full strength throughout the upper 10 meters of water, this corresponds to removal of 3 tons of oil a day, a significant amount. However, this figure assumes dispersed oil concentrations of at least

1.5 ppm over 10 meters, far higher than is likely to occur. Further,
copepod populations will be at their peak only at certain times of the
year. It should be pointed out that many other organisms ingest oil
particles without excreting them.

Summary of Subsurface Transport

Transport into and within the water column can be accomplished by
a number of mechanisms. Solution, dispersion and accommodation and
sedimentation are likely to take place shortly after the spill. There
is little data on how much oil can be taken up by sediments, though this
figure no doubt depends most heavily on the suspended solids load of the
water at the site of the spill. What scanty data exist suggest that
dissolution and dispersion between them will remove no more than a few
per cent of the slick, with dispersion being more important than dissolu-
tion. Neither mechanism is likely to be as important as evaporation in
removing oil from the slick except for very non-volatile residual oils.
But both mechanisms may be important from the biological standpoint.

After a few days, photochemical reactions become more important,
forming products which are more soluble than the reactants. Also,after
a few days, weathered oil might sink if it becomes heavy enough.

4.4.3 Emulsification

The formation of water-in-oil emulsions is one of the most important
processes affecting a surface slick, yet one of the least understood.
It can be considered to represent a positive flux term ϕ_B, in which a
new component, water, enters the slick. The volume of this flux may be
large enough to outweigh all the negative fluxes associated with evapora-
tion, dissolution and other weathering processes. Smith (1968), for

instance, found that the volume of emulsified oil impacting one beach after the Torrey Canyon spill was larger than the initial spill volume. Water-in-oil emulsions may contain between 10 and 80 per cent water and, as opposed to oil-in-water emulsions involved in mechanical dispersion of oil, they are very stable. Many crude oils, in fact, are initially produced as an emulsion and then dewatered.

Emulsification can change slick spreading properties more suddenly and more drastically than even evaporation. The viscosity of an emulsion may be 2 orders of magnitude or more higher than that of the oil alone (Atlantic Ocean Lab, 1970). Emulsions spread far more slowly than pure oil slicks and as a result are less susceptible to other forms of weathering. The higher the water content the greater these effects. When the water content rises above 50 per cent, the emulsion takes on a semi-solid, greaselike constituency which has been nicknamed "chocolate mousse" because it resembles the dessert in texture, if not in taste. Emulsions have been found after the Torrey Canyon, Arrow, World Glory and Santa Barbara spills.

No existing slick models adequately take emulsification into account. To do so requires an ability to predict when a slick will emulsify and what the water content will be, which in turn requires understanding the mechanisms of emulsification. The state of the art is just reaching this latter point.

The properties of the oil itself, as opposed to any environmental conditions, seem to be the most important factors in determining whether emulsions will form (Frankenfeld, 1973a). It is thought that surface active chemicals in the oil form a film on the oil-water interface, thereby

preventing the coalescence of water droplets that enter the oil when it is spilt. (Strassner, 1968). Berridge, Thew, et al. (1968) thought the agent came from the asphaltene content of oil. But other researchers (Atlantic Ocean Lab, 1970) did not find the same correlation between asphaltene content and emulsion stability. Based on a study of 45 crude oils, Strassner found that any oil with a film ratio greater than 20% and a viscosity of 6 cp or greater produced stable emulsions. Some 86 per cent of the oils fitted the correlation when only one of the two indices was applied.

As for kinetics, emulsification has been found to occur from shortly after the spill to 3 days after the spill (Atlantic Ocean Lab, 1970). Hence it can be grouped with evaporation and dissolution as an early weathering process.

4.4.4 Biodegradation

In the long run, biodegradation is an exceedingly important process in the removal of oil from the marine environment. It eventually takes care of most of the oil that remains after evaporation, dissolution and other quicker processes have run their course. However, the rate of biodegradation is so slow that the process will often not be important for modeling purposes, as shall be discussed.

When an oil pollution incident occurs in natural waters, the indigenous microbial population normally responds with a rapid decline in species diversity and a corresponding rise in the population of those species that can degrade the oil. More than 200 species have been identified which can utilize at least some of the hydrocarbons in oil (Zobell, 1973).

Some of the oil is decomposed completely to carbon dioxide and some is turned into cell biomass. There are also a large number of intermediate waste products formed such as aldehydes and ketones. These intermediate products either dissolve or evaporate or are in turn further decomposed by other microbial species.

Most bacteria are very specific as to which hydrocarbons they can utilize. All components of oil are subject to degradation, but it has been found that normal alkanes are oxidized most rapidly and aromatics least rapidly. This is because more species can utilize n-alkanes, which in turn might result from the fact that the simpler structure of n-alkanes makes them more susceptible to enzyme attack. In contrast to evaporation, the size of the molecule seems to have little effect on the susceptibility to biodegradation (Blumer et al., 1972).

The implications of the differential degradation rates for the kinetics of the process are as follows: Oil degradation will proceed rapidly at first as the easily degraded parts are attacked. Then the process will slow down noticeably. There may be a lag time before bio-degradation begins, however. This is the time needed for the proper bacterial populations to grow to large enough size and to become acclimated to the oil. Reports of lag times in experiments and in the environment vary from less than a day to more than two weeks, depending on various conditions (Atlas and Bartha, 1972a,b,c; Kinney et al., 1969).

The actual rates of biodegradation of oil in the marine environment cannot be easily predicted. Results of laboratory studies are usually not applicable to the real world, at least as far as rates are concerned, because most labs carry out degradation under nicely controlled, ideal

conditions. Lab biodegradation, therefore, is generally much faster

than would be the case under actual marine conditions. The actual rate of

microbial breakdown depends on a number of parameters, any one of which

might be a limiting factor under some circumstances. Among these are

nutrient (N and P) levels, oxygen, temperature, surface area of the slick

and the composition and size of the microbial population.

To get a very rough idea of how fast biodegradation might proceed,

a report by Arthur D. Little (1970) makes some quick and dirty calculations

for the cases in which oxygen and phosphorous are the limiting parameters.

It is estimated that 40 lbs. of O_2 can dissolve in the ocean per acre per

day and that oxidation of a pound of oil requires a minimum of 2 pounds of

oxygen. The most oil that can be broken down per day is thus 20 pounds

per acre, or 12,800 pounds per square mile, providing oxygen is the

limiting factor. For slicks on the open ocean, however, nitrogen or

phosphorous are more likely to be limiting. It was estimated that the

concentrations of phosphorous in the Atlantic would be enough to allow the

degradation of 5,440 pounds per square mile per day. A slick 1 mm thick

contains about 5,000,000 pounds of oil per square mile assuming a specific

gravity of .9. Thus O_2 limitation would allow the degradation of .2 per

cent of the slick each day and phosphorous limitation would permit half

that. If the slick is only .1 mm thick these figures become 2 and 1 per

cent. This figure is very crude in that it makes many untested assumptions

and it assumes a constant degradation rate, when actually the rate declines

as time proceeds. Nevertheless it does indicate that biodegradation will

not reduce the slick substantially for a couple of weeks at least. And

this figure assumes that the organisms will be present to do the degrading,

which is not always the case for the open ocean spills.

In many circumstances, especially when oil washes up on land or sinks into sediments, or even when it is floating out at sea, the rate of biodegradation may be imperceptibly slow. Examining shorelines contaminated with oil from the Arrow spill in Nova Scotia, Betancourt (1973) concluded that less than 20 per cent of the oil had disappeared in 18 months and Rashid (1974) noticed little degradation in low energy coastal areas 3 1/2 years after the same spill. Blumer and Sass (1972) noted a similar persistence of oil in sediments after the West Falmouth spill. For surface slicks in more productive near-shore areas the natural rate of degradation might be measured on a scale of months rather than years. Kinney et al. (1969) report that biodegradation of both large and small slicks in Alaska's Cook Inlet was "essentially complete" within two months, although disappearance of the oil was greatly aided by highly turbulent conditions.

Predictably, many laboratory tests do better than this for reasons already mentioned. For instance, Solig and Bens (1972) found a 50 per cent weight reduction in only 40 hours using a mixed culture with agitation, aeration and nutrient enrichment. Atlas and Bartha (1972) found that a pure culture of flavobacteria degraded 50 per cent of Swedish crude in 8 days, with degradation leveling off after that. Zobell (1969) found biodegradation to reduce the weight of the oil 26 to 98 per cent in 30 days with aeration and nutrient enrichment.

In summary, biodegradation of an oil spill will take a matter of months or years, though if ideal conditions are met the effects of the process will be seen beginning within 2 weeks of the spill. There is no

chance that biodegradation will be important in the first few days, except, perhaps, if the oil rapidly disperses into fine, widespread droplets. The lag time before biodegradation begins will be at least this long unless a high concentration of suitable organisms is already present at the site of the spill.

4.5 Summary and Conclusions Regarding Oil Slick Transformations

Perhaps the most important conclusion that may be drawn from the information presented in this chapter is the importance of the interactions between the following factors:

- physical and chemical oil properties

- the motion and composition of the water beneath the slick

- climatalogical conditions above the slick.

It is clear from the discussion of existing analytical approaches that most techniques do not attempt to consider the full range of potential inter- actions because of the complexity of the relationship involved. In addition it is evident that for many of the transformation processes there is a significant lack of data suitable for the purpose of testing the basic hypotheses of modeling efforts.

In spite of the complexities noted above, when the problem of predicting oil slick transformations is viewed from a perspective that emphasizes the total range of space and time scales involved, it becomes evident that for a particular application not all of the processes may be important. Also, for those processes that are judged to be significant, the precision of available methods may be adequate. The objective of this section is to illustrate these conclusions in the context of a simplified two-component oil mixture.

4.5.1 Two Component Slick Model

The two component slick computation is intended to typify the interactions between the following transformation processes:

- spreading

- dispersion

- evaporation

For simplicity, weathering processes other than evaporation are not included. Also, because of the lack of basic data on surface tension of mixtures, the net surface tension is assumed to be constant.

Oil Properties

The properties of the two oil types used in the computations are specified such that there will be a significant difference in their respective rates of evaporation as determined by the given oil vapor pressures. A summary of the properties of the two oil types is as follows:

Component #1

Density = ρ_1 = 0.73 g/cm^3

Vapor Pressure = P_1 = 1.3 x 10^3 dynes/cm^2

Molecular Weight = M_1 = 142

Component #2

Density = ρ_2 = 0.86 g/cm^3

Vapor Pressure = P_2 = 5 x 10^{-5} dynes/cm^2

Molecular Weight = M_2 = 288

The net surface tension of the mixture, f_n, is assumed to be constant and equal to 30 dynes/cm. Finally the initial concentrations of the two components are given by:

$$c_1 \Big|_{t=0} = 0.259 \text{ g/cm}^3$$

$$c_2 \Big|_{t=0} = 0.53 \text{ g/cm}^3$$

Mass Transfer Equation

The mass transfers in the two component mixture are treated using the following assumptions:

1. A circular slick of radius, R, and uniform thickness, h.

2. Horizontally and vertically uniform oil properties.

3. Evaporation flux, given by the following empirical relationship:

$$\phi_{e1} = kW \, p_i$$

where k = evaporation constant = $1 \times 10^{-12} \, \dfrac{sec^2}{cm^2}$

W = wind speed (cm/sec)

p_i = vapor pressure of oil fraction in the mixture

$(dyne/cm^2)$

For the above assumptions, the total mass conservation equations for the two oil components are as follows:

$$\frac{d}{dt} (c_1 hR^2) = -\phi_{e1} R^2$$

$$\frac{d}{dt} (c_2 hR^2) = -\phi_{e2} R^2$$

Using the volumetric relationship, $\dfrac{c_1}{\rho_1} + \dfrac{c_2}{\rho_2} = 1$, the above equations may be manipulated to yield:

$$\frac{dc_1}{dt} = \frac{c_1}{h} \left(\frac{\phi_{e1}}{\rho_1} + \frac{\phi_{e2}}{\rho_2} \right) - \frac{\phi_{e1}}{h}$$

$$\frac{dc_2}{dt} = \frac{c_2}{h} \left(\frac{\phi_{e1}}{\rho_1} + \frac{\phi_{e2}}{\rho_2} \right) - \frac{\phi_{e2}}{h}$$

$$\frac{dhR^2}{dt} = - \left(\frac{\phi_{e1}}{\rho_1} + \frac{\phi_{e2}}{\rho_1} \right) R^2$$

where the evaporative fluxes may be related to the oil properties using equation 4.4.17 and Raoult's Law (Equation 4.4-3).

$$\phi_{e1} = kW \left[\frac{c_1/M_1}{c_1/M_1 + c_2/M_2}\right]P_1$$

$$\phi_{e2} = kW \left[\frac{c_2/M_2}{c_1/M_1 + c_2/M_2}\right]P_2$$

in which the bracketed expression represents the mole fraction of each component in the slick.

Spreading and Dispersion

The spreading and dispersion calculations also assume the idealized slick geometry defined above. Spreading and dispersion are considered separately according to the following:

$$\left(\frac{dR}{dt}\right)_{Total} = \left(\frac{dR}{dt}\right)_{Spreading} + \left(\frac{dR}{dt}\right)_{Dispersion}$$

The rate of growth from spreading can be found from a balance of the various spreading forces discussed in section 4.3:

$$\underset{Gravity}{\beta_1(\rho_w-\rho)gh^2R} + \underset{\substack{Surface\\Tension}}{\beta_2 f_n R} = \underset{Spreading}{\frac{\beta_3\rho_w\nu_w R^2}{\sqrt{\nu_w t}}\left(\frac{dR}{dt}\right)} + \underset{spreading}{\overset{Dynamic\ Pressure}{\rho_w hR\left(\frac{dR}{dt}\right)^2}}$$

in which all terms are as defined in section 4.3. Solving the quadratic yields:

$$\left(\frac{dR}{dt}\right)_{\text{spreading}} = \frac{1}{2}\left\{-\beta_3 \frac{R}{h}\sqrt{\frac{\nu_w}{t}} + \sqrt{\beta_3^2\left(\frac{R}{h}\right)^2 \frac{\nu_w}{f} + 4\left[\beta_1\left(\frac{\rho_w-\rho}{\rho}\right)gh + \beta_2 \frac{f_n}{\rho_w h}\right]}\,\right\}$$

The above relationship is consistent with the constant volume relationships given in Table 4.3.1 provided that $\beta_1 = k_1^2/4$, $\beta_2 = 3/4\ k_3^2 k_1^4/k_2^6$ and $\beta_3 = k_1^4/k_2^6$. For mean values of k_1, k_2, k_3 given in Table 4.3.1, this yields:

$\beta_1 = 0.42$

$\beta_2 = 1.64$

$\beta_3 = 0.86$

The growth rate from dispersion is given as:

$$\left(\frac{dR}{dt}\right)_{\text{dispersion}} = Kt^n/R$$

This law agrees with data analyzed by Okubo (1962) if $K = .01$ and $n = 1.3$.

The above development provides four equations for the variables c_1, c_2, h, and R which may be solved for the given initial values of c_1 and c_2 and for reasonable initial choices of h and R that satisfy the relationship $\pi h R^2 = $ initial volume.

4.5.2   Results of the Computations

Figure 4.5.1 shows the results of the calculations using the model for three different initial volumes. The plot shows (1) the slick diameter (2) the relative percentage of oil fraction #1, and (3) the dominant processes as a function of time after the spill occurred. Figure 4.5.2 shows the same variables for calculations in which the following parameters were varied by a factor of two:

   - net surface tension, f_n

   - wind speed, W

   - dispersion coefficient, k

The results for these particular calculations seem to indicate that the rate of slick growth and evaporation are only slightly sensitive to changes in the parameters indicated. This seems to indicate that the evaporation and spreading have only a minor influence on each other. However, the model neglects the changes in the net surface tension that is likely to result from evaporation of volatiles. This change is likely to be very important in slowing the spreading of the slick.

The results presented in these figures support the following conclusions:

1. Dispersion and spreading processes enlarging the slick tend to overlap considerably in an intermediate region of length and time scales, indicating that neither alone may be an adequate representation of oil behavior. On the other hand, for times less than 1 day, spreading is clearly dominant while dispersion is the most important process at times greater than a week.
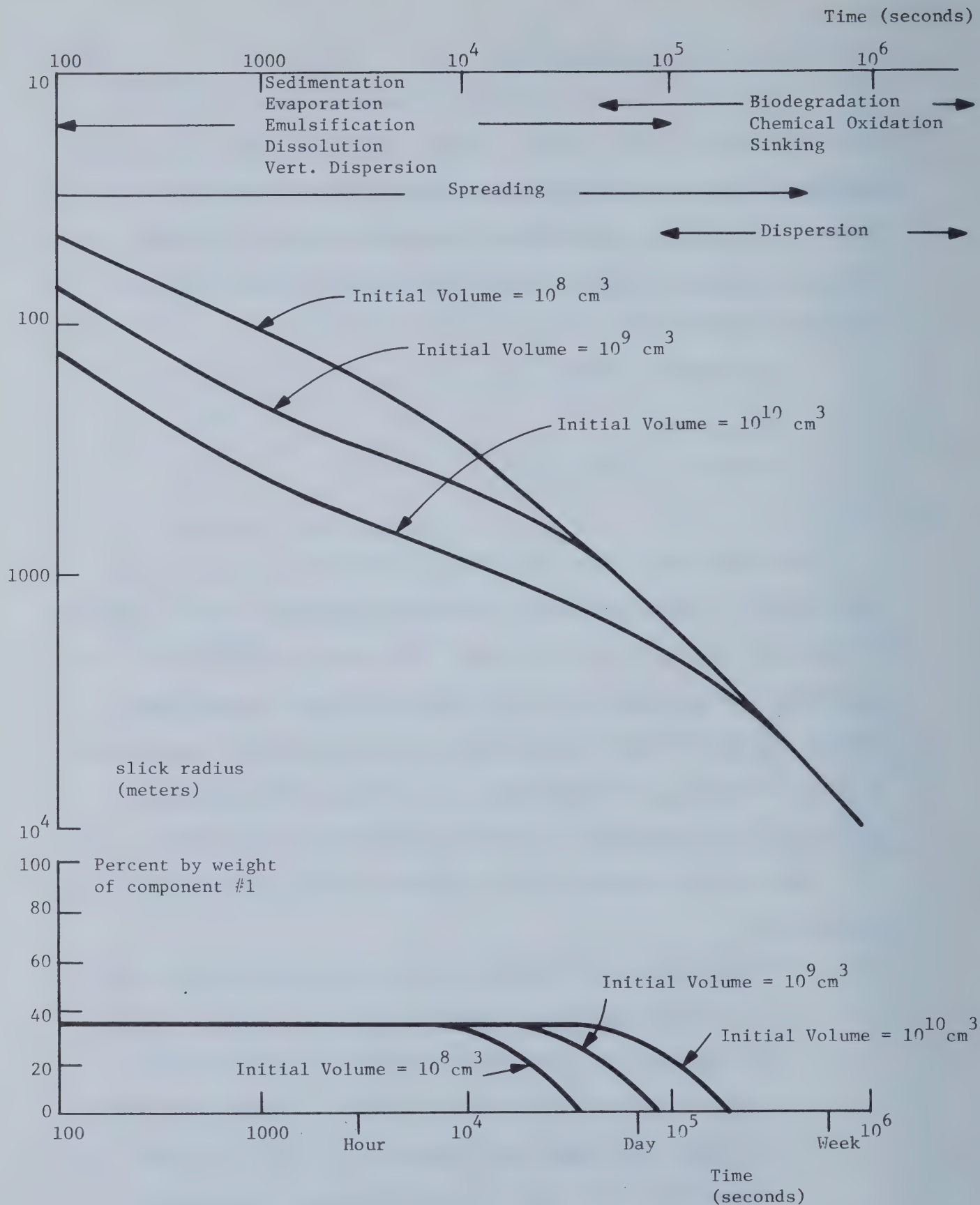
Figure 4.5.1   Results of the Two Component Oil Slick Computations for Three
Different Initial Volumes.

Figure 4.5.2 Sensitivity of Two-Component Oil Slick Behavior to Changes in the Parameters Representing Surface Tension, Evaporation, and Dispersion.

4-91
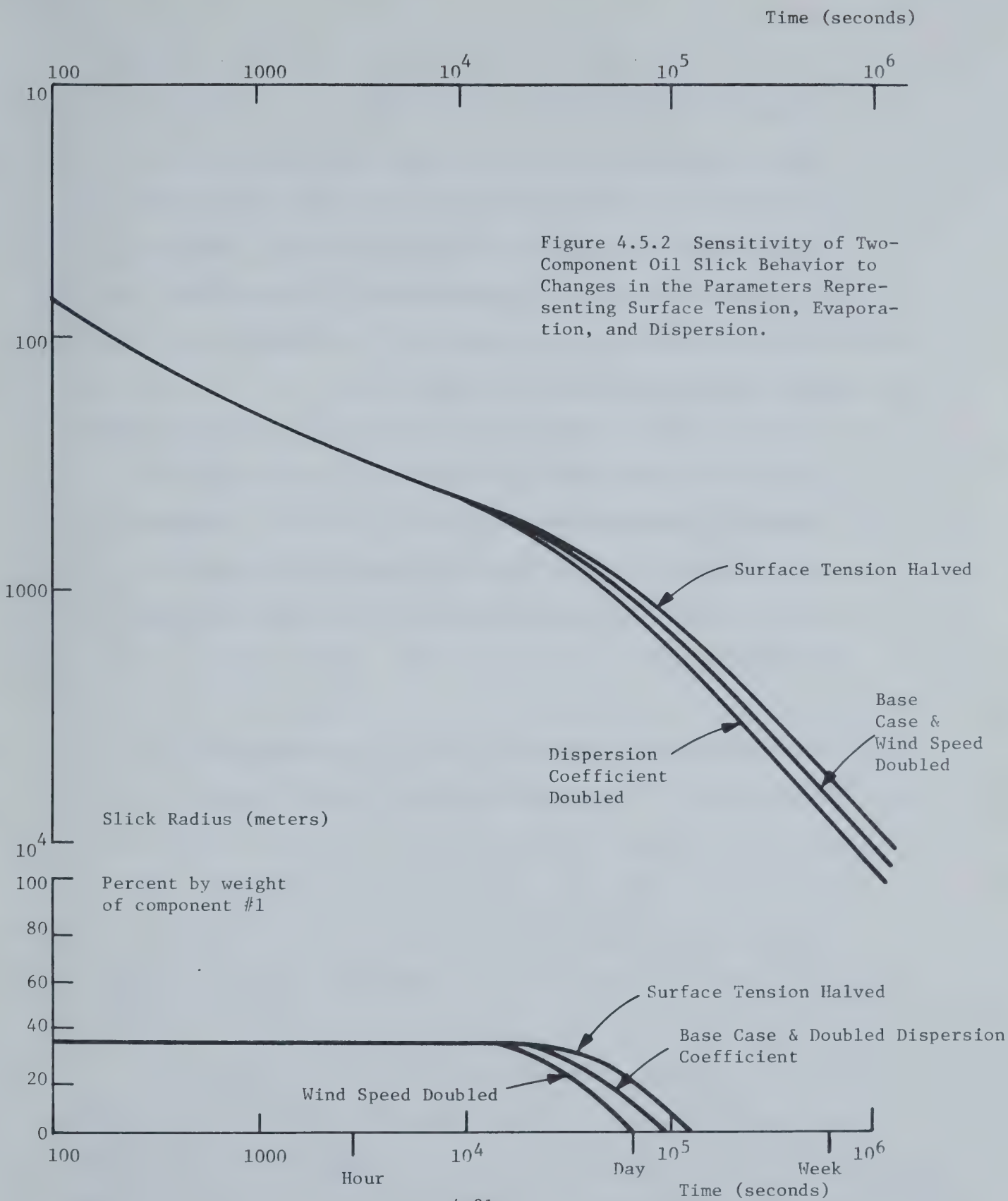
2. As illustrated by the evaporation process simulated by the two
   component calculations, the various weathering processes will
   important only within a relatively narrow range of times.
   For earlier times, the process may be neglected, and for later
   times it may be treated as a single step process. Thus for
   the example calculation, a sophisticated evaporation model
   would be required only if the period of time around a day
   after the spill occurred is of interest.

3. The effect of uncertainty in the different parameters describing
   the oil slick transformation is generally no greater than the
   variability associated with a range of initial oil volumes.
   This conclusion is of particular relevance to the use of oil
   spill models for risk assessment where the volume is not known
   a priori.

The significance of the length and time scale dependence of oil
spill transformation will be discussed further in the next chapter.

CHAPTER 5

COMPOSITE OIL SLICK MODELS

The preceding three chapters have presented detailed reviews of the
state-of-the-art in analyzing the basic environmental processes that are
relevant to the behavior of surface oil slicks. In presenting this
material, the emphasis was placed on delineating the various levels of
analysis, from the simple to the more complex, thus providing a comprehen-
sive treatment of the various techniques currently available for analysis
of these fundamental processes.

While essential, this knowledge is not sufficient in itself to deal
with the major issue of this review - modeling oil slick behavior. This
is true because at any given time an oil slick is affected by many of
these individual environmental processes; hence prediction inherently
requires a composite model. Existing composite models which combine
treatments of the wind field, oil slick advection, and oil transformations
into a single calculation scheme have not been mentioned in previous chap-
ters except where they were particularly relevant to the discussion of one
of the individual processes. Accordingly, the purpose of this chapter is
to review composite models in more detail. In addition to providing a
critical review of current capability, this section is also a useful
indicator of the needs for additional basic research to support modeling
efforts.

The detailed review of existing composite models is contained in
Section 5.2. Before reviewing these models, however, it is important to
address some of the general issues involved in the development of a composite
model. This is done in Section 5.1 which utilizes order of magnitude

arguments to examine the relative importance of various processes as a function of site-specific conditions. The last section of this chapter, 5.3, will present a summary of the various existing models along with some general conclusions concerning the weaknesses and strengths of state-of-the-art composite modeling. It is hoped that these sections together will be useful in addressing issues involving composite model application or development.

5.1 Structure Relationships for Composite Models

In reviewing models of oil slick behavior, there are two general measures that may be applied to the assumptions incorporated in each model. Firstly, for any of the model formulations the validity of the governing equations and the magnitude of associated parameters representing physical problems should be evaluated in light of the detailed information presented in Chapters 2 through 4. However, as previously noted, such an evaluation may be difficult in many cases because of the lack of basic data for comparison and the complexity of the interactions between the different processes governing oil slick behavior. Accordingly, it is useful to view these models from the perspective of the consistency with which the different parts of the model structure relate to each other and to the anticipated application of the model. This perspective is crucial not only to the task of model evaluation and selection, but also in the context of model development.

The relationship between the physical processes affecting oil slick behavior, are illustrated in Fig. 5.1.1 by the use of a length-time scale diagram in which the following processes are presented:
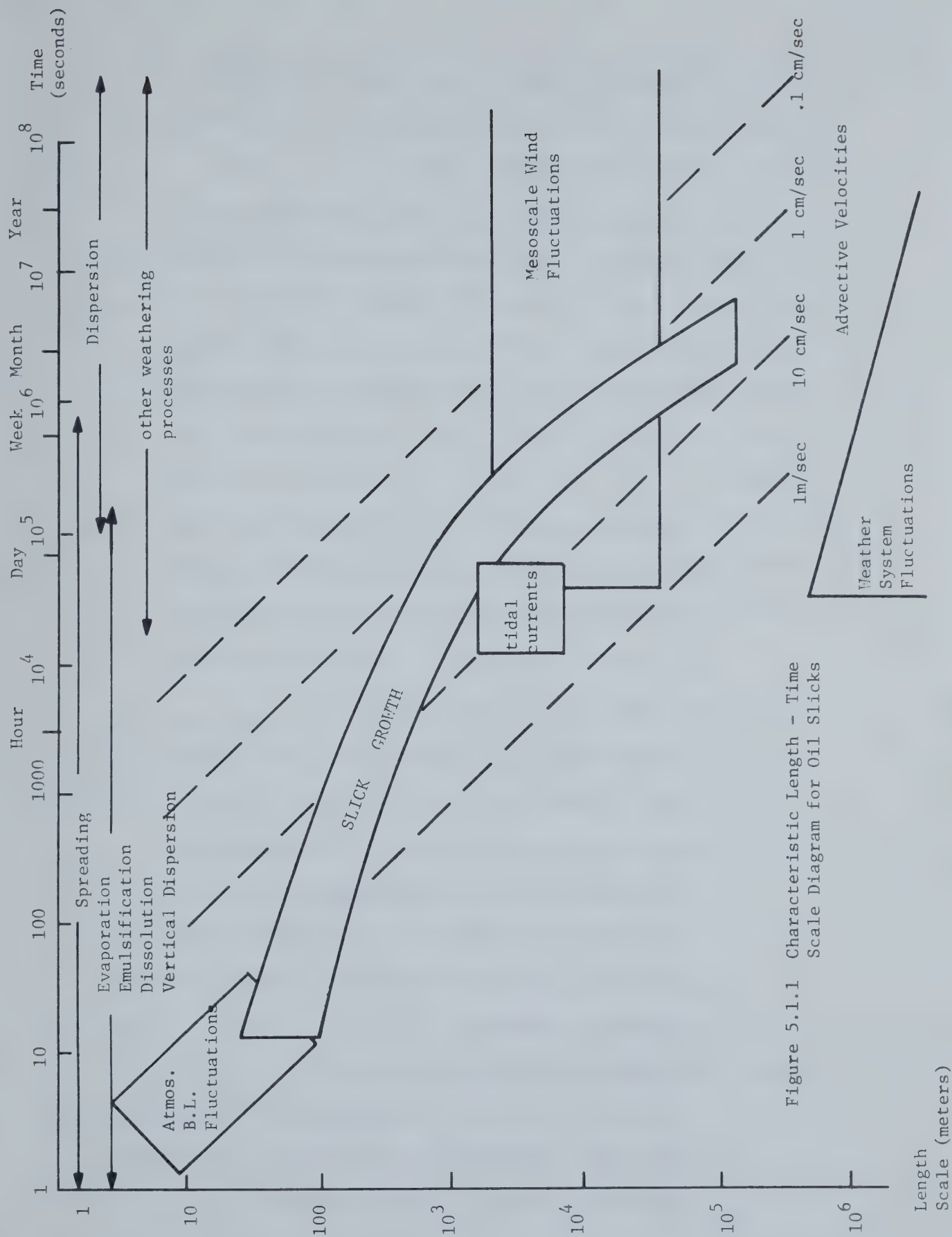
Figure 5.1.1 Characteristic Length - Time Scale Diagram for Oil Slicks

1. Net Slick Advection by various magnitudes of velocity.

    In this case the length scale represents the distance traveled
    by the slick in the associated time.

2. Spatial and temporal variations of the wind field and tidal
    advective movements. The regions indicated on the diagram denote
    the space and time scales that are characteristic of the three
    general categories of wind fluctuations discussed in Chapter 2
    and of tidal currents. The interpretation of these regions with
    respect to the total range of space and time scales is as
    follows:

    (i)   Any process (advection or slick growth) that takes place
            within an indicated region clearly will be affected by
            both the temporal and spatial variations of the
            associated meteorological or tidal fluctuations.

    (ii)   With respect to the time scale axis:
            -   processes that occur over smaller time scales than
                those indicated in the region will experience the wind
                or tide as a quasi-steady driving phenomenon.
            -   processes that occur over larger time scales will
                experience the wind or tide as rapidly varying "noise"
                that will cause no net advective movement but which
                may cause dispersion.

    (iii)   With respect to the space scale axis:
            -   processes that occur over smaller spatial scales
                than those indicated in the region will experience
                the wind or tide as spatially uniform.

- processes that occur over <u>larger</u> spatial scales than those indicated in the region will experience the wind or tides as small scale spatial features that produce no net effect but which may cause dispersion.

3. <u>Slick Growth processes</u> are indicated by a region of length and time scales that indicate the range of slick sizes as a function of time since the spill occurred. The relative importance of spreading and dispersion in causing slick growth is indicated on the time axis.

4. <u>Weathering processes</u> are designated in terms of the time scales within which they are significant. For time scales much smaller than the indicated range, a weathering process can generally be neglected. For larger times, the process can be viewed as a single step change.

The usefulness of a diagram such as Figure 5.1.1 lies in its capability to indicate the relationship between a number of separate processes within a single framework for any potential applications. The examples to be presented in this section assume that problems involving oil slick behavior may be characterized by the following:

- Initial distance to the shoreline
- Characteristic magnitude of net shoreward advection.

Given this information, the length-scale-time-scale diagram (Figure 5.1.1) may be used directly to deduce estimates of these additional features of the problem.

- The characteristic total time before the slick hits the shoreline

- The characteristic maximum slick size at time of shoreline contact

- The nature of the meteorological and tidal fluctuations that are significant in producing net advection

- The nature of the process responsible for slick growth (spreading or dispersion)

- The weathering processes that are significant during the time before shoreline contact.

It should be noted that for these cases, it is necessary to make a prior estimate of net shoreward velocities, based on whatever combination of site-specific wind and current information is appropriate. Clearly, this characterization does not apply to cases where offshore advection predominates.

Example #1 - A near shore spill

Figure 5.1.2 shows the use of the length-time scale diagram for a hypothetical oil spill that occurs 1 kilometer from the shoreline. If characteristic net shoreward advective velocities on the order of 10 cm/ sec are assumed (corresponding to 3% of a 3 m/sec wind speed) the following additional information may be deduced from the diagram:

- The characteristic total travel time will be on the order of several hours

- The characteristic final slick size will be on the order of 500 meters, with spreading being the dominant mode of slick growth

- Atmospheric boundary layer fluctuations will have no affect on the net slick movement

- Tidal advection, mesoscale wind fluctuations and weather system fluctuations will contribute to net slick advection but may be considered as steady in time and spatially uniform.

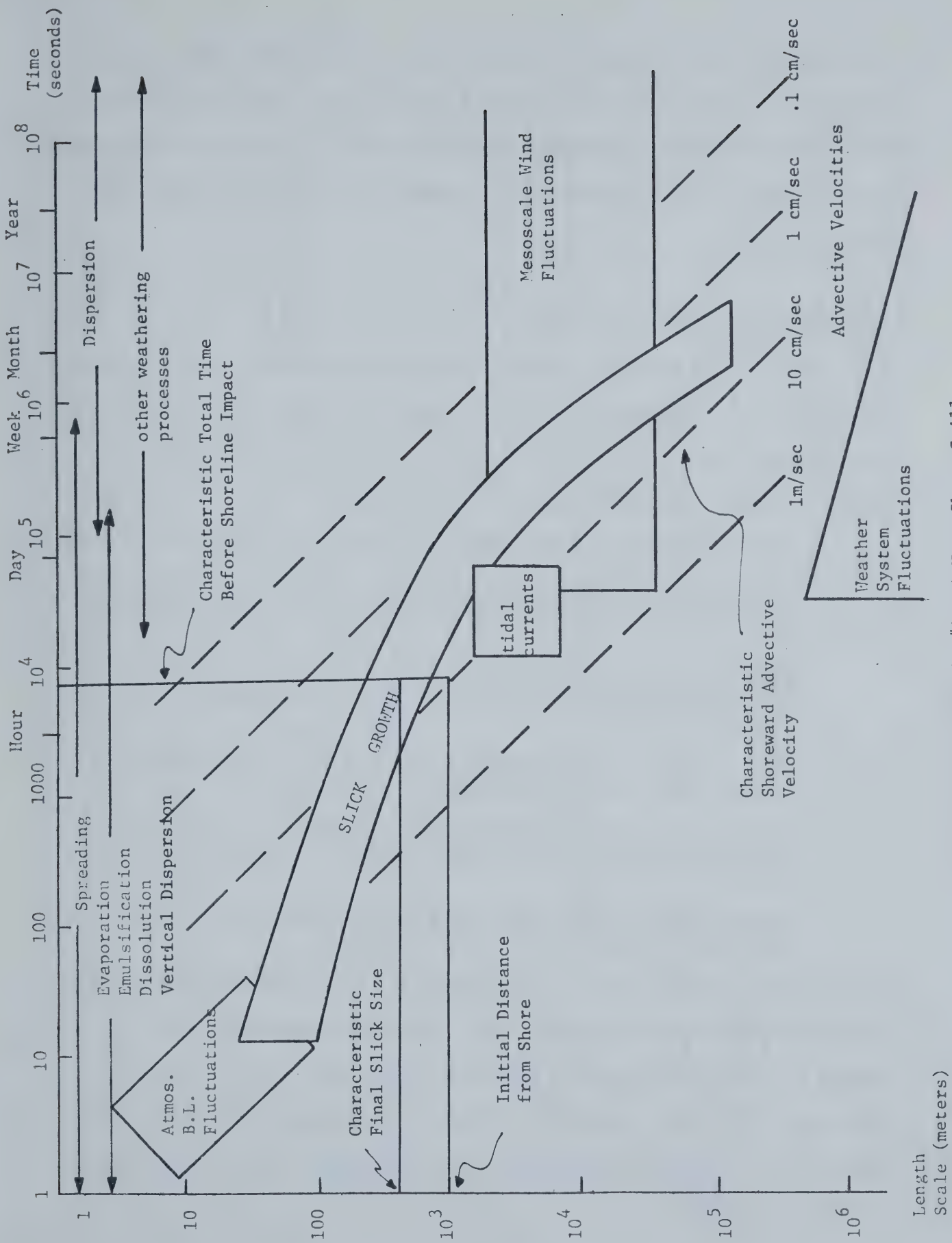- Evaporation and other short term processes will occur within the same time scale as slick movement.

Fig. 5.1.2 Example #1 - A Near Shore Spill

From these deductions, it may be concluded that an oil slick model to be applied to this case would not require a sophisticated advection representation but should rather emphasize the interaction of oil spreading and short term weathering. Slick advection can be assumed to be steady and spatially uniform.

Example # 2 - A far offshore spill

Figure 5.1.3 shows the length-time scale diagram for a spill assumed to have occurred a distance of 50 km from shore. Characteristic advective velocities are assumed to be 10 cm/sec as in the first example. The information gained from the diagram is as follows:

- The characteristic total travel time will be on the order of a week.

- The slick will obtain a characteristic size of about 10 km, with dispersion being the dominant slick growth mechanism determining final size

- Atmospheric boundary layer fluctuations and tidal advection will not affect the net slick movement but may contribute to slick dispersion.

- Both the spatial and temporal variations of the mesoscale wind fluctuations will be significant in slick advection

- The weather system fluctuations that contribute to net slick advection should be considered as spatially uniform but time-variable.

- Evaporation and other short term processes may be complete by the time the slick contacts the shoreline.

These factors indicate that the appropriate oil slick model should focus on mesoscale and weather system advection. Short term weathering may be modeled as a one-step process. Because of the small ratio of final slick size to distance traveled , it may not be necessary to model slick growth at all unless it is required by the representation of longer term weathering processes.
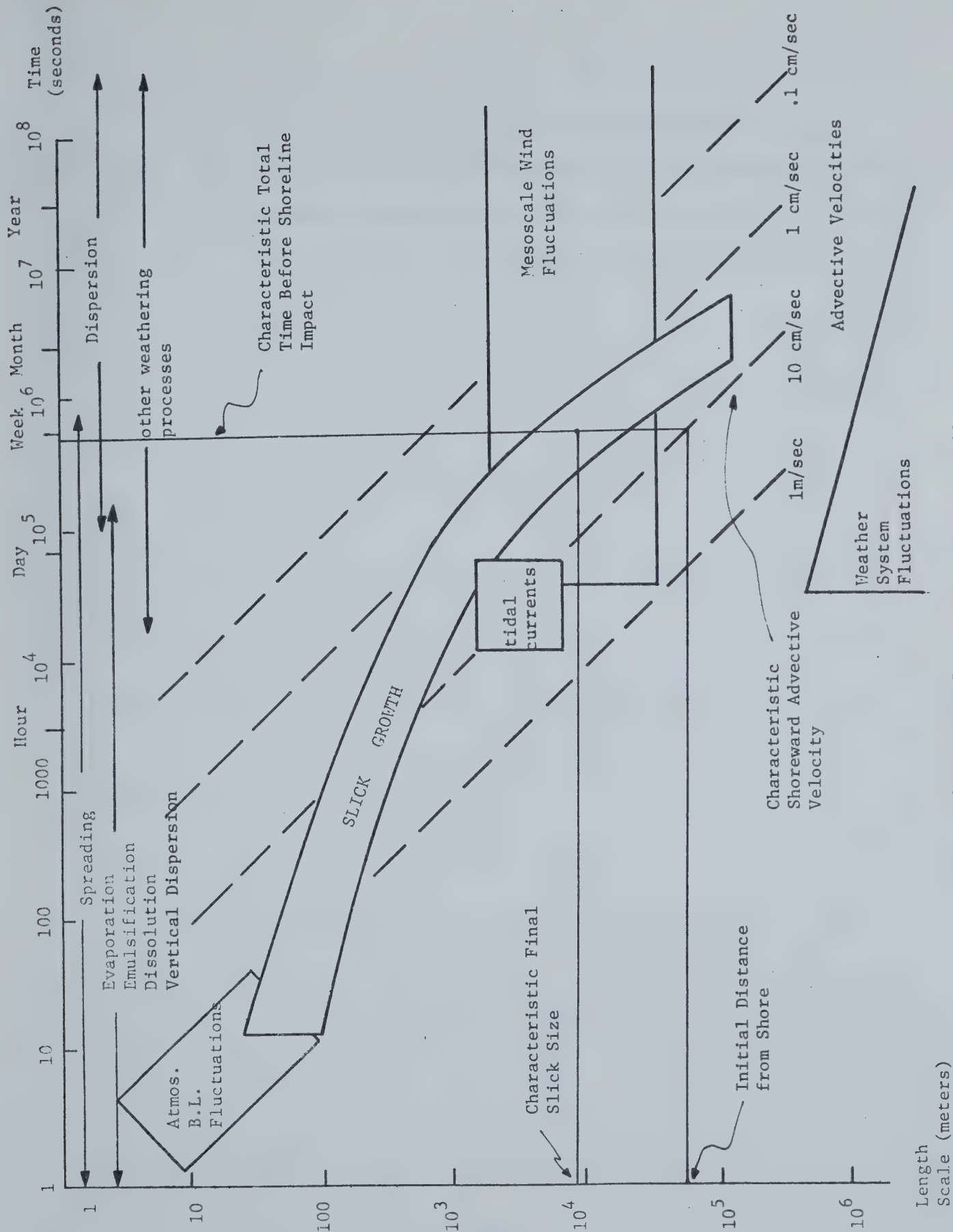
Fig. 5.1.3 Example #2 - A Far Offshore Spill

5-9

It is clear from the above examples that the required level of modeling is sensitive to the most basic features of an oil spill situation. This sensitivity will be significant in the review of existing models presented in the next section.

5.2   Review of Existing Composite Models

In selecting models to be reviewed in this section, the primary criterion was that the model should have been developed for the purpose of predicting total slick behavior, whether in an on-line or risk assessment mode.   Accordingly, techniques that were specifically designed to treat only one aspect of slick behavior (such as spreading models) are not discussed in this context.   However, as discussed in the preceding section and as will be clearly evident from the model review, a composite model may not necessarily include representation of all of the aspects of oil slick behavior.   Accordingly, there are in fact several models which consider advection only.   These models are included in this chapter since in certain applications an advection model may provide satisfactory estimates of oil transport.

This review was by necessity limited to those models for which adequate documentation was available.   The level of detail provided by the review of each model generally reflects the detail of the corresponding source of information.

5.2.1   Navy Model

Webb et al.(1970) developed a model for the U.S. Navy to provide movement forecasts for oil spills from naval vessels or other sources. Their approach consists of a linear vector summation of the effects of tides, permanent currents, geostrophic currents and wind induced drift. Or more exactly:

$$\vec{R}_s = \sum_{i=1}^{n} (\vec{D}_t + \vec{C}_p \Delta T_i + \vec{C}_g \Delta T_i + K_w \vec{W} \Delta T_i) \qquad (5.2.1)$$

where $\vec{R}_s$ is the slick centroid position up to time n and ΔT_i is the minimum time over which the currents can be assumed fixed. (For most cases wind duration and magnitude for a given direction will probably govern the value for ΔT_i).

The first term represents the influence of tidal currents and is given by

$$\vec{D}_t = [(\vec{C}_e \Delta T_e) + (\vec{C}_f \Delta T_f)] \qquad (5.2.2)$$

where $\vec{C}_e$ is the average ebb current

$\vec{C}_f$ is the average flood current

ΔT_e is the total hours of ebb current occurring in the time increment ΔT_i.

ΔT_f is the total hours of flood current occurring in the time increment ΔT_i.

$\vec{C}_e$ and $\vec{C}_f$ are taken from tidal current charts and tables.

The second term in Equation (5.2.1) represents the influence of permanent currents such as the Gulf Stream, Labrador Current, etc. A suggested source is NAVOCEANO Publication No. 700.

The third term in Equation (5.2.1) represents the effect of geo-strophic currents. As noted by the authors, calculations of such currents are quite complex and Webb et al. suggest use of a graph from James (1966) derived from actual cruise data of horizontal temperature gradient versus current for three areas of the Western Atlantic.

The fourth and last term in Equation (5.2.1) represents the wind induced drift. The wind factor K_w is based upon a relationship proposed by

Ekman (1905):

$$K_w = \frac{|\vec{V}|}{|\vec{W}|} = \frac{.0127}{\sqrt{\sin\phi}} \qquad\qquad (5.2.3)$$

where ϕ is the latitude, $\vec{V}$ is the water surface current and $\vec{W}$ the wind speed. As an example, for a latitude of 40° north the wind factor would be 1.6%.

Webb et al. also suggest that this fourth term can be found using a graph of surface drift as a function of wind velocity, fetch and wind duration. This graph was compiled by James (1966).

The Navy modellers suggest modifications which are appropriate for certain land boundaries. These include the neglect of tidal currents in deep water and the neglect of geostrophic and permanent currents in restricted or shallow water of less than 100 feet. The authors point out the difficulties with including influences from longshore currents, rivers and meanders from permanent currents but offer no specific solutions.

An important aspect of the Navy model is its dependence upon input values for wind and currents. While it is suggested that tidal current and permanent current charts and tables be used, it must be realized that these measurements are in most cases quite crude and are available for a very limited number of locations. The problem of obtaining wind input data is not discussed.

In summary the Navy model is clearly an advection model and thus neglects the effects of slick spreading, dispersion and degradation. The model does a thorough job of including the major driving forces involved in advection (except for waves) but these forces are accounted for in a very crude manner. For example, the authors suggest two methods for including the

influence of wind. This influence can vary by a factor of two, depending on which approach is taken. More specifically, if the modified wind factor approach (Equation 5.2.3) is taken for a latitude of 40° and wind speed of 35 knots then the surface current is .55 knots. If, on the other hand, James' graph is used, and assuming wind duration and fetch to be long (an assumption consistent with those on which Equation (5.2.3) is based), then the current is .9 knots. This discrepancy becomes increasingly worse as the latitude under consideration becomes larger.

5.2.2 Warner, Graham, Dean Model

Like the Navy model the Warner et al.(1972) model is purely an advection model, since it neglects degradation, spreading and wind forecasting. The model does not include wave effects nor, as it is applied by the authors, does it include currents other than local wind generated ones.

The assumptions behind the basic equation used in the model were given in Section 3.2.2. Using a form of Equation (3.2.33) Warner et al. applied a summation approximation and numerical integration to arrive at an explicit equation for the surface velocity which is dependent upon wind stresses up to 96 hours prior to the time that is being considered. Thus their model is effectively an Ekman-type model but with the capability of handling the unsteady effects of a fluctuating driving force (i.e. wind). The model, while theoretically more sound than the wind factor approach and requiring a modest degree of calculation, still cannot account for solid boundaries. In addition, it is based on an assumed constant vertical eddy viscosity. These deficiencies result in an unrealistically high deflection angle of 45° for the surface velocity for a steady wind. As was discussed in Section 3.2.7.3 the latter short-coming results in a parameter (i.e. vertical eddy viscosity) which is at best a simplification having no exact real world analog and for which little information is available.

Warner et al. applied their model in an attempt to hindcast the Arrow oil spill which occurred in 1970 off the coast of Nova Scotia. By varying the eddy viscosity parameter they were able to find a value such that the known trajectory was closely simulated by the model, whereas application of the 3% rule was much less accurate. The poor showing of

the 3% rule in forecasting the spill should not be surprising for reasons
cited in Section 3.2.2 and 3.3 and because all subsurface currents were
ignored. Conversely the good results obtained using the Warner et al.
model are easily explained since the model is in effect tuned to fit the
data. The fact that it can be tuned by a simple change in one parameter in
a range of reasonable values does indicate the model has promise in
certain applications. However, before it can be used in a predictive mode
several key problems must be addressed. First, as mentioned above, the
authors did not take into account the effect of large scale currents
(e.g. density driven, geostrophic, tidal, etc.) when applying their model
to the Arrow slick in spite of the fact that limited field data in the area
indicate a persistent current of the order 1/2 ft/sec. The authors also
indicate that the value for the vertical eddy viscosity used in the appli-
cation includes effects of these non-wind induced currents.

   The second major problem in using the model for prediction is
that of determining a value for the vertical eddy viscosity. It is safe
to say that for this model to be effectively used in forecasting, the
functional form of this very important parameter must be better defined.

   In summary,the Warner et al. model is essentially an unsteady Ekman-type
model. A major limitation of this type of model is its inability to include
moderately complex boundary conditions (i.e. shore line, variable depth,
etc.). This restricts the use of the model primarily to regions which
are far offshore, located in deep water and where the currents are primarily
wind induced. Use of the model is further restricted because the value for
the very important parameter (vertical eddy viscosity) remains very poorly
defined.

5.2.3 CEQ Model

The "CEQ report" (Stewart, Devanney and Briggs, 1974) contains
four studies: (1) an analysis of the number of platforms and amount and
type of petroleum transport activity implied by a range of hypothetical
offshore petroleum finds, (2) an analysis of the likelihood of oil spills
and spill volumes associated with these production activities, (3) an
analysis of the likely trajectories of such spills and (4) an exploratory
analysis of evaporation, spreading, and vertical diffusion of the
various components within the slick. Although each study is an important
component in an overall environmental impact assessment, the studies are
essentially independent and only the third study, which treats oil slick
advection,is discussed below.

The model compiles trajectory statistics (such as the distribution
of shoreline locations hit by slicks) for spills emanating from two types
of sites: potential Atlantic Coast terminals located on Buzzards Bay,
Delaware Bay and Charleston Harbor, and potential offshore production sites
off Georges Bank, the Mid-Atlantic Region, the South Atlantic Region and
the Gulf of Alaska. The oil drift velocity is assumed to be the sum of
3% of a time varying, spatially uniform wind field, spatially varying
tidal currents, and steady but spatially varying residual currents:

$$\vec{U}_{oil} = .03 \, \vec{U}_{wind} + \vec{U}_{tidal} + \vec{U}_{residual} \qquad (5.2.4)$$

The actual representation of each term depends on the type of region under
study.

For nearshore terminal areas the region was divided into a grid and hourly tidal currents for each element were estimated from tidal current charts. The accuracy of the assumed tidal currents was assessed by applying the continuity equation to the various grid elements for the case of Buzzards Bay, and comparing the implied water surface rise during one hour of a tidal cycle with the rise computed from tide tables. It was concluded that the average errors were in the range of .1 to .2 knots but that these were acceptable in comparison with other uncertainties of the analysis.

Winds were generated with a first-order discrete state Markov model involving a 33 x 33 state transition matrix (16 directions and two wind speeds, plus calm) and three-hour time steps. Variable wind speeds were obtained by sampling from the wind speed density function within each state. The transition matrices were compiled from three-hour wind data supplied by the National Weather Service at Otis Air Force Base, Mass.; Wilmington,Del.; and Charleston,S.C., respectively. All three stations are inland and since the simulation grids extend about 10 miles offshore there are likely to be locations for which the wind data are not representative.

Although the model does not account for spreading and dispersion directly, these effects are considered indirectly by tracking a number of slicks which originate at points surrounding the assumed spill center at radii corresponding to slick radii after various elapsed times.

For offshore production sites (typically located between 20 and 100 miles offshore) the tidal term was neglected by reasoning that the spill trajectories would either cover a sizeable number of tidal cycles, in which case the net transport due to tidal action would be quite small, or that

the tidal velocities would be small, or both.

Winds were generated in a manner similar to the nearshore areas except that a 9 x 9 state transition matrix was used (8 directions plus calm; wind speed determined from the wind speed distribution within each state). The coarser nature of this model was justified by the increased travel times of a typical trajectory and hence decreased sensitivity to the structure of the transition matrix.

The residual term, which was of minor significance for nearshore spills, was the least certain term for offshore spills. Long term deep-water current measurements, the geostrophy of the region and "considerable oceanographic intuition" were used to estimate steady, spatially varying currents. The estimates were then tested by comparing simulated trajectories with statistics gathered from drift bottle experiments. Because the residual term is assumed to be steady, meso-scale current fluctuations such as the eddies shed by the Gulf Stream are not modeled thus leaving all variability in drift to the wind term. Another assumption, noted by the authors, is that the wind drift factors for spilled oil and drift bottles are equivalent. This is important in as much as simulated trajectories showed strong sensitivity to the assumed residual current pattern.

In summary the "CEQ model" consists of two advection models - one for nearshore and one for offshore regions. The major constraints on the use of the former model are the availability of tidal current information and reliable wind measurements. In fact the choice of nearshore locations for the study was based, in part, on the availability of data. The accuracy of the calculations is limited by the approximation of a constant wind factor in shallow water. In the offshore model the major constraint is a reliable estimate of the residual currents.

5.2.4 Tetra Tech Model (TT Model)

Wang and Hwang (1974) developed a numerical model which includes advection (3% of the wind speed plus tidal current), spreading, and to a certain extent, dispersion. It does not account for weathering, and requires that the wind field (both in time and space) be input.

The model is unique relative to other existing models in that it features a numerical approximation of dispersive coupling between spreading and advection. This allows for the simulation of such commonly observed phenomena as non-radial spreading and weathercocking. To exactly solve for this coupling would require the solution to equations and boundary conditions similar to (4.3.6) and (4.3.4). Solutions to such a set of equations are far beyond the state of the art and hence Wang and Hwang's simulation is numerical and based upon physical intuition and limited field verification.

The basic idea is founded on the fact that when an oil slick is on water of uniform, steady current, the radial spreading may simply be superimposed onto the effect of the current. However, if the slick is exposed to spatial variations in currents on the order of the slick size, additional effective dispersion will occur as the slick is distorted from a non-radial shape. The formulation of the Tetra Tech model is intended to simulate this process by breaking up the slick into small enough subpatches such that simple superposition is valid.

Though Wang and Hwang's model description is not detailed, the model apparently behaves like the sequence depicted in Figure 5.2.1. The area of interest is discretized into a horizontal grid of equal squares. Water currents are supplied at the centroid of each grid for each time step.

The simulation scheme proceeds as follows. At the initiation of the spill, time t = 0, the spill of known volume is located at the centroid of a grid at the site of the spill. The situation at this time is shown in frame a where the vectors indicate the local water velocity (3% of wind speed plus tidal current) for the time step. These vectors are not shown in subsequent frames for the purpose of visual clarity. In general the velocity field will be different for each time step. It should be noted that the x in the frames indicates the site of the original spill at t = 0.

During the first time step the spill is allowed to spread according to Fay's radial spreading expressions (Table 4.3.1) and the center of mass is advected by the current at that node. Frame b depicts the situation at the end of time step 1. Note that in general the expanding slick will have overlapped into other grids. At this point, the slick is assumed to be of uniform thickness and thus the volume of the slick which has ex-panded into a given grid can be calculated and this is the volume of a new subslick considered to be at the centroid of the grid. The situation at this point is shown in frame c.

Now each subslick is allowed to spread and be advected by the respective current, independently of all other subslicks (i.e. frame d). The volumes from overlapping spills for a given grid are summed and a new
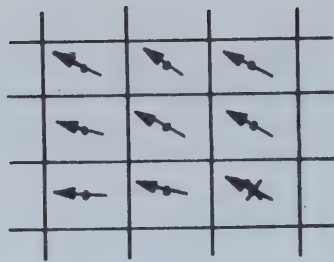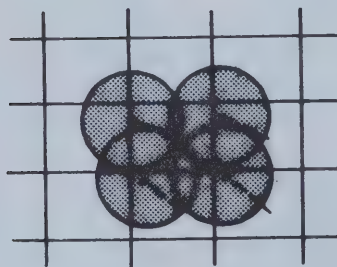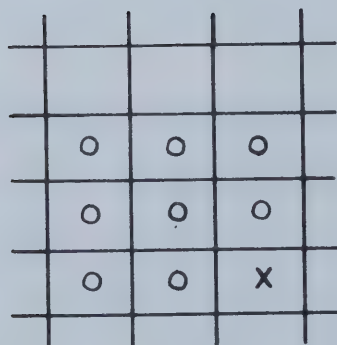
a) Time t = 0
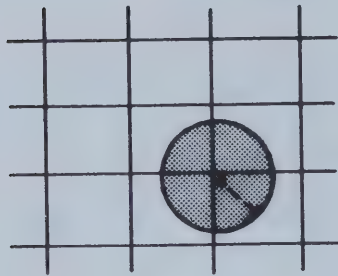
b) $t = \Delta t - \varepsilon$
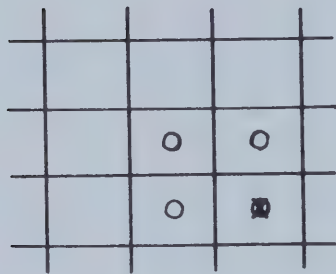
c) $t = \Delta t + \varepsilon$

d) $t = 2\Delta t - \varepsilon$

e) $t = 2\Delta t + \varepsilon$

Figure 5.2.1 Advective-Spreading Scheme Employed by Tetra Tech Model

5-22

composite subslick created at that node (i.e. frame e). And so the process continues.

Two key assumptions are made in this simulation that are not physically justifiable and the consequences of which are unclear. First, the scheme results in a numerical dispersion which has no real world analog. This can be easily seen by examining frames b and c of Figure 5.2.1. At the end of each time step, the oil volume which has overlapped into a grid is calculated and then "moved" to the centroid of the grid, where it is allowed to spread as a "new" slick without any previous spreading history. This numerical dispersion will be a function of grid spacing and time increment.

The second and perhaps most serious weakness results from the assumption that each subslick is advected and spreads independently of all other subslicks. This cannot be correct, since the equations used in governing the spreading of the subslick (i.e. Table 4.3.1) are based upon a lateral boundary condition (Equation 4.3.4) which does not include the important resistance supplied by surrounding subslicks.

In summary, the Tetra Tech model incorporates the effects of local water velocity variations upon the spreading of an oil slick. However, the scheme upon which it is based has little theoretical foundation and thus introduces complex numerical effects with no real world analog. If these shortcomings are accepted, use of the model is, as the authors note, still restricted primarily to enclosed water bodies such as bays and harbors where time and length scales are relatively short. This restriction is a result primarily of the grid scheme which requires a

well defined area of probable impact and because of the volume and detail of the input parameters needed for the model (i.e. tidal currents and wind velocities at each centroid). Such data is rarely available for open coastlines.

5.2.5 Coast Guard Model (New York Harbor)

Lissauer (1974) has developed a very site-specific model for predicting oil spill movement in New York Harbor. As in most harbors and bays, the surface currents in N.Y. Harbor are influenced primarily by tidal currents, wind induced currents and freshwater inflow (mainly from the Hudson River). Forecasting of course demands that the influence of each of these three major driving forces be calculated separately. To achieve this Lissauer assumed that the tidal component was given from tidal current charts and that the wind induced component was 3.5% of the wind speed. To derive the freshwater inflow component, Lissauer performed field measurements in the harbor utilizing anchored surface drifters. The freshwater inflow component was taken as the total velocity vector minus the tidal and wind induced current vectors. A plot of this calculated freshwater component versus outflow rate for the preceding day at an upstream dam on the Hudson showed a very good linear relation.

Spreading is accounted for in the model by a simple superposition of spreading using Fay's radial spreading formulas (Table 4.3.1) onto the calculated surface current. Weathering and dispersion are neglected.

To verify the advection model, further field experiments were carried out. Surface drifters consisting of 1 ft^2 cardboard squares were released and tracked for time periods varying from 10 minutes to more than 1 hour. For each experiment, the speed and direction were time averaged over the length of the particular experiment. In other words, for an experiment of 30 minutes in length, the starting position and position after 30 minutes were plotted and a straight line connecting the two points was drawn. The results showed that for the 2 experiments

of greater than an hour in length, the difference between predicted and observed distance traveled and direction was 10% and 3% respectively. For an experiment lasting 3 1/2 hours and time averaged every thirty minutes, the distance between the predicted and final position was about 3% of the total distance traveled. For experiments of less than one hour in length the discrepancies in distance traveled were much worse, varying from 20 - 70%.

In summary, Lissauer has developed a model which has been shown to be reasonably accurate over time spans of greater than one hour for a site-specific case, namely New York Harbor. The procedure used to develop the advection portion of the model was first to perform field experiments to measure surface current and then to perform a crude sensitivity analysis to determine the major driving forces. For New York Harbor these turned out to be tide, wind and freshwater inflow from the Hudson River. Using tidal current charts and assuming a 3.5% wind factor, Lissauer was able to calibrate the freshwater inflow component to dam outflow. The advection is assumed to apply to the center of mass of the slick and spreading governed by expressions from Fay is superimposed upon the slick-centroid movement.

The techniques used by Lissauer can no doubt be applied to other harbors, estuaries and bays. The primary disadvantages however are: (1) the large amount of field data needed to calibrate the model, (2) the questionable adequacy of the approach in areas close to shore since a fixed wind factor approach cannot account for shore effects, and (3) the need to know freshwater inflow rates of major rivers flowing into the harbor or bay.

5.2.6 SEADOCK Model

Williams et al. (1975) constructed a model to evaluate the proba-
bility of impact of an oil spill on the adjacent coastline and to help
organize a contingency program for clean-up of a spill originating
from SEADOCK, a proposed deepwater crude oil unloading facility off the
coast of Texas. The model keeps track not only of the surface slick but
also of the subsurface portion which originates through dissolution from
the surface slick. The model incorporates most of the more
important environmental influences for which some simple analytical
or empirical approximation is currently available.

As implied above, one use of the model is to evaluate risk and it
therefore makes use of wind and current data in simulating a hypothesized
oil slick's movement. The data used in the authors'application of the model
were collected by the promoters of SEADOCK and span a 23 month period. Off-
shore wind data was measured at an oil production platform near the SEADOCK
site. The onshore wind was taken from National Weather Bureau data at
a nearby city. To fill the inevitable gaps in the input data sequence,
Williams et al. make use of a first order Markov model. This type of
model is described in Section 2.3.2. Briefly, the direction data is dis-
cretized into 16 directions and averaged over a period of one month to
form a direction matrix. The magnitude (speed) data is combined with the
direction data to form a monthly probability distribution for each of the
16 directions for a discrete speed interval (e.g. 2.5 mph for wind). Thus
the model used to fill gaps, partially accounts for 1) seasonal changes
(on the time scale of one month) 2) the coupling that is known to exist

between direction and speed and 3) the lag dependency or "memory"
characteristic commonly found in wind and current data.

Knowing the space and time variation of winds and currents, the
oil transport can then be addressed. Advection of the surface slick
in regions farther than five miles offshore is given by:

$$\Delta R_{s_i} = (.03 \, \vec{W}_{F_i} + \vec{SC}_{F_i}) \Delta T_i \qquad\qquad (5.2.5)$$

where ΔR_{s_i} is the distance travelled in the ith time step, $\vec{W}_{F_i}$ is the
offshore wind during the ith time step, and $\vec{SC}_{F_i}$ is the subsurface
current during the ith time step. In the authors' application, both
$\vec{W}_{F_i}$ and $\vec{SC}_{F_i}$ (measured 10 feet below the surface) were supplied from the
SEADOCK data.

The length of the time step, i, varies from 3 hours (the time
increment between data points) initially to 24 hours for oil slicks that
have travelled for more than 20 days, except in the situation when the
slick is within 5 miles of shore in which case the time increment remains
3 hours.

To account for the Coriolis force, Williams et al. utilize a fixed
deflection angle. Acknowledging the uncertainty in this parameter, they
tried two values, 0° and 15°, and observed that there was little change in
the coastal impact point for a given slick for the SEADOCK site.

To account for shoreline effects, the modelers change the governing
advection formula when the slick is within 5 miles of the coast. For
the region between two and five miles from the coast, the advection is given by:

$$\Delta \vec{R}_{si} = .03(a\vec{W}_{Ni} + b\vec{W}_{Fi}) + s\vec{C}_i)\Delta T_i \qquad\qquad (5.2.6)$$

where $\Delta \vec{R}_{si}$ and $\vec{W}_{Fi}$ are defined as before and $\vec{W}_{Ni}$ is the onshore wind vector (i.e. measured at a land based station), $s\vec{C}_i$ is taken from applicable current charts, and a and b are weighting factors (a+b=1) determining the relative percentage of the two wind components to be applied and solely based on distance from shore. This added complexity is an attempt to account for the land/sea breeze effect which is discussed in Section 2.1.2.

When the slick reaches within two miles of the coast the governing advection relation is again modified. In this region, slick centroid movement is assumed to be 3% of the onshore wind plus the longshore current. The longshore current is taken from a nomograph by Paulus (1972). This is of course an empirical attempt to account for the no flow land boundary.

Spreading of the slick is based upon Fay's radial spreading expressions (Table 4.3.1) and is superimposed upon slick advection. Spreading is terminated when the total area reaches the value given by Fay's relationship, Equation (4.3.19).

Weathering is accounted for in the SEADOCK model in the form of evaporation, dissolution, and precipitation. For evaporation and dissolution a first order model utilizing the constants derived by Moore et al. (1973) is used. The important aspects of this approach are discussed in Section 4.4.1 and 4.4.2. The effects of precipitation are accounted for by reducing the volume of the slick by 1% during each time step when the slick is in shallow water and with wind speeds in excess of 20 miles per hour- conditions which result in turbidity

which is a favorable state for the occurrence of precipitation. However, the authors give no justification for the 1% value. Biodegradation and other long-term chemical changes are ignored, since these occur at time scales generally much larger than the time of interest for the SEADOCK site.

Williams et al. also include a submodel which predicts transport of the soluble fraction of the spilled oil that penetrates into the water column. The volume of these dissolved hydrocarbons at any given time is the total amount dissolved from the surface slick up to that time. The increase in volume of the subsurface spill is calculated at each time step until the incoming dissolution from the surface slick reaches a certain minimal amount (1% of total volume dissolved).

The subsurface model takes into account dispersion using a 3-D statistical dispersion model developed by Okubo (1962). The horizontal dispersion terms are assumed equal and proportional to the 4/3 power of the plume width as in Equation (4.3.30). The vertical dispersion coefficient is assumed constant and the maximum mixing depth for the SEADOCK application was taken as 60 ft. Thus the oil is taken to behave as a miscible substance, an assumption which would be incorrect if applied to the surface slick, but one which is probably appropriate for the subsurface component. Advection of the subsurface spill was based on the 10 and 30 ft. depth current data from SEADOCK.

In summary, Williams et al. have developed a model which includes treatment of all the major environmental processes thought to be important for the SEADOCK site and for which simple analytic techniques are available. Thus the SEADOCK model is the most extensive existing

composite model in the sense that it includes processes from all three of the major categories covered in the three previous chapters of this report (i.e. modeling of wind field, advection, and slick transformation).

The relative completeness of the model, however, should not over-shadow the fact that many of the analytic techniques used to model the individual processes are quite crude. For instance the model uses a fixed wind factor to determine local wind-induced currents and uses a "1% rule" to simulate mass loss due to vertical dispersion.

The model also suffers from a certain amount of internal in-consistency. This can perhaps best be seen by utilizing the techniques developed in Section 5.1. The hatched rectangular area in Figure 5.2.2 indicates the pertinent length and time scales for the SEADOCK site. From this figure it is evident that dispersion and not spreading will play the dominant role in slick growth rather than spreading alone as assumed by the model.
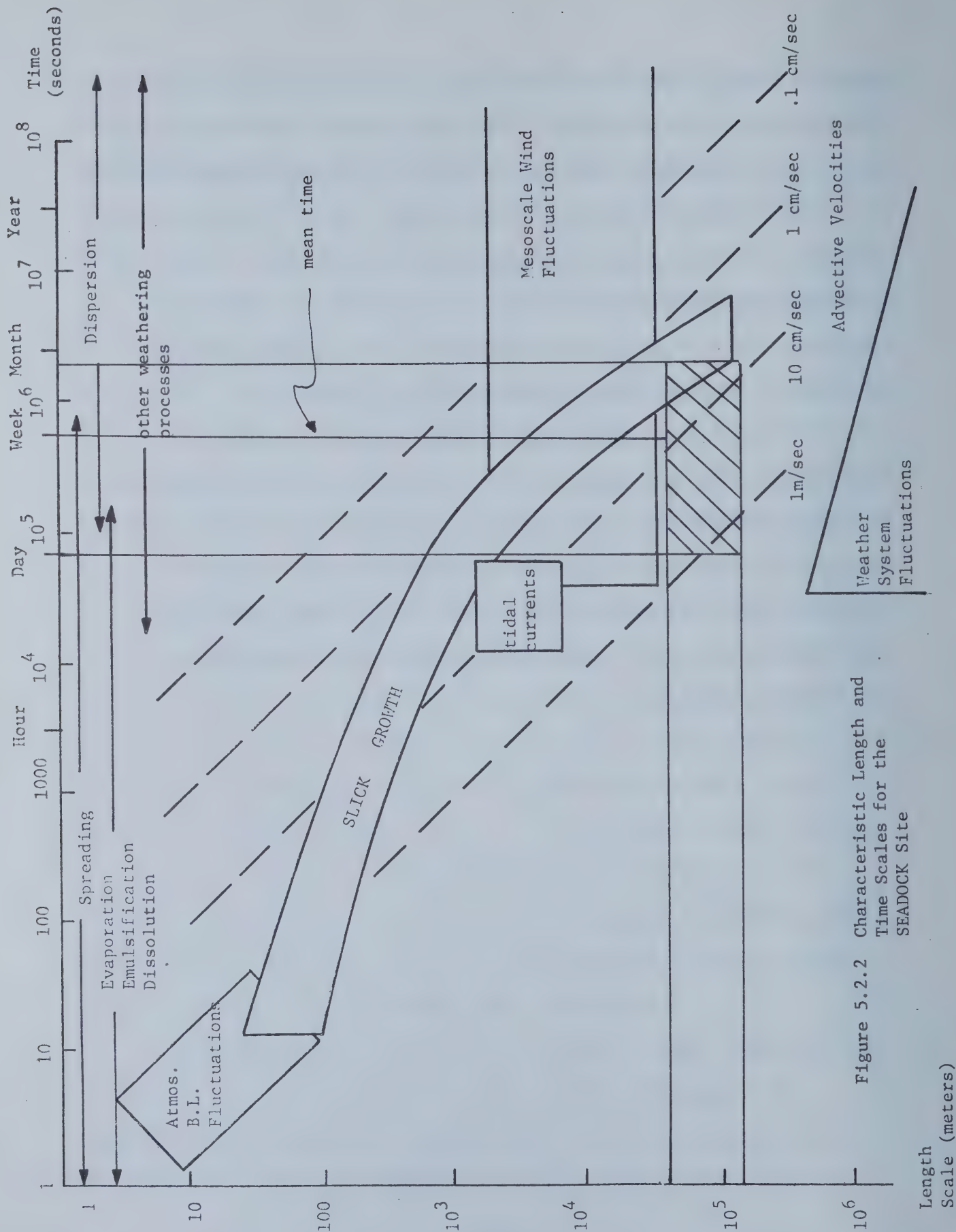
Figure 5.2.2 Characteristic Length and Time Scales for the SEADOCK Site

5.2.7 Coast Guard Model (New York Bight)

Miller et al. (1975) performed a study investigating the probable impact of oil spills originating from sites off the New Jersey and Delaware coasts. A numerical hydrodynamic model coupled with a wind generating model was used to produce water velocities and hence oil spill trajectories.

The wind field generation model is applicable primarily to storm systems and uses the geostrophic approximation, which is a balance of the pressure gradient forces against the Coriolis "force". A correction factor for frictional effects near the water surface is included. Input information includes storm radius, minimum and maximum pressure, storm center velocity and initial center location. The isobars are considered circular and spaced equally about the low pressure of the storm center. For the New Jersey application the authors "tuned" the model with data reported by ships during a two-day storm.

The wind velocities from the wind model are input into a numerical hydrodynamic model to derive water velocities. The hydrodynamic model is a depth-averaged model which can include dispersion of a pollutant. No verification of the model was attempted by the authors in their application to the N.J. coast.

Though many details are lacking in the report by Miller et al., one shortcoming of the model is obvious. The hydrodynamic model is based on a vertically averaged form of the governing equations and therefore the velocity is not a function of depth. This averaged velocity will in almost all cases not be a good indication of the wind induced surface current as was indicated in the two simple examples in Section 3.2.7.3.

5.2.8 Deepwater Ports Project Office Model (DPPO Model)

The Deepwater Ports Project Office of NOAA (1976) constructed a trajectory model to evaluate the risk of damage to states in the vicinity of the proposed deepwater ports known as SEADOCK and the LOOP. Though the model is less complex than the SEADOCK model described in section 5.2.6 it does contain many of the same components.

Advection is treated as a superposition of 3.1% of the wind speed plus the subsurface component due to observed permanent currents. Tidally induced currents are neglected primarily on the assumption that they induce no net drift. For the SEADOCK and LOOP application the modelers make use of extensive current data from previous investigators and current charts coupled with empirical arguments to derive permanent currents. Spreading is accounted for using Fay's expressions for radial spreading. Only the viscous and surface tension regimes are considered. Evaporation and dissolution are included in the same manner as employed by the SEADOCK model. Wind data are taken from the nearest coastal observation site.

A recent application of this approach (Bishop, 1976) utilizes theoretical calculations of baroclinic drift currents in New York Bight based on observed spatial density variations. For this application, spreading and weathering are neglected.

5.2.9. Delaware Model

Wang, Campbell and Ditmars (1975) constructed an interactive computer-based model for prediction of oil spill movement in Delaware Bay. The model includes treatment of advection, spreading, and dispersion and involves wind field modeling. Advection is taken as a superposition of the local wind induced current, other water currents, earth rotational effects, and waves. More specifically:

$$\vec{R}_s = \sum_{i=1}^{n} \{K_c \vec{C} + K_s K_w \vec{W}\} \Delta T_i \qquad (5.2.7)$$

where $\vec{R}_s$ is the surface slick's centroid position up to time n, $\vec{C}$ is the water current velocity vector originating from sources other than local wind, $\vec{W}$ is the surface wind velocity vector and ΔT_i is the time increment over which the parameters in parentheses can be considered constant. The values for $\vec{C}$ are taken from current charts by the U.S. Coast and Geodetic Survey (1960). The wind factor, K_w, is taken as .03 (i.e. 3% rule). The coefficient K_s represents the contribution to drift due to waves and is a function of wave steepness. The value for K_s is derived from laboratory experiments performed by Reisbig et al. (1973), some of the serious shortcomings of which were discussed in Section 3.1.2. The magnitude of K_s varies over a narrow range from 1 to .92 and thus, even if the doubts concerning the experiments are ignored, its inclusion in Equation (5.2.7) is superficial considering the uncertainty surrounding the wind factor, K_w.

The parameter K_c is called the tidal drift coefficient and is taken as a constant of 0.56. This value is based upon laboratory experiments

by Swartzberg (1971). In his report, Swartzberg offered no firm theoretical grounds for the existence of such a factor. This fact, coupled with the serious shortcomings of Swartzberg's experiment, which were pointed out in Section 3.3.3, and with the fact that Equation (5.2.7) obviously leads to erroneous results as the wind velocity approaches zero, casts serious doubt on the validity of this equation.

The effect of earth's rotation, or the Coriolis "force", is accounted for by deflecting the wind velocity vector by an angle α, derived from an Ekman solution:

$$\alpha = \arctan \left\{ \frac{\sinh(2\pi \frac{h}{D}) - \sin(2\pi \frac{h}{D})}{\sinh(2\pi \frac{h}{D}) + \sin(2\pi \frac{h}{D})} \right\}$$

(5.2.8)

$$D = \pi \sqrt{\frac{\nu_T}{\Omega}}$$

where D is the so-called "depth of frictional influence" and the other variables are as defined previously.

Recall from Section 3.2 that the value of the vertical eddy viscosity ν_T is poorly defined. Together with the weaknesses inherent in the Ekman approach (e.g. constant vertical eddy viscosity), this creates questions as to the usefulness of the above expression in calculating the deflection angle.

As mentioned previously, spreading is included in the model by means of Fay's spreading equations. However, the authors deviate somewhat from other modelers by only including the first two phases (i.e., gravity-inertia and gravity-viscous). The last regime (i.e. viscous-surface tension) is taken as negligible compared to the influence of dispersion.

This latter effect is included by use of a simple radial Fickian diffusion model which assumes a constant dispersion coefficient. The modelers do not suggest values for this constant.

Wind is input into the model in one of two ways. The user can choose to input wind data every two hours, which allows for the use of field data. The alternative method is a 4th order autoregressive model which requires much less data and is more probabilistic in nature. The autoregression coefficients and the variance of the random terms are based on measurements from a land-based station on Delaware Bay.

5.2.10 Battelle Oil Spill Model (BOSM)

S.W. Ahlstrom (1975) of Battelle Laboratories developed a model which is one of the more complex oil spill models. It includes wind field modeling and treats advection, spreading, dispersion, and to a very limited extent, slick volume changes. The model does not include degradation or advection due to waves.

In the model description, the author initially presents a form of the convective diffusion equation similar to that obtained by substituting Equation (4.3.21) into (4.3.20). However, no attempt is made to find a direct analytical or numerical solution to this equation. Rather, Ahlstrom simply uses the equation to categorize the important processes influencing an oil spill.

Ahlstrom suggests two methods to deal with the problem of simulating the wind field. First, wind velocity data from local stations can be used if available. An alternative method utilizes probabilistic techniques to simulate the wind and is primarily applicable to risk analysis. This method uses limited wind measurements to derive a monthly joint probability distribution function for wind direction (every 45°) and speed (every 5 knots). The wind input into the model is then derived every 4 hours by assuming that the wind vector occurs randomly with a probability of occurrence of each vector weighted with the appropriate monthly probability distribution. In other words, the wind at any point in time is assumed to be uncorrelated from the wind 4 hours previous. The weaknesses of this random walk approach were discussed in Section 2.3.1.

Like the Tetra Tech model, the Battelle model breaks the slick into "subpatches" or "parcels" and follows the movement of these individual

patches. Each parcel is assumed to move independently of all others. Thus the Battelle model, like the TT model, does not account for the important resistance to movement imposed by the surrounding subslicks. Unlike the TT model, the Battelle model evidently does not "collect" each subpatch into a new subpatch centered at the grid centroid at each time step and thus avoids some of the numerical dispersion inherent in the TT scheme. Instead, each parcel is followed in time until information on the total slick size is desired at which point a grid network is superimposed upon the spatially distributed ensemble of parcels. Each parcel is then associated with the nearest grid and the volume of the parcel is divided by the area of the grid to get an average concentration for that grid. It is at this point, where a certain amount of numerical dispersion in the BOSM model is likely and this dispersion will be a complex function of the grid pattern. It should be noted that no information is given as to the criteria for initially determining the size and number of parcels.

Centroidal movement of each parcel is broken into two components: one deterministic and the other probabalistic. Mathematically the parcel centroid position at any time n is given by:

$$x = \sum_{i=1}^{n} \left\{ K_w W_{x_i} + P_{x_i} + T_{x_i} + \frac{r_i}{\Delta T_i} \cos\theta_i \right\} \Delta T_i \qquad (5.2.9)$$

$$y = \sum_{i=1}^{n} \left\{ K_w W_{y_i} + P_{y_i} + T_{y_i} + \frac{r_i}{\Delta T_i} \sin\theta_i \right\} \Delta T_i$$

where K_w is the wind factor taken as .03, W_x and W_y are the wind velocity components, P is the permanent current, T is the tidal current and ΔT_i is the time increment over which the parameters in parentheses are considered

constant. The first three terms in parentheses represent the deterministic component and the values for W, T, and P are input into the model. The last term is the random component and is derived using a statistical treatment of turbulent diffusion. More specifically:

$$r_i = |R| \sqrt{12(D_E + D_\phi)\Delta T_i} \qquad (5.2.10)$$

$$\theta_i = |R| 2\pi$$

where R is a random number between zero and unity, D_E is the turbulent eddy dispersion coefficient for a homogeneous, isotropic water body, D_ϕ is an "equivalent dispersion coefficient" to account for spreading, and θ is an angle measured from the positive x axis. The value for D_ϕ is calculated using Fay's relationship for final slick size (Equation 4.3.19) and the relation for spreading in the surface tension regime. Utilizing these two expressions, the time t_s at which slick expansion ceases can be found. Knowing this time and assuming that spreading behaves in a manner analogous to two dimensional isotropic diffusion, a value for D_ϕ as a function only of initial slick volume can be calculated. For times greater than t_s, the "dispersion" due to spreading is taken as zero and the random component in Equation (5.2.8) is due solely to turbulent dispersion.

The Battelle approach to the modeling of oil spill movement is unique in many respects. Several weaknesses are apparent, however. First, Equation (5.2.10) is derived assuming that oil exhibits a Brownian-like random motion. This assumption, among other things, dictates that D_E

and D_ϕ are functions of neither time nor space. In the case of D_E this is generally a poor assumption,particularly in regard to the constancy of D_E with time.

Another major weakness apparent in Equation (5.2.10) is in the summation of D_ϕ and D_E. There is no physical basis for the assumption that these processes can be superposed in this manner.

As mentioned previously the Battelle Model does include, to a limited extent, slick volume changes. These occur in the form of beach deposits. The amount of oil deposited is calculated using a simple "sticking" function which is dependent on beach characteristics (e.g.if the beach is steep and rocky this factor is low; if the beach is sandy and gentle this factor is high), the phase of the tide (the factor for ebb tide is greater than for flood) and the ratio of the tide to the average maximum annual tide. No quantitative rules are given as to how these factors are determined.

5.2.11 Narragansett Bay Model

Premack and Brown (1973) of the University of Rhode Island construc-
ted a model for predicting oil spill movement which includes spreading
and advection. The model was applied by the authors to an actual con-
tinuous oil spill which occurred in Narragansett Bay.

Advection of the center of mass of the slick is modeled by
linear superposition of the tidal and local wind effects. The tidal
component is found using a two-dimensional finite difference numerical
model which is forced by changes in tidal elevation at the Bay inlet
and driven by wind. Local wind effects are accounted for by using a
slightly modified wind factor approach. However, instead of a constant
factor, a relation derived from experiments performed by Teeson et al.
(1970) is used. The relation is:

$$K_w = \frac{.04}{\sqrt{W}\sin\phi} \qquad\qquad (5.2,11)$$

where the variables are defined as in Equation (5.2,3) and W is in units
of meters/sec. The weaknesses of the experiment upon which this equation
is based were discussed in Section 3.3. A wind deflection angle of 20° is
used to account for earth's rotation.

The model includes slick spreading which is calculated using Fay's
spreading equations. Slick spreading is superimposed upon slick centroid
advection. All three regimes of spreading are included.

Rather than deal with the continuous nature of the spill directly,
Premack and Brown simplify the problem by discretizing the spill into
separate instantaneous subspills of equal volume occurring at equal

5-42

intervals in time. Thus for the 12-hour P.W. Thirtle spill, to which the model was applied, the authors use 12 subpatches released at hourly intervals. Each subspill is assumed to drift and to spread independently of the other subspills. Thus the interaction which would exist between subspills, particularly with regard to spreading, is ignored.

In application to the Thirtle Oil Spill, only limited qualitative data in the form of locations and approximate times of visual sightings of the spill were available for testing model predictions. Comparisons between the model and these visual observations were reasonable. It should be noted, however, that the spreading coefficient is varied to achieve a best fit and that the value finally chosen (5.7 dynes/cm) is somewhat low.

5.2.12 Puget Sound Model

Included in a review by Rath and Francis (1976) of oil spill
models is a model developed by Vagners and Mar (1972) for predicting spill
trajectories in Puget Sound. The model includes advection and spreading.
Advection is taken as the summation of the tidal current and the local
wind induced drift, which is taken as 3 1/3% of the wind speed with a zero
degree deflection angle. Both tidal and wind velocities are required
inputs to the model.   The edge of the slick is approximated by adding
a spreading component to the advection of the center of mass. Fay's
spreading equations are evidently used for determining this spreading
component.

5.2.13 San Francisco Bay Study

Another study included in the review by Rath and Francis (1976)
is that done by Conomos (1974). In his paper, Conomos utilized data
from U.S.G.S. surface and seabed drifters to compare with the known
movement of a major spill which originated near the release points.
Correlation between oil movement and both surface and bottom drifter
movement was evidently good.

5.2.14 USC Model

A group of researchers at the University of Southern California, under the direction of R.L. Kolpak, has been funded in the past few years by the American Petroleum Institute to develop an oil spill model. Though the model is not yet completed, a limited amount of information has been made available (Lasday, 1976).

The USC model will include advection and spreading and will place heavy emphasis upon the weathering processes. It will include the vertical and horizontal mechanisms of transport thus producing three-dimensional predictions. Emphasis is on predicting the ultimate fate of the oil.

To this end, the USC researchers have identified and modeled five regions in their composite model. These are the: (1) water surface, (2) water column, (3) atmosphere, (4) bottom sediments, and (5) nearshore zone. Interactions and transfers of oil between regions are included. Environmental factors such as wind condition, wave condition, currents, and water and air temperature are inputs into the model.

Unfortunately, no details are available as to what algorithms are used to model the various processes. Though the model represents a much more inclusive approach to the problem than previously taken, it cannot be any better than the submodels of the basic processes upon which it is based. And from previous discussions in Chapters 2-4 it is clear that many of these processes are not amenable to accurate quantitative modeling at this time.

5.2.15 AVCO Report

Waldman et al. (1973) published a report which many consider to include a model. In reality, however, it is a discussion of some of the basic environmental factors influencing oil spills and the methods currently available for modeling them. The factors discussed include spreading (Fay's expressions), dispersion, and transport (including wind, waves and Langmuir circulation). An analytical method to combine the nonlinear effects of spreading and transport is presented. The transport is induced by winds and subsurface currents which are assumed constant. Dispersion is discussed and the authors suggest use of a Fickian model based on Okubo's (1962) work to gain an order of magnitude estimate of the influence of dispersion on slick growth.

Once the basic state-of-the-art methods for modeling of these processes are introduced, the authors attempt to apply them to four actual spills for which some data are available. However, the lack of information concerning subsurface currents, local winds, and waves precludes any mean-ingful results or conclusions.

5.3 Summary and Conclusions

Table 5.3.1 summarizes the methods used by existing composite models in dealing with the important physical processes affecting oil spill movement. Several "models" which were discussed in the preceding section were not included in the table either because they are not truly models but rather studies or reports (e.g. AVCO) or because there were not enough specific details available concerning the model in question (e.g. USC model). From this table, several important observations on the state-of-the-art of composite models are readily apparent.

Advection is the primary component of each model. Despite the obvious importance of this process, there is a remarkable lack of diversity in the way in which the models treat advection. The apparent popularity of the simple wind factor approach should not be surprising in light of the discussion in Section 3.2. All but three models (WGD, the CG model of NY Bight and the Narragansett Bay Model) use the wind factor method to model surface drift. Recall that the WGD model was based on an unsteady Ekman formulation and that the CG model uses a vertically averaged numerical model. The latter results are probably not appropriate for surface drift. The Narragansett Bay model utilizes a modified wind factor which is a function of the wind speed and latitude.

With the exception of the first two models named above and the Delaware model, local wind drift is simply superimposed upon currents of other origins. In the case of the Delaware model a constant superposition factor of .56 is used, a value which has questionable basis. Currents of other origins (e.g. tides, freshwater currents) are typically derived from current charts, tables or measured data. The two exceptions to this are the CG Model of NY Bight and the Narragansett Bay model, which are based upon numerical hydrodynamic models which calculate total currents given

Table 5.3.1 SUMMARY OF EXISTING COMPOSITE MODELS

Environmental Process → Sub-model ↓	Wind Field			Advection					Dispersion		Spreading		Weathering	
	Measured	Simulated	Calculated	local wind drift: wind factor	local wind drift: others	other currents: meas-ured	other currents: others	other waves	Fickian	other	Fav	other	evaporation	subsurface
1. Navy	X			X		X								
2. WGD	X				X									
3. CEQ	X	X		X										
4. Tetra Tech	X	X		X		X				X	X	X		
5. Coast Guard	X	X		X		X					X			
6. SEADOCK	X		X	X	X	X	X		X		X		X	X
7. Coast Guard	X			X										
8. DPPO	X	X		X		X			X		X		X	X
9. Delaware	X	X		X		X		X	X	X	X			
10. BOSM	X	X		X	X	X	X			X	X	X		
11. Narragansett Bay	X			X	X	X	X				X			
12. Puget Sound	X			X		X					X			

5-48

certain forcing functions, primarily tides and winds.

Only one model (Delaware) explicitly includes the contribution of waves to slick advection. This model does so by multiplying the wind factor by a wave factor which varies from 1 to .92. The factor is based upon doubtful laboratory experiments and its maximum value is probably much nearer to 2. The reason for the omission of wave-induced advection, as explained in Section 3.1, is simply that until very recently, there has been no empirical or theoretical methods which have proven satisfactory in predicting wave mass transport, as was discussed in Section 3.1.

Spreading is included in the majority of the models and in all of these the governing formulas can be ultimately traced to those developed by Fay. All models which include spreading utilize the Fay expressions directly except for the Tetra Tech and BOS model. The latter model uses Fay's results to derive an equivalent diffusion-spreading coefficient and the TT model applies the Fay equations to independent subpatches instead of the entire slick. In all the models which include spreading, its effect is essentially superimposed upon advection and the effects of weathering upon density, spreading constants, etc., are ignored.

Dispersion of the surface slick is accounted for only in the Delaware, TT, BOS models and Coast Guard Model (New York Bight). The TT model treats dispersion in a non-Fickian manner which causes this process to become a complex function of the grid size and time increment of the numerical scheme. The BOS model includes dispersion in a classical Fickian model using dispersion coefficients applicable to miscible substances.

The general exclusion of dispersion by composite models cannot be easily justified on the grounds that it is not important. Figure 5.2.2 indicates, for instance, that for the time and velocity scales in the SEADOCK

application, dispersion was of importance. The obvious justification for omission is that little is known about this process with regard to oil slicks. Application of existing formulations for predicting dispersion of miscible fluids to oil slick dispersion is questionable,as was discussed in Chapter 4. Thus it is not surprising that modelers have simply avoided including dispersion, given their lack of knowledge about the process.

It is a similar lack of knowledge concerning the processes of weathering which is the major reason for the omission of these processes by all models except the DPPO and SEADOCK models. The latter model includes volume losses due to evaporation, dissolution, and precipitation. The DPPO includes the first two of these processes in a manner exactly the same as the SEADOCK model.

As for the modeling of the wind field, again a lack of diversity is evident. Only the CG model of NY Bight is not dependent upon measured wind velocities. Recall that this model uses atmospheric pressure data to derive the wind field. Several other models such as the CEQ model use a limited amount of actual wind data coupled with regression techniques to simulate continuous wind velocities.

In conclusion, it should be evident that the general state-of-the-art in existing composite models is quite crude. Though many composite models have been formulated, most have shown a lack of significant innovation. This should not be surprising, given the discussion in Chapters 2 to 4. It was clear in those sections that many basic environmental processes have virtually no analytical description available and hence must be ignored in any composite model. For other processes there may

exist a limited number of analytical techniques of varying complexity.
However, many of these techniques have not been proven or require complex
calculations. Hence existing composite models tend to use simple tech-
niques developed for previous models. These techniques did not necessarily
yield good results but required little computational effort and minimal
data inputs.

Yet despite these deficiencies, there are some geographic
locations such as harbors and small lakes and bays where careful appli-
cation of existing techniques can be applied with a reasonable amount of
success. Though not exhaustive, Lissauer's studies in New York Harbor
(Section 5.2.5) have more or less shown this to be true.

It is in more exposed environments such as open coastlines that
application of existing composite models is generally inadequate. Some
of the reasons for this are readily apparent if one considers Figure 5.1.1
once again. Unlike harbors and bays where travel times and length
scales are relatively small (e.g. hours and 100's of meters), slicks
in the open sea can experience travel times of days and distances of
miles. In open water other factors must be considered such as mesoscale
fluctuations, permanent currents (e.g. the Gulf Stream), and wave induced
drift. These are processes for which little predictive capability exists
at present and for which data collection programs are extremely expensive.

REFERENCES

Ahearn, D.G. and S.P. Meyers (eds.) (1973), The Microbial Degradation of Oil Pollutants, Center for Wetland Resources, Louisiana State University, Baton Rouge.

Ahlstrom, S.W. (1975), "A Mathematical Model for Predicting the Transport of Oil Slicks in Marine Waters," Battelle Pacific Northwest Laboratories, Richland, Washington (93 pages).

Alofs, J.D. and R.L. Reisbig, (1972), "An Experimental Evaluation of Oil Slick Movement Caused by Waves," J. of Physical Oceanography, 2, 439-443.

Anderson, J. (1976), "Sublethal Effects of Petroleum Hydrocarbons," Proceedings of NOAA Conference on Fate and Effects of Petroleum Hydrocarbons in Marine Ecosystems and Organisms, Seattle, Nov., 1976. In press.

Arthur D. Little, Inc. (1969), Combatting Pollution Created by Oil Spills, Vol. I: Methods, Report to Dept. of Transportation and the U.S. Coast Guard.

Arya, S.P.S. and J.C. Wyngaard (1975), "Effect of Baroclinicity on Wind Profiles and the Geostrophic Drag Law for the Convective Planetary Boundary Layer," Journal of the Atmospheric Sciences 32, 767-78.

Atlantic Oceanographic Laboratory (1970), Report of the Task Force - Operation Oil (clean-up of the Arrow oil spill in Chedabucto Bay) to the Minister of Transport, Bedford Inst., Dartmouth, Nova Scotia.

Atlas, R. and R. Bartha (1972a), "Biodegradation of Petroleum in Seawater at Low Temperatures," Canadian Journal of Microbiology 18, 1851-55.

Atlas, R. and R. Bartha (1972b), "Degradation and Mineralization of Petroleum by Two Bacteria Isolated from Coastal Waters," Biotechnology and Bioengineering 14, 297-308.

Atlas R. and R. Bartha (1972c), "Degradation and Mineralization of Petroleum in Seawater: Limitation by Nitrogen and Phosphorous," Biotechnology and Bioengineering 14, 309.

Bains, D.W. and D.J. Knapp (1965), "Wind Driven Currents," J. of the Hydraulics Div., ASCE, 91 (HY2), 205-221.

Barger, W.R., W.D. Garrett, E.L. Mollo-Christensen and K.W. Ruggles (1970), "Effects of an Artificial Sea Slick upon the Atmosphere and the Ocean," J. of Applied Meteorology, 9, 396-400.

Barnett, T.P. (1968), "On the Generation, Dissipation, and Prediction of Ocean Wind Waves," J. Geophys. Res. 73, 531-529.

Battelle Northwest (1970), "Oil Spill Treating Agents - Test Procedures, Status and Recommendations," Sponsored by American Petroleum Institute.

Benjamin, J.R. and C.A. Cornell (1970), Probability, Statistics and Decisions for Civil Engineers, McGraw-Hill Book Co., New York.

Berridge, S.A., R.A. Dean, F.G. Fallows and A. Fish (1968), "The Properties of Persistent Oils at Sea," Journal of the Institute of Petroleum 54 (539), 300-309.

Berridge, S.A., M.T. Thew and A.G. Loristen-Clarke (1968), "The Formation and Stability of Emulsions of Water in Crude Petroleum and Similar Stocks," Journal of the Institute of Petroleum 54 (530), 333-357.

Biesel, F. (1950), "Etude Theorique de La Houle en Eau Courante," Houille Blanche 5A, 279-285.

Bishop, J.M. and Overland, J.E. (1976), "Seasonal Drift on the Middle Atlantic Shelf," Deep-Sea Research in Press.

Bishop, J.M. (1976), "Surface Currents in the New York Bight as Related to a Simple Oil Trajectory Model," Proceedings of Conference on Coastal Meteorology, Sept. 1976, Published by American Meteorological Society, Boston, Mass.

Blackadar, A.K. and H. Tennekes (1968), "Asymptotic Similarity in Neutral Barotropic Planetary Boundary Layers," Journal of the Atmospheric Sciences 25, 1015-20.

Blokker, P.C. (1964), "Spreading and Evaporation of Petroleum Products on Water," Proc. 4th International Harbor Conference, Antwerp.

Blumer, M., M. Ehrhardt and J.H. Jones (1973), "The Environmental Fate of Stranded Crude Oil," Deep-Sea Research 20, 239-259.

Blumer, M. and J. Sass (1972), "Oil Pollution: Persistence and Degradation of Spilled Fuel Oil," Science 176 (4039), 1120-1122.

Boehm, P.D. and J.G. Quinn (1973), "Solubilization of Hydrocarbons by the Dissolved Organic Matter in Sea Water," Geochimica et Cosmochimica Acta 37, 2459-2477.

Borgman, L.E. (1969), "Ocean Wave Simulation for Engineering Design," Journal of Waterways and Harbors Division, ASCE, 95 (WW4), 556-583.

Box, J.P. and G.M. Jenkins (1970), Time Series Analysis Forecasting and Control, Holden Day.

Boylan, D.B. and B.W. Tripp (1971), "Determination of Hydrocarbons in Seawater Extracts of Crude Oil and Crude Oil Fractions," Nature 230, 44-47.

Bretschneider, C.L. (1966), "Wave Generation by Wind, Deep and Shallow Water," in Ippen, A.T. (ed.), Estuary and Coastline Hydrodynamics, McGraw-Hill, Chapter 3.

Brown, R.A., T.D. Searl and C.B. Koons (1976), "Measurement and Interpretation of Hydrocarbons in the Pacific Ocean," NOAA, Final Report on Contract No. 4-35266.

Buckmaster, J. (1973), "Viscous-gravity Spreading of an Oil Slick," Journal of Fluid Mechanics 49 Part 3, 481-491.

Burwood, R. and G.C. Speers (1974), "Photo-Oxidation as a Factor in the Environmental Dispersal of Crude Oil," Estuarine and Coastal Marine Science 2(2), 117-135.

Button, D.K. (1976), "The Influence of Clay and Bacteria on the Concentration of Dissolved Hydrocarbon in Saline Solution" Geochimica et Cosmochimica Acta 40, 435-440.

Cardone, V.J., W.J. Pierson, and E.G. Ward (1975), "Hindcasting the Directional Spectra of Hurricane Generated Waves," Proc. of 1975 Offshore Technology Conference.

Chang, M.S. (1969), "Mass Transport in Deep-water Long-Crested Random Gravity Waves," Journal of Geophysical Research 74 (6), 1515-1535.

Cochran, R.A. and P.R. Scott (1971), "The Growth of Oil Slicks and Their Control by Surface Chemical Agents," Journal of Petroleum Technology, 781-787.

Collins, I. (1968), "Inception of Turbulence at the Bed under Periodic Gravity Waves," J. Geophys, Res. 68, 6007-14.

Collins, I. (1972), "Prediction of Shallow-Water Spectra," J. Geophys. Res. 77, 2693-2707.

Conomos, T.J. (1974), "Movement of Spilled Oil as Predicted by Estuarine Nontidal Drift," Limnology and Oceanography 20(2), 159-173.

Crutcher, H.L. and L. Baer (1969), "Computations from Elliptical Wind Distribution Statistics," Journal of Applied Meteorology 1, 522-530.

Csanady, G.T. (1973), Turbulent Diffusion in the Environment, D. Reidel Publishing Co., Boston.

Csanady, G.T. (1976), "Mean Circulation in Shallow Seas," J. Geophys. Res. 81, No. 30, 5389-5399.

Dalrymple, R.A. (1974), "A Finite Amplitude Wave on a Linear Shear Current," J. Geophys. Res. 79, 4498-4504.

Dalrymple, R.A. (1976), "Symmetric Finite Amplitude Rotational Water Waves," to appear in J. Phys. Oceanography.

Davis, S.J. and C.F. Gibbs (1975), "The Effect of Weathering on a Crude Oil Residue Exposed at Sea," Water Research 9, 275-285.

Deepwater Ports Project Office (1976), "Analysis of the Risk of Damage to the States of Florida and Louisiana from the LOOP, Inc. Proposed Deepwater Port" and "Analysis of the Risk of Damage to the States of Florida and Texas from the SEADOCK, Inc. Proposed Deepwater Port," National Oceanographic and Atmospheric Administration, Dept. of Commerce, March 25.

DiSalvo, L.H. and H.E. Guard (1975), "Hydrocarbons Associated with Suspended Particulate Matter in San Francisco Bay Waters," Conference on Prevention and Control of Oil Pollution, American Petroleum Institute.

Ditlevsen, O. (1971), "Extremes and First Passage Times with Application in Civil Engineering," Ph.D. Thesis, Tech. University of Denmark, Copenhagen.

Doebler, H.J. (1966), "A Study of Shallow Water Wind Drift Currents at Two Stations off the East Coast of the U.S.," U.S. Navy Underwater Sound Lab., USL Report No. 755, New London, Conn.

Drapeau, G., W. Harrison, W. Bien and P. Leinonen (1974), "Oil Slick Fate in a Region of Strong Tidal Currents," Proc. Fourteenth Coastal Engineering Conference, Copenhagen, Vol. III, 2245-2259.

E.G. & G. Environmental Consultants (1975), "Summary of Oceanographic Observations in New Jersey Coastal Waters Near 39°28' N. Latitude and 74°15' W. Longitude During the Period May 1973 through April 1974," Waltham, Massachusetts, July.

Eagleson, P.S. and R.G. Dean (1966), "Small Amplitude Wave Theory,"in Ippen, A.T. (ed.) Estuary and Coastline Hydrodynamics, McGraw-Hill, New York, pp. 1-92.

Eganhouse, R.P. and J.A. Calder (1976), "The Solubility of Medium Molecular Weight Aromatic Hydrocarbons and the Effects of Hydrocarbon Co-solutes and Salinity," Geochimica et Cosmochimica Acta 40, 555-561.

Ekman, V.W. (1905), "On the Influence of the Earth's Rotation on Ocean Currents," Ark. Mat. Astron. Fys. 2, 1-53.

Ellison, T.H. (1956), "Atmospheric Turbulence," in Batchelor, G.K. and R.M. Davies (eds.), Surveys in Mechanics, Cambridge University Press, pp. 400-30.

Elworthy, P.H., A.T. Florence, C.B. MacFarlene (1968), Solubilization by Surface-Active Agents, Chapman and Hall, Ltd., London.

Endlich, R.M. (1961), "Computation and Uses of Gradient Winds," Monthly Weather Review 89, 187-91.

Estoque, M.A. (1961), "A Theoretical Investigation of the Sea Breeze," Quarterly Journal of the Royal Meteorological Society 87, 136-46.

Estoque, M.A. (1962), "The Sea Breeze as a Function of the Prevailing Synoptic Situation," Journal of the Atmospheric Sciences, 19, 244-50.

Fallah, M.H. and R.M. Stark (1976), "Random Model of Evaporation of Oil at Sea," Science of the Total Environment 5, 95-109.

Fasoli, U. and W. Numann (1973), "A Proposal for the Application of Monod's Mathematical Model to the Biodegradation of Mineral Oil in Natural Waters," Water Research 7, 409-418.

Fay, J.A. (1969), "The Spread of Oil Slicks on a Calm Sea," in Hoult, D.P. (ed.), Oil on the Sea, Plenum Press, pp. 53-63.

Fay, J.A. (1971), "Physical Processes in the Spread of Oil on a Water Surface," Proc. of the Joint Conf. on Prevention and Control of Oil Spills, Sponsored by API, EPA, and USCG, Washington, D.C., June 15-17, Publ. by Amer. Petrol. Inst., pp.463-467.

Feldman, M.H. (1973), "Petroleum Weathering: Some Pathways, Fate and Disposition on Marine Waters," Pacific Northwest Environmental Research Lab., Corvallis, Oregon, EPA 660 3 73 013, NTIS No. PB-227 278.

Ferrero, E.P. and D.T. Nichols (1972), "Analyses of 169 Crude Oils from 122 Foreign Oilfields," Bureau of Mines Information Circular 8542.

Fisher, E.L. (1960), "An Observational Study of the Sea Breeze," Journal of Meteorology 17, 645-60.

Fjeldstad, J.E. (1929), "Ein Beitrag zur Theorie der Winderzengten Meeresstrommungen," Beitrag zur Geophysik 23, 237-247.

Fjeldstad, J.E. (1930), Zeitschrift für Augewandle Mathematik und Mechanik, Vol. 10.

Floodgate, G.D. (1972), "Microbial Degradation of Oil," Marine Pollution Bulletin 3, 41 ff.

Forristall, G.Z. (1974), "Three-Dimensional Structure of Storm-Generated Currents," J. of Geophysical Research 79, 2721-1187,

Forrester, W.D. (1971), "Distribution of Suspended Oil Particles Following the Grounding of the Tanker Arrow," Journal of Marine Research 29(2), 141-170.

Frankenfeld, J.W. (1973a), "Weathering of Oil at Sea," Esso Research and Engineering Co., NTIS No. AD 787 789.

Frankenfeld, J.W. (1973b), "Factors Governing the Fate of Oil at Sea; Variations in the Amounts and Types of Dissolved or Dispersed Materials During the Weathering Process," Proc. Joint Conf. on Prevention and Control of Oil Spills, API, pp. 485-495.

Franks, F. (1966), "Solute-Water Interactions and the Solubility Behavior of Long-Chain Paraffin Hydrocarbons," Nature 210, 87-88.

Freegarde, M., C.G. Hatchard and C.A. Parker (1971), "Oil Spilt at Sea: Its Identification, Determination and Ultimate Fate," Lab Practice 20 (1), 35-40.

Gallant, R.W. (1970), Physical Properties of Hydrocarbons, Vols. 1 and 2, Gulf Publishing Co., Houston.

Galt, J.A. (1975), "Development of a Simplified Diagnostic Model for Interpretation of Oceanographic Data," NOAA Technical Report ERL 339-PMEL-25, Boulder, Colorado.

Gandin, L.S. (1965), Objective Analysis of Meteorological Fields, Israel Program for Scientific Translations, Jerusalem.

Glaeser, J.L. and G.P. Vance (1971), "A Study of the Behavior of Oil Spills in the Arctic," Coast Guard, Applied Technology Division, NTIS No. AD 717 142.

Godshall, F.A. and J.B. Jalickee (1976), "Statistical Analysis of Wind Climatology and Variation Between Shore and Marine Area Wind Observation," Proceedings of the Conference on Coastal Meteorology of the American Meteorology Society, Virginia Beach, Va.

Gordon, A.H. (1950),"The Ratio Between Observed Velocities of the Wind at 50 feet and 2000 feet Over the North Atlantic Ocean," Quart. J.R. Met. Soc., 344-48.

Gordon, A.H. (1952), "Angle of Deviation Between the Winds at 50 feet and 2000 feet over the North Atlantic Ocean," Met. Mag. 81, 59.

Harris, M.J., T. Higuchi and J.H. Rytting (1973), "Thermodynamic Group Contributions from Ion Pair Extraction Equilibria for Use in the Prediction of Partition Coefficients. Correlation of Surface Area with Group Contributions," J. Phys. Chem. 77, 2694-2703.

Harrison, W. (1974), "The Fate of Crude Oil Spills and the Siting of Four Supertanker Ports," Canadian Geographer 18 (3), 211-231.

Harrison, W., M.A. Winnik, P.T.Y. Kwong and D. MacKay (1975), "Disappearance of Aromatic and Aliphatic Components from Small Sea-Surface Slicks," Environmental Science and Technology 9(3), 231-234.

Haurwitz, B. (1941), Dynamic Meteorology, McGraw-Hill Book Company, New York.

Hay, J.S. and F. Pasquill (1959), "Diffusion from a Continuous Source in Relation to the Spectrum and Scale of Turbulence," Advances in Geophysics 6, 345 ff.

Hellmann, H. (1971), "The Behavior of Crude Oil on Water Surfaces as Indicated by Temporal Changes in Flow Characteristics," Erdoel-Kohle-Erdgas Petrochem. 24(6), 417-422 (in German).

Hermann, R.B. (1972), "Theory of Hydrophobic Bonding II. The Correlation of Hydrocarbon Solubility in Water with Solvent Cavity Surface Area," J. Phys. Chem. 76, 2754-2759.

Hidaka, K. (1933), "Nonstationary Ocean Currents. Part I," Mem. Imp. Marine Observatory Kobe 5, No. 3.

Hildebrand, F. (1965), Calculus for Applications, Prentice Hall.

Hino, M. (1965), "Digital Computer Simulation of Turbulent Diffusion," IAHR Congress, Leningrad, Paper #2-30.

Hinwood, J.B. and I.G. Wallis (1975), "Classification of Models of Tidal Waters," J. of Hydraulics Div., ASCE, 101 (HY10), 1315-1332.

Ho, C.L. and T. Karim (1976), "Impact of Surface Adsorbed Petroleum Hydrocarbons on Organisms," Proceedings of NOAA Conference on Fate and Effects of Petroleum Hydrocarbons in Marine Ecosystems and Organisms, Seattle, Nov., 1976. In press.

Hoult, D.P. (1972), "Oil Spreading on the Sea," in Annual Review of Fluid Mechanics, Vol. 4, M. Van Dyke, W.G. Vincenti, and J.F. Wehausen (eds.) pp. 341-368.

Houston, B.J. (1971), "Investigation of Sinking Methods for Removal of Oil Pollution from Water Surfaces. Phase I: Survey of the State-of-the-Art" U.S. Coast Guard Office of Research and Development Rept. No. 704110/A/001-1. NTIS No. AD 725 617.

Huang, N.E. (1970), "Mass Transport Induced by Wave Motion," Journal of Marine Research 28(1), 35-50.

Hughs, P. (1956), "A Determination of the Relation Between Wind and Sea-Surface Drift," Quarterly Journal of the Royal Meteorological Soc. 82, 494-502.

Hurst, H.E. (1951), "Long-Term Storage Capacity of Reservoirs," Trans. American Society of Civil Engineers, 116, pp. 770-808.

Isozaki, I. and T. Uji (1974), "Numerical Model of Marine Surface Winds and its Application to the Prediction of Ocean Wind Waves," Papers in Meteorology and Geophysics, 25, pp. 197-231.

James, R.W. (1966), Ocean Thermal Structure Forecasting, ASWEPS Manual, 5, U.S. Naval Oceanographic Office.

James, R.W. (1968), "Wind Drift Currents," Mariners Weather Log 12, 8-10.

Jeffery, P.G. (1973), "Large-Scale Experiments on the Spreading of Oil at Sea and Its Disappearance by Natural Factors," Proc. Joint Conf. on Prevention and Control of Oil Spills, Washington, D.C.

Kennedy, J.M. and E.G. Wermund (1971), "The Behavior of Oil on Water Derived from Airborne Infrared and Microwave Radiometric Measurements," Proc. Joint Conf. on Prevention and Control of Oil Spills, API, Washington, D.C., pp. 469-477.

Kenyon, K.E. (1969), "Stokes Drift for Random Gravity Waves," J. Geophys. Res. 74(28), 6991-6994.

Keulegan, G.H. (1951), "Wind Tides in Small Closed Channels," J. of Res. of the Nat. Bureau of Stand. 46(5), Res. Paper 2207, pp. 358-381.

Kim, Young (1974), "Oil Spreading on Coastal Waters," Paper presented at 14th Int. Conf. on Coastal Engineering, Copenhagen.

Kindle, E.C., J.E. Smith and C. Bhumralker (1976), "Results of Numerical Model Analysis of Strong Offshore Winter Winds," Proceedings of the Conference on Coastal Meteorology of the American Meteorological Society, Virginia Beach, Va.

Kinney, P.J., D.K. Button and D.M. Schell (1969), "Kinetics of Dissipation and Biodegradation of Crude Oil in Alaska's Cook Inlet," Proc. Joint Conf. on Prevention and Control of Oil Spills, API, Washington, D.C., pp. 171-177.

Kirk, R.E. and D.F. Othmer (eds.) (1955), "Vapor-liquid Equilibria and Vapor Pressure," Encyclopedia of Chemical Technology, Vol. 14, pp. 611-645.

Klein, A.E. and N. Pilpel (1974), "The Effects of Artificial Sunlight Upon Floating Oils," Water Research 8, 79 ff.

Koons, C.B. and D.E. Brandon (1975), "Hydrocarbons in Water and Sediment Samples from Coal Oil Point Area, Offshore California," Proc. Offshore Technology Conf., Dallas, Paper No. OTC 2387, pp. 513-521.

Koons, C.B., C.D. McAuliffe and F.T. Weiss (1976), "Environmental Aspects of Produced Waters from Oil and Gas Extraction Operations in Offshore and Coastal Waters," Proc. Offshore Technology Conference, Dallas, Paper No. OTC 2447, pp. 247-257.

Kreider, R.E. (1971), "Identification of Oil Leaks and Spills," Proc. of the Joint Conf. on Prevention and Control of Oil Spills, API, EPA and USCG, June 15-17, Washington, D.C., pp. 119-124.

Lai, M.G. and C.E. Adams (1974), "Determination of the Molecular Solubility of Navy Oils in Water," Naval Ordinance Lab., NTIS No. AD 784 414.

Lasday, A.H. and E.W. Mertens (1976), "Fate and Effects of Oil on Marine Life: Progress Report on Research Sponsored by the American Petroleum Institute," Proc. Offshore Technology Conf., Dallas, Paper No. OTC 2449, pp. 275-280.

Lasday, A.H. (1976), "Oil Spills - Historical Review and Characteristics," Seminar for U.S. Fish and Wildlife Service, New Orleans, La., April 26-27, (15 pages).

Lassiter, J.B., R.J. Powers and J.W. Devanney (1974), "The Role of Mass Transport in Oil Slick Weathering," Report to CEQ, MIT Sea Grant Report No. 74-20.

Lavoie, R.L. (1972), "A Mesoscale Numerical Model of Lake-Effect Storms," Journal of the Atmospheric Sciences 29, 1025-1040.

Lee, C.C., W.K. Craig and P.J. Smith (1974), "Water Soluble Hydrocarbons from Crude Oil," Bulletin of Environmental Contamination and Toxicology 12(2), 212-216.

Lee, R.A.S. (1971), "A Study of the Surface Tension Controlled Regime of Oil Spread," M.S. Thesis, Mechanical Engineering, M.I.T.

Leendertse, J.J. (1967), "Aspects of Computational Model for Long-Period Water-Wave Propagation," Memorandum, RM-5294-PR, Rand Corporation.

Leendertse, J.J. and S.K. Liu (1975), "Modeling of Three-Dimensional Flows in Estuaries," Symposium on Modeling Techniques, ASCE, Vol. 1, p. 625-642.

Leinonen, P.J. and D. MacKay (1973), "The Multicomponent Solubility of Hydro-carbons in Water," Canadian Journal of Chemical Engineering 51, 230-233.

Leinonen, P.J., D. MacKay and C.R. Phillips (1971), "A Correlation for the Solubility of Hydrocarbons in Water," Canadian Journal of Chemical Engineer-ing 49, 288-290.

Lissauer, I.M. (1974), "A Technique for Predicting the Movement of Oil Spills in New York," Coast Guard Research and Development Center, Groton, NTIS No. AD 786 627.

Longuet-Higgins, M.S. (1953), "Mass Transport in Water Waves," Phil. Trans. Roy. Soc., London, Ser. A., 245(903), 535-581.

Lyons, W.A. (1972), "The Climatology and Prediction of the Chicago Lake Breeze," Journal of Applied Meteorology 11, 1259-70.

Lysyj, I. and E.C. Russell (1974), "Dissolution of Petroleum-Derived Products in Water," Water Research 8, 863-868.

MacKay, D. and A.W. Wolkoff (1973), "Rate of Evaporation of Low-Solubility Contaminants from Water Bodies to Atmosphere," Environmental Science and Technology 7(7), 611-614.

MacKay, D. and P.J. Leinonen (1975), "Rate of Evaporation of Low Solubility Contaminants from Water Bodies to Atmosphere," Environmental Science and Technology 9(13), 1178-1180.

MacKay, D. and R.S. Matsugu (1973), "Evaporation Rates of Liquid Hydrocarbon Spills on Land and Water," Canadian Journal of Chemical Engineering 51, 434-439.

Madsen, O.S. (1977) "Wind Driven Currents in an Infinite Homogeneous Ocean," to appear in J. Phys. Oceanography, (reproduced in Appendix A of this report).

Majewski, J. and J. O'Brien (1974), "A Kinetic Study of a Fuel Oil Undergoing Photochemical Weathering," Environmental Letters 7(2), 145-161.

McAuliffe, C.D. (1966), "Solubility in Water of Paraffin, Cycloparaffin, Olefin, Acetylene, Cycloolefin and Aromatic Hydrocarbons," Journal of Physical Chemistry 70, 1267-1275.

McAuliffe, C.D. (1976a), "Dispersal and Alteration of Oil Discharged on a Water Surface," Proceedings of NOAA Conference on Fate and Effects of Petroleum Hydrocarbons in Marine Ecosystems and Organisms, Seattle, Nov., 1976. In press.

McAuliffe, C.D. (1976b), "Evaporation and Solution of C_1-C_{10} Hydrocarbons from Crude Oils on the Sea Surface," Proceedings of NOAA Conference on Fate and Effects of Petroleum Hydrocarbons in Marine Ecosystems and Organisms, Seattle, Nov., 1976. In press.

McAuliffe, C.D., A.E. Smalley, R.D. Groover, W.M. Welsh, W.S. Pickle and G.E. Jones (1975), "Chevron Main Pass Block 41 Oil Spill: Chemical and Biological Investigations," Conference on Prevention and Control of Oil Pollution, American Petroleum Institute.

McLean, A.Y. and D.A. Odedra (1974), "The Properties of Sable Island Crude Oil in Relation to its Behavior in the Event of a Spill at Sea," Proc. 6th Offshore Technology Conference, Dallas, pp. 449-460.

McPherson, R.D. (1970), "A Numerical Study of the Effect of a Coastal Irregularity on the Sea Breeze," Journal of Applied Meteorology 9, 767-77.

Mehia, J.M., D.R. Dawdy, and C.F. Nordin (1974), "Streamflow Generation 3. The Broken Line Process and Operational Hydrology," Water Resources Research 10(2), 242-5.

Mehia, J.M. and I. Rodriguez-Iturbe (1973), "Multidimensional Characterization of the Rainfall Process," R.M. Parsons Laboratory for Water Resources and Hydrodynamics, Technical Report No. 177, Dept. of Civil Engineering, M.I.T., November.

Milgram, J.H. (1977), "Mass Transport of Water and Floating Oil by Gravity Waves in Deep Water," Submitted for publication in J. Fluid Mechanics.

Miller, M.C., J.C. Bacon and I.M. Lissauer, (1975), "A Computer Simulation Technique for Oil Spills Off the New Jersey-Delaware Coastline," Coast Guard Report No. CG-D-171-75 (45 pages).

Mooers, C.N.K., J. Fernandez-Partages and J.F. Price (1976), "Meteorological Forcing Fields of the New York Bight (First Year)" Technical Report 76-8, Rosenstiel School of Marine and Atmospheric Science, University of Miami.

Moore, S.F., R.L. Dwyer and A.M. Katz (1973), "A Preliminary Assessment of the Environmental Vulnerability of Machias Bay, Maine to Oil Super-tankers," Report No. 162, Ralph M. Parsons Laboratory for Water Resources and Hydrodynamics, M.I.T.

Murray, S.P. (1972), "Turbulent Diffusion of Oil in the Ocean," Limnology and Oceanography 27(5), 651-660.

Murray, S.P. (1975), "Trajectories and Speeds of Wind-Driven Currents Near the Coast," J. of Physical Oceanography 5, 347-360.

Murty, T.S. and M.L. Khandekar (1973), "Simulation of Movement of Oil Slicks in the Strait of Georgia Using Simple Atmosphere and Ocean Dynamics," Conf. on Prevention and Control of Oil Spills, API, Washington, D.C., pp. 541-546.

National Academy of Sciences (1975), Petroleum in the Marine Environment, Washington, D.C.

Nelson, W.L. (1958), Petroleum Refinery Engineering, McGraw Hill, New York.

Neumann, G. (1968), Ocean Currents, Elsevier Oceanography Series, Elsevier Scientific Publishing Company, New York.

Neumann, H. (1966), "The Relation Between Wind on Surface Current Derived from Drift Card Investigations," Dt. Hydrogr. Z. 19, 253-266.

Neumann, J. and Y. Mahrer (1971), "A Theoretical Study of the Land and Sea Breeze Circulation," Journal of the Atmospheric Sciences 28, 532-42.

Okubo, A. (1962), "A Review of Theoretical Models of Turbulent Diffusion in the Sea," Technical Report 30, Chesapeake Bay Institute, Johns Hopkins University.

Overland, J.E. and W.H. Gemmill (1976), "Specification of Marine Winds in the New York Bight," National Meteorological Center, National Weather Service, paper to be published.

Pasquill, F. (1944), "Evaporation From a Plane, Free-liquid Surface into a Turbulent Air Stream," Proc., Royal Society of London $182\ A$, 75-95.

Paulus, W.S. (1972), "Physical Processes of the Marine Environment (Oil Movement Forecasting)," U.S. Naval Oceanographic Office, Washington, D.C.

Peake, E. and G.W. Hodgson (1966), "Alkanes in Aqueous Systems. I. Explora-tory Investigations on the Accommodation of C_{20} to C_{33} n-Alkanes in Distilled Water and Occurrence in Natural Water Systems," J. of American Oil Chemists' Society 43, 215-222.

Peake, E. and G.W. Hodgson (1967), "Alkanes in Aqueous Systems II. The Accommodation of C_{12} – C_{36} n-Alkanes in Distilled Water," J. American Oil Chemists' Society 44(12), 696-702.

Peregrine, D.H. (1976), "Interaction of Water Waves and Currents," In Advances in Fluid Mechanics, Vol. 16, in press.

Phillips, C.R. and V.M. Groseva (1975), "Separation of Multicomponent Hydrocarbon Mixtures Spreading on a Water Surface," Separation Science 10(2), 111-118.

Phillips, O.M. (1966) The Dynamics of the Upper Ocean, Cambridge University Press.

Pielke, R.A. (1974) "A Three-Dimensional Numerical Model of the Sea Breezes over South Florida," Monthly Weather Review 102, 115-139.

Pierson, W.J. and L. Moskowitz (1964), "A Proposed Spectral Form for Fully Developed Wind Seas Based on the Similarity Theory of S.A. Kitaigorodskii," J. Geophys. Res. 69(24), 5181-5190.

Plate, E.J. (1970), "Water Surface Velocities Induced by Wind Shear," J. of Eng. Mech. Div. ASCE, 96 (EM3), 295-312.

Plate, E.J. (1971), Aerodynamic Characteristics of Atmospheric Boundary Layers, U.S. Atomic Energy Commission, TID-25465.

Poirier, O.A. and G.A. Thiel (1941), "Deposition of Free Oil by Sediments Settling in Sea Water," Bulletin of the American Association of Petroleum Geologists 25(12), 2170-2180.

Premack, J. and G.A. Brown (1973), "Prediction of Oil Slick Motions in Narragansett Bay," Proc. Joint Conf. on Prevention and Control of Oil Spills, API, Washington, D.C., pp. 531-540.

Ramseier, R.O. (1971), "Oil Pollution in Ice-Infested Waters," Int. Symp. on Identification and Measurement of Environmental Pollutants, Ottawa, pp. 271-276.

Rashid, M.A. (1974), "Degradation of Bunker C Oil under Different Coastal Environments of Chedabucto Bay, Nova Scotia," Estuarine and Coastal Marine Science 2, 137-144.

Rath, R.J. and B.H. Francis (1976), "Modeling Methods for Predicting Oil Spill Movement," paper by Oceanographic Institute of Washington, Seattle, Washington 98109 (99 pages).

Reichardt, H. (1959), "Gesetzmassigkeiten der geradlinigen turbulenten Couette-stromung," Mitterlungen aus dem Max-Planck-Institut fur Stromun-forschung und der Aerodynamischen Ve suchsanstalt, No. 22, Göttingen, pp. 1-45.

Reid, R.O. (1975), "Analytical and Numerical Studies of Ocean Circulation," Reviews of Geophysics and Space Physics, U.S. National Report 1971-1974, Vol. 13, No. 3, pp. 607-609.

Reisbig, R.L., D.L. Alofs, et al. (1973), "Measurements of Oil Spill Drift Caused by the Coupled Parallel Effects of Wind and Waves," Memoires Societe Royale Des Sciences de Liege, 6 serie, Tome VI, pp. 65-75.

Regnier, Z.R. and B.F. Scott (1975), "Evaporation Rates of Oil Components," Environmental Science and Technology 9 (5), 469-472.

Rice, S.D. (1976), "Comparative Toxicities of Petroleum Hydrocarbons in Marine Organisms," Proceedings of NOAA Conference on Fate and Effects of Petroleum Hydrocarbons in Marine Ecosystems and Organisms, Seattle, Nov. In Press.

Roshore, E.C. (1972), "Investigation of Sinking Methods for Removal of Oil from Water Surfaces. Phase II: Methods of Test for Laboratory Evaluation of Oil Sinking Material," U.S. Coast Guard Office of Research and Development, NTIS No. AD-741 247.

Ruggles, K.W. (1970), "The Vertical Mean Wind Profile Over the Ocean in Light to Moderate Winds," J. Appl. Meteorology 9, 389-395.

Russel, R.C.H. and J.D.C. Osorio (1958), "An Experimental Investigation of Drift Profiles in a Closed Channel," Sixth Conf. on Coastal Eng., Chap. 10, pp. 171-193.

Ryan, P.J. and D.R.F. Harleman (1973), "Analytical and Experimental Study of Transient Cooling Pond Behavior," Technical Report No. 161, R.M. Parsons Laboratory for Water Resources and Hydrodynamics, Dept. of Civil Engineering, M.I.T., Cambridge, Mass.

Schlichting , H. (1968), Boundary-Layer Theory, McGraw-Hill, New York.

Shaw, D.G. (1976), "Hydrocarbons in the Water Column" Proceedings of NOAA Conference on Fate and Effects of Petroleum Hydrocarbons in Marine Ecosystems and Organisms, Seattle, Nov. 1976. In press.

Shemdin, O.H. (1972), "Wind Generated Current and Phase Speed of Wind Waves," Journal of Physical Oceanography 2, 411-419.

Shemdin, O.H. (1973), "Modeling of Wind Induced Current," J. of Hydraulic Research 11(3), 281-297.

Sheppard, P.A., H. Charnock and J.R.D. Francis (1952), "Observations of the Westerlies over the Sea," Quart. J.R. Met. Soc. 78, 563-82.

Sheppard, P.A. and M.H. Omar (1952), "The Wind Stress Over the Ocean from Observations in the Trades," Quart. J.R. Met. Soc. 78, 583-9.

Sheppard, P.A. (1954), "The Vertical Transfer of Momentum in the General Circulation," Arch. Met. Geophys. Bioklimat. A, 7, 114-24.

Shinozuka, M. and C.M. Jan (1972), "Digital Simulation of Random Processes and its Applications," Journal of Sound and Vibration 25(1), 111-28.

Shukla, D.K. and R.M. Stark (1974), "Random Movement of Oil Patches," The Science of the Total Environment 3, 117-25.

Sivadier, H.O. and P.G. Mikolaj (1973), "Measurement of Evaporation Rates from Oil Slicks on the Open Sea," Proc. Conf. on Prevention and Control of Oil Spills, API, Washington, D.C., pp. 475-484.

Smith, C.L. and W.G. MacIntyre (1971), "Initial Aging of Fuel Oil Films on Sea Water," Proc. Joint Conf. on Prevention and Control of Oil Spills, Sponsored by API, EPA, and USCG, Publ. by Amer. Petrol. Inst., Washington, D.C., pp. 457-461.

Smith, C.L. and W.G. MacIntyre, et al. (1974), "Investigations of Surface Films-Chesapeake Bay Entrance," EPA 670/2-73-099, U.S. Government Printing Office, Washington, D.C.

Smith, J.E. (1968), Torrey Canyon Pollution and Marine Life, Cambridge University Press.

Solig, G. and E.M. Bens (1972), "Bacteria which Attack Petroleum Hydro-carbons in a Saline Medium," Biotech and Bioeng 14, 319 ff.

Stewart, R.J., (1973), "Dispersion Predictions for Offshore Oil Slicks and a Bayesian Analysis of Spill Volume Distributions," S.M. Thesis, M.I.T., Department of Ocean Engineering.

Stewart, R.J., J.W. Devanney, and W. Briggs (1974), "Oil Spill Trajectory Studies for Atlantic Coast and Gulf of Alaska, Report to Council on Environmental Quality, MIT Sea Grant Report No. 74-20.

Stewart, R.J. (1976), "The Interaction of Waves and Oil Spills," Ph.D. Thesis, Department of Ocean Engineering, MIT, Cambridge, Mass.

Stokes, G.G. (1847), "On the Theory of Oscillatory Waves," Trans. Cambridge Phil. Soc., Vol. 8 and Supplement, Sci. Papers, Vol. 1.

Stommel, H. and Leetmaa, A. (1972), "Circulation on the Continental Shelf," Proc. National Academy of Sciences 69(11), 3380-3384.

Strassner, J.E. (1968), "Effect of pH on Interfacial Films and Stability of Crude Oil-water Emulsions," Journal of Petroleum Technology, pp. 303-312.

Strong, A.E. and I.S. Ruff (1970), "Utilizing Satellite-Observed Solar Reflections from the Sea Surface as an Indicator of Surface Wind Speeds," Remote Sensing of Environment 1, 181-185.

Stull, D.R. (1947), "Vapor Pressure of Pure Substances - Organic Compounds," Industrial and Engineering Chemistry 39, 517-550.

Sutton, C. and J.A. Calder (1974), "Solubility of Higher-Molecular-Weight n-Paraffins in Distilled Water and Seawater," Environmental Science and Technology 8(7), 654-657.

Sutton, O.G. (1947), "The Problem of Diffusion in the Lower Atmosphere," Quart. Journal of the Royal Met. Soc. 73, 257-381.

Swartzberg, H.G. (1971), "The Movement of Oil Spills," Proc. of the Jt. Conf. on Prev. and Cont. of Oil Spills, published by Amer. Petrol. Inst., Washington, D.C., pp. 489-494.

Tayfun, M.A. and H. Wang (1973), "Monte Carlo Simulation of Oil Slick Movements," ASCE WW3, pp. 309-23.

Taylor, G.I. (1921), "Diffusion by Continuous Movements," Proc. of the London Mathematical Society, Ser. 2, Vol. 20, pp. 196-212.

Teeson, D., F.M. White and H. Schenck (1970), "Studies of the Simulation of Drifting Oil by Polyethylene Sheets," Ocean Engineering 2, 1-11, Pergamon Press.

Thom, H.C.S. (1960), "Distributions of Extreme Winds in the United States," J. Structural Div., ASCE, ST4. 86.

Thomas, J.H. (1975), "A Theory of Steady Wind-Driven Currents in Shallow Water with Variable Eddy Viscosity," J. Physical Oceanography 5, 136-142.

Tobias, Leo (1971), "Feasibility Study of the Sand/Oil Sink Method of Combatting a Major Oil Spill in the Ocean Environment," U.S. Coast Guard Office of Research and Development, NTIS No. AD-742 949.

Tolbert, W.H. and G.G. Salsman (1964), "Surface Circulation of the Eastern Gulf of Mexico as Determined by Drift-Bottle Studies," J. Geophys. Res. 69, 223 ff.

Tomczak, G. (1964), "Investigations with Drift Cards to Determine the Influence of the Wind on Surface Currents," Oceanographize 10, 129-139.

Unluata, U. and C.C. Mei (1970), "Mass Transport in Water Waves," Journal of Geophysical Research 75(36), 7611-7617.

U.S. Army Corps of Eng. (1973), Shore Protection Manual, Government Printing Office, Washington, D.C.

U.S. Coast and Geodetic Survey (1960), Tidal Current Charts, Delaware Bay and River, Government Printing Office, Washington, D.C.

Vagners, J. and P. Mar (1972), Oil in Puget Sound, University of Washington Press, Seattle, Washington.

Van Dorn, W.G. (1953), "Wind Stress on an Artificial Pond," J. of Marine Research 12(3), 219-275.

Waldman, G.A., R.A. Johnson and P.C. Smith (1973), "The Spreading and Transport of Oil Slicks on the Open Ocean in the Presence of Wind, Waves, and Currents," Coast Guard Report No. CG-D-17-73, AD-765 926, (70 pages).

Wall, L.A., J.H. Flynn, S. Straus (1970), "Rates of Molecular Vaporization of Linear Alkanes," Journal Physical Chemistry 74 (17), 3237-3242.

Wang, H., J. Campbell and J.D. Ditmars (1975), "Computer Model of Oil Movement and Spreading in Delaware Bay," Coastal Engineering Report #5, Dept. of Civil Engineering, U. of Delaware, December.

Wang, J.D. and J.J. Connor (1975), "Mathematical Modeling of Near Coastal Circulation," TR No. 200, Ralph M. Parsons Laboratory for Water Resources and Hydrodynamics, MIT, Cambridge, Massachusetts.

Wang, S., and L. Hwang (1974), "A Numerical Model for Simulation of Oil Spreading and Transport and Its Application for Predicting Oil Spill Movement in Bays," Tetra Tech Inc., AD-780 424, (102 pages).

Warner, J.L., J.W. Graham and R.G. Dean (1972), "Prediction of the Movement of an Oil Spill on the Surface of the Water," Proc. Offshore Tech. Conf., Dallas, Paper No. OTC 1550.

Webb, L.E., R. Taranto and E. Hashimoto (1970), "Operational Oil Spill Drift Forecasting," paper presented at the 7th U.S. Navy Symposium of Military Oceanography, Annapolis, Maryland, May 12-14, 1970 (8 pages).

Welander, P. (1957), "Wind Action on a Shallow Sea: Some Generalizations of Ekman's Theory," Tellus 9(1), 45-52.

Wexler, R. (1946), "Theory and Observations of Land and Sea Breezes," Bulletin of American Meteorological Society 27, pp. 272-87.

Williams, G.N.,R. Hann and W.P. James (1975), "Predicting the Fate of Oil in the Marine Environment," Proc. of Joint Conference on Prevention and Control of Oil Spills, publ. by Am. Petrol. Institute, Washington, D.C.

Wilson, B.W. (1961), "Deepwater Wave Generation by Moving Wind Systems," J. of Waterways and Harbors Div., ASCE 87(WW2), 113-141.

Witten, A.J. and J.H. Thomas (1976), "Steady Wind-Driven Currents in a Large Lake with Depth-Dependent Eddy Viscosity," J. Physical Oceanography 6, 85-92.

Wu, J. (1968), "Laboratory Studies of Wind-Wave Interactions, J. Fluid Mech. 34(1), 91-111.

Wu, J. (1969), "Wind Stress and Surface Roughness at Air-Sea Interface," J. of Geophysical Res. 74(2), 444-55.

Wu, J. (1971), "Evaporation Retardation by Monolayers: Another Mechanism," Science 174(15), 283-285.

Wu, J. (1973), "Prediction of Near-Surface Drift Currents from Wind Velocity," J. of Hydraulics Div., ASCE 99(HY9), 1291-1302.

Wyngaard, J.C., O.R. Coté, and K.S. Rao (1974), "Modeling the Atmospheric Boundary Layer," Advances in Geophysics, Vol. 18A, Academic Press, pp. 193-211.

Zajic, J., B. Supplisson and B. Volesky (1974), "Bacterial Degradation and Emulsification of No. 6 Fuel Oil," Environmental Science and Technology 8(7), 664 ff.

ZoBell, C.E. (1969), "Microbial Modification of Crude Oil in the Sea," Proc. of the Joint Conf. on Prevention and Control of Oil Spills, Sponsored by API, FWPCA, Dec. 15-17, New York, pp. 317-326.

ZoBell, C.E. (1973), "Microbial Degradation of Oil: Present Status, Problems and Perspectives," in Ahearn, D.G. and S.P. Meyers (eds.), The Microbial Degradation of Oil Pollutants, Center for Wetland Resources, Louisiana State University, Baton Rouge.

Zwolinski, B.J. and R.C. Wilhoit (1971) Handbook of Vapor Pressures and Heats of Vaporization of Hydrocarbons and Related Compounds, API Research Project 44, Publication No. 101.

APPENDIX A:

A REALISTIC MODEL OF THE

WIND-INDUCED EKMAN BOUNDARY LAYER

ABSTRACT

A physically realistic and general model for the vertical eddy
viscosity in a homogeneous fluid is proposed. For an infinitely deep
ocean the vertical eddy viscosity increases linearly with depth from a
value of zero at the free surface. Based on this model a general theory
is developed for the drift current resulting from a time varying surface
shear stress. Explicit expressions are given for the temporal develop-
ment of the drift current in the vicinity of the free surface and for
the steady state response to a suddenly applied uniform shear stress.
The steady-state solution predicts the effective Ekman layer depth
to be proportional to the square root of the wind shear stress and
reproduces the experimentally observed logarithmic velocity deficit near
the free surface. The angle between the surface drift current and the
wind stress is found to be somewhat smaller, of the order 10°, than pre-
dicted by Ekman's classical solution. For the unsteady response to a
suddenly applied wind stress the present model predicts a much shorter
response time than that found by Fredholm based on a constant vertical
eddy viscosity assumption. The application of the proposed vertical eddy
viscosity model to finite depth conditions, including the effects of
slope currents, is outlined.

1. Introduction

In Ekman's (1905) classical study of wind driven currents a constant vertical eddy viscosity was assumed. For the steady wind driven current in an infinite homogeneous ocean the assumption of a constant vertical eddy viscosity leads to an angle between the wind shear stress and the surface current of $\pi/4$, a value generally considered to be on the high side. In shallower waters, where bottom friction comes into play, the assumption of a constant eddy viscosity in conjunction with a no-slip condition at the bottom leads to unrealistically low velocities as recently pointed out by Murray (1975), who circumvented this problem by introducing the somewhat artificial concept of a slip velocity at the bottom boundary. The shortcomings of a constant vertical eddy viscosity assumptions have long been recognized and the proper parameterization of the vertical eddy viscosity was recently identified by Reid (1975) as one of the major problems in the analysis of wind driven currents.

In relatively shallow water, when the depth h is smaller than or comparable to the thickness of the frictional layer, more realistic models than that of a constant vertical eddy viscosity have been proposed. Fjeldstad (1929), based on an analysis of field data, suggested that the vertical eddy viscosity, ν_T, was proportional to the 3/4 power of the distance, z_b, from the bottom, i.e., $\nu_T \propto z_b^{3/4}$. This model was recently employed by Murray (1975) in a study of nearshore wind driven currents. Thomas (1975) suggested a physically more realistic version of Fjeldstad's model by taking $\nu_T = \kappa |u_{*b}| z_b$, where κ is von Karman's constant ($\kappa = 0.4$) and $|u_{*b}|$ is the shear velocity based on the absolute value of the bottom shear stress, $|u_{*b}| = \sqrt{|\tau_b|/\rho}$, with ρ being the fluid density. Thomas'

model has several physically pleasing features. The magnitude of the vertical eddy viscosity depends on the flow itself and on the bottom boundary roughness, k_b, through $|u_{*b}|$, and it leads to the classical logarithmic velocity profile in the vicinity of the bottom. The added physical realism of Thomas' model is not achieved without a cost in terms of added computational difficulties. Thus, since the solution for the wind driven flow depends on the value assigned to v_T and since v_T itself depends on the flow characteristics a rather time-consuming iterative solution procedure must be adopted. This additional computational complexity apparently caused Witten and Thomas (1976) to abandon this model in favor of an explicit model for the vertical eddy viscosity. The eddy viscosity models referred to above are all restricted to application in shallow water. If they, despite this limitation, were adopted for deep water conditions they would effectively correspond to a constant vertical eddy viscosity assumption.

The purpose of this paper is to present a more realistic and more general model for the vertical eddy viscosity than those previously advanced in the context of wind driven ocean currents. The proposed model is simply that the vertical eddy viscosity is assumed to increase linearly with vertical distance from a sheared boundary, i.e., $v_T = \kappa |u_*| z$, where $|u_*|$ is the shear velocity and z is the distance from the sheared boundary, respectively. In the vicinity of the bottom, $z_b = 0^+$, this model is identical to the model proposed by Thomas (1975). Near the free surface, however, where $z_b = h^-$ the eddy viscosity given by the proposed model varies according to $v_T = \kappa |u_{*s}| (h - z_b)$, with $|u_{*s}|$ being the shear velocity based on the surface shear

stress. The model for the vertical eddy viscosity proposed here may be shown to agree with the model of steady turbulent shear flows proposed by Reid (1957). It leads to a logarithmic velocity profile near the bottom, as does Thomas' model, and a logarithmic velocity deficit in the vicinity of the free surface. The latter feature, which is absent in Thomas' model, has been observed experimentally in steady turbulent Couette flow by Reichardt (1959). Furthermore, Shemdin (1972) found the wind driven current in a laboratory wind wave facility, i.e., in the presnece of surface waves, to exhibit a logarithmic velocity deficit in the vicinity of the free surface. These observed features, which are reproduced by the proposed model for the vertical eddy viscosity, are taken to support the physical realism of the proposed model. In addition, the proposed model may be applied in deep as well as in shallow water and is therefore considered to be of a more general nature than previous models. It is noted that the present model, when applied to the case of infinite water depth, is identical to the model proposed by Ellison (1956) in the context of the atmospheric boundary layer.

The model for the vertical eddy viscosity is, of course, limited to the idealized conditions of a homogeneous ocean. It is applied here to the response of an infinitely deep homogeneous ocean of infinite lateral extent to a time-varying spatially uniform shear stress. Approximate expressions are derived for the temporal development of the pure drift current for a suddenly applied shear stress. The limit of this solution for large times is shown to be identical to Ellison's (1956) solution for the atmospheric boundary layer. The steady response is compared to the classical Ekman solution and reveals the angle between surface shear stress

and velocity to be approximately 10° as compared to the 45° predicted by Ekman (1905). The temporal development of the surface current resulting from a suddenly applied shear stress is compared with Fredholm's solution as given by Ekman (1905). The present solution shows the response to be nearly instantaneous when compared to the slow approach to steady state conditions exhibited by Fredholm's solution. The differences between the present and previous solutions as well as the implications of these differences are discussed in some detail. The problems associated with the application of the proposed model for the vertical eddy viscosity in the general case of finite depth and including the effects of a slope current are outlined.

2. General Analysis

For an infinitely deep, homogeneous ocean of infinite lateral extent the linearized form of the horizontal momentum equations may be written

$$\frac{\partial w}{\partial t} + i \, f \, w = \frac{\partial}{\partial \widehat{z}} \left(\nu_T \frac{\partial w}{\partial \widehat{z}} \right) \tag{1}$$

in which $i = \sqrt{-1}$,

$$w = u + i \, v \tag{2}$$

is the complex horizontal velocity in the $(\widehat{x}, \widehat{y})$ plane of the Cartesian coordinate system, $f = 2\omega_e \sin\phi$ is the Coriolis parameter, ω_e and ϕ being the radian frequency of earth's rotation and the latitutde, respectively, and $\widehat{z}$ is the vertical coordinate chosen positive upwards. The right hand side of (1) represents the contribution of frictional forces on horizontal planes and the terms expressing the horizontal force components associated

with a spatially varying atmospheric pressure and free surface elevation
are omitted to be consistent with the assumption of an ocean of infinite
lateral extent.

Introducing the more convenient vertical coordinate, $\hat{z} = -z$, which is
positive downwards and taking $z = 0$ in the free surface the proposed model
for the vertical eddy viscosity, ν_T, reads

$$\nu_T = \kappa u_* z \tag{3}$$

in which $\kappa = 0.4$ is von Karman's constant and $u_* = \sqrt{|\tau_s|/\rho}$ is the shear
velocity based on a representative value of the magnitude of the surface
shear stress, $|\tau_s|$. In problems where $|\tau_s|$ may be considered constant,
such as in the problem of a suddenly applied constant surface shear, there
is little ambiguity in the value to be assigned to u_*. For the flow re-
sulting from a time-varying surface shear stress the subsequent analysis
necessitates the use of a time-independent value of u_* in (3). The use of
a representative value of $|\tau_s|$ to define the magnitude of the vertical
eddy viscosity must in this case reflect the intended application of the
results.

With the shear stress on horizontal planes expressed in complex form
as $\tau = \tau_{\hat{x}} + i\ \tau_{\hat{y}}$ and defined in the usual manner in the right-handed
(x,y,z) coordinate system we have

$$\frac{\tau}{\rho} = \frac{\tau_{\hat{x}}}{\rho} + i\ \frac{\tau_{\hat{y}}}{\rho} = \nu_T \frac{\partial w}{\partial \hat{z}} = -\nu_T \frac{\partial w}{\partial z} \tag{4}$$

For the general problem of a flow starting from rest, i.e.,

$$w = 0 \qquad \text{for } t \leq 0 \tag{5}$$

and driven by a time-varying, spatially uniform surface shear stress, $\tau_s(t)$, (3) and (4) provide one of the necessary boundary conditions

$$\frac{\tau_s(t)}{\rho} = \frac{\tau_{s,\hat{x}}(t)}{\rho} + i\;\frac{\tau_{s,\hat{y}}(t)}{\rho} = - \kappa\, u_* z\,\frac{\partial w}{\partial z}\quad ; \;z \to 0,\; t \geq 0 \tag{6}$$

The remaining boundary condition to be satisfied by the solution of (1) is that of a vanishing motion with depth, i.e.,

$$w \to 0 \qquad \text{as } z \to \infty \tag{7}$$

Since the governing equation, (1), is linear and the coefficients independent of time the use of Laplace transforms, defined by

$$\overline{w} = \mathcal{L}\{w\} = \int_0^\infty e^{-st}\, w(t)\; dt \tag{8}$$

is convenient. Taking the Laplace transform of (1) and invoking the initial condition (5) the governing equation becomes

$$(s + i\; f)\; \overline{w} = \frac{\partial}{\partial z}\;(\kappa u_* z\;\frac{\partial \overline{w}}{\partial z}) \tag{9}$$

with the boundary conditions

$$- \kappa\, u_* z\,\frac{\partial \overline{w}}{\partial z} = \mathcal{L}\{\frac{\tau_{s,\hat{x}}(t)}{\rho} + i\;\frac{\tau_{s,\hat{y}}(t)}{\rho}\}\quad ; \quad \text{as } z \to 0 \tag{10}$$

and

$$\overline{w} \to 0\quad ; \quad \text{as } z \to \infty \tag{11}$$

Introducing the dimensionless vertical coordinate

$$\xi = \frac{z(s + i\; f)}{\kappa u_*} \tag{12}$$

(9) may be written

$$\frac{\partial}{\partial \xi} \left(\xi \frac{\partial \bar{w}}{\partial \xi} \right) - \bar{w} = 0 \tag{13}$$

whose general solution (Hildebrand, 1965) is

$$\bar{w} = A \quad I_0(2\sqrt{\xi}) + B \quad K_0(2\sqrt{\xi}) \tag{14}$$

where A and B are arbitrary constants and I_0 and K_0 are the zeroth order Modified Bessel Functions of the first and second kind, respectively.

By virtue of the exponential behavior of I_0 for large values of the argument it follows from (11) that A = 0 in (14), thus leaving us with

$$\bar{w} = B \quad K_0(2\sqrt{\xi}) \tag{15}$$

The constant B in (15) is determined from the free surface stress condition, (10), which in terms of the dimensionless vertical coordinate, ξ, may be written as

$$- \kappa u_* \ \xi \frac{\partial \bar{w}}{\partial \xi} = \kappa \ u_* \ \sqrt{\xi} \ B \quad K_1(2\sqrt{\xi}) =$$

$$\mathcal{L}\{\frac{\tau_{s,w}}{\rho} + i \ \frac{\tau_{s,y}}{\rho}\} = \mathcal{L}\{\frac{\tau_s}{\rho}\} ; \quad \text{as } \xi \to 0 \tag{16}$$

Introducing the asymptotic expansion of the first order Modified Bessel Function of the second kind, K_1, for small values of the argument we obtain from (16)

$$B = \frac{2}{\kappa u_*} \ \mathcal{L}\{\frac{\tau_s}{\rho}\} \tag{17}$$

and the Laplace transform of the solution to the stated problem has been found

$$\bar{w} = \frac{2}{\kappa u_*} \ \mathcal{L}\{\frac{\tau_s}{\rho}\} \ K_0(2\sqrt{\xi}) \tag{18}$$

To invert this Laplace transform it is recognized that

$$K_o(2\sqrt{\xi}) = K_o(\sqrt{\frac{4z}{\kappa u_*}} s + i \frac{4z}{\kappa u_*} f) \tag{19}$$

may be inverted by use of the table of Laplace transforms presented in Abramowitz and Stegun (1972, Chapter 29, Eqs. (29.2.14) and (29.3.120)). The result of this inversion may be written in terms of the function to which (19) is the Laplace transform, i.e.,

$$\mathcal{L}\{\frac{1}{2} e^{-ift} \frac{1}{t} e^{-\frac{z}{\kappa u_* t}}\} = K_o(2\sqrt{\xi}) \tag{20}$$

Inserting (20) in (18) it is readily seen that the use of the convolution theorem yields the general solution

$$w = \frac{1}{\kappa u_*} \int_0^t \frac{\tau_{s,\hat{x}}(t-\beta) + i \tau_{s,\hat{y}}(t-\beta)}{\rho} e^{-if\beta} \frac{1}{\beta} e^{-\frac{z}{\kappa u_* \beta}} d\beta \tag{21}$$

for the response of an infinite, homogeneous ocean to a time-varying, spatially uniform surface shear stress. The main assumption involved in obtaining the above solution, in addition to those made in the problem formulation itself, is that of a constant value of u_* based on a representative value of the surface shear stress, $|\tau_s| = (\tau_{s,\hat{x}}^2 + \tau_{s,\hat{y}}^2)^{1/2}$. This assumption is not unique to the present formulation of the problem and is made also when the solution is found based on an assumed constant vertical eddy viscosity. In this respect it may be worthwhile to point out that a spatially varying but time-independent vertical eddy viscosity has been employed successfully by Kajiura (1964 and 1968) in an analysis of turbulent oscillatory boundary layers.

3. Response to a Suddenly Applied Constant Surface Stress

To investigate in more detail the nature of the general solution obtained in the previous section the response to a suddenly applied constant surface shear stress in the $\hat{y}$-direction is considered here, i.e., we take

$$\tau_s = \begin{cases} 0 & t \leq 0 \\ i\tau_{s,y} & t \geq 0 \end{cases} \tag{22}$$

for which

$$u_* = \sqrt{\frac{\tau_{s,\hat{y}}}{\rho}} \tag{23}$$

For this problem, which corresponds to the problem solved by Fredholm based on a constant eddy viscosity assumption (Ekman, 1905), (21) becomes

$$w = u + i\,v = i\,\frac{u_*}{\kappa}\int_0^t \frac{1}{\beta}\,e^{-if\beta}\,e^{-\frac{z}{\kappa u_*\beta}}\,d\beta \tag{24}$$

The solution obtained here is remarkably similar in its appearance to Fredholm's solution (Ekman, 1905, Eqs. 11). The most striking difference between the two solutions is in their behavior in the vicinity of the free surface, i.e., as $z \to 0$. Taking $z = 0$ Fredholm's solution simplifies to Fresnel integrals, which are convergent, whereas the imaginary part of the present solution is a divergent cosine integral. This behavior of the present solution is, of course, a consequence of the assumed variation of the vertical eddy viscosity, in particular, the vanishing of ν_T as the free surface is approached. A similar peculiarity is exhibited by the classical solution for turbulent flow over a rough boundary (Schlichting, 1960) in the context of which the problem is resolved by satisfying the

no-slip condition a distance $z_{ob} = k_b/30$ above the theoretical bottom, where k_b is the equivalent sand roughness of the boundary. In analogy with the turbulent flow over a rough boundary we may therefore consider the surface velocity, w_s, obtained from the present solution to be the velocity evaluated from (21) or (24) corresponding to a value of $z = z_{os} = k_s/30$, where k_s is the equivalent sand roughness of the free surface.

The preceding argument, which is supported by the experimental findings of Reichardt (1959), removes the apparent singularity of our solution. It leaves us, however, with the rather unpleasant problem of estimating the value of the equivalent sand roughness, k_s, of the free surface. The equivalent sand roughness of a sea surface has been studied to some extent in the context of the atmospheric boundary layer. These results in conjunction with Shemdin's (1973) observation that the equivalent sand roughness of a free surface was of the same order whether the free surface was approached from above, $k_{s,air}$, or from below, k_s, may be used as a guide for estimating k_s. Analyzing wind velocity profiles above a sea surface Ruggles (1970) found the equivalent sand roughness of the sea surface to be essentially constant and of the order $k_{s,air} \simeq 4$ cm for wind speeds W_{10}, measured 10 meters above the still water level, ranging from 3 to 10 m/sec. In a similar study Wu (1969) found by re-analyzing wind data from both laboratory and field experiments that $k_{s,air} \simeq 8$ cm for wind speeds in excess of 15 m/sec. Although several problems regarding the sea surface roughness remain unresolved, including a discrepancy bewteen the values of $k_{s,air}$ obtained by Wu (1969) and

Ruggles (1970) for $W_{10} < 10$ m/sec and the equivalency of $k_{s,air}$ and k_s, the above discussion does provide an order of magnitude estimate of k_s. As we shall see the results obtained from (21) and (24) are relatively insensitive to the actual value assigned to k_s, so long as its order of magnitude is known.

Inspection of (24) shows that we may write the equation in the following form

$$w = u + i\,v = \frac{u_*}{\kappa} \int_0^{ft} \frac{\sin\alpha + i\,\cos\alpha}{\alpha}\, e^{-\frac{\zeta}{\alpha}}\, d\alpha \qquad (25)$$

in which

$$\alpha = f\,\beta \qquad (26)$$

is the nondimensional time and

$$\zeta = \frac{zf}{\kappa u_*} \qquad (27)$$

is the nondimensional vertical coordinate.

Equation (27) identifies the characteristic vertical length scale, ℓ, of the problem to be

$$\ell = \frac{\kappa u_*}{f} \qquad (28)$$

By taking $\kappa = 0.4$ and $u_* = 0.04 \sqrt{\rho_a/\rho}\; W_{10}$ as found by Ruggles (1970) with the ratio of air to fluid density, $\rho_a/\rho = 1/840$, (28) shows that

$$\ell \approx \frac{3.66\, W_{10}}{\sin\phi} \qquad (29)$$

where ℓ is in meters if W_{10} is in m/sec. The magnitude of ℓ is indicative

of the depth of frictional influence, as will be discussed later. In the present context (29) is established merely to show that the parameter ζ in (25) safely may be considered small in the uppermost meters of the ocean.

With the assumption of $\zeta \ll 1$ approximate expressions for (25) may be obtained in terms of tabulated functions. For example, we have from (25)

$$v = \frac{u_*}{\kappa} \int_0^{ft} \frac{\cos\alpha}{\alpha} e^{-\zeta/\alpha} d\alpha =$$

$$\frac{u_*}{\kappa} \left[\int_0^{\alpha_1} \frac{\cos\alpha}{\alpha} e^{-\zeta/\alpha} d\alpha + \int_{\alpha_1}^{ft} \frac{\cos\alpha}{\alpha} e^{-\zeta/\alpha} d\alpha \right] \tag{30}$$

Now, with $\zeta \ll 1$ and choosing $\zeta < \alpha_1 < 1$ we may expand $\cos\alpha = 1-\alpha^2/2$ in the first and $e^{-\zeta/\alpha} = 1 - \zeta/\alpha$ in the second integral of the right hand side of (30). Retaining only the leading term in the expansions and omitting the algebraic manipulations we obtain

$$v = \frac{u_*}{\kappa} \left[E_1\left(\frac{\zeta}{\alpha_1}\right) - Ci(\alpha_1) + Ci(ft) \right] ; \quad ft > \alpha_1 = 0.1 \tag{31}$$

in which

$$E_1\left(\frac{\zeta}{\alpha_1}\right) = \int_{\zeta/\alpha_1}^{\infty} \frac{e^{-\beta}}{\beta} d\beta \tag{32}$$

and

$$Ci(\alpha_1) = - \int_{\alpha_1}^{\infty} \frac{\cos\beta}{\beta} d\beta \tag{33}$$

are tabulated exponential integrals (Abramowitz and Stegun, 1972,

Chapter 5). By retaining the omitted terms in the expansions of $\cos\alpha$

and $e^{-\zeta/\alpha}$ utilized in obtaining (31), an error bound may be obtained and

the choice of $\alpha_1 = 0.1$ made here ensures us that the error in v is less

than 25 ζ u_*.

In a similar manner we may obtain from (25)

$$u \simeq \frac{u_*}{\kappa} [Si(ft) + \zeta(Ci(\zeta) - Ci(ft))] ; \quad ft > \zeta \tag{34}$$

in which

$$Si(ft) = \int_0^{ft} \frac{\sin\beta}{\beta} d\beta \tag{35}$$

is the tabulated sine-integral. The error term in (34) is $O(\zeta)$.

For $\zeta << 1$ the asymptotic behavior of $E_1(\beta) = -Ci(\beta) = -\gamma -\ln\beta$ as

$\beta \to 0$ may be introduced in (31) and (34) to give

$$u + iv \simeq \frac{u_*}{\kappa} [\frac{\pi}{2} + \zeta \ln\zeta + i (-2\gamma -\ln\zeta)]$$

$$+ \frac{u_*}{\kappa} [Si(ft) - \frac{\pi}{2} - \zeta Ci(ft) + i Ci(ft)] \tag{36}$$

in which $\gamma = 0.577..$ is Euler's constant. In the limit $ft \to \infty$ we have

$Si(ft) \to \pi/2$ and $Ci(ft) \to 0$ and the second bracketed term in (36) vanishes.

The steady state response is therefore expressed by the first bracketed

term in (36).

The exact steady state solution may be found from (24) by taking the

limit as $t \to \infty$. This procedure is rather time-consuming and involves

numerous changes of variables and contour integration to obtain an expres-

sion which by use of Abramowitz and Stegun (1972, Eq. 9.6.25) may be shown

to be identical to

$$u + i v = i \frac{2u_*}{\kappa} [ker (2\sqrt{\zeta}) + i kei (2\sqrt{\zeta})]= i \frac{2u_*}{\kappa} K_o(2\sqrt{\zeta} e^{i\pi/4}) \tag{37}$$

in which ker and kei are the zeroth order Kelvin Functions. It is, however, relatively simple to obtain (37), which is identical to Ellison's (1956) solution for the atmospheric boundary layer, by returning to (1) and solving this equation for $\partial/\partial t = 0$. It is reassuring to find that the asymptotic expansion of (37) for small values of $2\sqrt{\zeta}$ to $O(\zeta)$ is identical to the steady state solution obtained from (36).

4. Discussion of the Results

As discussed in the preceding section the value of the surface drift current is obtained from the general solutions corresponding to a value of $z = z_{os} = k_s/30$. With the order of magnitude of k_s being 5 cm and with ℓ given by (29) it is evident that $\zeta_{os} = z_{os}/\ell \ll 1$ so that the steady surface drift is obtained from (36)

$$w_s = u_s + i\ v_s = \frac{u_*}{\kappa}\{\frac{\pi}{2} + i(-1.15 + \ell n\ \frac{30\ell}{k_s})\} \tag{38}$$

Combining (36) and (38) it is seen that the velocity deficit, $w_s - w$, in the vicinity of the free surface is logarithmic as observed by Shemdin (1972). The value of the deflection angle, θ_s, between the surface shear stress and the steady surface drift current is found from (38) to be given by

$$\tan\theta_s = \frac{\pi/2}{-1.15 + \ell n\ \frac{30\ell}{k_s}} \tag{39}$$

where the deflection is to the right on the northern hemisphere.

With ℓ given by (29) the sensitivity of the predicted surface velocities and deflection angles to the value assigned to k_s is seen from Table 1 to be relatively insignificant. Thus, a change of the estimated value of k_s by a factor of two changes the nondimensional surface current,

Table 1: Values of Surface Drift Current and Deflection Angle for Various Wind Speeds and Surface Roughness.

W_{10} (m/sec)	5		10		15		20		30	
$k_s \sin\phi$ (cm)	$\kappa v_s/u_*$	θ_s °	$\kappa v_s/u_*$	θ_s °	$\kappa v_s/u_*$	θ_s °	$\kappa v_s/u_*$	θ_s °	$\kappa v_s/u_*$	θ_s °
10	7.47	11.9	8.16	10.9	8.57	10.4	8.85	10.1	9.26	9.6
5	8.16	10.9	8.85	10.1	9.26	9.6	9.55	9.3	9.95	9.0
2.5	8.85	10.1	9.55	9.3	9.95	9.0	10.24	8.7	10.65	8.4

$\kappa v_s/u_*$, as well as the deflection angle by only about 10 percent. The most striking difference between the results presented in Table 1 and the classical results of Ekman's (1905) theory is the much smaller value of the deflection angle. Observations of oil spill trajectories either real (Smith, 1968) or simulated (Teeson et al., 1970) have consistently shown values of the deflection angle of the order 10° or less and are therefore taken to support the present results. In the context of oil slick trajectories, which initially were the motivation for the present study, it is also interesting to note that the commonly employed rule of thumb that the speed of advection of an oil slick is three percent of the wind speed, W_{10}, follows from the results presented in Table 1. Thus, with the magnitude of the surface current $|w_s| = (u_s^2 + v_s^2)^{1/2}$ being essentially equal to v_s and adopting Ruggles' (1970) result $u_* = 0.04 \sqrt{\rho_a/\rho} \, W_{10}$ it follows that

$$|w_s| \simeq \frac{u_*}{\kappa} \left(\frac{\kappa v_s}{u_*}\right) = \sqrt{\rho_a/\rho} \, (0.1 \, \frac{\kappa v_s}{u_*}) \, W_{10} \tag{40}$$

Inspection of the values of $\kappa v_s/u_*$ presented in Table 1 and taking $\rho_a/\rho = 1/840$ show $|w_s| = 0.03 \, W_{10}$ to provide a reasonable approximation to (40). The preceding result should not be interpreted to support the "three percent rule" which clearly oversimplifies the problem. The effect of oil slicks on the water surface in reducing the apparent surface roughness (Barger et al., 1970) is not accounted for by the three percent rule, neither is the possible existence of a geostrophic current at large depths.

To examine the variation of the steady drift current with depth the solution given by (37) is plotted in Fig. 1. The velocity vector is indicated
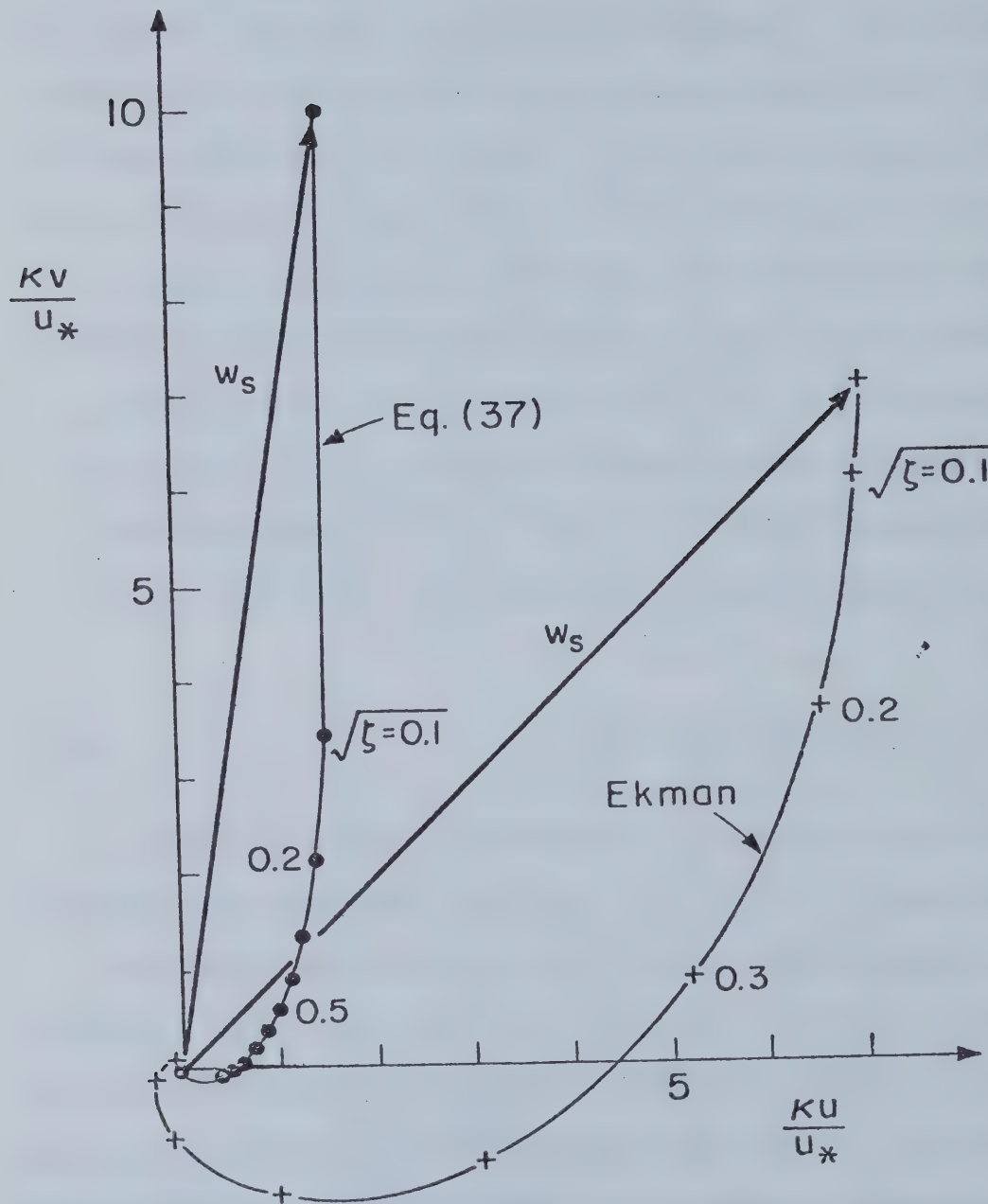
Figure 1: Vertical Velocity Structure of a Pure Drift Current in an Infinitely Deep Homogeneous Ocean of Infinite Lateral Extent. Comparison between the Turbulent Ekman Spiral (•) and the Classical Ekman Spiral (+).

at increments of $\sqrt{\zeta} = \sqrt{z/\ell}$ of 0.1, with the surface current given by (38)

rather than corresponding to $\zeta = 0$. The hodograph shown in Fig. 1 is

based on a value of $\kappa v_s/u_* = 10$ but is, except for the location of the point

indicating the surface current, quite general. The extremely rapid decrease

and rotation of the drift current with depth, a consequence of the

logarithmic velocity deficit near the surface, is noted. With ℓ given by

(29) it is seen that $\ell = O$ (100 m) for $W_{10} \simeq 20$ m/sec and the results pre-

sented in Fig. 1 indicate that for $z = 0.01 \, \ell \simeq 1$ m $(\sqrt{\zeta} = 0.1)$ the velocity

is only approximately a third of its value at the surface with a deflection

angle of 25° as compared to $\theta_s = 9^o$. It is also evident from Fig. 1 that

there is practically no motion at a depth corresponding to $\zeta = 1$, i.e., at

$z = \ell$, which shows that ℓ indeed is a measure of the extent of frictional

influence as previously mentioned. In this respect it is worthwhile noting

that (29) yields estimates of ℓ comparable to empirical formulas for this

quantity given in, for example, Neumann and Pierson (1966).

For comparison the classical Ekman spiral is also shown in Fig. 1.

From Ekman's (1905) solution we have that the magnitude of the surface drift

current is $w_s = u_*^2/\sqrt{\nu_e f}$ where ν_e is the constant value of the vertical

eddy viscosity. Requiring that the surface velocity be the same for the two

solutions leads to a determination of ν_e, which not surprisingly is similar

to formulas quoted by Neumann and Pierson (1966). With this formula for ν_e

the characteristic vertical scale of Ekman's solution becomes

$$a^{-1} = (\frac{2\nu_e}{f})^{1/2} = \sqrt{2} \, \frac{u_*}{\kappa v_s} \, \frac{\kappa u_*}{f} = \sqrt{2} \, \frac{u_*}{\kappa v_s} \, \ell \tag{41}$$

For $\kappa v_s/u_* = 10$, as chosen for the turbulent Ekman spiral, the proportion-

ality of a^{-1} and ℓ enables us to present the classical Ekman spiral in the nondimensional form used in Fig. 1. Aside from the difference in the value of the deflection angle at the surface the much more rapid decrease of the drift current with depth predicted by the present theory is noted. This feature may be of considerable importance in the design of offshore pile supported structures.

Despite the considerable differences between the details of the velocity structure predicted by the present theory and that of Ekman, the two solutions share a common feature. The total mass transport predicted by the present theory is found from (37) to be

$$q_x + i\, q_y = \frac{2u_*}{\kappa} \int_0^\infty [-\text{kei}\,(2\sqrt{\zeta}) + i\,\text{ker}\,(2\sqrt{\zeta})]\; dz =$$

$$\frac{u_* \ell}{\kappa} \int_0^\infty [-\beta\,\text{kei}\beta + i\beta\,\text{ker}\beta]\; d\beta = \frac{u_*^2}{f} \tag{42}$$

which is identical to the result obtained from Ekman's theory, as it should be since this result is independent of v_T.

In order to compare the unsteady response to a suddenly applied surface shear stress (31) and (34) are plotted in Fig. 2 corresponding to a value of the steady surface velocity $\kappa v_s/u_* = 10$, i.e., Fig. 2 represents the development of the surface current whose steady state solution was the one presented in Fig. 1. For comparison Fredholm's solution, based on an assumed constant value of the vertical eddy viscosity is shown. The temporal development is shown in terms of pendulum hours and the striking difference is the rapidity with which the present solution attains its steady state value. Whereas Fredholm's solution very slowly approaches the
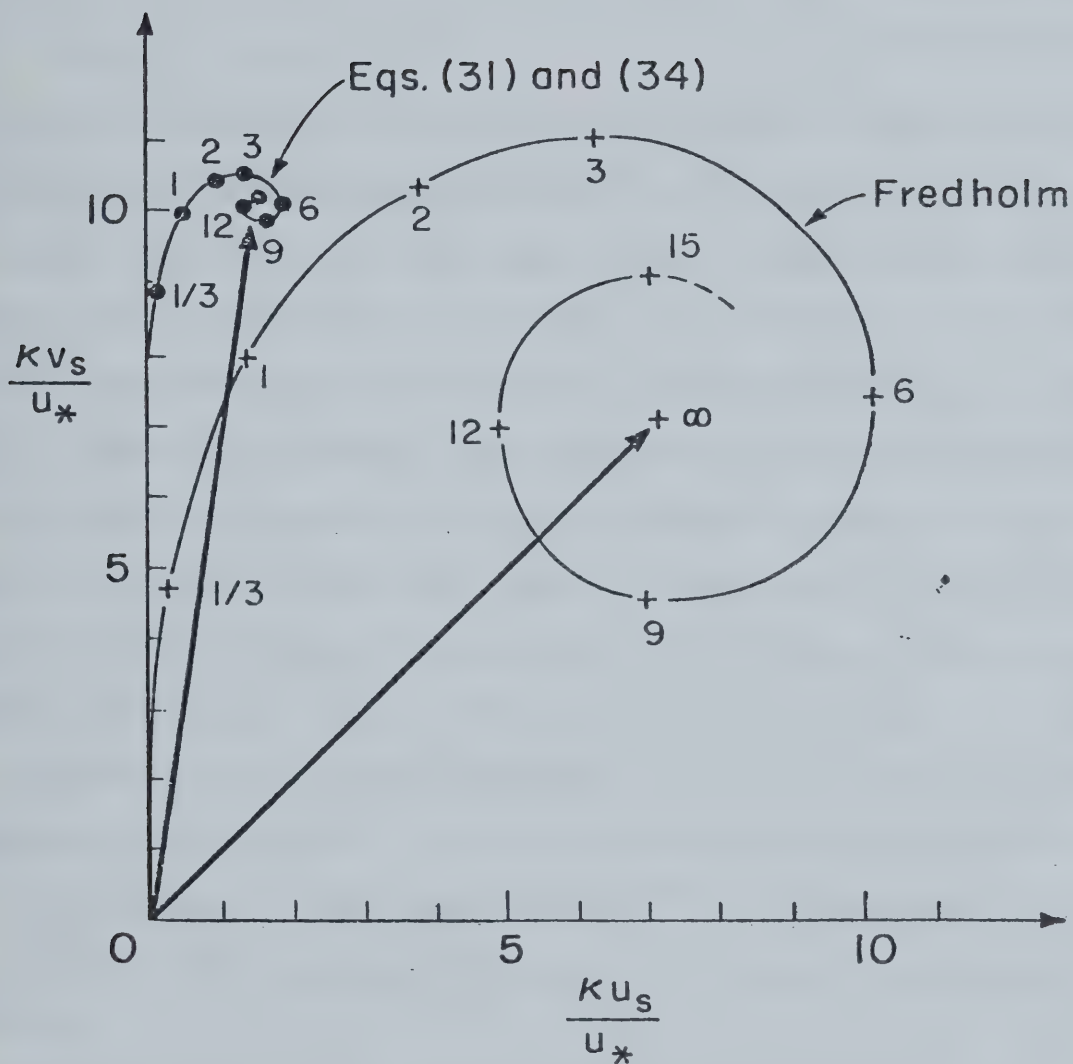
Figure 2: The Temporal Development of the Surface Drift Current due to a Suddenly Applied Uniform Surface Shear Stress. Time from Time of Application indicated in Pendulum Hours. Present Eddy Viscosity Model (•), Fredholm's Classical Solution (+).

steady state the present theory shows that the steady state is approximately reached within 3 pendulum hours. This extremely rapid response predicted by the present theory suggests that unsteadyness in many problems may be neglected and that a solution based on a quasi-steady analysis, i.e., assuming steady conditions to be reached immediately, therefore may lead to meaningful results.

A simple physical explanation for the much faster response predicted by the present model may be found by comparing the order of magnitude of the vertical eddy viscosity of the present model and the constant value, ν_e, assumed in the classical model. With ν_T being assumed to vary linearly with depth, an equivalent constant value of the vertical eddy viscosity corresponding to the present model would be ν_T evaluated at $z = \ell/2$. Thus, the present model corresponds to an equivalent constant value of $\nu_{T,e} = \kappa^2 u_*^2/(2f)$. This value may be shown to be considerably larger than the constant value ν_e obtained by requiring that the surface current be of the order three percent of the wind speed (by a factor of the order fifty). Since the difference between the instantaneous velocity vector during the unsteady response and the steady state velocity, according to the classical analysis is proportional to $\nu_e^{-1/2}$ it is evident that the present model, with its much larger apparent eddy viscosity, approaches steady state more rapidly.

The nature of the unsteady response at some finite depth below the free surface is readily envisioned by examining (36). With the first term on the right hand side of (36) expressing the steady state response, the second term is identified as expressing the manner in which steady state is approached. This term depends only weakly on the value of ζ so long as

$\zeta << 1$ and the manner in which steady state is approached is therefore that exhibited by the surface current development shown in Fig. 2. Since the magnitude of the steady state velocity decreases rapidly with depth the approach of steady state conditions will appear somewhat slower at greater depths.

6. Concluding Remarks

The results obtained in the previous sections for the pure drift current in an infinite homogeneous ocean were obtained based on a proposed model for the vertical eddy viscosity. This proposed model, which simply assumes that the vertical eddy viscosity increases linearly with distance from a sheared boundary is particularly simple to apply to the problem of the response of an infinitely deep ocean to a prescribed surface shear stress when it is assumed that the drift current vanishes at large depths. In a more general analysis the effects of a spatially varying atmospheric pressure, p_a, and free surface elevation, $\hat{z} = \eta = \eta(\hat{x}, \hat{y}, t)$, should be included.

For this more general problem formulation the governing equation replacing (1) reads

$$\frac{\partial w}{\partial t} + i f w = -P + \frac{\partial}{\partial \hat{z}} (\nu_T \frac{\partial w}{\partial \hat{z}}) \qquad (43)$$

in which

$$P = \frac{1}{\rho} \frac{\partial p_a}{\partial \hat{x}} + g \frac{\partial \eta}{\partial \hat{x}} + i (\frac{1}{\rho} \frac{\partial p_a}{\partial \hat{y}} + g \frac{\partial \eta}{\partial \hat{y}}) \qquad (44)$$

is the term giving rise to the slope current.

When the effects of a varying atmospheric pressure and free surface elevation are included in the analysis the current no longer vanishes at large depths. This, in turn, gives rise to the development of a bottom boundary layer in addition to the surface boundary layer treated in detail in the present paper. Thus, in the general case and assuming, for simplicity, steady state conditions (43) reads for the present vertical eddy viscosity model

$$i \, f \, w_s = -P + \frac{\partial}{\partial z_s} \left(\kappa |u_{*s}| z_s \frac{\partial w_s}{\partial z_s} \right) \qquad z_s \leq z_m \qquad (45a)$$

$$i \, f \, w_b = -P + \frac{\partial}{\partial z_b} \left(\kappa |u_{*b}| z_b \frac{\partial w_b}{\partial z_b} \right) \qquad z_b \leq h \leq z_m \qquad (45b)$$

in which z_s is the vertical coordinate, denoted by z in the main body of this paper, i.e., $z_s = 0$ in the free surface $\hat{z} = \eta \simeq 0$ and positive downwards, and z_b is zero at the bottom, $\hat{z} = -h$, and positive upwards. $|u_{*s}|$ and $|u_{*b}|$ are the shear velocities corresponding to the magnitudes of the surface shear stress and the bottom shear stress, respectively.

It is evident from the steady solution for the surface boundary layer presented and discussed in the previous sections that the character-istic vertical length scales of (45a) and (45b) are $\ell_s = \kappa |u_{*s}|/f$ and $\ell_b = \kappa |u_{*b}|/f$, respectively. Thus, for a water depth $h \gg \ell_s + \ell_b$ the depth is effectively infinite and the solution of (45a and b) is readily found to consist of a surface boundary layer, a frictionless layer in which the flow is geostrophic, i.e., $w = w_s = w_b = -P/if$, and a bottom boundary layer. Hence, for $h \gg \ell_s + \ell_b$ it follows that the choice of the matching location, $z_s = h - z_b = z_m$, is immaterial. In fact, the solution for the

bottom boundary layer becomes identical to the solution obtained by Ellison (1956) for the atmospheric boundary layer.

In the general case of a finite depth, i.e., $h \leq 0(\ell_s + \ell_b)$, the preceeding reasoning that the extent of the surface influence is ℓ_s and that of the bottom is ℓ_b, suggests the following general model for the vertical eddy viscosity

$$
\nu_T = \begin{cases} \kappa |u_{*s}| z_s & ; \quad z_s \leq \dfrac{|u_{*s}|}{|u_{*s}| + |u_{*b}|} h \\[4mm] \kappa |u_{*b}| z_b & ; \quad z_b \leq \dfrac{|u_{*b}|}{|u_{*s}| + |u_{*b}|} h \end{cases} \tag{46}
$$

This general model for the vertical eddy viscosity will reproduce the observed features of turbulent shear flows, i.e., the logarithmic velocity deficit near the free surface and the classical logarithmic velocity profile near solid boundaries. It is quite general, in that it may be applied in shallow as well as in deep water, and it is sufficiently simple to apply to be practical. In this respect it is noted that the problems associated with the application of (46) are similar to those associated with Thomas' (1975) model, i.e., the value of the bottom shear stress must first be estimated and a solution based on (46) must be obtained. Based on this solution an updated and improved estimate of $|u_{*b}|$ is obtained and the ultimate solution is approached in an iterative manner. This procedure is, of course, not trivial in the general case but is necessary if the details of the vertical velocity profile are to be resolved in a physically realistic manner.

References.

Abramowitz, M. and I. A. Stegun, (1972), Handbook of Mathematical Func-
tions, U.S. Dept. Interior, Nat. Bur. Standards, Appl. Math. Ser.,
No. 55, 1045p.

Barger, W. R., W. D. Garret, E. L. Mollo-Christensen and K. W. Ruggles,
(1970), "Effects of an Artificial Sea Slick upon the Atmosphere
and the Ocean" Jour. Appl. Met., Vol. 9, pp. 396-400.

Ekman, V. W., (1905), "On the Influence of Earth's Rotation on Ocean
Currents," Ark. Math. Astrono. Fys., Vol. 2, pp. 1-53.

Ellison, T. H., (1956), "Atmospheric Turbulence," Surveys in Mechanics,
G. K. Batchelor and R. M. Davis, Eds., Cambridge University Press,
pp. 400-430.

Fjeldstad, J. E., (1929), "Ein Beitrag zur Theorie der Winderzengten
Meeresströmungen," Beitr. Geophys., Vol. 23, pp. 237-247.

Hildebrand, F., (1965), Calculus for Applications, Prentice Hall,
Englewood Cliffs, New Jersey, 646p.

Kajiura, K., (1964), "On the Bottom Friction in an Oscillatory Current,"
Bull. Earthquake Res. Inst., University of Tokyo, Vol. 42,
pp. 147-174.

Kajiura, K., (1968), "A Model of the Bottom Boundary Layer in Water
Waves," Bull. Earthquake Res. Inst., University of Tokyo, Vol. 46,
pp. 75-123.

Murray, S. P., (1975), "Trajectories and Speeds of Wind-Driven Currents
Near the Coast," Jour. Phys. Ocean., Vol. 5, pp. 347-360.

Neumann,G. and W. J. Pierson, (1966), <u>Principles of Physical Oceanography</u>, Prentice Hall, Englewood Cliffs, New Jersey, 545p.

Reichardt, H., (1959), "Gesetzmässigkeiten der geradlinigen Turbulenten Couette-Strömung," <u>Mitteilungen aus dem Max-Planck-Institute für Strömungsforschung und der Aerodynamischen Versuchsanstalt</u>, No. 22, Göttingen, pp. 1-45.

Reid, R. O., (1957), "Modification of the Quadratic Bottom-Stress Law for Turbulent Channel Flow in the Presence of Surface Wind-Stress," <u>U.S. Army Corps of Engineers</u>, Beach Erosion Board, Tech. Memo. No. 93, 33p.

Reid, R. O., (1975), "Analytical and Numerical Studies of Ocean Circulation," <u>Reviews of Geophys. Space Phys.</u>, U.S. Nat. Rep. 1971-74, Vol. 13, No. 3, pp. 606-609.

Ruggles, K. W., (1970), "The Vertical Mean Wind Profile Over the Ocean in Light to Moderate Winds," <u>Jour. Appl. Met.</u>, Vol. 9, pp. 389-395.

Schlichting, H., (1960), <u>Boundary Layers</u> (4th Ed.) McGraw-Hill, New York.

Shemdin, O. H., (1972), "Wind Generated Current and Phase Speed of Wind Waves," <u>Jour. Phys. Ocean</u>, Vol. 2, pp. 411-419.

Shemdin, O. H., (1973), "Modelling of Wind Induced Currents," <u>Jour. Hydraulic Res.</u>, Vol. 11, No. 3, pp. 281-297.

Smith, J. E., (1968), <u>Torrey Canyon Pollution and Marine Life</u>, Cambridge University Press, 196p.

Teeson, D., F. M. White and H. Schenck, (1970), "Studies of the Simulation of Drifting Oil by Polyethylene Sheets," <u>Ocean Engineering</u>, Vol. 2, pp. 1-11.

Thomas, J. H., (1975), "A Theory of Steady Wind-Driven Currents in Shallow Water with Variable Eddy Viscosity," Jour. Phys. Ocean, Vol. 5, pp. 136-142.

Witten, A. J. and J. H. Thomas, (1976), "Steady Wind-Driven Currents in a Large Lake with Depth-Dependent Eddy Viscosity," Jour. Phys. Ocean, Vol. 6, pp. 85-92.

Wu, J., (1969), "Wind Stress and Surface Roughness of Air-Sea Interface," Jour. Geophys. Res., Vol. 74, No. 2, pp. 444-454.